

wiener klinische wochenschrift

The Central European Journal of Medicine

133. Jahrgang 2021 · Supplement 3

Wien Klin Wochenschr

<https://doi.org/10.1007/s00508-021-01884-1>

© Springer-Verlag GmbH Austria, part of Springer
Nature 2021



Abstracts

Österreichische Kardiologische Gesellschaft Jahrestagung 2021

„Alte Herzen – Neue Perspektiven“

Online-Congress – Vorträge live aus Salzburg
27. bis 29. Mai 2021

Tagungspräsident:

Univ.-Prof. Dr. Peter Siostrzonek

Tagungssekretär:

Univ.-Prof. Dr. Bernhard Metzler

Univ.-Prof. Dr. Daniel Scherr



BEST ABSTRACTS

Basic Science

Targeting IGF1 Signalling to Promote Cardiac Health and Longevity

M. Abdellatif¹, V. Trummer-Herbst¹, T. Pendl², S. Hofer², S. Durand³, J. Voglhuber¹, D. Von Lewinski¹, P. Rainer¹, D. Scherr¹, A. Zirlik¹, T. Eisenberg², G. Kroemer³, F. Madeo², E. Bisping¹, S. Sedej¹

¹Department of Cardiology, Medical University of Graz, Graz, Austria

²Institute of Molecular Biosciences, University of Graz, Graz, Austria

³Metabolomics and cell biology platforms, Institute Gustave Roussy, Villejuif, France

Introduction: Inhibition of IGF1 signalling is a conserved longevity-promoting mechanism across species. However, the effect of IGF1 inhibition on health and disease, with the exception of cancer, is largely controversial. Particularly in the heart, IGF1 signalling have been reported to exert both detrimental and beneficial effects. However, a common limitation in the previous cardiac studies is the focus on young mice. Furthermore, the lifelong impact of manipulating cardiac IGF1 signalling is surprisingly under-reported. Thus, it remains elusive as to whether (and how) IGF1 inhibition delays aging, meanwhile its activation promotes cardiac health.

Methods: We used male mice with cardiomyocyte-specific up- or down-regulation of IGF1 signalling induced by human IGF1 receptor overexpression (IGF1R Tg) or dominant negative phosphoinositide-3-kinase mutation (dnPI3K), respectively. Mice were examined at different life stages (young, middle-aged and aged) by echocardiography, haemodynamics and treadmill coupled to indirect calorimetry. Lifespan was assessed in independent longevity cohorts. Mitochondrial respiration, ATP synthesis capacity were measured by high-resolution respirometry and electrochemiluminescence-based assays, respectively. Autophagy flux was assessed by leupeptin-based LC3 lipidation and HPLC-MS was used for cardiac metabolome analysis. IGF1R and its downstream targets were immunoblotted in human explanted failing and non-failing hearts.

Results: When young, IGF1R Tg mice exhibited superior cardiac contractility and exercise capacity compared to WT mice, and more so compared to dnPI3K mice. With aging, however, IGF1R Tg mice showed a striking decline in cardiac function, leading to a full-blown heart failure phenotype, characterized by reduced ejection fraction, atrial dilation, lung congestion, and effort intolerance, as well as shortened maximum lifespan. Contrarily, sustained low activity of IGF1 signalling in old dnPI3K mice extended both cardiac healthspan and longevity, despite initially delaying cardiac development. Mechanistically, reduced autophagic flux in IGF Tg mice led to reduced mitochondrial oxidative capacity and metabolic rewriting towards energy production from glycolytic and anaerobic reactions. Supplementing the autophagy inducer spermidine to aged IGF1R Tg mice protected them from heart failure, indicating a causal role of autophagy. Along similar lines, the cardiac benefits observed in aged dnPI3K mutants were entirely abolished upon blocking autophagy by the protease inhibitor chloroquine. In humans, explanted failing hearts showed an increase in IGF1R expression and signalling activity as well as a decline in autophagy markers, compared to non-failing donors with compensated hypertrophy.

Conclusion: Fine-tuning of IGF1 signalling is essential to avoid its detrimental impact in the aging myocardium, but harness its benefits in during cardiac development. Therefore, at least the elderly might significantly benefit from available pharmacological inhibitors of IGF1, which are currently used in cancer therapy, to also prevent cardiac disorders associated with aging.

Altered spatio-specific CaMKII activation in autophagy deficient mice

J. Voglhuber¹, M. Abdellatif¹, N. Djalinac¹, V. Trummer-Herbst¹, S. Ljubojevic-Holzer¹, S. Sedej¹

¹Department of Cardiology, Medical University of Graz, Graz, Austria, Graz, Austria

Introduction: Autophagy is linked to preventing the development of cardiac hypertrophy and failure. While aberrant activation of Ca²⁺/calmodulin-dependent kinase II (CaMKII) promotes myocardial remodeling, the role of autophagy in maintaining cardiac Ca²⁺ homeostasis and regulating CaMKII signaling is unknown.

Methods: Young (10-15 weeks old) cardiomyocyte-specific autophagy protein 5-deficient mice (Atg5^{-/-}) mice and their littermate controls (Atg5^{+/+}) underwent comprehensive in vivo phenotyping using echocardiography, exercise tolerance and hemodynamic stress testing. In vitro assessment included gravimetry, qPCR of hypertrophy marker genes and cellular and nuclear dimensions of isolated ventricular myocytes. CaMKII activation was studied by immunocytochemistry in cardiomyocytes upon exposure to basal (1 Hz) or high (4 Hz) pacing frequency. Autophosphorylated CaMKII (pT286) signal was evaluated in different subcellular spaces (i. e. cytoplasm, nucleoplasm and nuclear envelope).

Results: Before symptomatic cardiac dysfunction occurred, Atg5^{-/-} mice showed compromised cardiac reserve in response to β -adrenergic stimulation (dp/dt max: 9475 \pm 126 vs 7364 \pm 496 mm Hg/s, $N=4-5$; $p=0.041$), despite similar maximum heart rate. Consequently, effort intolerance (distance run: 251 \pm 22 vs 152 \pm 13 m, $N=8$; $p=0.03$) and maximal oxygen consumption (2093 \pm 66 vs 1763 \pm 131 ml/h/kg, $N=8$; $p=0.04$) were reduced during treadmill exercise tolerance testing. Increased heart-to-body weight ratio (8.1 \pm 0.5 vs 10.2 \pm 0.8 $N=9$; $p=0.017$) was associated with elevated mRNA expression of hypertrophy marker NppB (278 % of Atg5^{+/+}, $N=5$; $p=0.016$) in Atg5^{-/-} mice, which showed enlarged cardiomyocytes and nuclei, as width-to-length ratio. Because Atg5^{-/-} cardiomyocytes exhibit elevated nuclear Ca²⁺ levels at high pacing frequency, we now measured subcellular CaMKII activation under the same experimental conditions. Interestingly, at 1 Hz, p -CaMKII was increased specifically at the nuclear envelope (154 % of Atg5^{+/+}, $N=5$ mice, 153-159 cells; $p=0.029$), but not in the cytoplasm or nucleoplasm. Increasing pacing frequency to 4 Hz did not alter p -CaMKII levels in Atg5^{+/+} cells. However, p -CaMKII was increased by ~30 % and ~20 % in the cytoplasm and nucleoplasm of Atg5^{-/-} cells respectively ($N=5$ mice, 153-155 cells).

Conclusion: Loss of ATG5-dependent autophagy causes cardiac hypertrophy and impaired cardiac reserve upon acute stress, which involves CaMKII activation, likely through the imbalance of nuclear Ca²⁺ load. Although, selective increase in p -CaMKII at the nuclear envelope in Atg5^{-/-} mice may temporarily protect from nuclear Ca²⁺ overload, excessive CaMKII activation in the cytoplasm and the nucleoplasm upon increased workload, likely drives hypertrophic signalling toward heart failure in autophagy-defective mice.

Therapeutic transdifferentiation of fibroblasts to functional endothelial cells

M. Graber¹, C. Tepekyözü-Gollmann¹, V. Schweiger¹, J. Hirsch¹, L. Pözl¹, F. Nägele¹, D. Lener², H. Hackl³, S. Sopper⁴, E. Kirchmair¹, S. Lechner¹, D. Lobenwein⁵, J. Vökl⁶, I. Tancevski⁷, M. Grimm¹, J.P. Cooke⁸, J. Holfeld¹

¹Universitätsklinik für Herzchirurgie Innsbruck, Innsbruck, Austria

²Universitätsklinik für Innere Medizin III Innsbruck, Innsbruck, Austria

³Zentrum für Bioinformatik der Medizinischen Universität Innsbruck, Innsbruck, Austria

⁴Universitätsklinik für Innere Medizin V Innsbruck, Innsbruck, Austria

⁵Universitätsklinik für Gefäßchirurgie Innsbruck, Innsbruck, Austria

⁶Institut für Physiologie, Johannes Kepler Universität Linz, Linz, Austria

⁷Universitätsklinik für innere Medizin II Innsbruck, Innsbruck, Austria

⁸Center for Cardiovascular Regeneration, Houston Methodist Research Institute, Houston, TX, United States,

Introduction: Regeneration of ischemic myocardium still displays a significant issue in modern cardiovascular medicine. Currently, there is a lack of efficient regenerative approaches, but reprogramming of cardiac fibroblasts towards functional endothelial cells could be a promising strategy. It has been shown, that activation of innate immunity, namely Toll-like receptor 3 (TLR3) is required for effective nuclear reprogramming. Shock wave therapy has shown distinct angiogenic effects in ischemic tissue via activation of TLR3. Thus, we hypothesized that the activation of TLR3 via SWT might enable reprogramming of resident fibroblasts towards endothelial cells in ischemic myocardium.

Methods: Human fibroblasts were treated with SWT or TLR3 agonist poly(I:C) and cultivated in endothelial differentiation medium. Upon 2 weeks, cells were analyzed for expression of endothelial-specific markers and FACS-sorting was performed. Cells positive for CD31 were declared as induced endothelial cells (iECs) and subjected to functional testing, including NO production and tube formation. iECs were suspended in Matrigel and injected subcutaneously in NGS mice. A lineage-tracing experiment in Fsp1-Cre/LacZ mice, which produce β -Galactosidase in FSP-1 expressing cells (fibroblasts), after coronary occlusion and subsequent SWT was performed. IF staining of β -Galactosidase and CD-31 has been performed and β -Galactosidase/CD31-positive cells were analyzed. Myocardial scarring was evaluated histologically and functional impairment was measured through assessment of the left ventricular function via transthoracic echocardiography. Chromatin remodeling and epigenetic plasticity were evaluated via Western Blot and ATAC sequencing.

Results: SWT activated TLR3 in cardiac fibroblasts and led to the induction of endothelial-specific genes like VEGFR, CD31 and VE-Cadherin. Fibroblasts, that were stained with IF upon SWT treatment and cultivation in endothelial differentiation medium were FACS-sorted and a newly formed CD31 positive population was found. These, as mentioned above, induced endothelial cells were capable of producing endothelial nitric oxide (NO) and forming tubular structures in vitro. In a Matrigel plug assay, injection of iECs led to a higher number of vessels and improved perfusion. In a lineage tracing experiment in FSP1-Cre/LacZ mice, we found higher numbers of

β -Galactosidase/CD31 positive cells after coronary occlusion and subsequent SWT, indicating transdifferentiation in vivo. Moreover, the LV function was ameliorated, while the area of dysfunctional scar tissue was decreased. Mechanistically, SWT enhanced epigenetic plasticity via a TLR3—NF κ B—IL-6—STAT3—PRDM14 axis. SWT and Poly(I:C) induced significant changes in chromatin organization, with chromatin being more accessible after both treatments.

Conclusion: We provide evidence, that mechanical stimulation via shock wave therapy induces transdifferentiation of resident fibroblasts towards endothelial cells dependent on activation of TLR3. These induced endothelial cells could be shown to be functional, enabling revascularization in ischemic areas. Hence, SWT displays an easy and feasible strategy for regeneration of ischemic myocardium.

Clinical Science

Serum-Laktat und MELD-XI-Score (Model for End-Stage Liver Disease Excluding INR) als Mortalitätsprädiktoren nach kardiopulmonaler Reanimation

R. Rezar¹, M. Lichtenauer¹, P. Schwaiger², C. Seelmaier¹, I. Pretsch¹, M. Ausserwinkler¹, J. Reichle¹, P. Jirak¹, C. Jung³, B. Strohm¹, U. Hoppe¹, B. Wernly¹

¹Department of Cardiology, Clinic of Internal Medicine II, Paracelsus Medical University of Salzburg, Salzburg, Österreich

²Department of Anesthesiology and Intensive Care, Paracelsus Private Medical University Salzburg, Salzburg, Österreich

³Division of Cardiology, Pulmonology, and Vascular Medicine, Medical Faculty, University Duesseldorf, Düsseldorf, Deutschland

Einleitung: Die Prognoseerstellung nach kardiopulmonaler Reanimation bleibt auch in der modernen Intensivmedizin eine Herausforderung für Kliniker. Trotz verschiedenen Tools wie laborchemischen Markern, Schnittbildgebungsverfahren und/oder neurophysiologischen Tests ist es oftmals schwierig, das individuelle PatientInnen-Outcome richtig einzuschätzen. Serum-Laktat ist ein in der Akutmedizin weit verbreiteter Marker zur Risikostratifizierung. Der Model for End-Stage Liver Disease Excluding INR (MELD-XI) Score wurde von Heuman et al. entwickelt, um der Limitation durch die Verwendung der INR bei antikoagulierten PatientInnen entgegenzuwirken. Mittlerweile wurde seine prognostische Wertigkeit auch abseits von chronischen Lebererkrankungen in verschiedenen Arbeiten bestätigt. In unserer retrospektiven Single-Center Analyse haben wir versucht, einen volatilen Schock-Marker (Laktat) mit einem stabileren Indikator (MELD-XI) für die Performance zweier vitaler Organsysteme (Leber und Niere) zu kombinieren, um die 30-Tages-Mortalität nach Reanimation abzuschätzen.

Methoden: In dieser Studie wurden 106 konsekutive PatientInnen nach kardiopulmonaler Reanimation analysiert, welche auf unsere internistische Intensivstation aufgenommen wurden. PatientInnen (1) <18 Jahre, (2) nach traumatischem Herz-Kreislaufstillstand, (3) mit einem Krankenhausaufenthalt <24 Stunden und/oder (4) fehlendem initialen Laktatwert wurden ausgeschlossen. Ein 30-Tages Follow-Up wurde telefonisch durchgeführt und beinhaltet das Erheben des CPC-Scores (Cerebral Performance Category) als neurologischem

Outcome-Marker. Ein positives Votum der lokalen Ethikkommission wurde eingeholt. Der erste an der Intensivstation erhobene Laktat-Wert wurde für die Analyse herangezogen. Der initiale MELD-XI-Score wurde nach folgender Formel erhoben: $5,11 \times \ln(\text{Serum Bilirubin in mg/dL}) + 11,76 \times \ln(\text{Serum Kreatinin in mg/dL}) + 9,44$. Als primärer Studienendpunkt wurde die 30-Tages-Mortalität verwendet. Die Baseline-Daten wurden für die gesamte Kohorte erfasst. Unterschiede zwischen den Gruppen wurden mittels U-Test berechnet, eine uni- und eine multivariate Cox-Regressions-Analyse für den Endpunkt durchgeführt. Weiters wurden eine ROC-Kurve und die AUCs für ein kombiniertes Modell, sowie den komplexeren Sequential Organ Failure Assessment (SOFA) Score berechnet. Weiters erfolgte die Berechnung von optimalen Cut-Off-Werten mittels Youden-Index.

Resultate: Sowohl Serum-Laktat, als auch der MELD-XI-Score waren unabhängige Prädiktoren für die 30-Tages-Mortalität nach Reanimation. Als optimale Cut-off Werte konnten ein Serum-Laktat von $\geq 2,5$ mmol/L bzw. ein MELD-XI-Score von >12 Punkten berechnet werden. Die PatientInnen wurden demnach in drei Gruppen aufgeteilt: (1) Laktat $<2,5$ mmol/L UND MELD-XI ≤ 12 Punkte („low-risk“; $n=32$), (2) Laktat $\geq 2,5$ mmol/L ODER MELD-XI >12 Punkte („medium-risk“; $n=39$), und (3) Laktat $\geq 2,5$ mmol/L UND MELD-XI >12 Punkte („high-risk“; $n=33$). PatientInnen in der „low-risk“-Gruppe wiesen eine Mortalität von 6 %, PatientInnen in der „medium-risk“-Gruppe eine Mortalität von 26 % und PatientInnen in der „high-risk“-Gruppe eine Mortalität von 61 % auf. Für dieses Modell konnte eine AUC von 0,78 errechnet werden (95 %KI 0,68–0,85; $p=0,03$), womit der deutlich komplexere SOFA-Score (AUC 0,66) outperformed wurde. Ein schlechteres neurologisches Outcome wurde in den „medium-risk“ und „high-risk“-Gruppen beobachtet (10,3 % und 9,1 % versus 6,25 % in der „low-risk“-Gruppe).

Schlussfolgerungen: In dieser Arbeit konnte mit einer Kombination aus zwei einfachen Parametern ein vielversprechendes Risiko-Stratifizierungs-Tool für PatientInnen nach kardiopulmonaler Reanimation gefunden werden. Im Gegensatz zu komplexen intensivmedizinischen Scores können alle hierfür benötigten Parameter schnell, einfach und kostengünstig erhoben werden. Mittels immer häufiger eingesetzten Point-of-Care Testgeräten könnte innerhalb kürzester Zeit ein solcher Score schon in der Notaufnahme berechnet werden.

Prädiktion von okkultem Vorhofflimmern bei kryptogenem Schlaganfall: Der Graz AF Score

E. Bisping¹, M. Kneihsl², D. Scherr¹, H. Mangge³, S. Fandler-Höfler², I. Colonna², M. Haidegger², S. Eppinger², F. Fazekas², C. Enzinger², T. Gattringer²

¹Klinische Abteilung für Kardiologie LKH Universitätsklinikum Graz, Graz, Österreich

²Klinische Abteilung für Neurologie LKH Universitätsklinikum Graz, Graz, Österreich

³Klinische Institut für Medizinische und Chemische Labordiagnostik LKH Universitätsklinikum Graz, Graz, Österreich

Einleitung: Vorhofflimmern (VHF) ist eine wichtige Differentialdiagnose der Ursachen eines kryptogen Schlaganfalls (KS). Die Kosten eines intensivierten Rhythmus-Monitorings über implantierbare Looprekorder (ILR) machen es aber erforderlich, die Patienten hierfür zu selektionieren. Wir haben daher einen klinischen Risikoscore zur Prädiktion von okkultem Vorhofflimmern entwickelt und seine Aussagekraft über ein einjähriges Follow up verfolgt.

Methoden: Literatursuche und Identifikation von Studien zur Assoziation folgender Einzelparameter mit der Detektion von Vorhofflimmern: Alter, NT-pro-BNP, linksatriale Größe, Ejektionsfraktion, supraventrikuläre Extrasystolen und Salven, früherer kortikaler Infarkt, multiterritorialer Infarkt, vorhergehende Thrombozytenaggregations-Hemmung. Graz AF Score: Anhand der publizierten Hazard Ratios (1,8 bis 13,7) Einteilung in Minor (1 Punkt) und Major Kriterien (2 Punkte) und Bildung eines Risikoscore von 0 bis 16 Punkten. Implantation von ILR mit präferentieller Empfehlung ab 4 Punkten. Prospektive Analyse der Detektionsrate des Risikoscores über 12 Monate Follow up monozentrisch an 150 Patienten mit KS (Einschlusszeitraum 5/2018 bis 8/2019). Analyse der Daten mittels Receiver Operating Charakteristik und Youden Index.

Resultate: Im Beobachtungszeitraum Detektion von VHF bei insgesamt 24 von 150 Patienten (16%); 6 von 24 Pat. mit ILR (25%); 18 von 126 Pat. ohne ILR (14%). Im Gesamtkollektiv zeigte der Risikoscore bei der ROC Analyse den höchsten Youden Index bei 4 Punkten, und dort eine Sensitivität von 92 %, Spezifität von 68 %, und einen negativ prädiktiven Wert von 98 %.

Schlussfolgerungen: Der Graz AF Score zeigt bei 12 Monaten Follow Up eine hohe Sensitivität und sehr gute negative Prädiktion bei adäquater Spezifität zur Detektion von Vorhofflimmern bei kryptogenem Schlaganfall. Der Score ist geeignet zur Präselektion von Patienten zur Looprekorderimplantation.

Prevention of early sudden cardiac death after myocardial infarction using the wearable cardioverter defibrillator—results from a real-life cohort

U. Rohrer¹, T. Odene¹, M. Manninger¹, C. Ebner², D. Mörtl³, H. Keller⁴, A. Dirninger⁵, G. Stix⁶, H. Alber⁷, C. Steinwender⁸, R. Binder⁹, M. Stühlinger¹⁰, D. Zweiker¹, A. Zirlik¹, D. Scherr¹

¹Medical University of Graz, Graz, Austria

²Elisabethinen Hospital Linz, Linz, Austria

³University Hospital St. Pölten, St. Pölten, Austria

⁴Klinik Landstraße, Vienna, Wien, Austria

⁵Hospital Hochsteiermark, Bruck/Mur, Austria

⁶Medical University of Vienna, Wien, Austria

⁷Hospital Klagenfurt, Klagenfurt, Austria

⁸Medical University of Linz, Linz, Austria

⁹Hospital Wels-Grieskirchen, Wels, Austria

¹⁰University Hospital Innsbruck, Innsbruck, Austria

Introduction: Patients are at elevated risk of sudden cardiac death (SCD) after acute myocardial infarction (MI). The VEST trial failed to show a significant reduction in arrhythmic mortality in patients prescribed with a wearable converter-defibrillator (WCD), having a lower than expected wearing compliance. We aimed to investigate the incidence of WCD treatments and

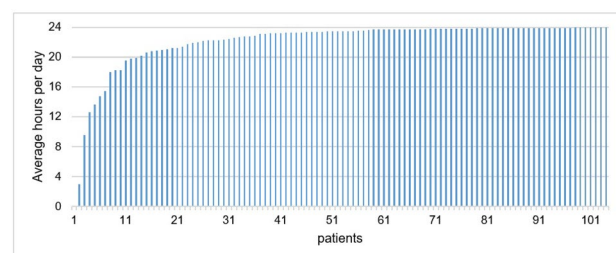


Fig. 1 Average wearing duration/day of Austrian cohort

outcomes of all patients with acute MI and LVEF $\leq 35\%$ in a real life and well-compliant cohort in Austria.

Methods: We performed a retrospective analysis of all patients meeting the in- and exclusion criteria of the original VEST trial within the Austrian WCD registry between 2010 and 2019.

Results: 105/896 patients (12 %) with an average age of 64 ± 11 years (12 % female; LVEF $28 \pm 6\%$) registered in the Austrian WCD registry met the VEST in- and exclusion criteria. 104/105 patients were revascularized and prescribed with a WCD prescription for 69 (1;277) days, the median wearing duration was 23.5 (0;24) hours/day. 4/105 (3.8 %) patients received 9 appropriate WCD shocks, the per patient shock rate was 2 (1;5). No inappropriate shock was delivered. During follow-up, 46/105 patients (44 %) received an ICD after the WCD period, 4/105 (3.8 %) patients died during follow-up. Arrhythmic mortality (1.9 % Austria vs. 1.6 % VEST, $p=ns$), as well as all-cause mortality (3.8 % vs. 3.1 %, $p=ns$) in the Austrian cohort were comparable to the VEST cohort.

Conclusion: The WCD is a safe treatment option in a highly selected cohort of patients with a LVEF $\leq 35\%$ after acute myocardial infarction. However, despite excellent WCD compliance as opposed to the VEST study, only 3.8 % of patients receive appropriate WCD shocks and the arrhythmic mortality rate was not significantly improved.

Ist Vielfalt gefährlich? – Magnetresonanztomographie-Untersuchungen bei Patient*Innen mit Schrittmachern oder Defibrillatoren mit Komponenten verschiedener Hersteller

C. König¹, F. Tinhofer¹, T. Puntus¹, A.L. Burger¹, K. Huber¹, M. Nürnberg¹, D. Zweiker¹

¹3. Medizinische Abteilung mit Kardiologie, Klinik Ottakring, Wien, Österreich

Einleitung: Viele Patienten mit elektronischen Schrittmachern oder Defibrillatoren (SM/ICD) müssen sich einer Magnetresonanztomographie (MRT) unterziehen. Ein erheblicher Teil der Patienten verfügt jedoch über ein SM/ICD-System, mit Generatoren und Sonden von jeweils unterschiedlichen Herstellern („Misch-Systeme“), wodurch das ganze System nicht MRT-tauglich ist, obwohl die einzelnen Komponenten per se MRT-tauglich sind. Die bisherige Datenlage zu diesen Patienten mit einem „gemischten“ SM/ICD-System, die sich einer MRT-Untersuchung unterziehen, ist bislang sehr begrenzt.

Methoden: Es wurde eine retrospektive Monocenter-Studie durchgeführt, an der alle SM/ICD-Patienten teilnahmen, die sich in einem Zeitraum zwischen Januar 2013 und Mai 2020 einem MRT unterzogen. Kurz- und Langzeitergebnisse wurden zwischen beiden Gruppen verglichen. Primäre Endpunkte waren der Tod oder unerwünschte MRT-bezogene Ereignisse, die einen Krankenhausaufenthalt oder eine SM/ICD-Revision erforderlich machten. Sekundäre Endpunkte waren Anzeichen für beginnendes Generator- oder Sondenversagen, oder Unwohlsein des Patienten während des MRTs.

Resultate: Insgesamt wurden 227 MRT-Untersuchungen, darunter auch 10 MRTs im Thoraxbereich, an 158 verschiedenen Patienten durchgeführt, mit 1 bis 9 MRTs pro Patienten. Das Durchschnittsalter betrug 73 Jahre und 52 (32,9 %) der Patienten waren weiblich. Wir identifizierten 38 Patienten, mit 54 MRT-Untersuchungen, die in die Gruppe der „gemischten“ Systeme fielen und 89 Patienten, mit 134 MRT-Untersuchungen, die der Gruppe der MRT-tauglichen Systeme zuzuordnen waren. Bei 31 Patienten, mit 39 MRT-Untersuchungen, konnte

die MRT-Konditionalität nicht bestimmt werden und sie mussten exkludiert werden. Patienten mit Misch-Systemen waren älter als Patienten mit MRT-tauglichen Systemen (Mittelwert 77 vs. 72 Jahre, $p=0,003$). Der primäre Endpunkt trat bei 0 % in der Gruppe der „gemischten“ SM/ICD-Systeme und bei 2,2 % in der Gruppe der „MRT-tauglichen“ Systeme auf ($p=1,000$). Die Komplikationen waren wie folgt: Zwei Patienten entwickelten ein neu diagnostiziertes Vorhofflimmern, das direkt im Zusammenhang mit der vorherigen MRT-Untersuchung gebracht wurde, wobei einer dieser Patienten zusätzlich eine vorübergehende SM/ICD-Dysfunktion hatte. Kein Patient in der „gemischten“ Gruppe und drei Patienten (3,4 %) in der MRT-tauglichen Gruppe erfüllten die Kriterien für die sekundären Endpunkte ($p=0,554$). Bei Patienten mit unbestimmbarer MRT-Konditionalität war die Komplikationsrate ähnlich (0 % sowohl für die primären als auch für die sekundären Endpunkte).

Schlussfolgerungen: Die Komplikationsrate von SM/ICD-Patienten, die sich einem MRT unterzogen, war insgesamt niedrig. Es fanden sich keine Anzeichen für ein erhöhtes Komplikationsrisiko bei Patienten mit einem „gemischten“ SM/ICD-System ohne MRT-taugliche Zertifizierung, im Vergleich zu Patienten mit komplett MRT-tauglichen SM/ICD-Systemen.

Principal morphomic and functional components of secondary mitral regurgitation

G. Heitzinger¹, P. Bartko¹, G. Spinka¹, N. Pavo¹, S. Prausmüller¹, S. Kastl¹, H. Arfsten¹, C. Gebhard¹, J. Mascherbauer¹, C. Hengstenberg¹, G. Strunk², M. Hülsmann¹, G. Goliash¹

¹Medizinische Universität Wien/AKH Wien, Universitätsklinik für Innere Medizin II/Abteilung für Kardiologie, Wien, Austria
²Complexity Research, Wien, Austria

Introduction: Secondary mitral regurgitation in patients with heart failure and reduced ejection fraction (sMR) typically results from distortion of the underlying cardiac architecture. The morphological components which may account for the clinical impact of sMR have not been systematically assessed or correlated with clinical outcomes. Our aim was to identify the key morphologic and functional features in sMR and their prognostic impact on outcome.

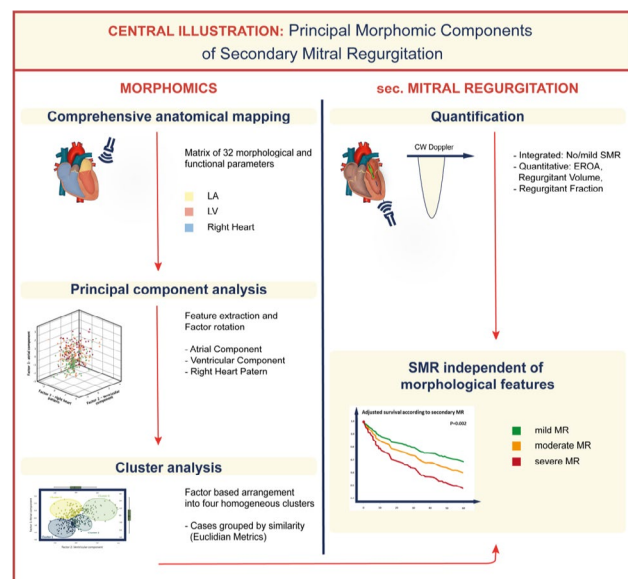


Fig. 1 Central Illustration

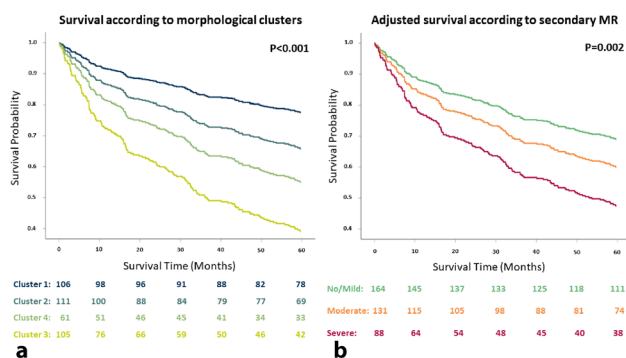


Fig. 2 Survival according to morphological clusters and sMR

Methods: Morphomic and functional network profiling was performed on a cohort of stable heart failure patients optimized on guideline based medical therapy. Principal component analysis was then used to condense the information into a simple factor-based solution relating sMR and clinical outcomes. Four homogenous clusters were derived based on the factors and identified to be associated with sMR (Fig. 1).

Results: Morphomic and functional data from 383 patients were profiled and subsequently condensed into factors. Factor 1 describes high loadings of left atrial morphological information, factor 2 high loadings of left ventricular topology. Based on these factors, four homogenous clusters were derived. sMR was most prominent in cluster 3 and 4 with the morphological difference being left ventricular size (end diastolic volume 188 ml (160–224) versus 315 ml (264–408), $P < 0.001$). Clusters were associated with mortality ($P < 0.001$), however, sMR remained independently associated with mortality after adjusting for the clusters (adj. HR 1.42, 95% CI 1.14–1.77; $P < 0.01$) (Fig. 2/Panel B). The detrimental association of sMR with mortality was mainly driven by cluster 3 (HR 2.18, 95% CI 1.32–3.60; $P = 0.002$), the “small LV cavity” phenotype (Fig. 2/Panel A).

Conclusion: These results challenge the current perceptions that sMR in heart failure with reduced ejection fraction results exclusively from global or local LV remodeling and are suggestive of a potential role of the left atrial component as a pathophysiologic mechanism. The association of sMR with mortality cannot be purely attributed to cardiac morphology alone, supporting other complementary key aspects of mitral valve closure consistent with the force balance theory. The association of sMR with mortality entirely driven by the small LV cavity phenotype refines the prognostic impact of sMR at the interface of anatomic variability.

Evaluation of long-term success of cryoballoon pulmonary vein isolation using an implantable loop recorder

A. Petzl¹, M. Granner¹, L. Haindl¹, M. Ladenbauer¹, N. Doruska¹, M. Martinek², B. Frey¹

¹Klinische Abteilung für Innere Medizin 3, Universitätsklinikum St. Pölten, St. Pölten, Austria

²Interne 2 mit Kardiologie, Angiologie und Intensivmedizin, Ordensklinikum Linz Elisabethinen, Linz, Austria

Introduction: Pulmonary vein isolation (PVI) is the cornerstone of current catheter-based therapy of atrial fibrillation (AF). Recurrence rates have been reported to be as high as 10–50% in different studies. Reported outcomes are usually based on intermittent electrocardiogram (ECG) monitoring, such as Holter ECG. However, paroxysmal episodes of AF are

Table 1 showing parameters significantly associated with atrial fibrillation recurrence

	AF recurrence	no AF recurrence	p value
Age (mean)	62,65 ± 12,37	56,89 ± 10,75	0.006
parox. AF	55.70%	44.30%	0.05
pers. AF	35.50%	64.50%	0.05
OSAS	6.30%	0.00%	0.056
CHADS2Vasc <2	35,90%	64,10%	0.004
CHADS2Vasc ≥2	62,50%	37,50%	0.004

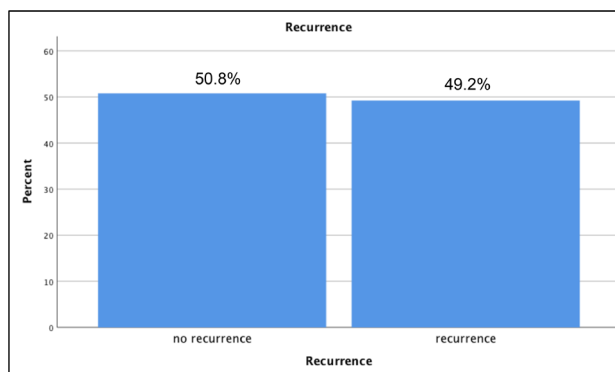


Fig. 1 Proportion of patients with atrial fibrillation recurrence after cryoballoon pulmonary vein isolation

easily missed with non-continuous monitoring. Therefore, we conducted a study evaluating the risk of AF recurrence after PVI with cryoballoon using an implantable loop recorder (ILR).

Methods: A total of 128 consecutive patients were included in the analysis. All underwent cryoballoon PVI and ILR implantation (usually at the same hospital admission) for paroxysmal or persistent AF. Episodes identified by the ILR as AF, atrial tachycardia and tachycardia were manually revised. If confirmed, these episode were counted as AF if the duration was 2 minutes or longer. A telephone follow-up on symptoms was performed.

Results: Mean follow-up time was 747 days (± 239), during which 62 patients (48.4%) experienced at least one episode of AF recurrence, while only 32 of these patients (52.5%) were symptomatic on the follow-up. In the AF burden analysis only 47 patients (36.7%) had AF recurrence with a burden >0.1%. We found patient age ($p = 0.006$), persistent AF ($p = 0.05$) and CHADS2Vasc Score ≥2 ($p = 0.004$) to be significantly associated with AF recurrence. Interestingly, we observed that the higher the CHADS2Vasc Score was, the higher was the AF burden in patients with AF recurrence. the presence of obstructive sleep apnoea syndrome (OSAS) ($p = 0.056$) was trending towards an increase in recurrence.

Conclusion: This study with an exceptionally long and continuous follow-up with ILR shows a long-term AF free survival after cryoballoon PVI of 51.6% (Table 1). Only 36.7% of patients had AF recurrence with a burden of >0.1%. Only about half of the recurrence episodes were symptomatic. Patient age, persistent AF and CHADS2Vasc Score ≥2 were significantly associated with AF recurrence and OSAS was borderline significant. Higher CHADS2Vasc Score was associated with higher AF burden.

Efficacy and safety of percutaneous pulmonary CTO intervention in chronic thromboembolic pulmonary hypertension

C. Gerges¹, R. Friewald², M. Gerges¹, I. Shafran¹, R. Sadushi-Kolici¹, N. Skoro-Sajer¹, B. Moser³, S. Taghavi⁴, W. Klepetko³, I. Lang¹

¹Medizinische Universität Wien, Universitätsklinik für Innere Medizin II, Klinische Abteilung für Kardiologie, Wien, Austria
²Universitätsklinikum Krems, Klinische Abteilung für Innere Medizin 1, Krems, Austria
³Universitätsklinik für Thoraxchirurgie, Medizinische Universität Wien, Wien, Austria

Background: Balloon pulmonary angioplasty (BPA) is an emerging percutaneous therapy for patients with inoperable chronic thromboembolic pulmonary hypertension (CTEPH), and patients with mean pulmonary artery pressure (mPAP) ≤30 mm Hg have an excellent survival [1, 2]. Common vascular lesion types are ring-like stenoses (type A), web lesions (type B), subtotal occlusions (type C), chronic total occlusions (CTO, type D) and tortuous lesions (type E). Occlusive lesions (i. e. subtotal occlusions and CTOs) are most challenging [3]. Risk and benefit of pulmonary occlusive lesion intervention in CTEPH has not been studied. We evaluated the impact of percutaneous pulmonary CTO intervention on BPA treatment response.

Methods: 120 patients underwent 712 BPA procedures between April 2014 and October 2019. Clinical features and hemodynamics were assessed at baseline and 6–12 months after the last BPA session (Fig. 1).

Results: A total of 2542 lesions were targeted; 720 occlusions (28.3 %; 352 CTOs and 368 subtotal occlusions) and 1822 non-occlusion lesions (71.7 %). Complications occurred in 6.0 % of all procedures (severe complications in 0.4 % of all procedures). 45 patients completed BPA treatment after a median of 6 (4;10) procedures per patient. In these patients, mPAP dropped from

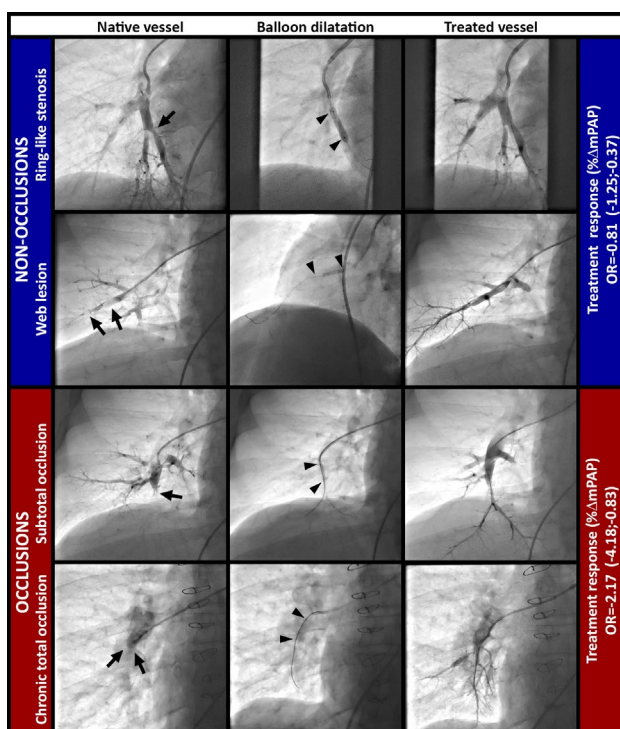


Fig. 1

Table 1 Clinical and hemodynamic data at baseline and follow-up of patients with „complete BPA“.

	n=45		
	Baseline	Follow-up	p-value
WHO FC	3 (3;3)	1 (1;2)	<0.001†
Nt-proBNP-pg/mL	579 (182;1385)	198 (70;429)	<0.001†
SaO ₂ -%	91.3 ± 4.2	93.3 ± 4.3	<0.001*
HR-beats/min	72.7 ± 11.5	65.6 ± 12.9	<0.001*
CO-L/min	5.2 ± 1.4	5.4 ± 3.1	0.541*
mRAP-mm Hg	6.8 ± 4.3	4.8 ± 2.9	0.010*
sPAP-mm Hg	65.6 ± 19.1	44.4 ± 11.8	<0.001*
dPAP-mm Hg	23.2 ± 8.4	14.9 ± 4.2	<0.001*
mPAP-mm Hg	38.8 ± 10.7	25.5 ± 5.2	<0.001*
mPAWP-mm Hg	9.7 ± 3.8	8.6 ± 3.5	0.161*
DPG-mm Hg	13.6 ± 9.0	6.3 ± 4.1	<0.001*
CPA-mL/mm Hg	2.1 ± 1.4	3.4 ± 3.1	0.004*
PVR-WU	6.2 ± 2.9	3.5 ± 1.7	<0.001*

p-values are results from paired samples t-test (*) and Wilcoxon signed rank test (†).
 BPA = balloon pulmonary angioplasty; CO = cardiac output; CPA = pulmonary arterial compliance; dPAP = diastolic pulmonary artery pressure; DPG = diastolic pulmonary vascular pressure gradient; HR = heart rate; mPAP = mean pulmonary artery pressure; mPAWP = mean pulmonary arterial wedge pressure; mRAP = mean right atrial pressure; Nt-proBNP = N-terminal pro-brain natriuretic peptide; PEA = pulmonary endarterectomy; PVR = pulmonary vascular resistance; S_aO₂ = arterial oxygen saturation; sPAP = systolic pulmonary artery pressure; WHO = World Health Organization; WU = Wood units.

40.1 ± 10.8 to 25.6 ± 5.1 mm Hg (*p* < 0.001), without significant change in cardiac output (5.2 ± 1.4 to 5.5 ± 3.1 L/min, *p* = 0.409). In the overall cohort, success rate for recanalization of occlusions was 81 % (subtotal occlusions (type C lesions): 98 %; CTOs (type D lesions) 50 %). Number of successfully treated lesions of any type (OR -0.86 [-1.19;-0.53]; *p* < 0.001), number of successfully treated occlusions (OR -2.17 [-3.38;-0.97]; *p* = 0.001) and number of successfully treated non-occlusion lesions (OR -0.81 [-1.25;-0.37]; *p* < 0.001) emerged as predictors of relative change in mPAP. The impact on relative change in mPAP was higher for CTOs (OR -5.88 [-10.49;-1.26]; *p* = 0.014) than for subtotal occlusions (OR -2.51 [-4.18;-0.83]; *p* = 0.004).

Conclusion: The number of successfully treated vascular lesions predicts treatment response to BPA, while the number of successfully recanalized occlusions (particularly CTOs) appears to have the strongest impact on change in mPAP (Table 1). Our data highlight the importance of advanced BPA technique.

Untergewicht als Mortalitätsrisiko bei Sepsis

P. Schwaiger¹, T. Danninger¹, R. Rezar², B. Mamandipoor³, D. Dankl¹, A. Koköfer¹, C. Jung⁴, V. Osmani³, B. Wernly¹

¹Universitätsklinik für Anästhesie, perioperative Medizin und allgemeine Intensivmedizin, Uniklinikum Salzburg, Salzburg, Österreich

²Universitätsklinik für Innere Medizin II, Kardiologie und Internistische Intensivmedizin, Salzburg, Österreich

³Fondazione Bruno Kessler Research Institute, Trentino, Italien

⁴Klinik für Kardiologie, Pneumologie und Angiologie, Universitätsklinikum Düsseldorf, Düsseldorf, Deutschland

Einleitung: Sowohl Übergewicht, als auch Untergewicht stellen Gesundheitssysteme weltweit vor erhebliche Herausforderungen. Verschiedene Studien an septischen PatientInnen konnten bereits einen Überlebensvorteil übergewichtiger Individuen mit Sepsis im Vergleich zu normal- oder untergewichtigen Personen zeigen. Diese Studie untersucht die Behandlungsstrategien und Überlebensraten von septischen PatientInnen aus der multizentrischen e-ICU-Datenbank in Relation zum Body Mass Index (BMI).

Methoden: Insgesamt wurden 16.612 Patienten aus der eICU Collaborative Research Database in die Analyse eingeschlossen. Demographische und klinische Basischarakteristika wurden erhoben. Als primärer Endpunkt wurde die Mortalität auf der Intensivstation definiert. Eine multinomiale logistische Regressionsanalyse wurde durchgeführt, um drei sequenzielle Regressionsmodelle zu schätzen. So wurde der Einfluss der drei BMI Kategorien (BMI <18,5 kg/m², BMI 25 bis 29 kg/m², BMI >29 kg/m²) auf das primäre Outcome untersucht. Anschließend wurden die Daten über 2 Modelle sowohl an Patientencharakteristika (Modell-2), als auch dieverwendeten Behandlungsstrategien (Modell-3) angepasst.

Resultate: Es konnten keine signifikanten Unterschiede hinsichtlich der verschiedenen Behandlungsstrategien zwischen den BMI-Untergruppen gezeigt werden. Untergewichtige PatientInnen wiesen eine erhöhte Mortalität auf. Dieser Unterschied blieb auch nach Anpassung mittels Modell-2 (aOR 1,54 95 %KI 1,15–2,06; $p=0,004$) und Modell-3 (aOR 1,57 95 %KI 1,16–2,12; $p=0,003$) signifikant. Zwischen normal- und übergewichtigen (BMI 25–30 kg/m²) PatientInnen zeigte sich kein Unterschied hinsichtlich der Mortalität, jedoch konnte eine höhere Überlebenswahrscheinlichkeit von adipösen (BMI >30 kg/m²) Individuen im Vergleich zu normalgewichtigen PatientInnen gezeigt werden (Modell-3: aOR 0,82 95 %KI 0,68–0,98; 0,03).

Schlussfolgerungen: Wir konnten in unserer Analyse von über 16.000 Individuen eine höhere Mortalität von untergewichtigen septischen PatientInnen zeigen. Adipöse PatientInnen hingegen wiesen eine niedrigere Sterblichkeit auf. Unsere Analyse unterstützt die These des „Adipositas-Paradoxon“.

COVID-19 & Herz

Copeptin refines the prognostic value of high-sensitive cardiac troponin i in hospitalized patients with COVID-19: a prospective single-center study

C. C. Kaufmann¹, A. Ahmed¹, M. Kassem¹, M. Freynhofer¹, B. Jäger¹, G. Aicher¹, S. Equiluz-Bruck¹, A. Spiel¹, G. Funk¹, M. Gschwantler¹, P. Fasching¹, J. Wojta², K. Huber¹

¹Wilhelminenspital, Wien, Austria

²Medizinische Universität Wien, Wien, Austria

Introduction: COVID-19 has been associated with a high prevalence of myocardial injury and increased cardiovascular morbidity. Copeptin, a marker of vasopressin release, has been previously established as a risk marker in both infectious and cardiovascular disease.

Methods: This prospective, observational study of patients with laboratory-confirmed COVID-19 infection was conducted from June 6th to November 26th, 2020 in a tertiary hospital. Copeptin and high-sensitive cardiac troponin I (hs-cTnI) levels on admission were collected and tested for their association with the primary endpoint of ICU admission or 28-day mortality.

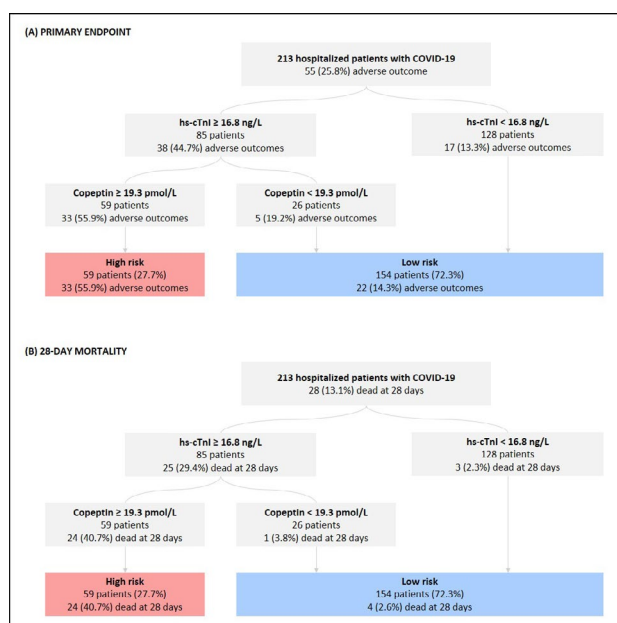


Fig. 1

Results: A total of 213 eligible patients with COVID-19 were included of whom 55 (25.8%) reached the primary endpoint. Median levels of copeptin and hs-cTnI at admission were significantly higher in patients with an adverse event (Copeptin 29.6 pmol/L, [IQR, 16.2–77.8] vs 17.2 pmol/L [IQR, 7.4–41.0] and hs-cTnI 22.8 ng/L [IQR, 11.5–97.5] vs 10.2 ng/L [5.5–23.1], $P < 0.001$). ROC analysis demonstrated an optimal cut-off of 19.6 pmol/L for copeptin and 16.2 ng/L for hs-cTnI and an increase of either biomarker was significantly associated with the primary endpoint. The combination of raised hs-cTnI and copeptin yielded a superior prognostic value to individual measurement of biomarkers and was a strong prognostic marker upon multivariable logistic regression analysis (OR 4.274 [95% CI, 1.995–9.154], $P < 0.001$). Addition of copeptin and hs-cTnI to established risk models improved C-statistics and net reclassification indices (Fig. 1).

Conclusion: The combination of raised copeptin and hs-cTnI upon admission is an independent predictor of adverse events in hospitalized patients with COVID-19.

Hypertrophic hearts are more susceptible for myocardial SARS-CoV-2 infection

F. Nägele¹, M. Graber¹, J. Hirsch¹, L. Pölzl¹, A. K. Stadler Cramm², M. Grimm¹, T. Alexander², I. Tancevski³, J. Holfeld¹, C. Gollmann-Tepeköylü¹

¹Universitätsklinik für Herzchirurgie, Medizinische Universität Innsbruck, Innsbruck, Austria

²Institute of Medical Genetics and Pathology, Basel, Switzerland

³Universitätsklinik für Innere Medizin II, Medizinische Universität Innsbruck, Innsbruck, Austria

Introduction: The coronavirus disease 19 (COVID-19) crisis caused by SARS-CoV-2 infections is a rapidly emerging global threat to healthcare systems. To date, cardiac involvements in SARS-CoV-2 infections have been identified with unclear clinical significance. Patients with pre-existing cardiomyopathies are hypothesized to be prone to myocardial infections due to a disease-related upregulation of its putative receptor Angio-

tensin-converting enzyme 2 (ACE2). In this study, we aimed to verify correlations between myocardial SARS-CoV-2 infections and structural heart disease.

Methods: Cardiac tissue of 23 autopsy cases with lethal COVID-19 course was obtained. Myocardial presence of SARS-CoV-2 was assessed via PCR. Cardiac expression levels of ACE2 were determined in immunofluorescence staining. Cardiac weight was assessed and cardiomyocyte hypertrophy was evaluated in Hematoxylin/Eosin (H/E) staining. Expression levels of atrial natriuretic peptide (ANP) and brain natriuretic peptide (BNP) as indicators of increased myocardial stretch and volume overload were measured with qPCR. Clinical data were collected and cardiac hypertrophy was assessed via echocardiography in a cohort of 150 patients tested positive for SARS-CoV-2.

Results: SARS-CoV-2 viral load could be detected in 15 hearts (65 %) of 23 autopsy cases. Myocardial SARS-CoV-2 infection clearly correlated with shorter survival. Cardiac ACE2 expression was significantly downregulated in hearts with myocardial SARS-CoV-2 viral load. Cardiac tissue positive for SARS-CoV-2 showed increased expression levels of ANP and BNP as well as increased myocardial hypertrophy in H/E staining. Analysis of echocardiographies in a cohort of 150 patients tested positive for SARS-CoV-2 revealed a correlation of cardiac hypertrophy with a prolonged hospital stay.

Conclusion: Myocardial SARS-CoV-2 infections are more frequent in patients with hypertrophic hearts. Although SARS-CoV-2 typically does not induce fulminant myocarditis, our data shows a clear association of myocardial infections with a more severe clinical course of COVID-19. Myocardial SARS-CoV-2 infections were more likely in patients with signs of increased volume load and patients with pre-existing cardiac hypertrophy showed increased hospitalization rate as well as prolonged hospital stay. Thus, cardiac hypertrophy may be considered as a distinct risk factor for a severe clinical course in SARS-CoV-2 infections.

Seroprevalence of SARS-CoV-2 antibodies in healthcare workers and an unselected all comer patient population

M. Riesenhuber¹, C. Nitsche¹, C. J. Binder², E. S. Schernhammer³, T. Stamm⁴, E. Anwar¹, V. Geyik¹, A. Gruber¹, F. Hamidi¹, J. Heger¹, P. Hemetsberger¹, F. Jakse¹, C. Kohns¹, H. Haslacher², T. Perkmann², C. Hengstenberg¹, T. A. Zelniker¹

¹Medizinische Universität Wien, Universitätsklinik für Innere Medizin II, Klinische Abteilung für Kardiologie, Wien, Austria

²Medizinische Universität Wien, Klinisches Institut für Labormedizin, Wien, Austria

³Medizinische Universität Wien, Zentrum für Public Health, Abteilung für Epidemiologie, Wien, Austria

⁴Medizinische Universität Wien, Zentrum für Medizinische Statistik, Informatik und Intelligente Systeme, Institut für Outcomes Research, Wien, Austria

Introduction: Healthcare workers and patients are at high risk of COVID-19. SARS-CoV-2-specific antibodies are usually detectable 10 to 14 days after exposure to SARS CoV 2. Serological antibody tests, therefore, can identify individuals who have been exposed to SARS-CoV-2 and who have developed immunity. Knowledge of the antibody status can help estimate the rate of asymptomatic infections and guide personal protection precautions and restriction policies. This study aimed to estimate the seroprevalence and seroconversion rate of SARS CoV 2

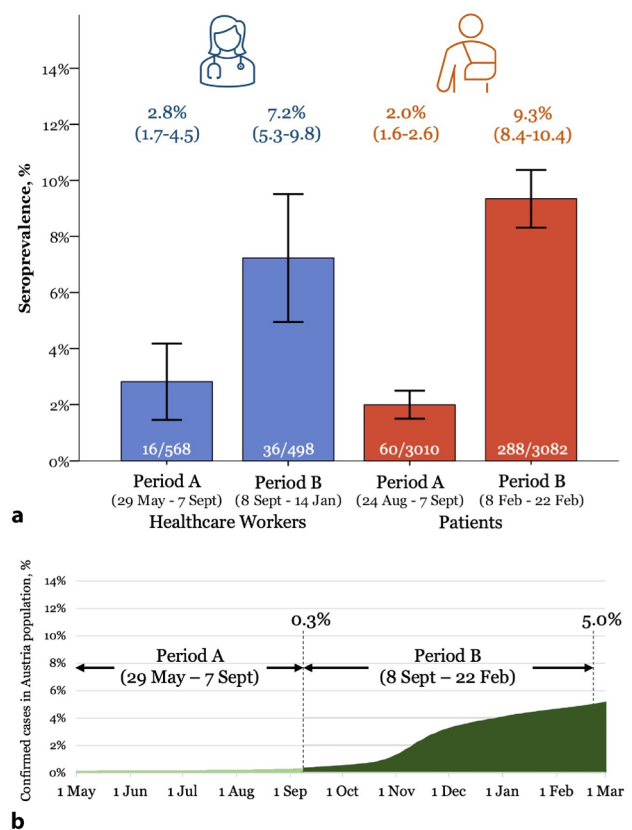


Fig. 1 Panel a: Seroprevalence of SARS-CoV-2 in healthcare workers (blue) and an unselected patient population (red) during the first and second waves of SARS-CoV-2 in Austria. Panel b: Proportion of confirmed SARS-CoV-2 cases in the Austrian population (Source: AGES)

in healthcare workers and an unselected patient population at a tertiary academic center.

Methods: The present prospective study (ClinicalTrials.gov NCT04407429) had two parts: First, we collected serial blood samples from healthcare workers at baseline and at 1, 2, 3, 6, and 12 months. Secondly, we consecutively measured SARS-CoV-2 antibodies from leftover diagnostic serum samples in a total of 6,092 patients at 2 time points ($n=3,010$: August 24–September 7, 2020; $n=3,082$: February 8–22, 2021). Electronic health records were used to collect patients' demographics, medical history, and available laboratory measurements. Antibodies against the SARS-CoV-2 nucleocapsid antigen were measured using a sandwich electrochemiluminescence assay (Elecsys, Roche Diagnostics). We estimated the seroprevalence and 95 % confidence intervals (CI) according to the Wilson's score method during the first and second waves of SARS-CoV-2 in Austria (Period A: May 29, 2020 until September 7, 2020; Period B: September 8, 2020 until February 22, 2021). Moreover, to select the most informative variables and overcome the limitations of stepwise regression procedures, we performed a least absolute shrinkage and selection operator (LASSO) logistic regression in a model that incorporated age, sex, diabetes, heart failure, peripheral artery disease, acute and chronic coronary syndrome, atrial fibrillation, pneumonia, chronic obstructive pulmonary disease, liver disease, cancer, and smoking in combination with 10-fold cross-validation.

Results: Between May 29 and September 7, 2020 (Period A), 16 of 568 healthcare workers had detectable antibodies against SARS-CoV-2. This resulted in a seroprevalence of 2.8 % (95 %

CI 1.7 % to 4.5 %; Fig. 1), which was similar to that of an unselected patient population enrolled in September 2020 (60/3010 patients: 2.0 %, 95 % CI 1.6 % to 2.6 %). In the subsequent period (September 8, 2020 until February 22, 2021), we measured antibodies against SARS-CoV-2 in 36 of 498 healthcare workers, resulting in a seroprevalence of 7.2 % (95 % CI 5.3 % to 9.8 %). Compared with healthcare workers, the seroprevalence was numerically but not statistically higher amongst patients enrolled in February 2021, where 288 of the 3,082 patients had detectable antibodies against SARS-CoV-2, yielding a seroprevalence of 9.3 % (95 % CI 8.4 % to 10.4 %). The proportions of healthcare workers and patients with antibodies were significantly higher than the proportion of confirmed cases in Austria's general population at both time points (all $P < 0.01$). Among healthcare workers who developed antibodies, 4 (11 %) were asymptomatic, and 13 (34 %) were not aware of previous exposure to SARS-CoV-2. Of note, 2 healthcare workers with confirmed PCR testing (1 asymptomatic) lost their antibody status after 1 and 2 months, respectively. With LASSO regression, the strongest association for the presence of SARS-CoV-2 antibodies in an all-comer patient population was obtained for a history of acute coronary syndrome (odds ratio 2.13).

Conclusion: Healthcare workers and patients had a higher infestation rate than the general population. The seroprevalence of SARS-CoV-2 antibodies was numerically higher among an unselected patient population than among healthcare workers. These results indicate that measures for the protection of healthcare workers are essential to mitigate the risk of SARS-CoV-2 exposure through patient contact. In this study, a history of an acute coronary syndrome had the strongest association with SARS-CoV-2 antibodies in an all-comer patient population, warranting attention to possible COVID-19 related long-term sequelae in this vulnerable patient population. Funding: Austrian Science Funds (FWF KLI-876)

AKUTES KORONARSYNDROM

1.1

Association of plasma Interleukin-6 with infarct size, reperfusion injury and adverse remodeling after ST-elevation myocardial infarction

C. Tiller¹, M. Reindl¹, M. Holzknacht¹, I. Lechner¹, J. Schwaiger², C. Brenner¹, A. Mayr³, G. Klug¹, A. Bauer¹, B. Metzler¹, S. Reinstadler¹

¹Innere Medizin III, Kardiologie & Angiologie, Innsbruck, Austria

²Innere Medizin, Kardiologie, Hall in Tirol, Austria

³Radiologie Innsbruck, Innsbruck, Austria

Introduction: Little is known about the clinical relevance of interleukin (IL)-6 in patients with acute ST-elevation myocardial infarction (STEMI). This study examined the possible associations of plasma IL-6 concentrations with infarct size (IS), reperfusion injury and adverse left ventricular remodeling (LVR), in STEMI patients treated with primary percutaneous coronary intervention (PCI).

Methods: We prospectively included 170 consecutive STEMI patients (median age 57 years, 14 % women) treated with primary PCI between 2017-2019. Blood samples for biomarker analyses including IL-6 were collected at day 2. Left ventricular ejection fraction (LVEF), IS, and reperfusion injury (microvascular obstruction [MVO] and intramyocardial haem-

orrhage [IMH]) were determined using cardiac magnetic resonance imaging at day 4 (interquartile range [IQR]:3-6). LVR was defined as ≥ 10 % increase in left ventricular end-diastolic volume from baseline to 4 months CMR follow-up.

Results: Patients with IL-6 concentrations \geq median (17 ng/l) showed a significantly lower LVEF (43 % vs. 52 %, $p < 0.001$), larger IS (22 % vs. 13 %, $p < 0.001$), larger MVO (1.9 % vs. 0.0 %, $p < 0.001$), and more frequent IMH (52 % vs. 18 %, $p < 0.001$). LVR was more common in patients with IL-6 \geq median (24 % vs. 9 %, $p = 0.005$). In both linear and binary multivariable regression analysis, IL-6 remained independently associated with lower LVEF (odds ratio [OR]: 0.10, 95 % confidence interval [CI] 0.02-0.42, $p = 0.002$), larger IS (OR: 5.29, 95 % CI 1.52-18.40, $p = 0.009$), larger MVO (OR: 5.20, 95 % CI 1.30-20.85, $p = 0.020$), with presence of IMH (OR: 3.73, 95 % CI 1.27-10.99, $p = 0.017$) and adverse LVR (OR: 2.72, 95 % CI 1.06 to 6.98, $p = 0.038$). Patients with IL-6 concentrations ≥ 17 ng/l were more likely to experience major adverse cardiac events ($p = 0.028$) during a median follow-up of 12 (IQR: 5-14) months.

Conclusion: High concentrations of circulating plasma IL-6 at day 2 after primary PCI for STEMI were independently associated with worse myocardial function, larger infarct extent, more severe reperfusion injury and a higher likelihood for LVR, suggesting IL-6 as a useful biomarker of more serious outcome and potential therapeutic target.

1.2

Angiotensin-converting enzyme inhibitors and angiotensin receptor blockers in acute coronary syndrome: implications for platelet reactivity?

M. Tscharre¹, P. Wadowski², C. Weikert², J. Pultar², B. Eichelberger³, S. Panzer³, T. Gremmel²

¹Wiener Neustadt, Department of Internal Medicine, Cardiology and Nephrology, Wr. Neustadt, Austria

²Medical University Vienna, Department of Internal Medicine II, Wien, Austria

³Medical University Vienna, Department of Blood Group Serology and Transfusion Medicine, Wien, Austria

Introduction: In patients with acute coronary syndrome (ACS) angiotensin-converting enzyme (ACE) inhibitors are preferred over angiotensin-receptor blockers (ARBs). However, in a recent pilot-study treatment with ACE inhibitors was associated with increased platelet reactivity compared to ARBs. Therefore, we sought to investigate the impact of renin-angiotensin-aldosterone system (RAAS) blockade with ACE inhibitors and ARBs on platelet aggregation in patients with ACS undergoing percutaneous coronary intervention.

Methods: On-treatment residual platelet reactivity in response to arachidonic acid (AA), adenosine diphosphate (ADP), SFLLRN, AYPGKF and collagen was assessed by multiple electrode aggregometry (MEA) in 197 ACS patients on dual antiplatelet therapy (DAPT) with aspirin and either prasugrel or ticagrelor.

Results: One-hundred-sixty-five (83.7 %) patients were treated with ACE inhibitors, 32 (16.3 %) with ARBs. On-treatment residual AA- and ADP-inducible platelet reactivity was significantly higher in patients with ACE inhibitors (both $p < 0.05$; Fig. 1). Likewise, SFLLRN was significantly higher in patients with ACE inhibitors ($p = 0.036$) and there was a trend for higher AYPGKF- and collagen-inducible platelet reactivity ($p = 0.053$ and $p = 0.082$). The incidence of high on-treatment residual

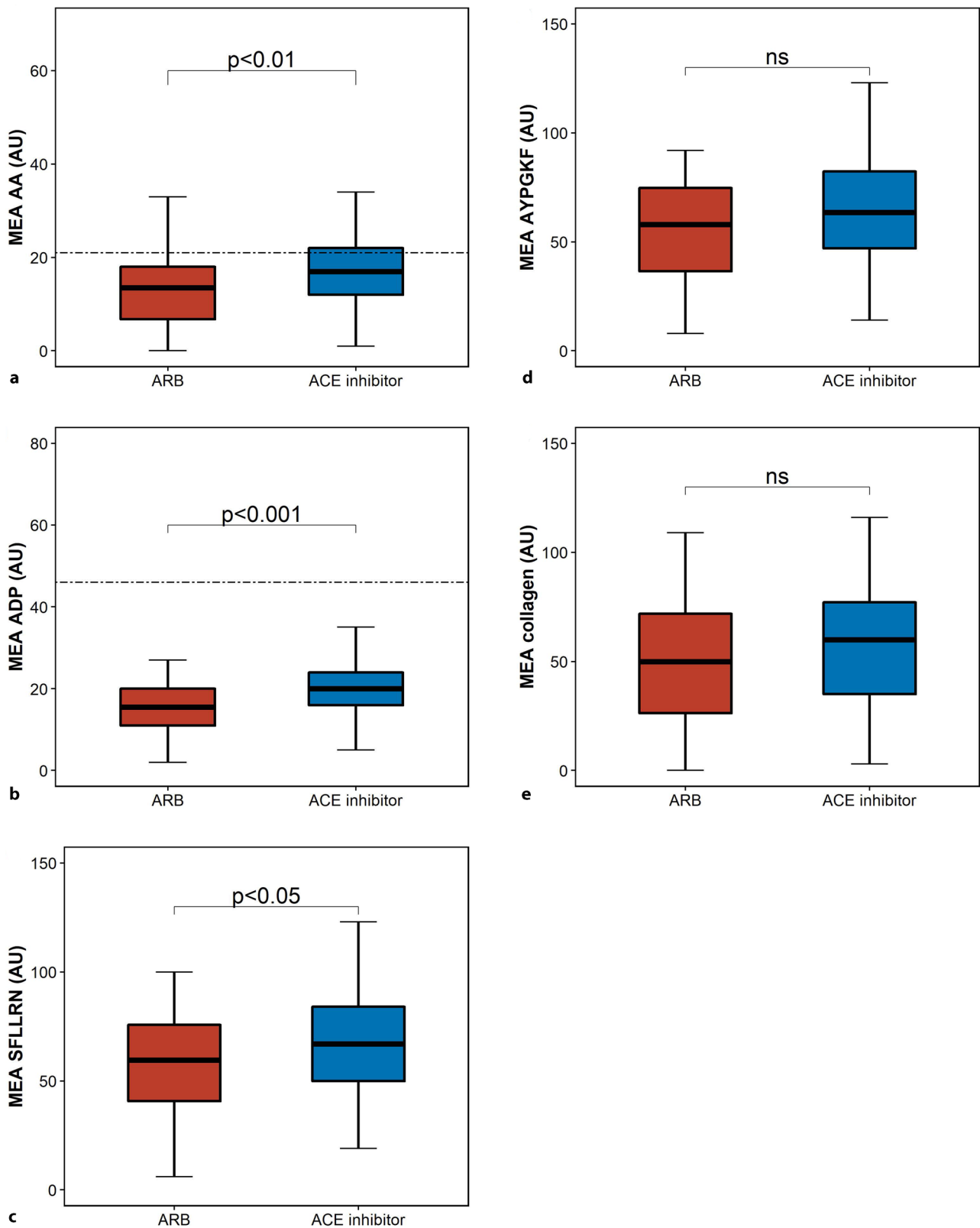


Fig. 111.2 Aggregation units (AU) by multiple electrode aggregometry (MEA) in response to AA (panel a), ADP (panel b), SFLLRN (panel c), AYPGKF (panel d) and collagen (panel e) stratified for patients with angiotensin-converting enzyme (ACE) inhibitors and angiotensin-receptor blockers (ARBs). Cut-off values for high on-treatment residual platelet reactivity are indicated by the dashed lines. The boundaries of the box show the lower and upper quartile of data, and the line inside the box represents the median. Whiskers are drawn from the edge of the box to the highest and lowest values that are outside the box but within 1.5 times the box length

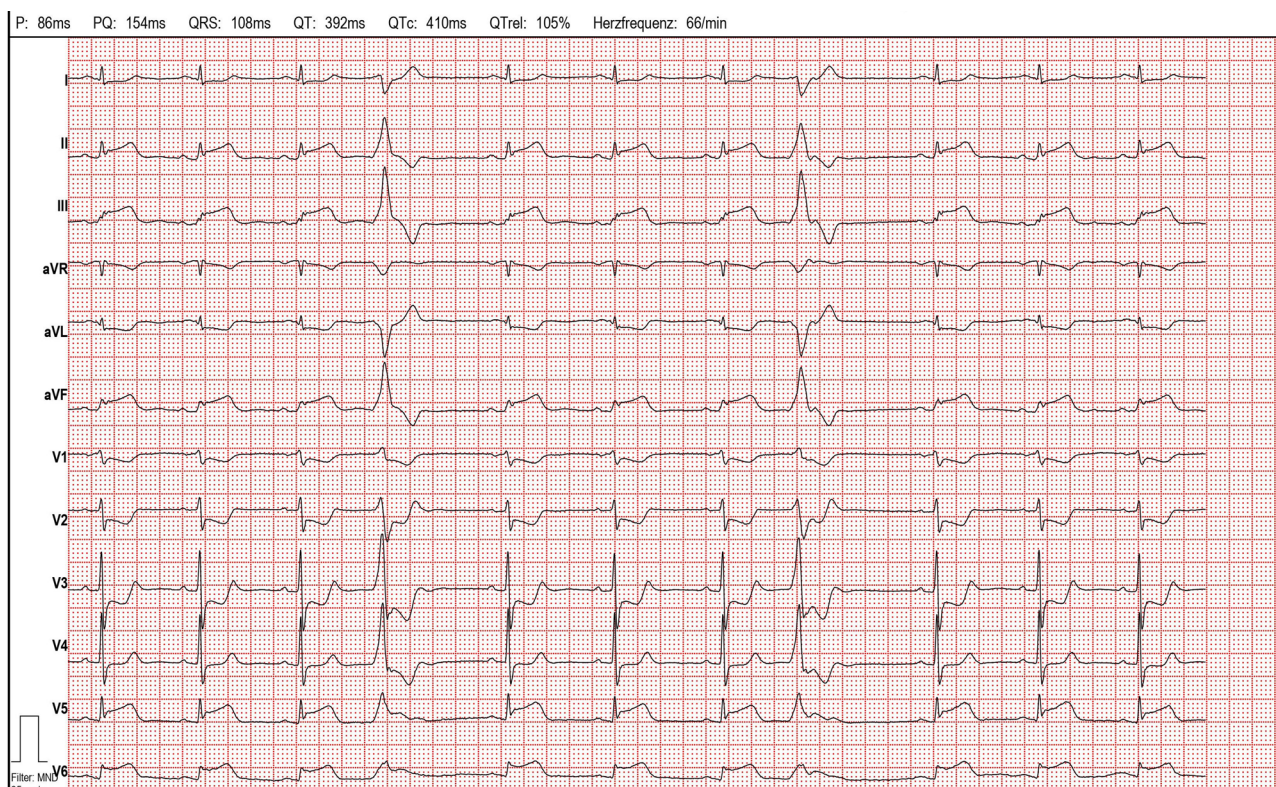


Fig. 111.3

platelet reactivity AA was significantly higher in patients with ACE inhibitors (52 [31.5 %] vs. 3 [9.4 %] patients; $p=0.019$).

Conclusion: ACE inhibitors are associated with increased on-treatment residual platelet reactivity in ACS patients with potent DAPT. Further clinical trials are needed to elucidate the role of RAAS blockade with ACE inhibitors and ARBs in ACS patients treated according to current standards.

1.3

Posterolateral STEMI in patient with coronary artery anomaly

N. Kohls¹, D. Spiel¹, K. Huber¹, M. Edwards-Nikfardjam¹

¹Klinik Ottakring, Vienna, Austria

Background: Anomalous origin of the left coronary artery from the right sinus of Valsalva (left-ACAOS) is one of the rarest coronary artery anomalies (CAA) with a reported prevalence of 0.02–0.05 %. Based on the anatomical relationship of the anomalous artery to the aorta and pulmonary artery, the traditional classification differentiates between a malignant variant with an inter-arterial course, which carries a risk of sudden cardiac death (SCD) in young athletes, and low-risk courses such as retro-aortic, pre-pulmonary or transseptal. We describe a case of a patient with a benign variant, presenting with symptoms reflecting an acute coronary syndrome (ACS).

Case Report: An 80-year-old male patient with no history of coronary artery disease (CAD) presented with persistent chest pain and increased sweating. The initial electrocardiogram showed ST-segment elevation in leads II, III, aVF and V5-V6 and concomitant ST-segment depression in leads V1-V3, indica-

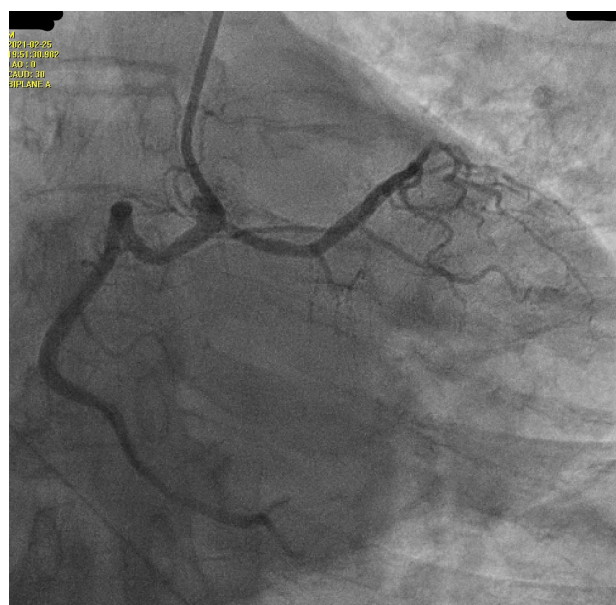


Fig. 211.3

tive for inferior wall ST-elevation myocardial infarction (Fig. 1). Cardiac troponin was above 125.000 ng/L at admission. Acute coronary angiography (CAG) revealed unexpectedly an anatomic anomaly of the coronary artery system: A single coronary artery originated from one main stem ostium that arose from the right coronary sinus. A large-sized right coronary artery (RCA) coursed regularly, but also supplied the inferior parts of the left ventricle and reached until far toward the anterior wall (Fig. 2). In the periphery of the RCA, we found an occlusion of the posterolateral artery (PLA) as well as a high-grade posterior

descending artery (PDA) stenosis. Both lesions were successfully treated by angioplasty with stent implantation (Synergy 2.5 × 16 mm and Supraflex 2.25 × 20 mm). The left coronary artery (LCA) arose from the proximal RCA and gave rise to a hypoplastic left anterior descending artery (LAD). The circumflex artery (CX) was small and without significant stenosis. For further clarification of the coronary anatomy, we performed a coronary CT which confirmed the complex CAA with a retro-aortic course of the singular coronary artery without involvement of the aortic root.

Discussion: Usually, benign variants of left-ACAOS are only found by coincidence on CAG as observed in this case. The cause of the detected peripheral lesions is unlikely due to the described CAA although there exists in principle the possibility that the change of hemodynamics in anomalous coronary arteries might affect the development of CAD or myocardial infarction.

Conclusion: This case underlines the importance of coronary CT as an imaging tool for the detection of rare coronary anomalies which can help to define the type of left-ACAOS.

1.4

Ein pflegegeleitetes Sekundärpräventionsprogramm bei Menschen nach einem akuten Koronarsymptom aus der Perspektive von Gesundheitsexpertinnen und -experten in Österreich – eine qualitative Studie

H. Qin¹, D. Bonderman², S. Brunner³, T. Großbichler⁴, H. Mayer⁵

¹Klinische Abteilung für Kardiologie, Universitätsklinik für Innere Medizin II, Medizinische Universität Wien, Wien, Österreich

²Klinik Favoriten, Wiener Gesundheitsverbund, Wien, Österreich

³Stadt Zürich Stadtspital Waid, Zürich, Schweiz

⁴FH-Campus Favoriten, Wiener Gesundheitsverbund, Wien, Österreich

⁵Institut für Pflegewissenschaft, Universität Wien, Wien, Österreich

Einleitung: Menschen nach akutem Koronarsyndrom haben weiterhin ein hohes kardiovaskuläres Risiko. Dennoch belegen Studien, dass deren Adhärenz zu der empfohlenen Lebensstilmodifikation noch mangelhafte ist. Daher ist es erforder-

Tab. 111.4 Soziodemografische Daten der Gesundheitsexpertinnen und -experten

Interview Nr	Alter	Sex	Beruf	Berufsjahr	Setting
E11	45J	m	Kardiologe	20J	Ambulantes Rehabilitationszentrum
E12	70J	m	Allgemeinmediziner	40J	Primärversorgung
E13	54J	m	Internist	32J	Primärversorgung
E14	55J	w	Kardiologin	29J	Primärversorgung
E15	58J	m	Internist	18J	Akutkrankenhaus
E16	60J	m	Soziologe	35J	Akutkrankenhaus
E17	53J	w	Kardiologin	29J	Akutkrankenhaus
E18	56J	m	Kardiologe	30J	Akutkrankenhaus
E19	46J	m	Kardiologe	16J	Akutkrankenhaus
E110	43J	w	Kardiologin	14J	Akutkrankenhaus
E111	54J	w	DGKP	32J	Akutkrankenhaus
E112	48J	w	DGKP	30J	Stationäres Rehabilitationszentrum
E113	53J	w	Kardiologin	18J	Akutkrankenhaus
FD1	58J	m	DGKP	39J	Akutkrankenhaus
	54J	m	DGKP	20J	
	50J	m	DKGP	19J	
	35J	m	DGKP	12J	
	52J	w	DGKP	31J	
	47J	w	DGKP	26J	
	43J	w	DGKP	22J	
FD2	38J	m	Allgemeinmediziner	9J	Stationäres Rehabilitationszentrum
	54J	w	Kardiologin	30J	
	53J	w	Diätologin	33J	
	45J	w	DGKP	25J	
	37J	w	Physiotherapeutin	14J	
	29J	w	Psychologin	2J	
	49J	w	DGKP	24J	

DGKP = Diplomierter Gesundheits- und Krankenpflegerin/Diplomierter Gesundheits- und Krankenpfleger; El = Einzelinterview; FD = Fokusgruppe-Diskussion; J = Jahr

Tab. 211.4 Haupt- und Unterthemen

Hauptthemen	Unterthemen
Kontinuierliche Begleitung für Mensch nach akutem Koronarsyndrom	Notwendigkeit der Errichtung einer Anlaufstelle Einen personenzentrierten Ansatz verfolgen
Kardiale Rehabilitation Nurse (KR-Nurse)	Speziell ausgebildetes Pflegepersonal als KR-Nurse Kommunikation als eine erforderliche Kompetenz Als Koordinatorin/Koordinator in der interdisziplinären Zusammenarbeit
Erforderliche Prioritätensetzung für die Patientenedukation im Akutkrankenhaus	
Erhöhte Bereitschaft zur Krankheitsbewältigung	Verbessertes Krankheitsverständnis Angstreduktion

derlich, eine pflegerische Intervention dafür zu entwickeln. Dabei soll die Perspektive aller in der Versorgung beteiligten Personengruppen miteinbezogen werden, vor allem die Sicht der Gesundheitsexpertinnen und -experten. Ziel der Studie war es, Empfehlungen aus dem Expertenwissen der unterschiedlichen Gesundheitsberufe für ein zu entwickelndes pflegegeleitetes nichtmedikamentöses Sekundärpräventionsprogramm für Menschen nach einem akutem Koronarsyndrom abzuleiten. Die folgende Forschungsfrage wurde in dieser Arbeit beantwortet: Was könnte ein pflegegeleitetes Sekundärpräventionsprogramm für Menschen nach einem akutem Koronarsyndrom vom Akutkrankenhaus zur Primärversorgung in Österreich aus Sicht der Gesundheitsexpertinnen und -experten umfassen?

Methoden: Es fanden zwei Fokusgruppen-Diskussionen und 13 Einzelinterviews mit 27 Gesundheitsexpertinnen und -experten aus den Akutkrankenhäusern, stationären oder ambulanten Rehabilitationszentren und Arztpraxen der Primärversorgung für Allgemeinmedizin oder Kardiologie statt. Die Datenanalyse der Interviews erfolgte anhand der thematischen Analyse nach Braun and Clarke (2006). Die zuständige Ethikkommission stimmte der Untersuchung zu (EK Nr. 1811/2018).

Resultate: Von November 2018 bis Oktober 2019 nahmen 27 Gesundheitsexpertinnen und -Experten davon 15 Frauen und 12 Männern im Alter von 29 bis 70 Jahren an der Studie teil. Die Gesundheitsexpertinnen und -Experten kamen aus drei Akutkrankenhäusern, drei Rehabilitationszentren und Arztpraxen der Primärversorgung. Die durchschnittliche Berufserfahrung der Teilnehmenden betrug 24,0 Jahre. Aus der Datenanalyse ergaben sich folgende vier Hauptthemen: Kontinuierliche Begleitung für Menschen nach akutem Koronarsyndrom, kardiale Rehabilitation Nurse, erforderliche Prioritätensetzung für die Patientenedukation im Akutkrankenhaus und erhöhte Bereitschaft zur Krankheitsbewältigung. Die Ergebnisse zeigen, dass Menschen nach akutem Koronarsyndrom ein pflegegeleitetes Sekundärpräventionsprogramm benötigen und dafür eine Anlaufstelle eingerichtet werden soll. Das speziell, ausgebildete Pflegepersonal ist dafür geeignet, dieses Programm anzubieten. Die Gesundheitsexpertinnen und -experten empfehlen einen personenzentrierten Ansatz, was zu einer erhöhten Bereitschaft zur Krankheitsbewältigung führen kann. Sowohl die Prioritätensetzung für die Patientenedukation im Akutkrankenhaus als auch eine verstärkte sektorenübergreifende Vernetzung sind die Voraussetzungen für die Ausführung dieses Programms. Zudem soll das speziell, ausgebildete Pflegepersonal neben dem kardiologischen Fachwissen über ausgeprägte Kommunikations- und Sozialkompetenz verfügen.

Schlussfolgerungen: Diese Studie liefert einen ersten Einblick über das zu entwickelnde pflegegeleitete Sekundärpräventionsprogramm und weist auf einer personenzentrierten Praxis hin, welche auf die Bedürfnisse der Patientinnen und Patienten nach akutem Koronarsyndrom abzielt und von speziell ausgebildetem Pflegepersonal wie z. B. Nurse Practitioner als zentrale Ansprechperson geleitet wird. Das darauf aufgebautes

Sekundärpräventionsprogramm kann die Selbstmanagementfähigkeit und die Krankheitsbewältigung der Patientinnen und Patienten fördern, indem die Patientinnen und Patienten bei der Lebensführung kontinuierlich begleitet werden.

1.5

The age-specific prognostic impact of platelet-to-lymphocyte ratio on long-term outcome after acute coronary syndrome

N. Kazem¹, F. Hofer¹, L. Koller¹, A. Hammer¹, T. Hofbauer¹, C. Hengstenberg¹, A. Niessner¹, P. Sulzgruber¹

¹Division of Cardiology, Department of Internal Medicine II, Medical University of Vienna, Wien, Austria

Background: Personalized risk stratification after acute coronary syndrome (ACS) within the ageing society including easily applicable age-specific strategies for the prediction of fatal adverse events remain scarce, but of utmost importance. Platelet activity and inflammation play a key role during ACS. Therefore, we aimed to evaluate the age-specific prognostic potential of the platelet to lymphocyte ratio (PLR) on long-term cardiovascular mortality after ACS.

Methods: Patients presenting with ACS admitted to the Vienna General Hospital between December 1996 and January 2010 were recruited within a clinical registry including assessment of peripheral blood samples. The impact of the PLR on survival was assessed by Cox-regression hazard analysis.

Results: We included a total of 681 patients with a median age of 64 years (IQR:45–84). 200 (29.4 %) individuals died during the median follow-up time of 8.5 years. A strong and independent association of the PLR with cardiovascular mortality was found in the total study population (adjusted [adj.] hazard ratio [HR] per one standard deviation [1-SD] of 1.52 [95 %CI:1.18–1.96; $p < 0.001$]). After stratification in individuals <65 years ($n = 339$) and ≥ 65 years ($n = 342$), a prognostic effect of the PLR on cardiovascular mortality was solely observed in elderly patients ≥ 65 years (adj. HR per 1-SD of 1.32 [95 %CI: 1.01–1.74]; $p = 0.045$), but not in their younger counterparts <65 years (adj. HR per 1-SD of 1.08 [95 %CI: 0.60–1.93]; $p = 0.804$).

Conclusion: The present investigation highlights a strong and independent age-specific association of the PLR with cardiovascular mortality in patients with ACS. The PLR allows to identify only elderly patients at high risk for fatal events after ACS—even from a long-term perspective.

1.6

Trimethylamine N-oxide (TMAO) as a potential biomarker of individual severe stress perception in posttraumatic stress disorder (PTSD)-vulnerable patients after acute myocardial infarction

D. von Lewinski¹, D. Enko², H. Rothenhäusler³, O. Amouzadeh-Ghadikolai⁴, H. H. Arpf⁵, L. Harpf⁵, H. Traninger⁵, B. Obermayer-Pietsch⁶, M. Schweinzer³, C. K. Braun³, A. Meinitzer², A. Baranyi³

¹Division of Cardiology, Department of Internal Medicine, Medical University of Graz, Graz, Austria

²Clinical Institute of Medical and Chemical Laboratory Diagnostics, Medical University of Graz, Graz, Austria

³Department of Psychiatry and Psychotherapeutic Medicine, Medical University of Graz, Graz, Austria

⁴Department of Psychiatry and Psychotherapy I, State Hospital Graz II, Graz, Austria

⁵ZARG Zentrum für ambulante Rehabilitation GmbH, Graz, Austria

⁶Division of Endocrinology and Diabetology, Department of Internal Medicine, Medical University of Graz, Graz, Austria

Background: Acute myocardial infarction is not only a somatic disease but potentially triggers psychological effects, too. Post-traumatic stress disorder (PTSD) is a common stress-related disorder. It is characterized by numerous symptoms, such as flashbacks, intrusions, nightmares and severe anxiety, as well as uncontrollable, intense and disturbing thoughts and feelings related to the traumatic experience. However, with regard to the development of PTSD, individual stress perception might be crucial since not every serious traumatic experience leads to PTSD. To date, almost no biological correlates of an individual's perception of stress have been identified as being associated with the long-term development of PTSD. Objective: The aim of the study was to determine whether blood levels of TMAO vary immediately after AMI (1) in patients with or without depression, and (2) in patients with AMI induced PTSD symptomatology (subsyndromal PTSD and full PTSD). Furthermore, we investigated whether

TMAO is a potential biomarker that might be useful in the prediction of PTSD symptomatology in the long term.

Methods: A total of 114 AMI patients were assessed with standardized clinical psychiatric interviews based on the Hamilton Depression Scale (HAMD-17) after admission to the hospital and 6 months later. In addition, the CAPS-5 was used to explore PTSD symptoms (subsyndromal PTSD and full PTSD) 6 months after AMI. To assess patients' TMAO status, serum samples were collected at hospitalization and 6 months after AMI.

Results: Study participants with post-myocardial infarction PTSD symptomatology (subsyndromal PTSD and full PTSD) had significantly higher TMAO levels immediately after AMI than patients without PTSD symptoms (ANCOVA: TMAO (PTSD x time), $F=4.544$, $df=1$, $p=0.035$). In contrast, depressive symptomatology 6 months after AMI had no influence on TMAO levels (TMAO (depression x time), $F=0.083$, $df=1$, $p=0.774$). With the inclusion of additional clinical predictors in a hierarchical logistic regression model, TMAO becomes a significant predictor of PTSD symptomatology.

Conclusion: An elevated TMAO level immediately after AMI might reflect severe stress in PTSD-vulnerable patients, which might also lead to a short-term increased gut permeability to trimethylamine (TMA), the precursor of TMAO. Thus, elevated TMAO might be a biological correlate for stress that is associated with vulnerability to PTSD and might help to identify patients at increased risk.

1.7

Transiente ST Hebung nach lokaler Suprareninapplikation im Zuge einer Bronchoskopie

A. Fellner¹, S. Rechberger¹, C. Reiter¹, B. Strasser², T. Lambert¹, D. Hrnčić¹, A. Nahler¹, C. Steinwender¹

¹Kepleruniklinikum Linz, Abteilung für Kardiologie und internistische Intensivmedizin, Linz, Österreich

²Kepler Universitätsklinikum Linz, Institut für medizinische und chemische Labordiagnostik, Linz, Österreich

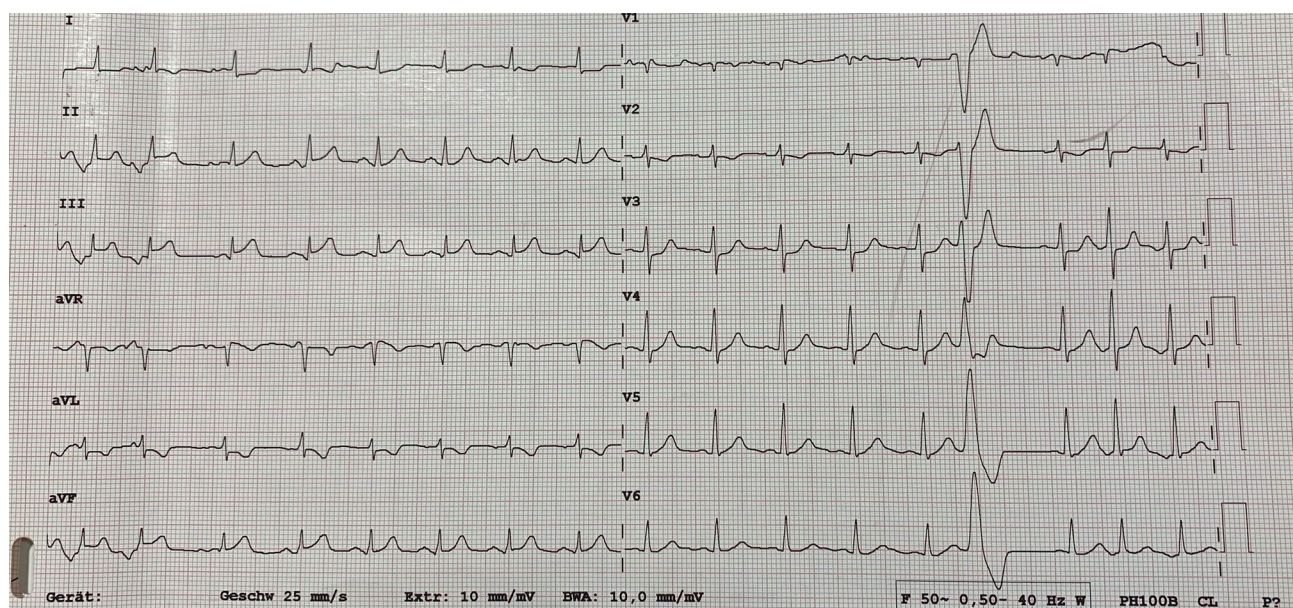


Abb. 111.7

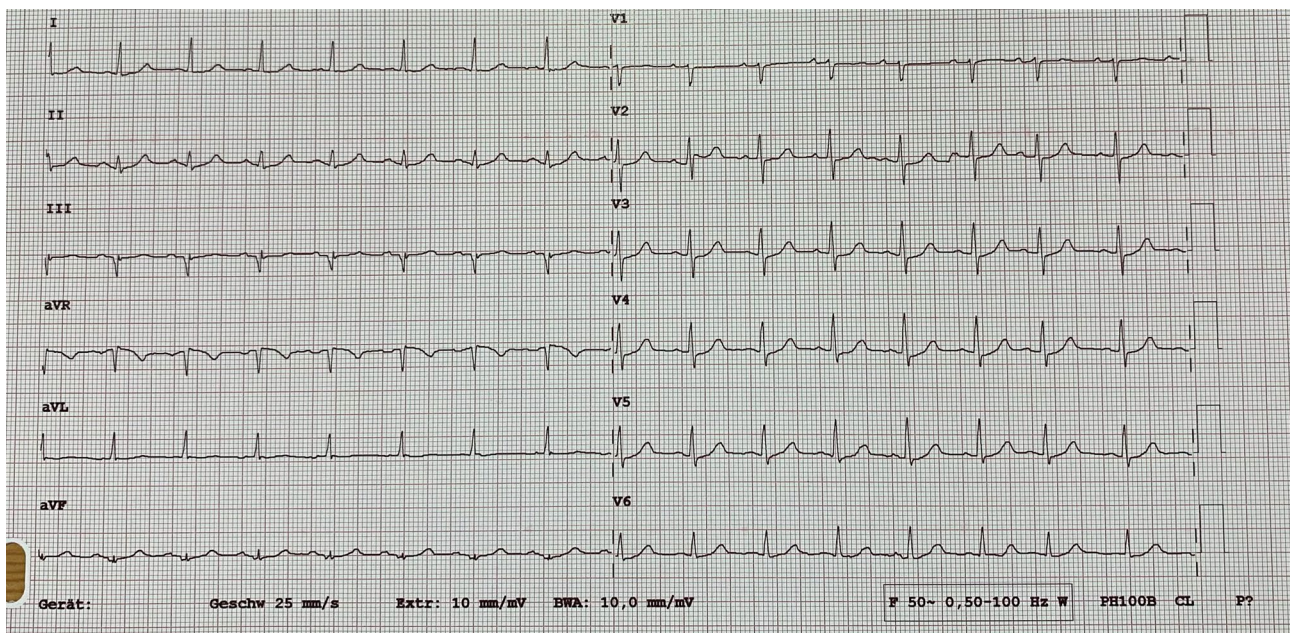


Abb. 211.7

Einleitung: Bei einem 63-jährigen Patienten wurde aufgrund einer CT gesicherten pulmonalen Raumforderung zur weiteren Abklärung eine Bronchoskopie durchgeführt. Nach endoskopischer Probenexzision kam es zu einer Blutung, welche unter lokaler Suprareninapplikation (1 mg) sistierte. Umgehend daran kam es zu ST Hebungen in den Ableitungen II, III, aVF, und ST Senkungen in den Ableitungen I und aVL, sowie zu einem Blutdruckabfall auf 80/60 mm Hg (siehe Abb. 1). Nach raschem Aufklaren nach der Narkose negierte der Patient Thoraxschmerzen oder Dyspnoe, und war wieder normoton. Bereits nach Verlegung auf die hiesige kardiologische Intensivstation waren dort die ST Hebungen nicht mehr nachweisbar, die ST Strecke isoelektrisch (Abb. 2). Es konnten keine Wandbewegungsstörungen bei hyperdynamen linken Ventrikel in der Echokardiographie nachgewiesen werden. Zum Ausschluss eines akuten Koronarsyndroms wurde binnen kurzer Zeit nach Eintreffen auf der Intensivstation eine Koronarangiographie durchgeführt, in welcher sich keine signifikanten Koronarstenosen zeigten. Auch in den repetitiv durchgeführten Troponin Kontrollen wurde keine relevante Dynamik beobachtet. Der Patient konnte nach unauffälliger Observanz und persistierender Beschwerdefreiheit am Folgetag zur weiteren Abklärung der pulmonalen Raumforderung auf die Normalstation verlegt werden.

Schlussfolgerungen: Durch lokale Applikation von Suprarenin kann es zu vorübergehenden ST Strecken Hebungen im EKG ohne relevante Koronarstenosen kommen. Dies ist bereits der zweite Patient binnen 2 Jahren, bei welchem die Autoren eine ST Streckenhebung bei lokaler Suprarenininstillation im Zuge einer Bronchoskopie festhalten konnten.

2 BASIC SCIENCE

2.1

Effects of short term adiponectin receptor agonism on cardiac function and energetics in diabetic db/db mice

A. Tarkhnishvili¹, J. Gollmer², C. Koentges¹, N.J. Byrne², K. Pfeil², T.B. Mwinella¹, D. Wolf¹, C. Bode¹, A. Zirlik², H. Bugger²

¹Universitäts-Herzzentrum Freiburg-Bad Krozingen, Freiburg, Germany

²Klinische Abteilung für Kardiologie, Medizinische Universität Graz, Graz, Austria

Introduction: Impaired cardiac efficiency is a hallmark of diabetic cardiomyopathy in models of Type 2 diabetes. Adiponectin receptor 1 (AdipoR1) deficiency impairs cardiac efficiency in non-diabetic mice, suggesting that hypoadiponectinemia in Type 2 diabetes may contribute to impaired cardiac efficiency due to compromised AdipoR1 signaling. Thus, we investigated whether targeting cardiac adiponectin receptors may improve cardiac function and energetics, and attenuate diabetic cardiomyopathy in type 2 diabetic mice.

Methods: Eight week-old db/db mice or C57BLKS/J control mice received intraperitoneal injections of the non-selective adiponectin receptor agonist, AdipoRon, or vehicle for 10 consecutive days. Cardiac function and dimensions were investigated using echocardiography, and contractility and rates of energy substrate metabolism were investigated using the isolated working heart model.

Results: Based on echocardiography, AdipoRon treatment did not alter ejection fraction, left ventricular diameters or left ventricular wall thickness in db/db mice compared to vehicle-treated mice. In isolated working hearts, an impairment in cardiac output and efficiency in db/db mice was not improved by AdipoRon. Mitochondrial respiratory capacity, oxygen con-

sumption in the presence of oligomycin, and levels of 4-hydroxynonenal were similar among all groups. However, AdipoRon induced a marked shift in the substrate oxidation pattern in db/db mice towards increased reliance on glucose utilization. In parallel, the diabetes-associated increase in serum triglyceride levels in vehicle-treated db/db mice was blunted by AdipoRon treatment, while an increase in myocardial triglycerides levels in vehicle-treated db/db mice was not altered by AdipoRon treatment.

Conclusion: Thus, AdipoRon treatment shifts myocardial substrate preference towards increased glucose utilization, likely by decreasing fatty acid delivery to the heart, but was not sufficient to improve cardiac output and efficiency in db/db mice.

2.2

Cardiac fibrosis and endothelial dysfunction in duchenne muscular dystrophy: the role of Tenascin C

P. L. Szabo¹, O. Hamza¹, M. Inci¹, J. Ebner², K. Hilber², A. Dietmar³, S. Trojanek³, S. Costantino⁴, F. Paneni⁴, B. K. Podesser¹, A. Kiss¹

¹Ludwig Boltzmann Institute for Cardiovascular Research at the Center for Biomedical Research, Medical University of Vienna, Vienna, Austria

²Center for Physiology and Pharmacology, Medical University of Vienna, Vienna, Austria

³Center for Anatomy and Cell Biology, Division of Cell and Developmental Biology, Medical University of Vienna, Vienna, Austria

⁴Center for Molecular Cardiology, University of Zurich and University Heart Center, Cardiology, University Hospital Zurich, Zürich, Switzerland

Background: Besides skeletal muscle degeneration, Duchenne muscular dystrophy (DMD) patients also suffer from dilated cardiomyopathy, which significantly contributes to morbidity and mortality. However, the exact underlying mechanisms contributing to the cardiovascular dysfunctions in DMD are still largely unknown. More recently, our group demonstrated that upregulation of Tenascin C in post-myocardial infarction and left ventricular (LV) hypertrophy led to adverse LV remodelling and cardiac fibrosis. Aims: Our study was aimed to characterize vascular and cardiac dysfunction in longitudinal study (3-, 6- and 10-months old mice) and 2) elucidate the vascular dysfunction and cardiac fibrosis in link to TNC in a mouse model of DMD.

Methods: Male mdx and wt mice were used. Transthoracic echocardiography was performed to assess left ventricular (LV) function and morphology. To test the vascular reactivity wire myography was used on isolated aortic rings. To investigate the causative role of oxidative stress in endothelial dysfunction, aorta segments were incubated with NADPH oxidase inhibitor (Apocynin or Setanaxib). Cardiac fibrosis, TLR-4 and TN-C expression in LV tissue were assessed by immunohistochemistry and RT-qPCR. Levels of TN-C in plasma was measured by ELISA and epigenetic regulation of TN-C was assessed by DNA methylation in LV tissue. To further evaluate the role of TN-C in endothelial dysfunction, human umbilical vein endothelial cells (HUVEC) were treated either with human recombinant TN-C (10 µg/ml) or combination with TLR-4 inhibitor (TAK-242, 50 nM). Lung endothelial cells were isolated from mdx mice,

then the expression of NADPH oxidase 1 and 4 (NOX1, NOX4), and interleukin-6 (IL-6) were assessed by RT-qPCR.

Results: LV dilation and cardiac fibrosis were markedly enhanced in mdx mice (6-10 months) compared to age-matched controls, ($p < 0.05$). This was accompanied by the significant upregulation of TN-C in plasma ($p < 0.01$ vs control). Both TN-C expression and DNA methylation of TNC promoter were significantly increased in LV tissue as well as TLR-4 expression was upregulated in perivascular regions of mdx mice in comparison to control. In line with these findings, vascular endothelial function (6 and 10 months of age) was markedly impaired in mdx mice ($p < 0.01$). Of importance, this effect was markedly improved by applying NADPH oxidase inhibitor. HUVEC incubated with TN-C showed increased expression of IL-6 and oxidative stress-related markers and application of TLR-4 inhibitor markedly reversed these impairments. In line with that endothelial cells were isolated from mdx mice also showed a significant upregulation of IL-6 or NADPH oxidase mRNA expression.

Conclusion: Presence of TN-C in plasma and cardiac tissue is accompanied by LV dysfunction, dilatation and fibrosis and vascular dysfunction. Collectively, TN-C created an intracellular environment that facilitated fibrosis and oxidative stress, which, in turn, resulting in cardiomyocyte and endothelial cell dysfunction. Thus, TN-C may be a critical mediator in the progression of cardiac fibrosis and endothelial dysfunction in DMD and represent a new target for therapy.

2.3

Autophagy-related gene 5 (Atg5) is required for maintaining subcellular calcium homeostasis during acute cardiac stress

N. Djalina¹, J. Voglhuber¹, S. Ljubojević-Holzer¹, S. Sedej¹

¹Medizinische Universität Graz, Graz, Austria

Introduction: Autophagy exerts protective effects during cardiac stress inflicted by β -adrenergic stimulation and pressure overload. Contrarily, deletion of the cardiac-specific Atg5 gene contributes to left ventricular hypertrophy and contractile dysfunction, resulting in dilated cardiomyopathy. Heart failure is characterized by perturbations of excitation-contraction coupling (ECC) underlying alterations in intracellular calcium signaling. In this study, we aimed to understand whether loss of basal autophagy due to Atg5 deletion specifically in cardiomyocytes contributes directly to disturbances in subcellular calcium cycling.

Methods: Cardiac-specific Atg5^{-/-} and Atg5^{+/+} mice were used to isolate ventricular cardiomyocytes, which were loaded with 8 µM Ca²⁺ indicator Fluo4/AM. Isolated cells were electrically stimulated and subjected to elevated workload by increasing pacing frequencies from 1 to 4 Hz. Cytosolic and nuclear calcium transients (CaTs) were recorded in line-scan mode using a laser scanning confocal microscope. Pharmacological inhibition of autophagic flux was performed by an intraperitoneal injection of 40 mg/kg leupeptin to Atg5^{+/+} mice.

Results: At baseline (1 Hz) stimulation the amplitude and kinetics of calcium transients were comparable between Atg5^{-/-} and Atg5^{+/+} cells. However, after progressive increase of the pacing rate from 1 Hz to 4 Hz, Atg5^{-/-} cardiomyocytes displayed reduced cytoplasmic and nuclear CaT amplitude, but increased nuclear time-averaged CaTs compared to controls. Such increase in nuclear calcium load could stimulate

Ca²⁺-dependent transcriptional activity, and involve CaMKII-mediated pro-hypertrophic gene program and, thus, contribute to cardiac remodelling. In addition, we observed increased occurrence of arrhythmic events in *Atg5*^{-/-} hearts at high pacing frequency, indicative of intracellular calcium overload and disturbed ECC. Acute pharmacological autophagy inhibition failed to elicit direct changes in time-averaged CaTs in the cytoplasm and nucleoplasm, suggesting that loss of *Atg5*-dependent autophagy seems to induce adverse cardiac remodelling that involves increased CaMKII activity due to the imbalances in nuclear Ca²⁺ levels.

Conclusion: Specific loss of *ATG5* protein impairs calcium cycling during acute stress exposure by reducing CaT amplitudes, promoting arrhythmia, and increasing nuclear calcium load, which may induce hypertrophic gene expression. Further work is needed to identify key components mediating autophagy-related cardioprotection to develop strategies against cardiac remodeling and its progression to heart failure.

2.4

Expression of the long non coding RNA TRDN-AS in the ischemic heart

D. Traxler¹, J. Mester-Tonczar¹, E. Hasimbegovic¹, A. Spannauer¹, N. Kastner¹, K. Zlabinger¹, M. Riesenhuber¹, M. Gyöngyösi¹

¹Medizinische Universität Wien, Klinische Abteilung für Kardiologie, Wien, Austria

Introduction: Triadin (TRDN) as part of the calcium release complex plays an important role in intracellular calcium homeostasis in cardiomyocytes. Alternative splicing results in the production of two isoforms (TRDN-short or cardiac isoform and TRDN-long or skeletal isoform). Triadin antisense (TRDN-AS) is a long non coding RNA (lncRNA) that is localised at the opposite strand of the protein encoding gene and overlaps with TRDN-long. The function of antisense transcripts is still unknown, however, a role in gene regulation on the transcriptional and post-transcriptional level has been proposed. Previous data showed increased TRDN RNA, but decreased protein expression in human failing hearts. Coronary ligation in mice resulted in lower expression of TRDN after 24 hours. Mutations of TRDN are associated with a genetic form of ventricular arrhythmia and sudden cardiac death. Interestingly ablation of TRDN was not lethal in mice. In our previous work (unpublished) we have determined the de-regulation of lncRNAs by sequencing in porcine reperfused myocardial infarction (AMI) 3 days after the infarction, and found a significant downregulation of TRDN-long in the infarcted, and TRDN-short in the border, and TRDN-AS both in the infarcted and border area as compared to non-ischemic heart. We hypothesized, that ischemic preconditioning may reverse down regulation of the TRDN, its two isoforms and the corresponding lncRNA form (TRDN-AS) in a translational animal model of ischemic cardiomyopathy.

Methods: We performed cardiac ischemic remote intrinsic pre-conditioning (IRIPC) by each three cycles of 10 minutes ischemia (percutaneous balloon occlusion in the mid left anterior descending coronary artery (LAD)) followed by 10 minutes reperfusion in 13 pigs (IPC), and sham procedure in 10 pigs (control). One day later (2nd window of protection) all pigs underwent percutaneous reperfused acute myocardial infarction (AMI) by 90 min occlusion of the left circumflex coronary artery (LCX). Tissue samples from the LCX AMI, border and remote and the conditioning area (distal LAD) were collected

on day 3 ($n=5$ and $n=5$, IRIPC and control, respectively) and month 1 after AMI ($n=8$ and $n=5$, IRIPC and control, respectively). TRDN, TRDN-short, TRDN-long and TRDN-AS were assessed using qPCR in all myocardial regions. Cardiac MRI + late enhancement was performed on day 3 and month 1 to assess left ventricular function parameters and infarct size.

Results: Scar size was significantly reduced after one month in the IRIPC group (mean \pm SD: $8.4 \pm 3.7\%$, vs $14.0 \pm 1.8\%$, $p < 0.01$), without a difference between the groups regarding left ventricular ejection fraction. All TRD isoforms and its corresponding lncRNA were downregulated on day 3. However, we observed a 17.3 times decreased expression of TRDN-AS ($p=0.03$) and 5.1 times decreased TRDN-long expression ($p=0.03$) in the control group after one month, with a trend towards downregulation of the TRDN and its short isoform (8.3 times and 7.4 times respectively) in the control group. In the border, remote and LAD conditioning region there was no significant dysregulation of TRDN, its isoforms or TRDN-AS.

Conclusion: Our in vivo translational model of reperfused AMI revealed a down-regulation of TRDN, TRDN-long, TRDN-short and TRDN-AS in the infarct zone on day 3 in both groups, but only in the control group after one month, suggesting a long-term benefit of IRIPC on preservation of contractility of the infarcted area.

2.5

Initial analysis of myocardial samples and explanted materials from the pediatric patients with complex cardiac diseases registry (PETTICOAT)

E. Hasimbegovic¹, I. Pavo², N. Kastner¹, A. Spannauer¹, J. Mester-Tonczar¹, D. Traxler-Weidenauer¹, D. Zimpfer³, I. Michel-Behnke², M. Pavone-Gyöngyösi¹

¹Department of Cardiology, Medical University of Vienna, Wien, Austria

²Department of Pediatric Cardiology, Medical University of Vienna, Wien, Austria

³Department of Heart and Thoracic Surgery, Medical University of Vienna, Wien, Austria

Introduction: The rarity of complex paediatric cardiac diseases, the interindividual variability of the cardiac anatomy, existing comorbidities, previous surgery and limited sample availability are among the reasons for the scarcity of data characterising tissues in paediatric cardiac patients. [1, 2] The Pediatric paediatric patients with Complex cardiac diseases registry (PETTICOAT) aims to accumulate and characterise myocardial samples and explanted cardiac materials from this patient collective.

Methods: As part of the PETTICOAT registry, we have collected samples from 78 paediatric patients with complex cardiac diseases thus far. For the initial analysis we examined a total of 20 explants and 18 right ventricular myocardium samples. The myocardium samples were embedded in paraffin and stained using standardised haematoxylin eosin (HE) and Picro-Sirius Red (PSR) protocols. The HE images were used to conduct manual cardiomyocyte circumference measurements. The PSR images were analysed using ImageJ software to obtain the relative surface area of interstitial collagen fibres. A standardised immunohistochemistry (IHC) protocol was used to detect tumour necrosis factor alpha (TNF- α) in the myocardium. We developed and optimised a Technovit[®] 7200 solution-based

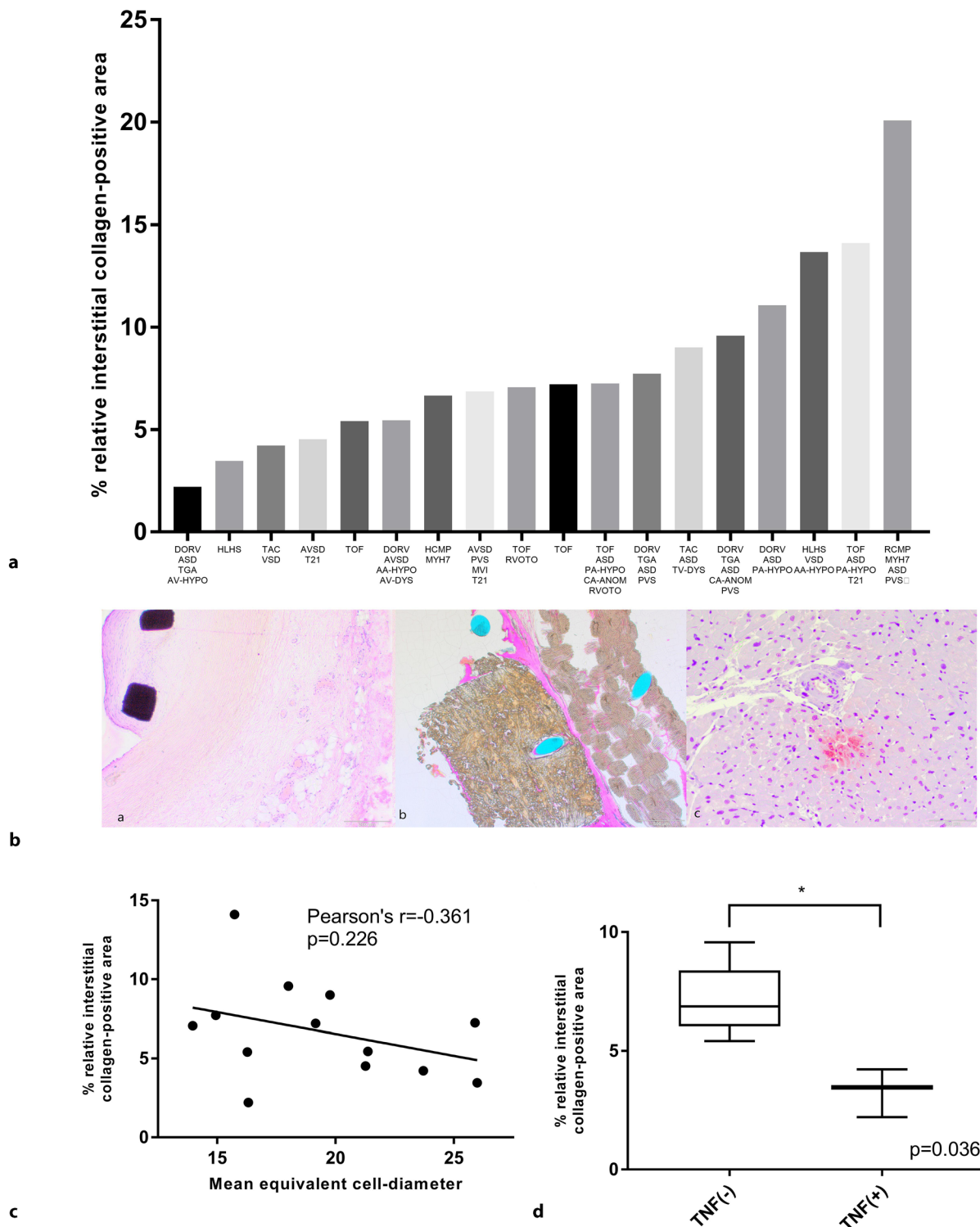


Fig. 1125 Initial PETTICOAT analysis. 1A) Percentage relative interstitial collagen area in right ventricle myocardium in individual paediatric patients. Relevant cardiac conditions are listed on the x-axis for each patient. 1B) a) HE-stain of a Technovit® 7200 embedded PDA stent b) HE-stain of a Technovit® 7200 embedded explanted right ventricular outflow tract conduit c) Positive right ventricle myocardium Tnf- α IHC stain with Vector® Red 1C) Correlation between equivalent cell diameter and relative PSR-positive area 1D) Relative interstitial collagen area of right ventricle myocardium samples stratified using Tnf- α IHC staining. Abbreviations: ASD – atrial septal defect, AA-Hypo – aortic arch hypoplasia, AV-Dys/Hyp – aortic valve hypo-/dysplasia, atrioventricular septal defect, CA-ANOM – coronary artery anomaly, DORV- double outlet right ventricle, HCMP – hypertrophic cardiomyopathy, HLHS – hypoplastic left heart syndrome, MVI – mitral valve insufficiency, MYH7 – MYH7 gene mutation, PA-Hypo – pulmonary artery hypoplasia, PVS – pulmonary stenosis, RCMP – restrictive cardiomyopathy, RVOTO – right ventricular outflow tract obstruction, TAC – common truncus arteriosus, TGA – transposition of the great arteries, TOF – tetralogy of Fallot, TV-Dys – tricuspid valve dysplasia, T21 – Down syndrome, VSD – ventricular septal defect

plastic embedding and slicing protocol for explanted cardiac devices. We used the newly established protocol to embed and slice the hard explants from the PETTICOAT registry and stained the slides with an adapted HE protocol.

Results: The collected explants included 5 patent ductus arteriosus (PDA) stents, 4 aortic coarctation (CoA) stents, 5 right ventricular outflow tract (RVOT) conduits, 4 pulmonary artery branch stents and 2 Fontan tunnel conduits. These were successfully embedded, cut and stained using an adapted HE protocol. The fibrotic remodelling of the right ventricle was assessed in 18 patients (mean age: 4.98 (IQR: 2.07–26.86) months) who most commonly suffered from the tetralogy of Fallot (TOF, 27.8%), a double outlet right ventricle (DORV, 27.8%), pulmonary artery stenosis (22.2%) and combined atrial-ventricular septum defects (16.7%). The cardiomyocyte diameter was measured for 13 samples from this collective and a TNF- α IHC stain was successfully conducted in eight patients. The median interstitial collagen-positive area was $8.08 \pm 4.39\%$ in the overall collective, $8.20 \pm 3.38\%$ in TOF and $7.20 \pm 3.50\%$ in DORV. There was no significant correlation between the amount of interstitial collagen and frequency of previous cardiac surgery or age. However, we found significantly less interstitial collagen-positive areas in samples that stained positive for TNF- α ($p=0.036$). The median cardiomyocyte size of the overall collective was $19.42 \pm 4.04 \mu\text{m}$, $18.21 \pm 4.69 \mu\text{m}$ in TOF and $17.66 \pm 2.77 \mu\text{m}$ in DORV patients. There was a trend towards an inverse correlation between the cell diameter and the relative collagen area, but it did not reach significance (Pearson's $R = -0.361$, $p=0.226$).

Conclusion: We successfully established a protocol that allows the detailed examination of hard explanted paediatric cardiac devices and preserves their structural integrity. In a preliminary analysis of soft-tissue samples of right ventricle myocardium, we have found a significant inverse correlation between TNF- α and interstitial collagen. As the sample size in our biobank increases, we will be able to use these protocols to generate increasingly robust data on this scarce and highly complex patient collective.

2.6

HDAC modification improves cardiomyocyte function via modulation of the myofilament

D. M. Eaton¹, T. G. Martin², M. Kasa³, N. Djalilac³, J. P. Johnson¹, E. Kolesnik³, S. Ljubojevic-Holzer³, D. von Lewinski³, H. Maechler³, A. Zirlik³, J. A. Kirk², S. R. Houser¹, P. P. Rainer³, M. Wallner³

¹Lewis Katz School of Medicine at Temple University, Philadelphia, United States

²Loyola University Chicago Stritch School of Medicine, Chicago, United States

³Medical University of Graz, Graz, Austria

Introduction: Approximately 50% of all patients with heart failure (HF) can be classified as having HF with preserved Ejection Fraction (HFpEF). We previously established a large animal model of slow progressive pressure overload that recapitulates key clinical features of HFpEF, which was then used as a platform to test the effects of the pan-HDAC inhibitor suberanilohydroxamic acid (SAHA). SAHA reversed and prevented the development of diastolic, systolic, and pulmonary dysfunction. This study was designed to assess the effects of SAHA at the level of cardiomyocyte and contractile protein function to investigate how it modulates cardiac function in parallel studies using cardiac tissue from humans and large mammals with similar physiological features (ie. long action potential, similar myosin heavy chain isoform).

Methods: Adult feline ventricular cardiomyocytes (AFVM) were isolated from male domestic short hair cats and treated with 2.5 μM SAHA or vehicle (DMSO) for 90 minutes, then incubated with a calcium (Ca²⁺) indicator (Fluo-4AM) and electrically stimulated (0.5 Hz) to record Ca²⁺ transients and contractions. Skinned myocytes were isolated from treated AFVM and functional experiments were performed to assess myofilament Ca²⁺ sensitivity and passive stiffness. The effects of SAHA on human cardiac tissue was assessed using left ventricle (LV) trabeculae isolated from non-failing donor hearts treated with 10 μM SAHA or vehicle for 120 minutes while being electrically stimulated (1 Hz). Developed force and relaxation parameters were recorded. Skinned myocytes were then isolated for calcium sensitivity and passive stiffness experiments.

Results: There was both a significant increase in contractility (fractional shortening) and relaxation kinetics (time to 50% baseline, return velocity), but no difference in peak Ca²⁺ transients in SAHA treated AFVM. These findings are indicative of an increase in myofilament Ca²⁺ sensitivity and to directly assess this, skinned myocytes (used to assess myofilament function) were isolated from treated AFVMs. Myofilament Ca²⁺ sensitivity was significantly improved and passive stiffness was significantly decreased with SAHA. In parallel experiments using SAHA treated trabeculae isolated from non-failing human hearts, there was a decrease in diastolic tension and increase in developed force, with a similar systolic peak force. Skinned myocytes were then isolated from these trabeculae and had a similar response to AFVMs, with an increase in myofilament Ca²⁺ sensitivity and decrease in passive stiffness.

Conclusion: These findings suggest that SAHA can modulate cardiac function at the level of the cardiomyocyte and myofilament in human and feline myocardium by increasing myofilament calcium sensitivity and reducing diastolic tension. These changes are in line with functional data observed in human trabeculae and in-vivo hemodynamics in a feline model with features of HFpEF.

2.7

Boosting NAD⁺ metabolism improves diastolic dysfunction in animal models of aging, obesity and hypertension

M. Abdellatif¹, V. Trummer-Herbst¹, F. Koser², S. Durand³, R. Adao⁴, D. Von Lewinski¹, P. Rainer¹, D. Scherr¹, A. Zirlik¹, A. Leite-Moreira⁴, J. Alegre-Cebollada⁵, S. Kiechl⁶, W. Linke², G. Kroemer³, S. Sedej¹

¹Department of Cardiology, Medical University of Graz, Graz, Austria

²University of Muenster, Institute of Physiology II, Münster, Germany

³Metabolomics and cell biology platforms, Institute Gustave Roussy, Villejuif, France

⁴Department of Surgery and Physiology, Faculty of Medicine University of Porto, Porto, Portugal

⁵National Centre for Cardiovascular Research (CNIC), Madrid, Spain

⁶Department of Neurology, Medical University of Innsbruck, Innsbruck, Austria

Introduction: Heart failure with preserved ejection fraction (HFpEF) is a highly prevalent and intractable form of cardiac decompensation commonly associated with diastolic dysfunction.

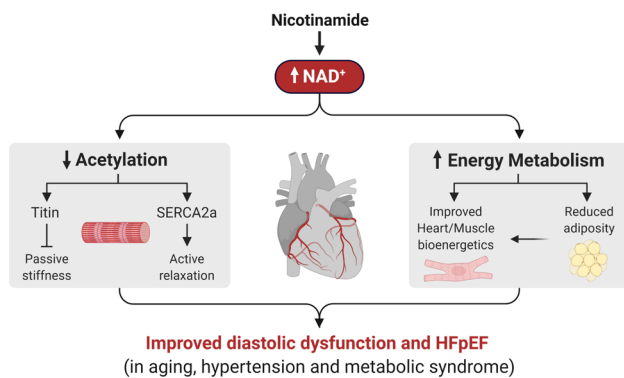


Fig. 112.7

tion. HFpEF, at least in animals, is intimately linked to metabolic perturbations in mitochondrial fatty acid oxidation, redox reactions, and ATP synthesis. Since all these processes are nicotinamide adenine dinucleotide (NAD⁺)-dependent, we speculated that NAD⁺ metabolism is deranged in HFpEF and, thus, it might be therapeutically targeted.

Methods: To induce local NAD⁺ deficiency, we generated mice with partial deletion of nicotinamide phosphoribosyltransferase (NAMPT) specifically in cardiomyocytes. We also used ZSF1 obese rats as a model of metabolic syndrome-induced HFpEF, whereas age- and hypertension-related diastolic dysfunction were examined in 2-year-old C57BL/6J mice and Dahl salt-sensitive rats, respectively. We applied a multitude of *in vivo* and *in vitro* assays, including invasive hemodynamics, serial echocardiography and blood pressure measurements, exercise testing, indirect calorimetry, cardiac histology, acetylome and metabolome profiling, myocardial and skeletal muscle bioenergetics, as well as calcium kinetics, sarcomere shortening, and titin mechanics in isolated cardiomyocytes. The translational potential of the study was examined in cardiac biopsies of HFpEF and non-failing donors, and in a human cohort with 20 years of follow-up.

Results: HFpEF in patients and ZSF1 obese rats was associated with a cardiac deficit in NAD⁺, and mimicking this in NAMPT-haploinsufficient mice caused premature diastolic dysfunction. Contrarily, elevating NAD⁺ levels by oral supplementation of its precursor, nicotinamide, improved diastolic dysfunction induced by metabolic syndrome, salt-sensitive hypertension or old age. This effect was mediated partly through alleviated systemic comorbidities and enhanced myocardial bioenergetics. Simultaneously, nicotinamide directly improved cardiomyocyte passive stiffness and calcium-dependent active relaxation through increased deacetylation of titin and SERCA2a, respectively. Finally, in a long-term human cohort study, high dietary intake of naturally-occurring NAD⁺ precursors was associated with lower blood pressure and reduced risk of cardiac and all-cause mortality.

Conclusion: NAD⁺ precursors, and especially nicotinamide, hold promise as potential therapeutic agents against diastolic dysfunction and clinical HFpEF.

2.8

Analysis of the fibrotic substrate and post-operative ventricular arrhythmias in patients undergoing surgery due to valvular aortic stenosis and left ventricular outflow tract obstruction

V. Paar¹, M. Haslinger¹, P. Krombholz-Reindl², M. Neuner³, P. Jirak¹, T. Kolbitsch¹, B. Minnich⁴, F. Schrödl⁵, M. Lichtenauer¹, C. Granitz¹, R. Seitelberger², A. Brunauer³, M. Kirnbauer³, U. C. Hoppe¹, C. Dinges², L. J. Motloch¹

¹Division of Cardiology, Department of Internal Medicine II, Paracelsus Medical University, Salzburg, Austria

²Department of Cardiac Surgery, Paracelsus Medical University, Salzburg, Austria

³Department of Anesthesiology, Perioperative Medicine and Intensive Care Medicine, Paracelsus Medical University of Salzburg, Salzburg, Austria

⁴Division of Vascular and Exercise Biology, Department of Biosciences, University of Salzburg, Salzburg, Austria

⁵Institute for Anatomy, Paracelsus Medical University, Salzburg, Austria

Introduction: Valvular pathologies and/or subvalvular alterations are the two major pathologies of aortic stenosis and often require cardiac surgery. Both manifestations are associated with cardiac hypertrophy that potentially results in tissue fibrosis. However, molecular and histological differences in the severity of fibrosis in both etiologies were not investigated yet. Furthermore, clinical implications on post-operative arrhythmias, which potentially might depend on fibrosis, are unknown.

Methods: To investigate this issue, we analyzed left ventricular septal specimen of cardiosurgical patients undergoing myectomy and/or aortic valve replacement due to valvular (AVS, *n*=7) versus subvalvular (ASVS, *n*=8) pathologies by histological (Masson's trichrome stain) and molecular (western blots of fibrosis-related proteins) analyses. Additionally, to evaluate clinical implication on post-operative arrhythmias, 48 hours rhythm monitoring at the intensive care unit, as well as Holter monitoring at the fifth post-operative day, were investigated. Healthy post-mortem septal cardiac specimen served as a control group.

Results: While echocardiographic parameters were similar in both pathology groups, such as left ventricular ejection fraction (AVS: 61.4 ± 11.1 % vs. ASVS: 64.0 ± 5.7 %, *p*=0.58), peak trans-aortic velocity at rest (AVS: 4.6 ± 0.8 m/s, vs. ASVS: 3.6 ± 1.4 m/s, *p*=0.12), and intraventricular septum diastolic (AVS: 16.0 ± 3.3 mm vs. ASVS: 21.4 ± 6.4 mm, *p*=0.06), we observed a higher incidence of premature ventricular extra-beats on the fifth post-operative days in AVS (24 h incidence of PVB >5000, AVS: *n*=3/4 vs. ASVS: *n*=0/4). Histological analyses revealed that in both, AVS and ASVS, there is a trend towards a higher fibrotic burden in comparison to healthy control tissue (AVS: *p*=0.13, ASVS: *p*=0.07). This was confirmed by the significant increase of the fibrotic proteins Smad3 and TGF-β1 in both pathologies. However, there was no difference in AVS and ASVS concerning histologically determined fibrosis (relative fibrotic area: AVS: 3.5 ± 4.1 % vs. ASVS: 4.2 ± 4.3 %, *p*=0.75), as well as in the protein levels analyzed by western blot.

Conclusion: In comparison to healthy control tissue, AVS and ASVS are associated with progressive fibrotic remodeling, though without differences between AVS and ASVS. While this finding could also promote a higher incidence of post-operative ventricular arrhythmias in cardiosurgical patients it does

not seem to contribute to a higher arrhythmogenicity in AVS. Further studies need to investigate the association of fibrosis and post-operative arrhythmias in cardiosurgical patients. This study was supported by Paracelsus Medical University (R18/02/106-PAA).

2.9

Blockade of K-ras signalling attenuates the coagulatory phenotype of alternatively activated macrophages

P. Haider¹, M. Salzman¹, J. Pointner¹, C. Hengstenberg¹, W. Speidl¹, J. Wojta¹, P. Hohensinner¹

¹Medical University of Vienna, Vienna, Austria

Introduction: Macrophages are a heterogeneous population of phagocytic cells which can be polarized by the tissue environment into distinct subsets to fulfil specific tasks. Alternative polarization of macrophages (alternatively activated macrophages, AAM) within a Th2 environment by interleukin-4 and interleukin-13 leads to a macrophage phenotype characterized by increased tissue factor (TF) production and release of extracellular vesicles [1]. Further, plasminogen activator inhibitor 1 (PAI-1) is upregulated in AAMs, inhibiting urokinase-type plasminogen activators (uPA) ability to activate membrane-bound matrix metalloproteases on macrophages, leading to impaired proteolysis by these cells [2]. Increased TF expression and a pro-coagulatory environment are observed in cancer patients bearing tumours with mutations in the K-ras gene [3].

Methods: We studied the role of K-ras in human AAM by inhibiting K-ras signalling via the approved drug fendiline in vitro. Macrophages were generated over 7 days from peripheral blood mononuclear cells through isolation and seeding in cell culture medium containing macrophage colony-stimulating factor. The cells were pre-treated with fendiline before polarizing them into AAMs by interleukin-4 and interleukin-13. K-ras signalling was assessed by measuring the intracellular phosphorylation of a central downstream target, ERK1/2 by flow cytometry and immunofluorescent staining. Polarization of macrophages was evaluated by qPCR, flow cytometry and ELISA of AAM specific cytokines. The coagulatory and fibrinolytic phenotype was studied by qPCR, ELISA, flow cytometry of extracellular vesicles as well as rotational thromboelastometry of conditional culture medium using the ROTEM system.

Results: Alternative activation by interleukin-4/interleukin-13 led to a significant and continuous phosphorylation of ERK1/2 compared to unstimulated macrophages. Phosphorylation was highest after 30 minutes of polarization and was detectable up to 48 hours after stimulation. Addition of fendiline significantly reduced the phosphorylation of ERK1/2. Inhibition of K-ras prior to polarization into AAM led to a significant reduction in the expression of AAM associated CD206 as well as in the production of interleukin-10. Further, the release of AnnexinV+ extracellular vesicles was diminished in fendiline treated AAMs. When we assessed the coagulatory potential of conditioned culture medium by rotational thromboelastometry, culture medium of K-ras treated AAM had significantly prolonged coagulation times compared to medium of untreated cells. TF, uPA as well as PAI-1 mRNA and protein was reduced in fendiline treated AAM compared to untreated cells.

Conclusion: By blocking intracellular K-ras signalling in human alternatively activated macrophages, we reduced the coagulatory phenotype of these cells. Mechanistically, fendiline

led to a reduction of phosphorylated ERK1/2 and a downregulation of the coagulatory proteins TF, uPA and PAI-1. These cellular alterations led to a prolonged coagulation potential measured by rotational thromboelastometry. Overall, we showed that the coagulatory phenotype of alternatively activated macrophages can be targeted specifically by pharmacological inhibition of K-ras signalling.

2.10

Vascular graft storage solution preserves endothelial function

A. Kiss¹, L.P. Szabo¹, C. Dostal¹, Z. Arnold¹, D. Geissler², I. Crailsheim², S. Folkmann², M. Grabenwöger², B. Podesser¹, B. Winkler²

¹Ludwig Boltzmann Institute for Cardiovascular Research at the Center for Biomedical Research, Medical University of Vienna, Vienna, Austria, Wien, Austria

²Department of Cardio-Vascular Surgery Clinic Vienna North and Karl Landsteiner Institute for Cardio-Vascular Research, Wien, Austria

Introduction: Saline is still the most widely used storage solution in cardiovascular procedures despite knowing evidence of its negative influence on the human endothelium. Aim of this study was to assess the effect of DuraGraft® (Somaluthion Inc, Jupiter FL, USA), a novel intraoperative graft treatment solution, on human saphenous vein segments, rat aortic segments and human umbilical vein endothelial cells (HUVECs) in comparison to saline.

Methods: From Patients undergoing aortocoronary bypass surgery, saphenous vein graft segments were randomized to DuraGraft® ($n=12$) or saline ($n=12$) solution before intraoperative storage. These segments and additionally rat aortic segments underwent assessment of vascular function in a multichamber isometric myograph system in comparison to Krebs-Henseleit solution (KHS). Human umbilical vein endothelial cells (HUVECs) were used for cell viability tests.

Results: KCl-induced contraction showed a significant response when treated with DuraGraft® compared to normal saline in human vein segments (24.73 ± 16.22 vs. 15.59 ± 9.53 N/m², $P < 0.066$). Segments treated with DuraGraft® preserved endothelium-dependent vasorelaxation in response to cumulative dosage of bradykinin compared to saline treated segments. In rat aorta segments stored in saline showed significantly impaired vasoconstriction (3.59 ± 4.20 , $p < 0.0001$) and vasorelaxation compared to KHS and DuraGraft® ($p < 0.0001$). Saline at 30 and 60 minutes markedly inhibited cell viability ($p < 0.0001$). In contrast, cell viability was similar between KHS and the DuraGraft® group after 30 and 60 minutes.

Conclusion: DuraGraft® demonstrated a favorable effect on graft relaxation and contraction indicating preservation of vascular endothelial function. Saline is inferior to a specialized solution and can show harmful effects on the human endothelium.

2.11

Deep RNA sequencing identified a novel circular RNA, circ-RCAN2 in pig hearts with potential regulatory functions in acute myocardial infarction

J. Mester-Tonczar¹, P. Einzinger², J. Winkler¹, N. Kastner¹, A. Spannauer¹, K. Zlabinger¹, D. Traxler-Weidenauer¹, D. Lukovic¹, E. Hasimbegovic¹, G. Goliash¹, N. Pavo¹, M. Gyöngyösi¹

¹Medizinische Universität Wien, Wien, Austria
²Technische Universität Wien, Wien, Austria

Introduction: First described in 1976 in viroids, circular RNAs (circRNAs) are covalently closed RNA molecules and belong to the class of long non-coding RNAs. Unlike linear RNAs such as messenger RNAs (mRNAs), circRNAs do not have 3' poly(A) tails nor 5' cap structures, making them more stable than mRNAs due to their resistance to exonucleases. In the past decade, circRNAs have been shown to play a central role in gene regulatory networks and disease development however, circRNA expression patterns in myocardial infarction (MI) is currently insufficiently explored. Here, we used deep RNA sequencing to identify circRNA expression in a porcine model of myocardial infarction.

Methods: Three days after closed-chest reperfusion MI by temporary 90 min percutaneous balloon occlusion of the mid LAD or sham surgery in domestic pigs, porcine myocardium samples were harvested and stored at -80 °C in RNAlater. RNA was extracted using the miRNeasy Mini kit (Qiagen, Hilden, Germany). Cardiac circRNAs were identified by deep RNA-sequencing of rRNA-depleted RNA. Bioinformatics analysis was performed using the CIRIfull and KNIFE algorithms. CircRNAs identified with both algorithms were further investigated by differential expression analysis using qPCR. Sanger sequencing was performed to check for circularity of the qPCR product. In addition, our in vivo data was checked in vitro by using hypoxic and normoxic porcine cardiac progenitor cells (pCPCs).

Results: Novel identified circ-C12orf29 and circ-RCAN2 were significantly downregulated in infarcted myocardial tissue compared to healthy pig myocardium ($p=0.004$ for circ-C12orf29 and $p=0.027$ for circ-RCAN2). The backsplice junctions of the circular transcripts were confirmed by Sanger sequencing. Interestingly, in vitro hypoxic pCPCs did not show any significant changes in differential expression of circ-C12orf29. In contrast with the in vivo data, circ-RCAN2 exhibited significant ischemia-time-dependent upregulation in hypoxic pCPCs, validated by qPCR.

Conclusion: Our results reveal novel cardiac circRNAs identified in infarcted and healthy pig hearts by deep RNA-sequencing. Deviated expression patterns of circ-RCAN2 were observed in vivo in acute MI in pigs and in pCPCs in vitro, highlighting the importance of translational experiments. Our findings will

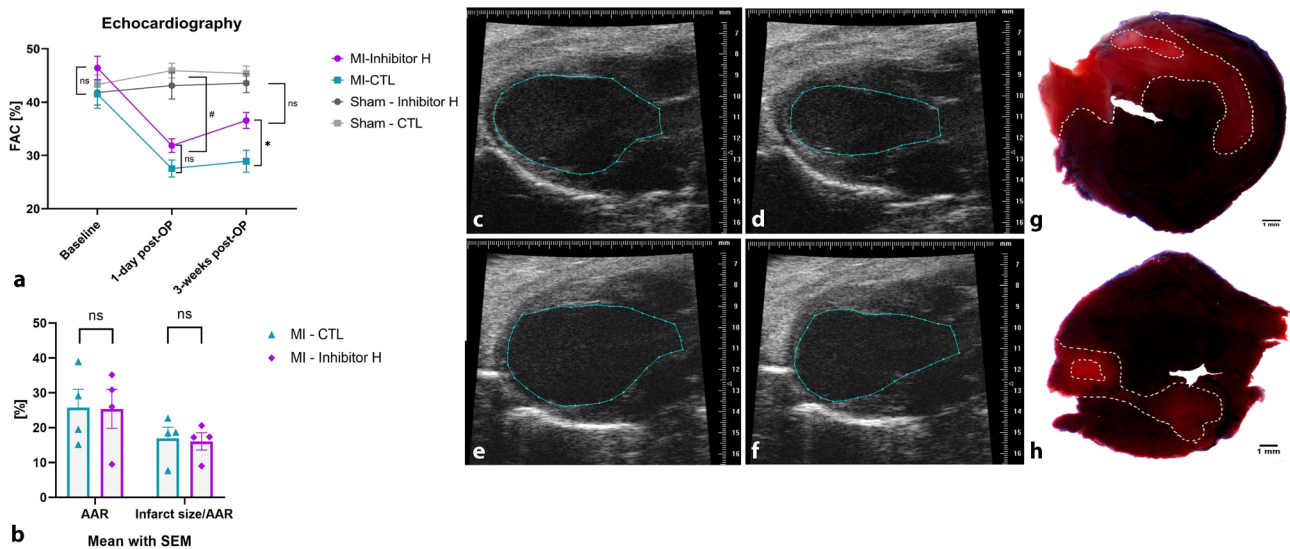


Fig. 112.12 Echocardiography and Infarct size. Sham-CTL (Sh-C), Sham-Inhibitor H (Sh-I); MI-CTL (M-C); MI-Inhibitor H (M-I). **a** Echocardiography: Four different groups, Inhibitor H treated group and with control (CTL) substance treated, each with an MI and as Sham operated groups. Echocardiography before operation (baseline), one day after operation and after 3 weeks right before end of experiment. 30 min Ligation followed by reperfusion and daily injections. FAC: endocardial systolic fractional area change. Statistics with two-way ANOVA. Baseline: No significant difference at baseline within all groups. Day 1: No significant difference within the operated groups and within the Shams. a significant difference between the M-I and the SH-I ($p=0.0426$), between M-C and Sh-I ($p=0.0065$), highly significant difference ($p<0.0001$) between M-I and Sh-C as well as between M-C and Sh-C. 3 weeks: no significant difference between M-I and Sh-I as well as between the two Sham groups. Significant differences between M-I and M-C ($p=0.0454$), M-I against Sh-C ($p=0.0055$), M-C against Sh-I ($p=0.0007$) and highly significant between M-C and Sh-C ($p<0.0001$). **b** Quantification of infarct size 1 day after 30 min ligation and afterward reperfusion, treated with Inhibitor H and CTL; Statistics: ARR: Mann-Whitney U test, Infarct size/AAR: unpaired t test; $n=4$ per group. Area at risk (AAR); no significant difference. Infarct size normalised to AAR; no significant difference. **c** Echocardiography parasternal long axis after 3 weeks in diastole, Inhibitor H. **d** Echocardiography parasternal long axis after 3 weeks in systole, Inhibitor H. **e** Echocardiography parasternal long axis after 3 weeks in diastole, CTL. **f** Echocardiography parasternal long axis after 3 weeks in systole, CTL. **g** 1 mm heart slice of CTL treated MI stained with Evans blue and 2,3,5-Triphenyltetrazolium chloride (TIC). **h** 1 mm heart slice of Inhibitor H treated MI stained with Evans blue and 2,3,5-Triphenyltetrazolium chloride (TIC)

advance our knowledge and understanding of circRNA regulation during acute MI.

2.12

STING-Inhibition after myocardial infarction

L. Rech¹, M. Abdellatif¹, M. Pöttler¹, V. Stangl¹, E. Ulcar¹, M. Gülen², A. Ablasser², P.P. Rainer¹

¹Medizinische Universität Graz, Graz, Austria

²Ecole Polytechnique Fédérale de Lausanne, Lausanne, Switzerland

Introduction: Myocardial infarction (MI) is one of the prevalent causes of death in the world, with some patients developing heart failure from myocardial remodelling after infarction. Inflammatory processes trigger remodelling post-MI. One inflammatory factor is Type 1 Interferon which can be released by cytosolic dsDNA, sensed via the STING-receptor. The aim of this study was to reduce this inflammatory response by inhibiting the STING-receptor and thus reduce post-infarctional remodelling.

Methods: Surgery was performed to trigger infarction for 30 minutes by ligating of the proximal LAD in 22 wildtype male mice (C57BL6/J), another 10 mice have undergone sham operation. Echocardiographic assessment of the endocardial systolic fractional area change (FAC) was carried out before, one day after and three weeks after surgery. The mice with ligation

were separated into two groups with eleven individuals each, as well as the sham operated mice in five each group. One group was treated with the STING-Inhibitor while the other received a control substance. Treatment was applied intraperitoneally once per day for three weeks.

Results:

- Procedural success was good as evidenced by immediate FAC decline in MI animals.
- One day post-op no significant difference in FAC and infarct size can be seen between the two groups of MI mice
- Three weeks post-op a highly significant difference in FAC can be observed in the group treated with STING-Inhibitor compared to the control group in the MI mice
- The sham operated mice never showed any difference between the groups at any time.
- Fibrosis and Cross sectional area were significantly reduced in treated MI group compared to control

Conclusion: STING-Inhibitor potentially improves outcome after a myocardial infarction.

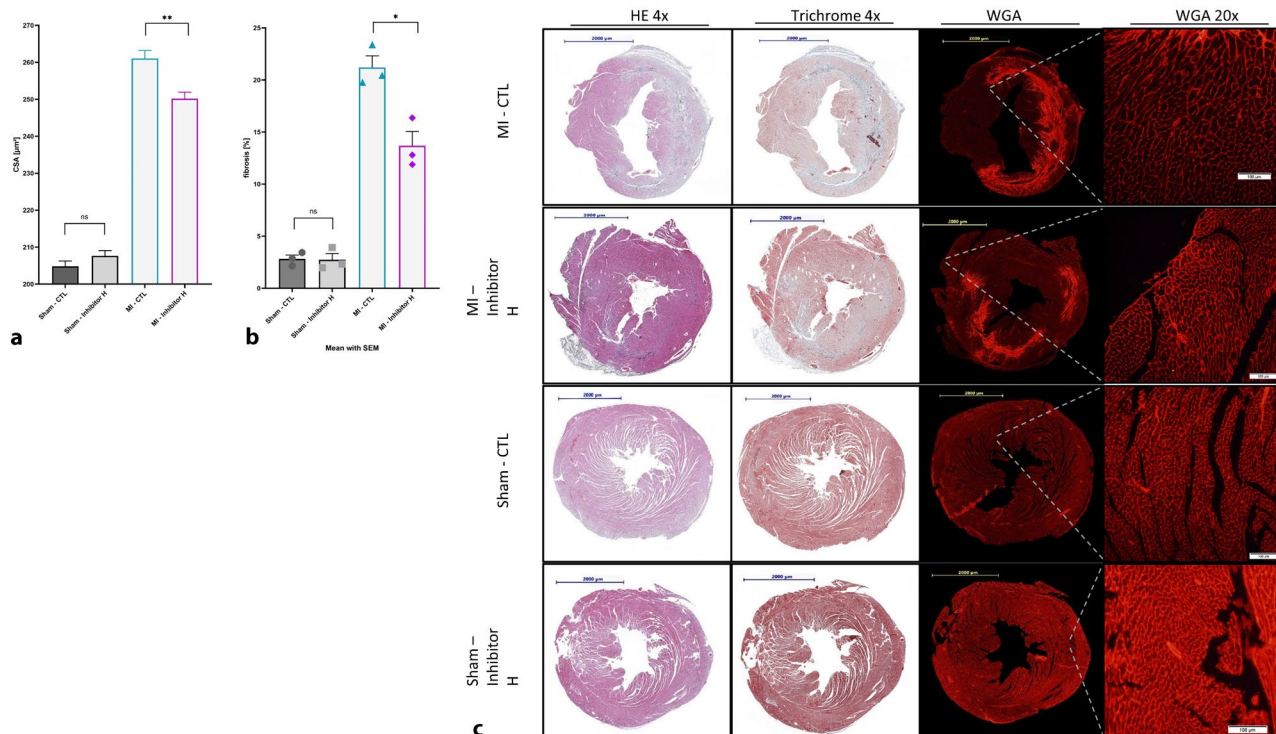


Fig. 212.12 Fibrosis and Cross sectional area. A cell surface area quantified by WGA ICH staining ($n=3$ per group; in average >1100 cells per n). No significance in between the Sham groups, highly significantly difference ($p < 0.0001$) between all Sham groups compared to all MI groups, great significant difference between both MI groups ($** p = 0.0016$); Kruskal-Wallis test. b fibrosis quantified by Masson Trichrom staining ($n=3$ per group). No significance in between the Sham groups. Significant between Sh-C and M-C ($p < 0.0001$), Sh-C and M-I ($p = 0.0016$), Sh-I and M-C ($p = 0.0001$), Sh-I and M-I ($p = 0.0018$), as well as M-C and M-I ($* p = 0.0129$); tTest. c Examples slides for each group in HE staining, Masson Trichrome staining and WGA ICH staining. Scale bar 2 mm (2000 p.m) in 4x; scale bar 100 p.m in 20x

2.13

Identifying of circulating miRNAs responsible for acute myocardial ischemia-related malignant ventricular arrhythmias in a translational study

M. Riesenhuber¹, A. Spannauer¹, D. Traxler¹, K. Zlabinger¹, D. Lukovic¹, N. Kastner¹, E. Hašimbegović¹, J. Mester-Tonczar¹, S. Batkai², T. Thum², M. Gyöngyösi¹

¹Medizinische Universität Wien, Universitätsklinik für Innere Medizin II, Klinische Abteilung für Kardiologie, Wien, Austria
²Cardior Pharmaceuticals GmbH, Hannover, Germany

Introduction: Peri-infarction malignant ventricular arrhythmias are responsible for the vast majority of sudden cardiac deaths. Conduction properties of myocardial tissue are tightly regulated at the genetic and protein expression level. MicroRNAs are powerful post-transcriptional regulators of mRNAs translation and can be investigated using deep sequencing technologies. In our large animal model of reperfused acute myocardial infarction (AMI) we have observed ventricular arrhythmias (often leading to ventricular tachycardia (VT) and fibrillation (VF)) during the first 20–25 min of coronary occlusion. We hypothesized that acute ischemic myocardial tissue releases miRNAs, playing a role in induction of malignant ventricular arrhythmias. The aim of this project is to identify circulating miRNAs associated with early peri-infarction ventricular tachycardia and fibrillation.

Methods: Closed-chest reperfused AMI was induced in 114 domestic pigs by occlusion of the mid LAD for 90 minutes, followed by reperfusion. Blood samples were collected routinely 25 min after initiation of coronary occlusion or at the start of ventricular arrhythmias before medical treatment or cardioversion. Cardiac MRI was performed after 3 days. Out of 114 pigs, 14 suffered from VT or VF, and 2 died before cardiac MRI was completed (Arrhythmia-Group). 14 pigs without arrhythmias (Non-Arrhythmia-Group) were matched to the Arrhythmia-Group for left ventricular (LV) end-diastolic volume (ml), ejection fraction (%), LV mass (ml), and scar (% of LV mass). After isolating miRNA from EDTA-plasma, next-generation sequencing was conducted for 28 samples (14 per group, false discovery rate <0.1). Expression levels are reported as counts per million reads (CPM). Targeted genes for differentially expressed miRNAs were combined with Gene Ontology analysis with terms associated with cardiac conduction and arrhythmia. All genes with interaction between differentially expressed miRNAs and cardiac conduction/arrhythmia were outlined in Fig. 1.

Results: Cardiac MRI resulted in similar LV parameter: LV end-diastolic volume 52.6 ± 10.4 ml vs. 53.1 ± 7.7 ml, LV ejection fraction 43.8 % ± 10.7 vs. 42.9 % ± 8.1, LV mass 65.6 ± 11.5 ml vs. 64.0 ± 9.2 ml, scar (% of LV mass) 35.5 % ± 10.7 vs. 34.5 % ± 9.0, cardiac output 1.77 ± 0.41 l/min vs. 1.86 ± 0.42 l/min, and right ventricular ejection fraction 50.5 % ± 11.7 vs. 52.3 % ± 12.9 in the Arrhythmia-Group vs. Non-Arrhythmia-Group, respectively. MiR-4492, miR-4454, miR-363-3p, and miR-378a-3p were significantly upregulated in the Arrhythmia-Group, while miR-181d-5p, miR-181c-5p, miR-125b-5p, miR-223-3p, miR-28-3p, and miR-125b-2-3p were significantly down-regulated. Gene ontology analysis revealed association with target genes relevant for cardiac conduction and cardiac arrhythmia, displayed in Fig. 1. The most common genetic targets were myocyte potassium channels, for example KCNC2, KCNE4, KCNH6 or KCNJ11.

Conclusion: Next-generation sequencing identified 10 differentially regulated miRs between the groups. Identified

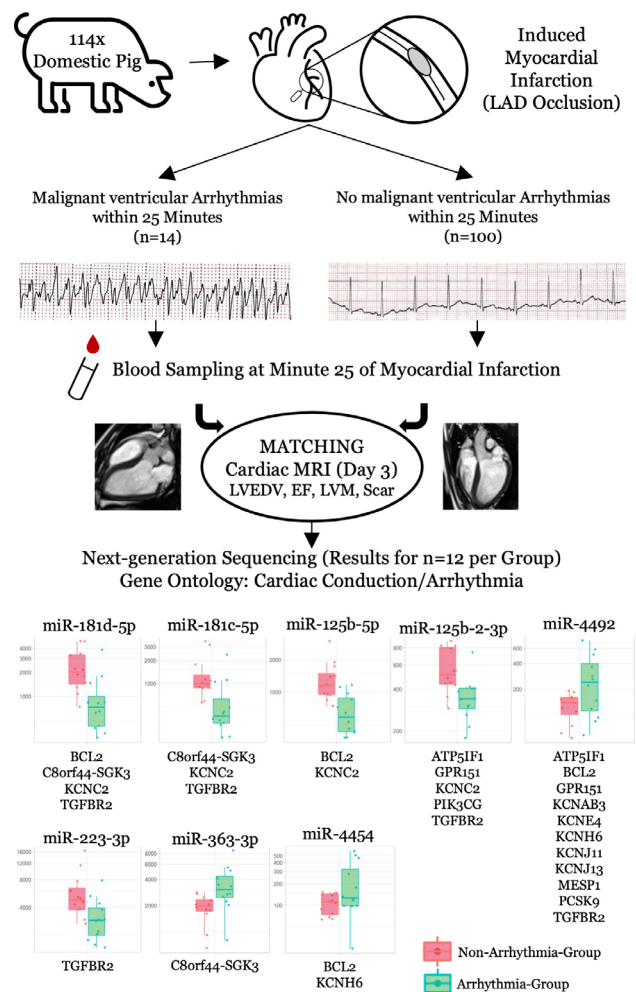


Fig. 112.13 Flowchart and results of the trial. Differentially regulated miRNAs with gene targets in the Gene Ontology analysis are displayed in counts per million reads. Gene targets are displayed below each miR

miRs will undergo large-scale qPCR testing, and the verified candidates will be potentially suitable for antagomir design and in-vivo trials to assess prevention of acute myocardial ischemia-related malignant arrhythmias. Funding: Projektbezogenes Stipendium (2019) der Österreichischen Kardiologischen Gesellschaft and Cardior Pharmaceutical GmbH (Hannover, Germany) for the pig experiments (did not influence the results).

2.14

Progesterone promotes spontaneous coronary artery dissection

J. Hirsch¹, A. Volland², A. Nikolajevic³, M. Graber¹, F. Nägele¹, L. Pölz⁴, J. Begele¹, R. Hilbe⁵, S. Lechner¹, M. Grimm¹, J. Holfeld¹, C. Gollmann-Tepeköylü¹

¹Medical University of Innsbruck, Department of Cardiac Surgery, Innsbruck, Austria

²Department of Virology, Innsbruck Medical University, Innsbruck Austria, Innsbruck, Austria

³Daniel Swarovski Research Laboratory, Department of Visceral-, Transplant- and Thoracic Surgery, Innsbruck Medical University, Innsbruck Austria, Innsbruck, Austria

⁴Medical University of Innsbruck, Department of Anatomy, Innsbruck, Austria

⁵Department of Internal Medicine II, Innsbruck Medical University, Innsbruck Austria, Innsbruck, Austria

Introduction: Spontaneous coronary artery dissection (SCAD) is a common cause of myocardial infarction (MI) in young women. Here pathologic remodelling of the coronary artery extracellular matrix (ECM) causes intimal tear, resulting in coronary occlusion and infarction. However, the underlying molecular mechanisms of SCAD are poorly understood. Mainly females are affected, with an incidence peak shortly after pregnancy. Therefore hormones might play vital role in the disease development. Accordingly a recent publication could show that Progesterone, softens the uterus to enable embryonal implantation. We therefore hypothesized that progesterone mediates the development of SCAD via ECM softening and

Methods: Human aortic smooth muscle cells (SMC) were treated with progesterone and analysed for ECM gene expression. To further elucidate the effects of progesterone on a single receptor, we performed lentiviral transfection of SMCs for stable upregulation of progesterone receptor (PR). Subsequently, ECM proteins were analysed utilizing qPCR. To identify the transcription factor responsible for ECM changes, we performed next-generation sequencing after lentiviral PR transfection and progesterone stimulation. To translate our hypothesis in vivo, we analysed uteri of mice treated with progesterone and analysed the sections for ECM alterations via Histology

Results: Progesterone regulates the transcription of a number of ECM-modulating genes including Fibrillin, MMP-9, ADAMTS5, Col4a1, Col5a1 and TGFbeta all known for their involvement in arterial dissections. RNA sequencing revealed Klf15 Foxo1 and Bcl6 as potential downstream pathways regarding ECM remodelling. In vivo, mason trichrome staining revealed progesterone treatment to be responsible for arterial degradation and leakage.

Conclusion: Progesterone induces ECM remodelling and likely predisposes coronary arteries to dissection. We thereby uncover a novel risk factor for the development of SCAD and further our understanding of this diseases development, potentially leading to novel therapeutic approaches and prevention strategies.

2.15

Use of novel strain parameters to assess anthracycline-induced cardiotoxicity

A. Spannauer¹, N. Kastner¹, J. Mester-Tonczar¹, E. Hašimbegović¹, V. Schweiger¹, D. Traxler-Weidenauer¹, M. Riesenhuber¹, J. Bergler-Klein¹, M. Gyöngyösi¹

¹Medizinische Universität Wien, Wien, Austria

Introduction: Anthracycline induced cardiotoxicity continues to be an interdisciplinary challenge for both cardiologists and oncologists. While global longitudinal strain (GLS) is finding more and more acceptance as a diagnostic and prognostic tool in anthracycline induced cardiotoxicity, other parameters can be derived from the development of longitudinal strain over the average heart cycle. Recent investigations have shown that parameters such as the appearance of early systolic lengthening, which is a passive stretching of the ventricle in the early systolic phase, is an independent predictor of cardiovascular events in STEMI patients [1]. Furthermore, the phenomenon of post-systolic shortening, which is the continued contraction of the LV after aortic valve closure, can be used to diagnose coronary artery disease and predict future cardiovascular events [2]. In this study, we have investigated whether these parameters are also affected by cardiotoxicity in a porcine model [3].

Methods: In a porcine model of cardiotoxicity, 11 pigs (sus scrofa) received either Doxorubicin (DOX, $n=5$) or Myocet (MYO, $n=6$) which is a liposomal formulation of DOX which has been shown to be less cardiotoxic than doxorubicin. Intravenous treatments of DOX or MYO were scheduled in each 21. days. After 60 days of follow up, cardiac MRIs were analyzed, including speckle tracking longitudinal, radial and circumferential strain. Additionally, the novel strain parameters of postsystolic shortening, postsystolic index and early systolic lengthening were evaluated by averaging the longitudinal strain curves from 2-, 3- and 4-chamber views for each animal.

Results: After 60 days of follow-up, the standard strain measurements of GLS (-13.0 ± 2.9 vs. -16.5 ± 1.8 , $p=0.035$), circumferential strain (-12.6 ± 5.2 vs. -18.8 ± 1.7 , $p=0.023$) and peak negative strain (-12.9 ± 2.9 vs. -16.2 ± 2.0 , $p=0.049$) differed significantly between DOX and MYO groups, favoring MYO. End systolic strain (-12.5 ± 2.9 vs. -16.2 ± 2.0 , $p=0.034$), wall thickness (12.2 ± 0.2 vs. 14.2 ± 1.0 , $p=0.002$) as well as novel strain parameters of postsystolic shortening (-0.5 ± 0.3 vs. -0.2 ± 0.2 , $p=0.043$) and postsystolic index (4.5 ± 3 vs. 0.9 ± 1.3 , $p=0.030$) were significantly better in MYO treated animals. No early systolic lengthening was observed in either group.

Conclusion: Our data demonstrate the usefulness of new cardiac MRI parameters to assess cardiotoxicity in chemotherapy-treated animals. Beside the standard strain parameters such as GLS and circumferential strain, which were significantly better in MYO vs. DOX, our results show that the novel strain parameter of postsystolic shortening, which was previously only associated with coronary artery disease, is also affected by anthracycline induced cardiotoxicity. Future investigations with higher sample sizes are necessary to investigate whether post-systolic shortening is a predictor of anthracycline induced cardiotoxicity independent of a reduction in GLS.

Novel strain parameters

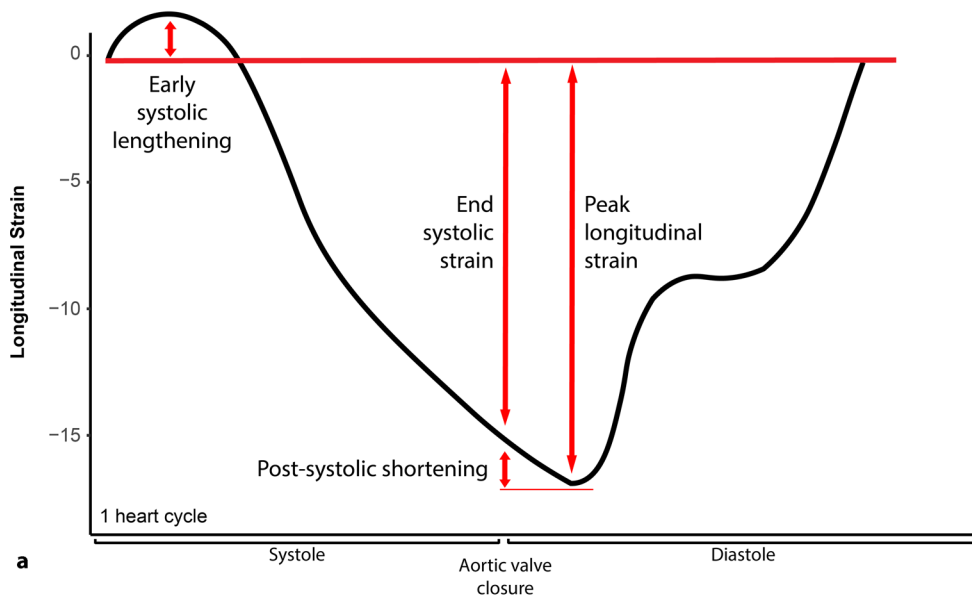
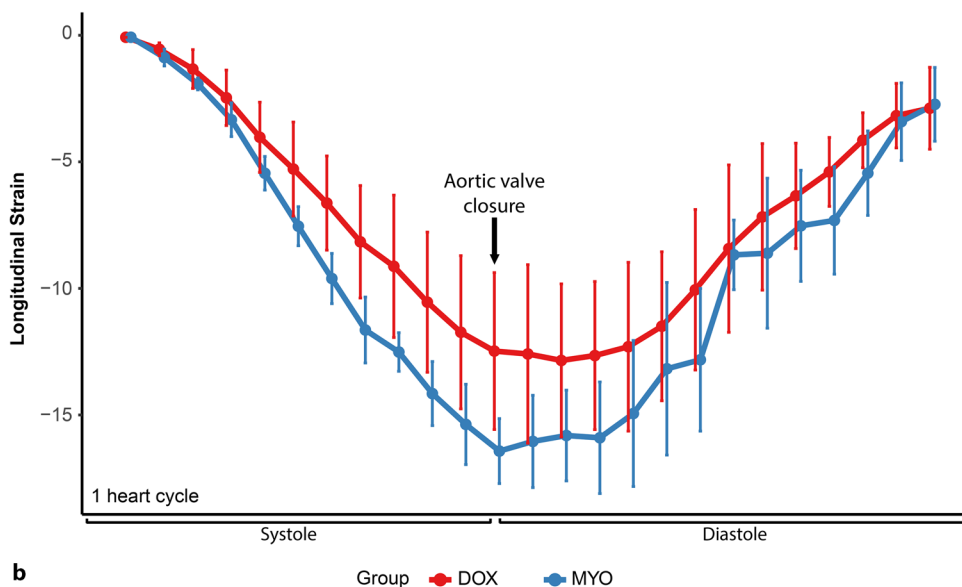


Fig. 112.15 a Schematic of the development of longitudinal strain over one heart cycle. Early systolic lengthening is a positive strain (=stretching) value early on during systole. Post systolic shortening is a continued contraction of the ventricle after closure of the aortic valve. **b** Average strain curves obtained in DOX and MYO pigs. More negative longitudinal strain denotes better LV function, which was observed in the MYO group. Notice the lack of early systolic lengthening (no longitudinal strain above 0) and the visible post-systolic shortening in the DOX group. Also notice the difference in the general shape of the strain curves

Doxorubicin vs. Myocet



b Group ● DOX ● MYO

2.16

Knockdown of AMI-related circRCAN2 with siRNA to elucidate its role during ischemia in porcine cardiac progenitor cells in vitro

N. Kastner¹, J. Mester-Tonczar¹, P. Einzinger², D. Traxler¹, E. Hasimbegovic¹, M. Riesenhuber¹, A. Spannbaauer¹, K. Zlabinger¹, M. Pavone-Gyöngyösi¹

¹Medizinische Universität Wien, Wien, Austria

²Technische Universität Wien, Wien, Austria

Introduction: Circular RNAs (circRNAs) are non-coding RNAs which functions and role in myocardial infarction are still unknown. RNA-sequencing of the long noncoding circular RNA (circRNA) in a previous pre-clinical experiment revealed that porcine myocardial infarcted tissue exerts significantly differently expressed circRCAN2 as compared to nonischemic porcine heart tissue. Since the linear transcript of circRCAN2 is linked to calcineurin signaling pathway, which is associated with activated calcium-sensitive intracellular signaling leading to heart failure, we aimed to elucidate its circular function by knock-down of circRCAN2 by siRNA.

Methods: Porcine cardiac progenitor cells (pCPCs) were cultured and characterized with immunofluorescence staining with alpha smooth muscle actin, BNP, Connexin-43, car-

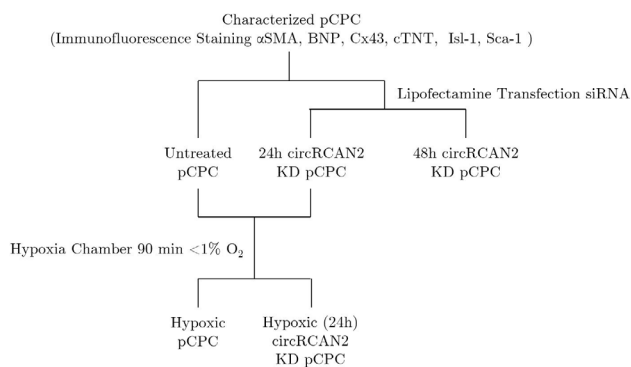


Fig. 112.16 Study Design of circRCAN2 knockdown (KD) in pCPCs

diac Troponin T, Islet-1 and Sca-1. A knockdown siRNA was designed to range over the backsplice junction of circRCAN2, not affecting the linear transcript of RCAN2. Cells were transfected with siRNA using Lipofectamine LTX with PLUS reagent for 24 hours (group 24 h-KD-pCPC) or 48 hours (group 48-KD-pCPC). To simulate ischemia, untreated (group Hyp-pCPC) and 24 hours transfected pCPCs (group Hyp-24-KD-pCPC) were placed in hypoxia chamber (<1 % O₂) for 90 minutes to analyze the effects of circRCAN2 knockdown on hypoxic pCPCs cell function (Fig. 1). Expression of circRCAN2 was measured with RT-qPCR, as well as proliferation and cytokinesis markers Ki67 and RhoA and apoptosis marker Cas3 of the experimental groups. Metabolic activity was analyzed with a MTT assay in all samples. Each experiment was repeated with pCPCs from three different pigs, each in four technical replicates.

Results: Native cultured pCPCs showed expression of cell specific markers. Lipofectamine transfection with a high concentration of siRNA achieved knockdown of circRCAN2 in pCPCs, with significantly ($p < 0.01$) downregulated circRCAN2 expression after 24 h and 48 h when compared to the untreated pCPCs. Proliferation markers Ki67 and RhoA were significantly upregulated in normoxic knockdown pCPCs (groups 24 h-KD-pCPC and 48-KD-pCPC) in comparison to untreated pCPCs, which effect was completely abolished after hypoxia. Knockdown of circRCAN2 did not affect the expression of the apoptosis marker Cas3 under normoxia, but it led to significant downregulation of Cas3 expression under hypoxia (Fig. 2). The MTT assay revealed that the circRCAN2 knockdown in the pCPCs did not significantly alter metabolic activity of the pCPCs neither under normoxic, nor hypoxic conditions.

Conclusion: Knockdown of circRCAN2 in pCPCs led to significant upregulation of the proliferation markers Ki67 and RhoA under normoxic condition, while additional hypoxia revoked it, and resulted in downregulation of the apoptosis marker. Our data suggest a promising opportunity for circRCAN2 as new therapeutic target in patients with heart failure of ischemic and non-ischemic origin.

2.17

Make it right: reverse cardiac remodeling

L. Pölzl¹, J. Hirsch¹, J. Eder¹, S. Lechner¹, F. Nägele¹, M. Graber¹, V. Schweiger¹, R. Gronauer², H. Hackl², M. Grimm¹, J. Holfeld¹, C. Gollmann-Tepeköylü¹

¹Universitätsklinik für Herzchirurgie Innsbruck, Innsbruck, Austria

²Institute of Bioinformatics, Medizinische Universität Innsbruck, Innsbruck, Austria

Introduction: Progressive fibrosis results in myocardial stiffening and dysfunction in patients with heart failure contributing to ventricular remodeling and impaired contractility. Despite high global burden and intensive research, there are no therapies available to remove excessive fibrosis and thus, induce reverse remodeling. The right (RV) and the left ventricle (LV) differ markedly in their embryonic development, anatomy and function. In this project we aimed to (a) elucidate mechanistic differences between RV and LV regeneration and (b) thus, reveal novel therapeutic targets for LV regeneration.

Methods: LV and RV heart failure were induced using absorbable sutures in a murine transaortic constriction (TAC) or pulmonary artery banding (PAB) procedure. Sutures were absorbed after 2 weeks, mimicking afterload relieve. Right and left ventricular function and mass were evaluated weekly via transthoracic echocardiography during a 4-week follow-up. Hearts were harvested and analyzed for cardiomyocyte size, myocardial thickness and myocardial fibrosis in histological sections. LV and RV were subjected to next generation RNA sequencing. To determine the adaption of the RV upon birth, hearts of newborn mice were harvested on day 1, 3, 7 and 14. Micro-CT and histological analysis were performed for evaluation of structural changes in myocardial thickness and myocardial fibrosis upon birth.

Results: Surgical bandings resulted in an increase of the mean gradient over the aorta or the main pulmonary artery

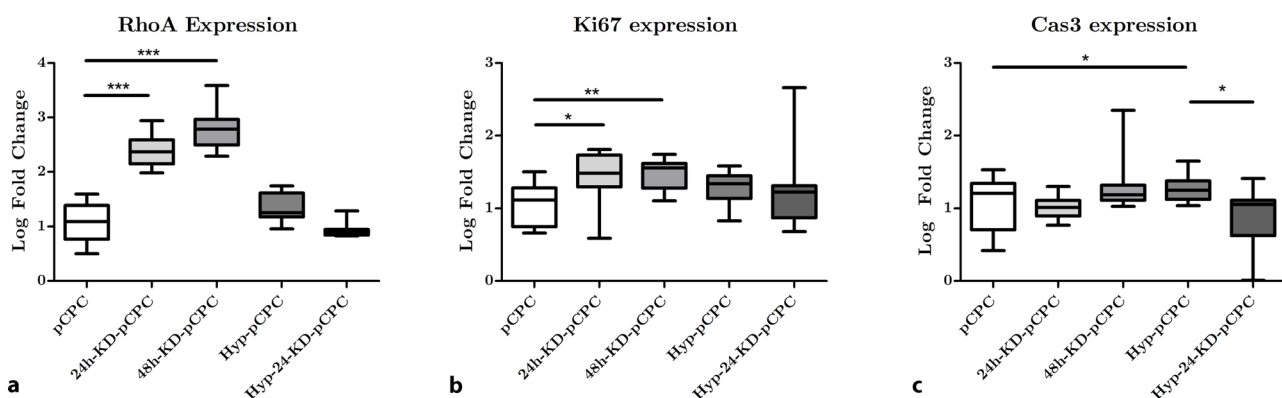


Fig. 212.16 Log Fold Changes of Gene Expression in pCPC (untreated normoxic pCPC), 24 h-KD-pCPC (24 h knockdown of circRCAN2 of pCPCs), 48 h-KD-pCPC (48 h knockdown of circRCAN2 of pCPCs), untreated Hyp-pCPC (hypoxic pCPCs) and Hyp-24-KD-pCPC (24 h knockdown of circRCAN2 of pCPCs). A) RhoA expression. B) Ki67 expression. C) Cas3 expression

respectively. RV and LV free wall thickened for 35.81 % or 31.44 % due to the increased afterload within 2 weeks. Absorption of bandings resulted in a reduction of the mean gradient to base line levels. Upon afterload relieve myocardial mass of the left ventricle remained increased after 4 weeks (23 %), however, the right ventricle remodeled to baseline level thickness. Next-generation RNA sequencing revealed differential gene expression profile of left and right ventricle upon afterload relieve. Within first days of life, the afterload of the RV decreased markedly due to the adaptation of the circulatory system. Micro-CTs showed a significant reduction of RV thickness between day 1 and day 3 after birth without any signs of fibrosis.

Conclusion: The RV remodels without any signs of fibrosis in contrast to the LV. This might be due to an innate mechanism necessary for physiological remodeling after birth. Gene expression profiles differ markedly between RV and LV upon afterload relieve. Understanding the mechanism of RV remodeling could reveal novel therapeutic targets to promote LV remodeling.

2.18

Dapagliflozin triggers left ventricular reverse remodeling in a mouse model of pressure overload-induced hypertrophy

N. Baumgartner¹, P. M. Pilz¹, L. Weber¹, P. L. Szabo¹, Z. Arnold¹, A. Kiss¹, B. K. Podesser¹

¹Ludwig Boltzmann Institute for Cardiovascular Research at the Center for Biomedical Research, Medical University of Vienna, Wien, Austria

Introduction: Regression of left ventricular (LV) hypertrophy due to mechanical unloading e. g. aortic valve replacement is characterized by a marked reduction in left ventricular mass (LVM) and the improvement of cardiac function. Recently, the new antidiabetic drugs, sodium-glucose-cotransporter-2(SGLT2) inhibitors have shown favorable effects on cardiac function among heart failure patients without diabetes. However, the underlying signaling mechanism and whether SGLT2 inhibition stimulates reverse remodeling upon LV hypertrophy are still unknown. This study aimed to investigate whether SGLT2 inhibitor, Dapagliflozin (DAPA) improves LV function and regression of LV hypertrophy in a mouse model of pressure overload-induced LV hypertrophy.

Methods: Male C57BL/6J mice (body weight 20–25 g) were used. LV hypertrophy was induced by transverse aortic constriction (TAC) surgery. Mice were allocated into the following groups: 1) Sham (no TAC operation), 2) TAC for 8 weeks, 3) TAC and DAPA treatment for 8 weeks and 4) 6 weeks after TAC operation DAPA treatment started for 2 weeks. DAPA was provided via drinking water (1 mg DAPA/kg bodyweight). Echocardiography was performed to assess cardiac function and hemodynamic function was invasively measured at day of sacrifice. To further evaluate the effects of DAPA treatment on LV mass, lung congestion and kidney morphology the following parameters were measured: heart weight (HW)/body weight (BW) ratio, lung weight(LW)/BW ratio and kidney weight/BW ratio.

Results: Six and eight weeks of TAC resulted in a significant reduction in LV ejection fraction (EF) compared to Sham operated group (LVEF SHAM: 56 ± 12 % vs 8 weeks TAC 27 ± 12 %, $p < 0.05$). This was associated with an increase of LV mass and HW/BW ratio in compared to Sham group and significant increase in LV systolic pressure and end-diastolic pressure, respectively ($p < 0.05$). All these morphological and functional changes were markedly improved in mice treated with DAPA

for 8 weeks, respectively ($p < 0.05$). Notably, DAPA treatment only for 2 weeks could effectively improve LVEF and regress LV hypertrophy in comparison with 8 weeks TAC group (LVEF 8 weeks TAC: 27 ± 12 % vs 2 weeks DAPA 41 ± 11 %; LV mass: 8 weeks TAC 163 mg ± 73 mg vs 104 mg ± 20 mg, $p < 0.05$). Furthermore, DAPA treatments also markedly reduced the sign of lung congestion, respectively ($p < 0.05$).

Conclusion: In our mouse model LV hypertrophy and cardiac dysfunction was markedly improved by the administration of DAPA in a preventive indication. Most important, DAPA treatment in existing LV hypertrophy triggered and resulted in reverse remodeling referring to LV hypertrophy regression and improvement of LV function. Therefore, administration of DAPA in patients with LV hypertrophy and heart failure may be an effective therapeutic approach for boosting LV reverse remodeling.

2.19

Ivabradine rescues vascular abnormalities in a mouse model of duchenne muscular dystrophy

M. P. K. Kuruppu Appuhamilage¹, P. L. Szabo¹, S. Trojaneck², D. Abraham², K. Hilber³, B. K. Podesser¹, A. Kiss¹

¹Ludwig Boltzmann Institute for Cardiovascular Research at Center for Biomedical Research, Medical University of Vienna, Vienna 1090, Austria, Wien, Austria

²Center for Anatomy and Cell Biology, Medical University of Vienna, Vienna 1090, Austria, Wien, Austria

³Department of Neurophysiology and Pharmacology, Center for Physiology and Pharmacology, Medical University of Vienna, Vienna 1090, Austria, wien, Austria

Introduction: Duchenne muscular dystrophy (DMD) is a rare genetic disorder initiated by the absence of dystrophin and is primarily differentiated by skeletal muscle degeneration and cardiac dysfunction. More recent studies underlined the importance of vascular abnormalities such as augmented arterial stiffness and endothelial dysfunction in the progression of cardiac complications. Ivabradine, a selective inhibitor of “If” channels in the heart improves adverse left ventricular remodelling and vascular dysfunction in various cardiovascular diseases. However, whether ivabradine treatment could improve the vascular complications in DMD is largely unknown.

Methods: In this study, we examined the vascular abnormalities in both dystrophin and utrophin deficient (mdx-utr) mice, a severe and progressive animal model of DMD. Mice (4–6 weeks old) were subjected to ivabradine (10 mg/kg/day in drinking water) or vehicle treatments for 3 to 4 weeks. At the end of the treatment, aorta and lung tissue were collected to assess the vascular reactivity, employing wire myograph and angiotensin-converting enzyme (ACE) activity measurement respectively.

Results: We depict that similar to DMD patients, mdx-utr mice also exhibit vascular abnormalities and cardiac fibrosis. Ivabradine-treated mice demonstrated a significantly improved endothelium-dependent vasodilation ($p < 0.05$) and decreased vascular stiffness compared to vehicle-treated mdx-utr mice ($p < 0.01$). In addition, lung ACE activity was significantly reduced in the treated mice in comparison to the control group ($p < 0.01$) indicating less activation in the renin-angiotensin-aldosterone system, which can contribute to the progression of cardiac fibrosis and vascular dysfunction.

Conclusion: In conclusion, our study for the first time shows the beneficial effects of ivabradine on the progression of cardiac vascular complications in DMD and this may present a novel therapeutic approach.

3 BILDGEBUNG

3.1

Cardio-pulmonary transit-time by cardiac magnetic resonance imaging: associates to infarct severity and adverse events after reperfused STEMI

F. Troger¹, M. Reindl², M. Pamminger¹, C. Tiller², M. Holzknacht², I. Lechner², S. Reinstadler², A. Bauer², B. Metzler², G. Klug², A. Mayr¹

¹Universitätsklinik für Radiologie, Innsbruck, Austria

²Universitätsklinik für Innere Medizin III, Kardiologie und Angiologie, Innsbruck, Austria

Introduction: Cardiopulmonary-transit-time (cpTT) may serve as surrogate parameter for integrative cardiac performance and has been linked to heart failure. Cardiac magnetic resonance (CMR) data on cpTT and its associates with infarct characteristics and clinical outcome after reperfused ST-elevation myocardial infarction (STEMI) are lacking so far.

Methods: A total of 207 patients (179 men [87 %], median age 55 [interquartile range (IQR) 49–64] with acute STEMI underwent CMR on day 3 [IQR 2–4] and 4 months (m) [IQR 4–5] after primary percutaneous coronary intervention. cpTT was taken as the time between the peaks of time-intensity curves of gadolinium contrast to pass from the right ventricle (RV) to the left ventricle (LV). Infarct size, extent of microvascular obstruction (MVO), RV and LV dimensions and function were assessed at both occasions.

Results: cpTT decreased significantly between baseline and 4 m CMR scan (8.6 seconds [IQR 7.5–9.6] to 7.8 sec [IQR 7–8.7], respectively, $p < 0.0001$). Patients with presence of MVO had significantly prolonged cpTT at baseline and 4 m follow-up (all $p < 0.022$). According to Cox regression analysis (“functional model”) baseline cpTT (hazard ratio (HR) 1.5, 95 % confidence interval (CI) 1.1–2.2; $p = 0.008$) remained significantly associated to the occurrence of major adverse cardiac events (MACE) after adjustment for LV ejection fraction (EF) and cardiac index.

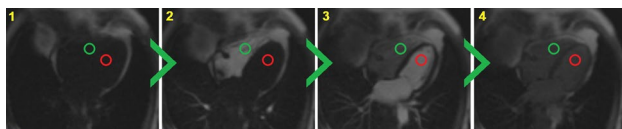


Fig. 113.1 First-pass dynamic of gadolinium-bolus through the RV (green) and LV (red)

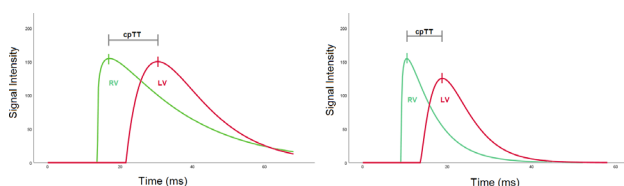


Fig. 213.1 Computation of cardio-pulmonary transit time as the time difference between peak signal intensities of RV and LV

According to Cox regression analysis (“tissue model”) baseline cpTT (HR 1.462, 95 % CI 1.02–2.09, $p = 0.039$) as well as extent of MVO (HR 1.196, 95 % CI 1.081–1.324, $p = 0.001$) remained significantly associated to MACE after adjustment for infarct size. Baseline cpTT (area under the curve [AUC]: 0.725, 95 % confidence interval [CI] 0.57–0.88; $p < 0.009$) was significantly higher for the prediction of MACE compared to LV ejection fraction (AUC: 0.686, 95 % CI 0.51–0.87; $p = 0.031$. AUC difference: 0.039, $p < 0.03$). In Kaplan-Meier analysis, cpTT ≥ 9 sec was associated with clinical adverse cardiovascular events ($p = 0.008$).

Conclusion: Following reperfused STEMI, cpTT predicts prognosis independently of infarct size and systolic function. Moreover, cpTT provides significantly higher prognostic implication in comparison with LV ejection fraction.

3.2

Safety and image quality of cardiac magnetic resonance imaging in patients with retained epicardial pacing wires after heart transplantation

C. Gatterer¹, M. Stelzmüller², A. Kammerlander¹, A. Zuckermann², M. Krššák³, C. Loewe⁴, D. Beitzke⁴

¹Medical University of Vienna, Department of Medicine II, Division of Cardiology, Vienna, Austria, Wien, Austria

²Medical University of Vienna, Department of Surgery, Division of Cardiac Surgery, Vienna, Austria, Wien, Austria

³Medical University of Vienna, Department of Medicine III, Division of Endocrinology and Metabolism, Vienna, Austria, Wien, Austria

⁴Universitätsklinik für Radiologie und Nuklearmedizin, Abteilung für kardiovaskuläre und interventionelle Radiologie, Wien, Austria

Introduction: Temporary epicardial pacing wires, implemented in patients during heart transplantation, are routinely removed before discharge. However, in some cases, these wires may remain in situ and are often considered as a contraindication for magnetic resonance imaging in the future. Therefore, we aimed to provide data about safety and image quality of cardiac magnetic resonance (CMR) in those patients.

Methods: This is a report on a subpopulation out of eighty-eight patients after heart transplantation that were included in a prospective cohort study and underwent multiple CMR in their post-transplant course. During CMR, patients were monitored by ECG and all examinations were observed by a physician to document potential adverse events. Additionally, image quality was assessed by an imaging specialist.

Results: Nineteen of 88 patients included had temporary pacing wires in situ. These patients underwent a total of 51 CMR. No major adverse event and only one single, mild sensory event could be documented. All CMR studies showed preserved diagnostic image quality. Temporary pacing wires were visible in 100 % of HASTE and CINE sequences. In less than 50 percent of the examinations, temporary pacing wires were also visible in T1 and T2 Mapping, STIR, and LGE sequences, without any impairment of image quality.

Conclusion: With a low event rate of only one mild adverse event during 51 CMR examinations (1.96 %), CMR appears to be safe in patients with retained temporary epicardial

3.3

Prognostic value of depressed cardiac index after STEMI: a phase-contrast magnetic resonance study

J. Schwaiger¹, S. Reinstadler², M. Holzknrecht², C. Tiller², M. Reindl², J. Begle², I. Lechner², C. Lamina³, A. Mayr⁴, I. Graziadei¹, A. Bauer², B. Metzler², G. Klug²

¹Abteilung für Innere Medizin, LKH Hall, Hall in Tirol, Austria
²Universitätsklinik für Innere Medizin III – Kardiologie und Angiologie, Innsbruck, Austria
³Institut für Genetische Epidemiologie, Department für Genetik und Pharmakologie, Medizinische Universität Innsbruck, Innsbruck, Austria
⁴Universitätsklinik für Radiologie, Innsbruck, Austria

Introduction: An invasively measured Cardiac Index (CI) of $\leq 2.21 \text{ l/min/m}^2$ is one of the strongest prognostic indicators after ST-elevation myocardial infarction, however knowledge is mainly based on invasive evaluations performed in the present era. Velocity-encoded Phase Contrast Cardiac Magnetic Resonance (PC-CMR) allows non-invasive determination of CI.
Methods: In this prospective study CMR was performed in 406 stable and contemporarily revascularized patients a median of 3 days after STEMI. Forward stroke volume was assessed at the level of the ascending aorta by PC-CMR. Left ventricular ejection fraction (LVEF) and global longitudinal strain (GLS) were determined by cine CMR. Major adverse cardiac events (MACE) were defined as the composite of death, myocardial infarction or hospitalization for heart failure.

Results: Median CI was 2.52 l/min/m^2 , 27 % of patients had $\leq 2.21 \text{ l/min/m}^2$. Median LVEF was 53 %, median GLS was -12.2% . During a median follow-up of 13.6 (12.1;62.9) months, 38 patients (9.3 %) experienced a MACE. A depressed CI was significantly associated with MACE after adjustment for LVEF, GLS, TIMI risk score and infarct size (HR=2.91 (95 %CI 1.39-6.07); $p=0.004$) and led to significant discrimination improvement (NRI 0.58 (95 % CI 0.21-0.94); $p=0.002$).

Conclusion: A CI of 2.21 l/min/m^2 or less as measured by PC-CMR was present in 27 % of clinically stable patients after STEMI and strongly and independently predicted medium-term MACE. The prognostic value of a depressed CI was superior and incremental to LVEF, GLS, TIMI risk score and infarct size.

3.4

Determinants and prognostic relevance of aortic stiffness in patients with recent ST-elevation myocardial infarction

I. Lechner¹, M. Reindl¹, C. Tiller¹, M. Holzknrecht¹, A. Mayr², G. Klug¹, C. Brenner¹, A. Bauer¹, S. J. Reinstadler¹, B. Metzler¹

¹Universitätsklinik für Innere Medizin III – Kardiologie und Angiologie, Medizinische Universität Innsbruck, Innsbruck, Austria
²Universitätsklinik für Radiologie, Medizinische Universität Innsbruck, Innsbruck, Austria

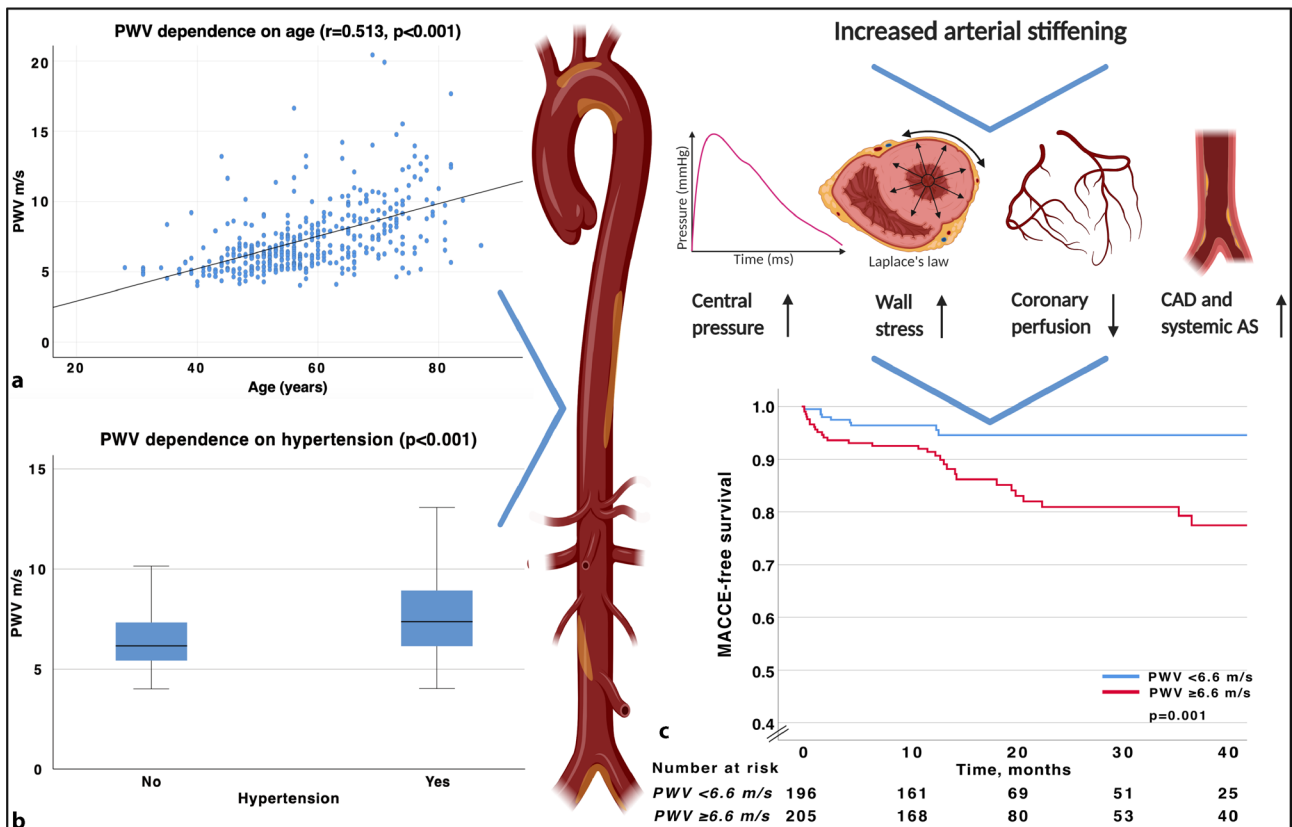


Abb. 113.4 Central Illustration (Created with Biorender)

Introduction: The association between aortic stiffness, cardiovascular risk factors and prognosis in patients with recent ST-elevation myocardial infarction (STEMI) is poorly understood. We analyzed the relationship between cardiovascular risk factors and arterial stiffening and assessed its prognostic significance in patients with recent STEMI.

Methods: We prospectively enrolled 408 consecutive patients who sustained a first STEMI and underwent primary percutaneous coronary intervention (PPCI). Aortic pulse wave velocity (PWV), a direct measure of aortic stiffness, was determined by the transit-time method using velocity-encoded, phase-contrast cardiac magnetic resonance imaging. Patient characteristics were acquired at baseline and major adverse cardiac and cerebrovascular events (MACCE) were assessed at 13 (interquartile range [IQR] 12–31) months. Cox regression and logistic regression analysis were performed to explore predictors of PWV and MACCE.

Results: Median aortic PWV was 6.6 m/s (IQR 5.6–8.3 m/s). In multivariable analysis, age (odds ratio [OR] 1.10, 95 % confidence interval [CI], 1.08–1.14, $p < 0.001$) and hypertension (OR 2.45, 95 % CI, 1.53–3.91, $p < 0.001$) were independently associated with increased PWV. Sex, diabetes, smoking status, dyslipidemia, and obesity were not significantly associated with PWV in adjusted analysis (all $p > 0.05$). High PWV significantly and independently predicted occurrence of MACCE in adjusted analysis (hazard ratio [HR] 2.45, 95 % CI 1.19–5.04, $p = 0.014$).

Conclusion: In patients with recent STEMI, the impact of classical cardiovascular risk factors on aortic stiffness is mainly dependent on age and increased blood pressure. Increased aortic stiffness is associated with adverse clinical outcome post-STEMI, suggesting it as a relevant therapeutic target in this population.

3.5

Assessment of apical wall motion for optimized identification of left ventricular thrombi following st-elevation myocardial infarction

M. Reindl¹, I. Lechner¹, M. Holzknrecht¹, C. Tiller¹, A. Mayr², F. Troger², M. Theurl¹, G. Klug¹, C. Brenner¹, A. Bauer¹, B. Metzler¹, S. Reinstadler¹

¹University Clinic of Internal Medicine III, Cardiology and Angiology, Medical University of Innsbruck, Innsbruck, Austria

²University Clinic of Radiology, Medical University of Innsbruck, Innsbruck, Austria

Introduction: Compared with transthoracic echocardiography (TTE), cardiac magnetic resonance (CMR) imaging has a considerably higher sensitivity for left ventricular (LV) thrombus detection in patients after ST-elevation myocardial infarction (STEMI). However, CMR imaging is not routinely available to screen all STEMI patients. The aim of this study was to establish a simple and robust TTE algorithm that identifies specific patients for additional CMR to optimize LV thrombus detection post-STEMI.

Methods: In total, 659 consecutive STEMI patients underwent TTE and CMR 3 (interquartile range:2–4) days after infarction (median time difference between both modalities 0.5 days). LV ejection fraction (LVEF) and two different apical wall motion scores (AWMS), one using the 17-segment-model (AWMS17Seg) and one using the 16-segment-model (AWMS16Seg), were evaluated by TTE. Primary endpoint was defined as presence of LV thrombus by CMR.

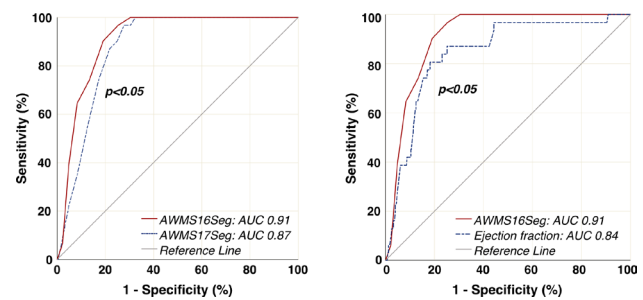


Fig. 113.5

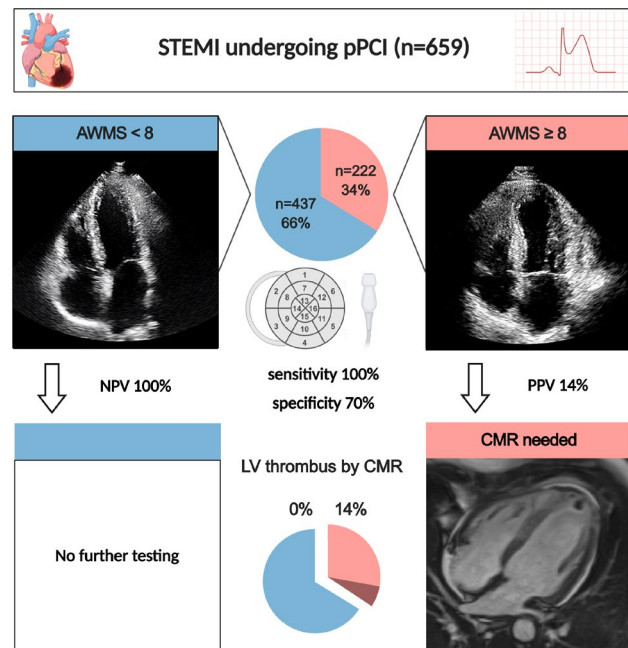


Fig. 213.5

Results: A LV thrombus was present in 31 patients (5%). The AWMS16Seg showed highest predictive value (area under the curve [AUC]:0.91 [95 %CI:0.89–0.93]; $p < 0.001$), which was significantly higher (both p -values for difference: < 0.05) compared to LVEF (AUC:0.84 [95 %CI:0.82–0.87]; $p < 0.001$) and AWMS17Seg (AUC:0.87 [95 %CI:0.85–0.90]; $p < 0.001$). The relation between AWMS16Seg and LV thrombus remained significant after adjustment for LVEF and AWMS17Seg (odds ratio 1.65 [95 %CI:1.16–2.35]; $p = 0.006$) as well as for clinical (hypertension, hyperlipidemia, peak troponin) and angiographic (culprit lesion, post-interventional TIMI flow) predictors of LV thrombus (both $p < 0.001$). Dichotomization at AWMS16Seg ≥ 8 ($n = 222$, 34 %) allowed detection of all LV thrombi (sensitivity:100 %), with a corresponding specificity of 70 % (negative and positive predictive value 100 % and 14 %, respectively).

Conclusion: AWMS16Seg by TTE served as simple and very robust predictor of CMR-verified LV thrombi post-STEMI. An AWMS16Seg-based TTE algorithm to identify patients for additional CMR imaging offers great potential to optimize detection of LV thrombi following STEMI.

3.6

Prevalence and outcomes of cardiac amyloidosis in all-comer referrals for bone scintigraphy

C. Nitsche¹, K. Mascherbauer¹, T. Wollenweber², M. Koschutnik¹, C. Dona¹, V. Dannenberg¹, A. Kammerlander¹, F. Hofer¹, C. Hengstenberg¹, M. Hacker², J. Mascherbauer¹

¹Medical University of Vienna – AKH of Vienna – Cardiology Clinic, Wien, Austria
²Medical University of Vienna – AKH of Vienna – Nuclear Medicine Clinic, Wien, Austria

Objectives: Cardiac amyloidosis (CA) is increasingly identified as a cause of heart failure due to diagnostic advances and enhanced disease awareness. Screening ascertainment have unveiled a significant proportion of (coexisting) CA for various cardiac conditions, but the true prevalence of CA in the general population as well as prognostic implications remain unknown.

Methods: Consecutive all-comer referrals for 99mtechnetium-3,3-diphosphono-1,2-propanodicarboxylic acid (DPD) bone scintigraphy between January 2010 and August 2020 were included retrospectively. CA was defined as positive cardiac tracer uptake (Perugini grade 0: negative; grades 1 to 3: increasingly positive). Owing to the study design, CA subtype (transthyretin vs. light chain) was not assessed. Indications for DPD, laboratory, and clinical data were retrieved from medical records. Mortality was captured from the Austrian death registry. Combined hospitalization for heart failure (HHF) and all-cause death was defined as study endpoint. Outcome analysis was performed using Kaplan Meier estimates and multivariate Cox regression.

Results: 17.202 scans from 11.549 subjects (61.2 ± 16.1 y/o, 62.9 % female, 73.7 % cancer patients) were analyzed. Follow-up scans for patients with >1 test yielded identical Perugini grades in all cases. Prevalence of CA for the overall population was 5.5 % (n=638/11.549; grade 1: 4.0 %, grade 2/3: 1.5 %), increased with age (<60 y/o: 2.5 %, 60–70 y/o: 5.4 %, 70–80 y/o: 7.6 %, >80 y/o: 14.2 %, p < 0.001, Fig. 1), and was higher in men vs. women (7.4 % vs. 4.4 %, p < 0.001). Also, CA was more prevalent in cardiac (19.1 %, n=207/1081) vs. non-cardiac referrals (4.1 %, n=431/10.468; p < 0.001). Across all age groups of non-cardiac referrals, CA patients more often had atrial fibrillation and cardiomyopathy, and displayed worse renal function (p for all < 0.05). Following DPD, 3490 patients (30.2 %) had reached the study endpoint (84 HHF, 3313 death, 93 both) after 5.9 ± 3.3 years. By Kaplan Meier estimates, the presence of CA among all-comers predicted adverse outcomes (log-rank, p < 0.001, Fig. 1).

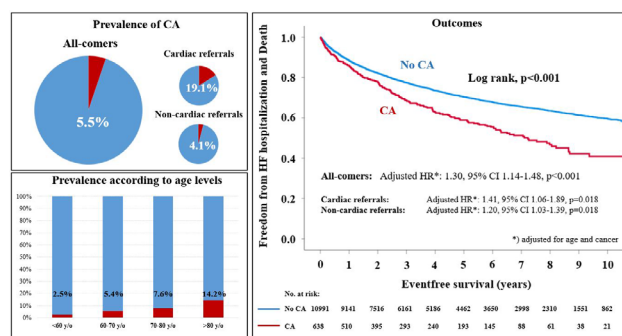


Fig. 113.6 Prevalence and outcomes of cardiac amyloidosis (CA) in bone scintigraphy referrals

After adjustment for age and cancer, CA remained significantly associated with outcomes by multivariate Cox regression (hazard ratio [HR]: 1.30, 95 % confidence interval [CI] 1.14–1.48, p < 0.001). This effect was consistent across subgroups of cardiac (HR: 1.41, 95 % CI 1.06–1.89, p = 0.018) and non-cardiac referrals (HR: 1.20, 95 % CI 1.03–1.39, p = 0.018). Outcomes were similar in grade 1 vs. 2/3 CA patients (p > 0.05).

Conclusion: Cardiac tracer uptake is present in 1 in 20 patients referred for bone scintigraphy, and independently predicts prognosis—even in this population with significantly reduced life expectancy due to the high rate of malignancy. With novel CA-specific drugs available—especially for transthyretin CA—diagnosis of CA is even more crucial to improve patient outcomes.

3.7

Towards reducing segmentation labeling costs for CMR imaging using explainable AI

A. Stria¹, A. Agibetov¹

¹Institut for Artificial Intelligence and Decision Support, Medizinische Universität Wien, Wien, Austria

Introduction: Segmented cardiac magnetic resonance (CMR) images allow us to computationally quantify important morphological and pathological changes, such as stroke volume or ejection fraction. These features are essential in cardiac disease quantification and non-invasive pre-clinical diagnosis [1]. To facilitate the computation of such features, deep-learning-based cardiac segmentation algorithms have been recently proposed in the literature [2–4]. While these algorithms promise the creation of (semi-)automatic segmentation tools, their successful application is heavily conditioned on the availability of large amounts of labeled segmented data. Unfortunately, obtaining segmented MR images is a tedious and time-consuming delineation task that represents a big challenge in the cardiac imaging domain. Here we present our preliminary results and a vision, funded by the ÖKG Forschungsstipendium, for a computational framework to reduce sample size-dependence for automated segmentation in CMR imaging. Our main hypothesis is that a (pre-trained) AI classification model could be used as a template for segmentation labels. The segmentation framework

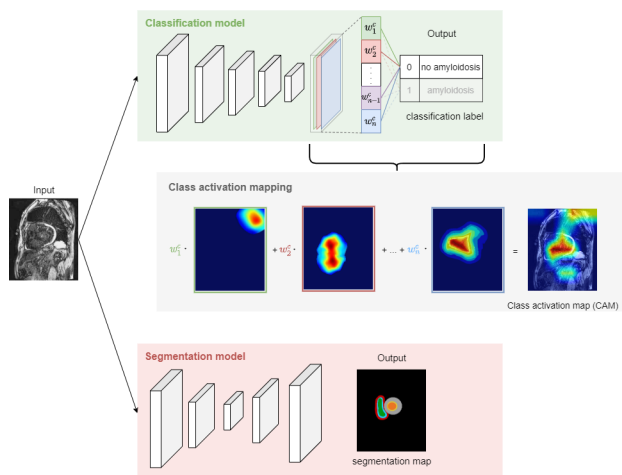


Fig. 113.7

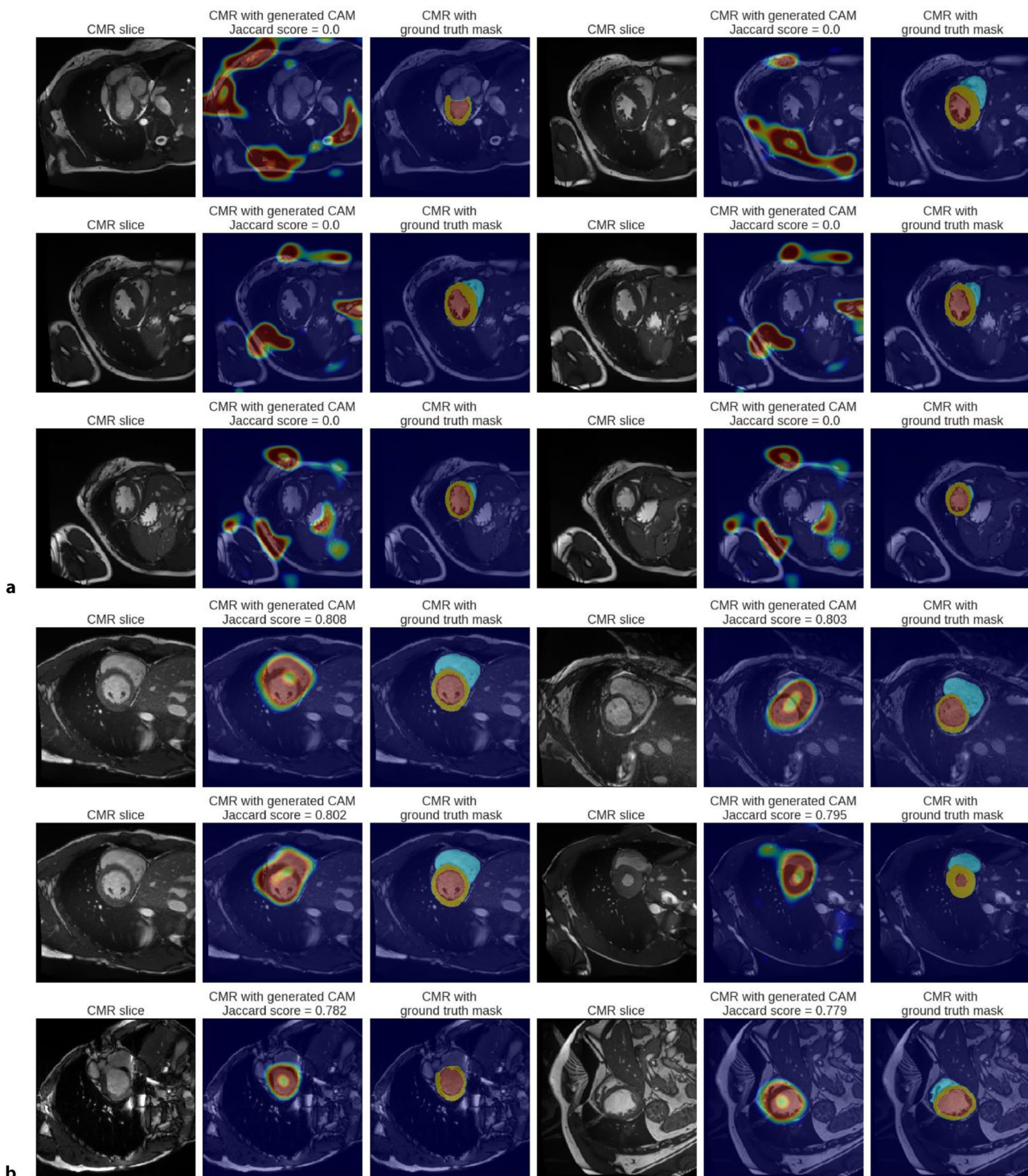


Fig. 213.7

uses the anatomical priors extracted from a classification model with explainable artificial intelligence (XAI) techniques.

Methods: The proposed methodology re-purposes a pre-trained classification model by obtaining the class activation maps (CAMs [5]) as segmentation priors. CAM is an explainable AI technique that generates a localization map, which highlights the important regions of the image with respect to the prediction of the deep learning model. These proxy labels guide the training process of a segmentation model, by penalizing the algorithm whenever it proposes segmentation maps that dif-

fer too much from the anatomical prior. For development and evaluation, the Automatic Cardiac Diagnosis Challenge (ACDC) dataset from the University Hospital of Dijon is used. We took cine MR images from 100 patients, which are split equally into five different disease groups (healthy, previous myocardial infarction, dilated cardiomyopathy, hypertrophic cardiomyopathy, abnormal right), as well as their segmentation ground truth masks for our deep learning model. We trained a convolutional neural network (CNN) as our multiclass classification model and evaluated its performance with the accuracy met-

rics, the area under the receiver-operating characteristic curve (ROC AUC) and F1-score. Then, we extracted CAMs from our classification network and compared them to the ground truth using the Jaccard index. This index measures the similarity of two segmentation masks by computing the ratio of their overlapping area to their union.

Results: The ROC AUC for the five different diagnoses, normal, previous myocardial infarction, dilated cardiomyopathy, hypertrophic cardiomyopathy, and abnormal right ventricle, were 0.55, 0.41, 0.80, 0.40, 0.69, respectively. A random model would have a ROC AUC of 0.5 for either of these categories. Overall, our pre-trained classification model achieved a weighted F1 score of 0.23 for this five-class prediction problem. This is only slightly better than a pure random performance, which would have an F1 score of 0.2 for 5 categories. However, by visually examining the class activation maps of this pre-trained model we noticed that it was attending closer to the heart region as a whole. In fact, it was able to produce really good segmentation maps. On some slices, the Jaccard score was as high as 0.8, i. e., 80 % of overlap with the ground truth segmentation. Expectedly, in the worst cases, there was no overlap (Jaccard score = 0), which, actually, represents a random prior at the start of training a segmentation model. The average Jaccard index for the whole holdout test set was 0.18, i. e., 18 % overlap on all cine MR image slices.

Conclusion: Our preliminary results open a promising research direction that shows that even a far from perfect pre-trained classification model could be used to produce sensible segmentation masks, with an average overlapping index of 18 % (Jaccard score). This is particularly encouraging because the AI model was not trained on segmentation labels at all. The big assumption is that a good classification prediction model understands the underlying structure of the input image, by “attending” to the anatomic heart region in the image. We are currently testing the limits of our hypothesis and measuring the effective impact on the reduction of sample size dependency that it can bring. Compared to segmentation labels, obtaining classification labels, e. g., patient’s diagnosis, is much easier to get. Indeed, a cardiologist may need to look at a few MR slices and establish the diagnosis, whereas manual segmentation may take hours. Our generic methodology might well support the creation of automatic segmentation tools in cardiac MRI that drastically reduce the dependence on time-consuming delineation labels. Eventually, we intend to open-source our framework for the cardiological community.

3.8

Echokardiographie des rechten Vorhofes zur Abschätzung der Fibrose bei herzchirurgischen Patienten

M. Haslinger¹, V. Paar¹, P. Krombholz-Reindl², M. Neuner³, P. Jirak¹, M. Lichtenauer¹, C. Granitz¹, F. Föttinger¹, R. Seitelberger², M. Kirnbauer³, U. C. Hoppe¹, C. Dinges², L. J. Motloch¹

¹Universitätsklinikum für Innere Medizin II, PMU Salzburg, Salzburg, Österreich

²Universitätsklinik für Herzchirurgie, Gefäßchirurgie und endovaskuläre Chirurgie, PMU Salzburg, Salzburg, Österreich

³Universitätsklinik für Anästhesiologie, perioperative Medizin und allgemeine Intensivmedizin, PMU Salzburg, Salzburg, Österreich

Einleitung: Die Genese der kardialen bzw. atrialen Dysfunktion ist von mehreren Faktoren geprägt, wobei das Ausmaß der Fibrose hierbei eine wichtige Rolle spielt. Die Abschätzung des Fibrosegrades stellt eine Schwierigkeit in der klinischen Praxis dar. Echokardiographische Messungen des rechten Atriums sind eine etablierte Methode um dessen Funktion abzuschätzen. Inwieweit diese echokardiographischen Werte die histologisch gemessene Fibrose widerspiegeln, war das Ziel dieser Studie.

Methoden: 18 herzchirurgische PatientInnen (66,6 % männlich, mittleres Alter 69,3 Jahre) wurden in dieser prospektiven Studie eingeschlossen, wobei vorbekanntes Vorhofflimmern ein Ausschlusskriterium war. Im Rahmen der Herzoperation wurde Gewebe aus dem rechten Vorhof gewonnen und histopathologisch aufgearbeitet. Außerdem wurde die SMAD-3 Expression mittels Western Blot analysiert, um mögliche Zusammenhänge mit TNF-alpha abhängigen Fibrosemechanismen zu zeigen. Quantitative Messungen des rechten Vorhofes (Fläche, Volumen, Volumen/Körperoberfläche, RVEDD und TAPSE) wurden erhoben und mit den Ergebnissen korreliert.

Resultate: Echokardiographische Messungen des rechten Vorhofes wie Fläche (Durchschnitt = 18,2 ± 3,1 cm², r = 0,78, p = 0,02) Volumen (Durchschnitt = 52,7 ± 15,0 ml, r = 0,77, p = 0,03) und Volumen/Körperoberfläche (Durchschnitt = 27,9 ± 9,3 ml/m², r = 0,81, p = 0,02) waren signifikante Prädiktoren der histopathologischen Fibrose, zeigten jedoch keine Korrelation mit SMAD-3. Der rechtsventrikuläre enddiastolische Durchmesser und die TAPSE waren weder prädiktiv für das Ausmaß der Fibrose, noch zeigten sie eine Korrelation mit der Expression von SMAD-3.

Schlussfolgerungen: Die Volumetrierung und Flächenberechnung des rechten Vorhofes sind starke Prädiktoren für das Ausmaß der kardialen Fibrose. Weitere Untersuchungen über mögliche Zusammenhänge zwischen echokardiographischen Parametern und zugrundeliegender Fibrosierung sind nötig.

3.9

Evolution of myocardial tissue injury over a decade after ST-Elevation myocardial infarction: a cardiac magnetic resonance study

A. Mayr¹, G. Klug², M. Reindl², C. Tiller², M. Holzknicht², I. Lechner², M. Pamminger¹, F. Troger¹, A. Bauer², S. Reinstadler², B. Metzler²

¹Universitätsklinik für Radiologie, Innsbruck, Austria

²Universitätsklinik für Innere Medizin III, Kardiologie und Angiologie, Innsbruck, Austria

Introduction: In patients with first ST-elevation myocardial infarction (STEMI), the evolution of myocardial tissue injury parameters over a decade as assessed by cardiac magnetic resonance (CMR) has not yet been described. This study examined long-term myocardial tissue injury dynamics in STEMI patients treated with primary percutaneous coronary intervention (PCI), as well as its association with patient characteristics.

Methods: Sequential CMR studies (after 3 days [interquartile ranges (IQR) 2–4], 4 months (m) [IQR 4–5] and 9 years (y) [IQR 8–10]) were conducted in a total of 104 STEMI patients to assess left ventricular (LV) dimensions and function, infarct size and microvascular obstruction (MVO). T2* mapping was added at 9y scan to assess the presence of iron within the infarct core.

Results: Infarct size decreased progressively from 13.3 % of LV myocardial mass [IQR 6.5–20.5] to 10.2 % [IQR 5.2–16.1] to 7.7 % [IQR 2.4–12.2] (all p < 0.001), with an average reduction

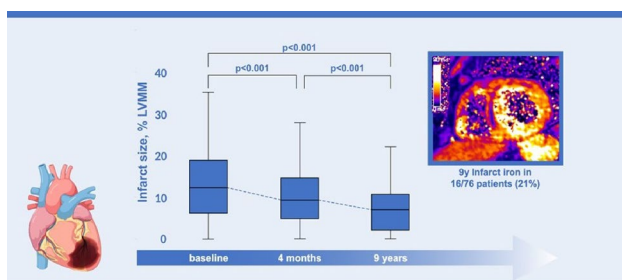


Fig. 113.9 Infarct size involution is a dynamic process beyond the first months and for several years after STEMI

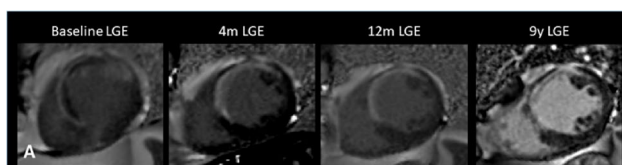


Fig. 213.9 Evolution of late gadolinium enhancement in a STEMI patient after 4 months, 12 months and 9 years

rate of 6.3 % per year [IQR 3.7–9] and a relative reduction of 43 % [IQR 18–66] over a decade. MVO was present in 60 % (60/104) of patients at baseline, but in none of the follow-up examinations. Sixteen patients (16/76, 21 %) had persistent iron within the infarct core at 9y CMR. Persistent iron was associated to a younger patient age ($p=0.022$), greater infarct size on any occasion (all $p < 0.01$) as well as presence of MVO ($p < 0.002$). Patients with persistent iron showed a lower relative regression of infarct size (34 % [IQR 24–49] versus 53 % [IQR 22–70], $p=0.037$) over a decade and greater endsystolic volumes on any occasion (all $p < 0.035$).

Conclusion: The involution of infarct size is a dynamic process that extends well beyond the first few months after STEMI. While MVO vanishes in the first few weeks, persistence of infarct iron occurs up to a decade after reperfused STEMI and is associated with initial infarct severity and worse infarct healing.

3.10

Radiation induced valvular heart disease and cardiotoxicity induced cardiomyopathy is common

R. Badr Eslam¹, M. Frey¹, C. Kronberger¹, M. Pavone-Gyöngyösi¹, M. Schneider¹, J. Bergler-Klein¹

¹Universitätsklinik für Innere Medizin II – Abteilung für Kardiologie, Wien, Austria

Introduction: Oncologic treatments allow increasing survival of malignancies such as breast cancer or lymphomas. Mediastinal radiotherapy causes direct linear damage of the myocardium, inflammatory atherosclerosis and early valve calcification depending on the field applied, typically occurring with a latency of 10–20 years after exposure to radiation therapy. This study aims to demonstrate typical findings of radiation induced valve disease (RIVD) in the long-term follow up.

Methods: Prospective patients with different malignancies or survivors of childhood cancer, after radiation therapy with or without additional chemotherapy were evaluated due to cardiac symptoms or before further chemotherapy. Transthoracic

echocardiography and speckle tracking strain were performed in all pts in our cardio-oncology clinic.

Results: 51 pts were included (37 female, 14 male). The mean age was 66.1 ± 11.6 y (35–82 y). During the study period 17 (33 %) of the pts died. In echocardiography, typical thickening and calcification of the basal and mid part of the anterior mitral leaflet, calcific aortic valve sclerosis or stenosis with intervalvular fibrosa thickening of the aorto-mitral curtain and mitral ring calcification were observed in most patients, leading to valve stenosis and/or regurgitation. Mean LVEF was 54 % (29–70 %). Cardiotoxic cardiomyopathy with reduced systolic LVEF was present in 20 pts (39 %), reduced RVF in 15 pts (29 %). 36 pts showed typical thickening of the AMVL, sparing the leaflet tips. Thickening and typical sclerosis of the AV cusps was present in almost all pts. Surgical or transcatheter AVR was performed in 15 pts (29 %) and 9 pts underwent MVR (18 %). Concomitant coronary disease with simultaneous CABG or PCI was frequent, as well as peripheral atherosclerosis of the carotids, subclavian artery or aorta, or presence of porcelain aorta.

Conclusion: Thickening of mitral valve and calcification of aortic valve are common after thoracic or mediastinal irradiation, typically leading to aortic stenosis and stiffening of the anterior mitral leaflet. After chemotherapy, cardiotoxicity induced cardiomyopathy is often present in addition. After radiation, echocardiography should be performed regularly after 5–10 years. AVR or MVR/MV repair if feasible are accompanied by increased surgical risk. Interventional techniques e.g. TAVR are an enticing option pending mitral, coronary and peripheral comorbidities.

3.11

Hepatic T1-times on cardiovascular magnetic resonance imaging reflect liver fibrosis and predict outcome in an all-comer cohort

K. Mascherbauer¹, C. Donà¹, M. Koschutnik¹, C. Nitsche¹, V. Dannenberg¹, C. Bardach¹, D. Beitzke¹, C. Loewe¹, J. Mascherbauer¹, C. Hengstenberg¹, A. Kammerlander¹

¹Medizinische Universität Wien, Wien, Austria

Introduction: Non-alcoholic fatty liver disease (NAFLD) is associated with dismal outcomes in patients with cardiac disorders but infrequently assessed by cardiologists. Cardiovascular magnetic resonance (CMR) is evolving as one-stop-shop imaging modality in cardiology, allowing for non-invasive myocardial tissue characterization by T1-mapping. On standard CMR exams, hepatic tissue is also assessable on T1-maps. However, it is unknown whether hepatic T1-times are associated with 1) myocardial T1-times, 2) established NAFLD scores, and 3) outcomes in patients referred for CMR.

Methods: In consecutive patients undergoing CMR we assessed hepatic and myocardial T1-times, and the NAFLD Fibrosis Score (NFS). Correlation analyses were used to test the association between hepatic and myocardial T1-times as well as the NFS. We used Kaplan-Meier estimates and Cox-regression models to investigate the association between hepatic T1-times and a composite endpoint of heart failure hospitalization and cardiovascular death.

Results: 513 patients were included (57 ± 18 y/o, 49 % female). Hepatic T1-times were 588 ± 98 ms on average and were correlated with myocardial T1-times ($r=0.42$, $p < 0.001$) and weakly with the NFS ($r=0.11$, $p=0.04$). Patients with severe liver fibrosis or cirrhosis ($n=47$) had significantly higher

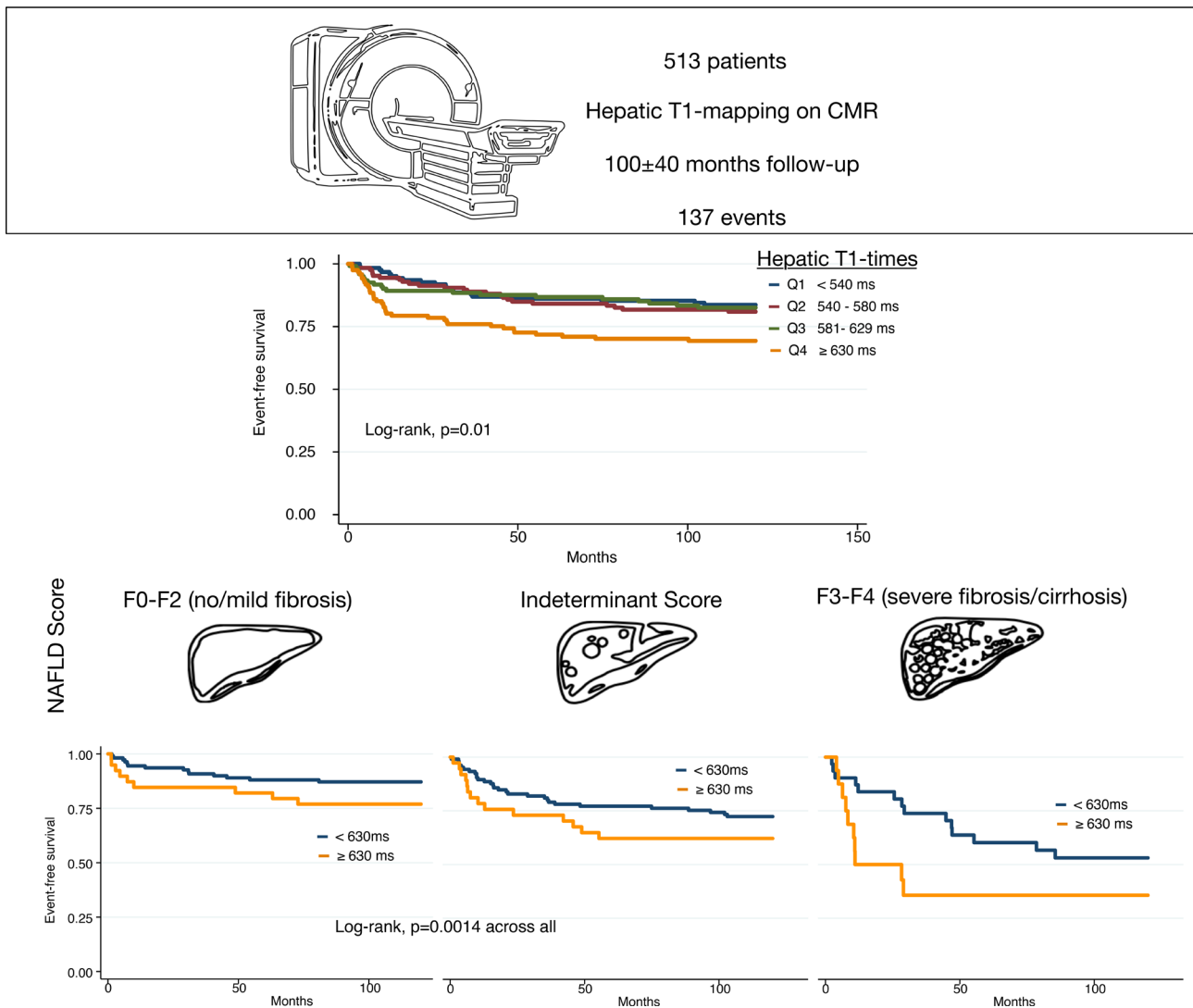


Fig. 113.11

hepatic T1-times as compared to patients with no or mild fibrosis based on the NFS (635 ± 197 ms versus 588 ± 80 ms, $p=0.02$). During follow-up (100 ± 40 months), a total of 137 (27 %) events occurred. When stratified by quartiles, patients in the highest hepatic T1-time quartile (>700 ms) were at higher risk for events compared to all other quartiles (log-rank, $p=0.01$), which was consistent across different NAFLD risk groups based on the NFS (no/mild fibrosis, indeterminant score, severe fibrosis/cirrhosis). On Cox regression analyses, higher hepatic T1-times yielded significantly higher risk estimates for events (adj. HR 1.20 [95 %CI: 1.04–1.38] per 1-SD increase, $p=0.01$) even when adjusted for age, sex, left and right ventricular ejection fractions, and myocardial T1-times.

Conclusion: Hepatic T1-times assessed on standard CMR reflect severity of NAFLD and predict outcome on top of established risk factors, including myocardial T1-times, in an all-comer CMR cohort.

3.12

Kardiale Magnetresonanztomographie bei Morbus Fabry: T1-Mapping und Strain als frühe Marker für kardiale Krankheitsprogression

C. Gatterer¹, G. Mundigler¹, D. Beitzke², C. Hengstenberg¹, G. Sunder-Plassmann³, S. Graf¹

¹Medizinische Universität Wien, Universitätsklinik für Innere Medizin II, Abteilung für Kardiologie, Wien, Österreich

²Medizinische Universität Wien, Universitätsklinik für Radiologie und Nuklearmedizin, Abteilung für kardiovaskuläre und interventionelle Radiologie, Wien, Österreich

³Medizinische Universität Wien, Universitätsklinik für Innere Medizin III, Abteilung für Nephrologie, Wien, Österreich

Einleitung: Zirka 50 % der PatientInnen mit der lysosomalen Speicherkrankheit Morbus Fabry, entwickeln im Laufe ihres Lebens eine kardiale Beteiligung, auch Fabry Kardiomyopathie genannt. Neben der Echokardiographie wird die kardiale Magnetresonanztomographie (CMR) für die Untersuchung

der PatientInnen empfohlen, da sie neben der nicht-invasiven Gewebecharakterisierung auch die morphologische und funktionelle Beurteilung erlaubt. Der myokardiale Strain, gemessen in der CMR mittels feature-tracking, konnte bereits bei anderen Erkrankungen erfolgreich für die Detektion mechanischer Dysfunktion angewandt werden. T1-Mappings, ermöglicht den Nachweis von Glykosphingolipidakkumulation im Myokard. Ziel der vorliegenden Studie war die Untersuchung der prognostischen Bedeutung der verschiedenen CMR Parameter.

Methoden: Im Rahmen des KarMA Projekts (kardiale Beteiligung bei Morbus Anderson-Fabry) wurden mittels der CMR Post-processing Software „Medis Suite MR“ CMR Sequenzen in einer Kohorte von PatientInnen mit Morbus Fabry analysiert. Linksventrikuläre Masse (LVM), endsystolisches- und enddiastolisches Volumen (LVEDV, LVESV), Ejektionsfraktion (EF), durchschnittliche T1 Relaxationszeiten des linksventrikulären Myokards (T1) sowie der globale longitudinale, regionale und zirkumferentielle Strain (GLS, GRS, GCS) des linken Ventrikels mittels feature-tracking wurden mittels CMR erhoben. Die statistischen Auswertungen beinhalten T-Test und Spearman Korrelationen.

Resultate: CMR Daten von 33 PatientInnen wurden analysiert (davon 22 Frauen). 17 PatientInnen waren zu Baseline therapie-naiv und 16 unter spezifischer Therapie. Bei 31 PatientInnen war eine zweite MRT Untersuchung möglich. Die Auswertung des myokardialen Strains zu zwei Zeitpunkten war bei 18 PatientInnen möglich. Das Durchschnittsalter betrug zum Zeitpunkt der Baseline-Untersuchung 40,8 ($\pm 16,3$) Jahre. Durchschnittliche T1 Zeiten, LVM, LVEDV, LVESV, LVEF sowie GLS, GCS und GRS blieben über den Follow-up Zeitraum von 43 (± 17) Monaten stabil. Allerdings fand sich eine signifikante Korrelation der Baseline T1 Zeiten ($967 \pm 84,5$ ms) mit den Follow-up Werten für LVM ($84,9 \pm 32,7$ g/m²; $p=0,02$, $\rho=-0,462$), LVEDV ($63,0 \pm 17,6$ g/m² $p=0,049$ $\rho=-0,398$) und GRS ($70,2 \pm 14,2$ % $p=0,011$ $\rho=-0,5$). Des Weiteren korrelierten die T1 Zeiten der Baseline Untersuchungen mit einer Veränderung der LVM ($p=0,036$ $\rho=-0,44$) und Veränderungen des GCS ($p=0,043$ $\rho=-0,618$) im Verlauf von Baseline- zu Follow-up-Untersuchung. Auch die Veränderung der T1 Zeiten zwischen den beiden Untersuchungen korrelierte mit dem GLS ($-19,47 \pm 3,57$ $p=0,044$, $\rho=-0,414$) und GRS ($69,1 \pm 18,7$ $p=0,003$, $\rho=-0,588$) zum Zeitpunkt des Follow-ups.

Schlussfolgerungen: Die Messung der T1-Relaxationszeiten, als Indikator für Glykosphingolipidakkumulation, könnte frühzeitig Veränderungen der Morphologie (LVM, LVEDV) sowie der Funktion (GRS) prognostizieren. Darüber hinaus gehen Veränderungen der T1-Zeiten mit einer Verschlechterung der linksventrikulären Funktion, gemessen mittels Strain (GLS, GCS und GRS) einher. T1-Mapping, und Feature-tracking Strain Messungen sind somit als prognostisch wichtige Parameter für das Monitoring von PatientInnen mit Morbus Fabry anzusehen.

3.13

Multimodal imaging of the cardiac vagal innervation to visualize the vago-cardial anatomy and topography

B. Kronsteiner¹, P. Heimel², G. Oberoi³, M. Andreana³, L. Reissig⁴, R. Blumer⁴, S. Geyer⁴, P. Slezak², W. Weninger⁴, B. K. Podesser⁵, A. Kiss⁶, F. Moscato³

¹Center for Medical Physics and Biomedical Engineering, Medical University of Vienna, Vienna, Austria; Ludwig Boltzmann Institute for Cardiovascular Research, Medical University of Vienna, Vienna, Austria, Wien, Austria

²Ludwig Boltzmann Institute for Experimental and Clinical Traumatology, AUVA Research Center, Vienna, Austria; Austrian Cluster for Tissue Regeneration, Vienna, Austria; Karl Donath Laboratory for Hard Tissue and Biomedical Research, University Clinic of Dentistry, Medical University of Vienna, Vienna, Austria, Wien, Austria

³Center for Medical Physics and Biomedical Engineering, Medical University of Vienna, Vienna, Austria, Wien, Austria

⁴Division of Anatomy, Medical University of Vienna, Vienna, Austria, Wien, Austria

⁵Department of Biomedical Research, Medical University of Vienna, Vienna, Austria, Wien, Austria

⁶Center for Biomedical Research, Medical Univ. of Vienna, Vienna, Austria; Ludwig Boltzmann Insit. for Cardiovascular Research, Medical University of Vienna, Vienna, Austria, Wien, Austria

Introduction: Heart transplantation is the gold standard approach in the treatment of patients with end-stage heart failure. However, patients may suffer from negative side-effects of cardiac denervation after heart transplantation, such as sympathico-vagal imbalance at rest and insufficient chronotropic response during exercise [1]. Within this project, we are addressing this clinical problem by mapping the anatomy of the cardiac Vagus Nerve to establish a multimodal imaging cluster providing structural and functional in-detail information for selective vago-cardial neuromodulation. Four different imaging modalities, i. e., optical coherent tomography (OCT) [2], micro-computed tomography (μ CT) [3], high-resolution episcopic microscopy (HREM) [4], and Immunofluorescence microscopy (IF) [5] were used to provide essential 3D- information of the Vagus Nerve on anatomical, histological, and molecular level as basis for development of a regenerative neural interface of the cardiac VN.

Methods: Cervical Vagus Nerve (CVN) and subsequent cardiac branches were carefully isolated from the cadavers of New-Zeeland female rabbits ($n=4$; 3 kg) and male domestic pigs ($n=4$; 60–92 kg). VN samples were divided into 2 groups, of which one was topographically mapped to visualize the vagal course from the cervical to the cardiac level as well as the tissue structure using contrast-enhanced μ CT and HREM. Based on the data obtained, a 3D-rendered model from the cervical level to the cardiac branch of VN anatomy and histology was performed. The other group was scanned using OCT, which provide access to detailed information about tissue structure and molecular composition in a fast, label-free manner and Immunohistochemistry with antibodies labeling, Neurofilament (NF), Myelin Basic Protein (MBP), choline Acetyltransferase (ChAT) and Tyrosine Hydroxylase (TH).

Results: Multimodal Imaging provides anatomically and morphologically relevant information of the Vagus Nerve, such as the course of single fascicles from cardiac branches up to CVN as well as their main features, such as diameter, myelin sheaths, fascicle number, fascicle area, internal branching, and

twisting. Inter-species comparison showed that the pig model was in closest to the humans, for example in in respect to size and diameter of the VN. However, our study approach was the first one that was mainly focusing on mapping the course of the CVN down to the cardiac branches to create an anatomical model for selective stimulation of the cardiac VN. Anatomical differences between these species, such as the branching patterns, and the course of the CVN down to the heart, should

be taken into account, especially with regard to translational research for human medicine.

Conclusion: This imaging pipeline can provide a novel anatomical and structural information for selective cardiac Vagus Nerve Stimulation and thus, support the design, development and test of a novel, smart cardiac neuroprosthesis for HTx patients.

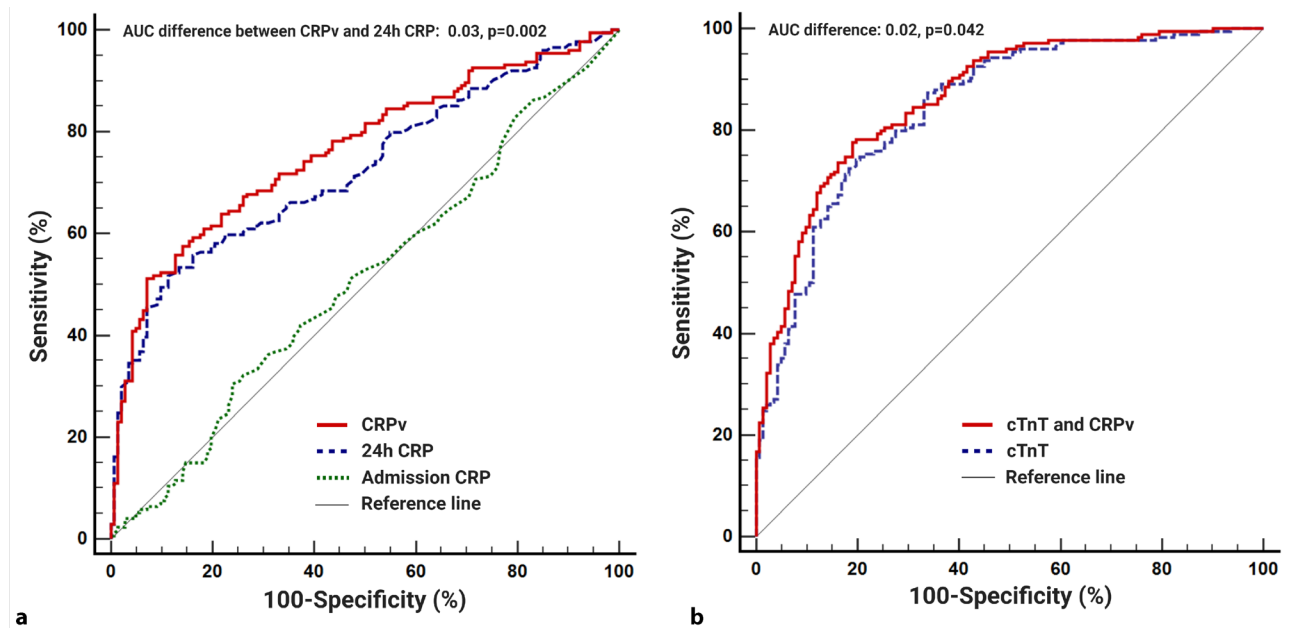


Fig. 113.14 ROC analysis for the prediction of MVO. A) Admission CRP failed to predict MVO (AUC 0.51, 95 % 0.44–0.57, $p=0.803$), whereas CRPv was a better predictor of MVO than 24 h CRP (AUC 0.76, 95 % CI 0.71–0.81, p

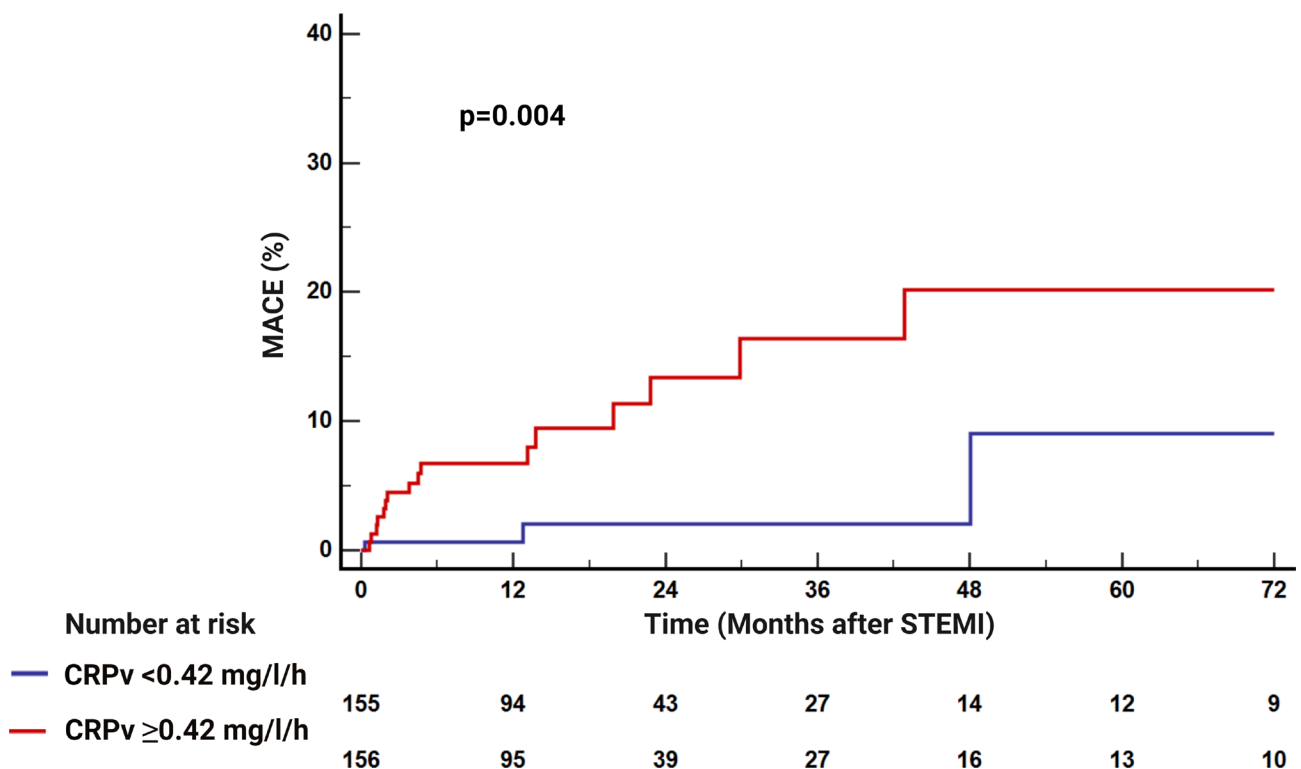


Fig. 213.14 CRPv and clinical outcome. Kaplan-Meier curve displaying the MACE-free survival in relation to median CRPv

3.14

C-reactive protein velocity predicts microvascular pathology after acute st-elevation myocardial infarction

M. Holzknrecht¹, C. Tiller¹, M. Reindl¹, I. Lechner¹, F. Troger², A. Mayr², C. Brenner¹, G. Klug¹, A. Bauer¹, S.J. Reinstadler¹, B. Metzler¹

¹University Clinic of Internal Medicine III, Cardiology and Angiology, Medical University of Innsbruck, Innsbruck, Austria
²University Clinic of Radiology, Medical University of Innsbruck, Innsbruck, Austria

Introduction: The role of C-reactive protein velocity (CRPv) as an early and sensitive marker of an excessive inflammatory response in the setting of acute ST-elevation myocardial infarction (STEMI) is only poorly understood. The aim of this study was to investigate, in patients with STEMI treated with primary percutaneous coronary intervention (PCI), the association of CRPv with microvascular infarct pathology.

Methods: This prospective cohort study included a total of 316 patients with STEMI undergoing PCI. CRPv was defined as the difference between CRP 24±8 h and CRP at hospital admission, divided by the time (in h) that have passed during the two examinations. The association of biomarker levels with cardiac magnetic resonance (CMR)-determined microvascular obstruction (MVO) was evaluated.

Results: CMR was performed at a median of 3 [interquartile range 2-4] days after PCI. After adjustment for cardiac troponin T (cTnT), culprit lesion location and TIMI-flow post-PCI, CRPv (odds ratio 3.36, 95% confidence interval (CI) 1.72-6.57; *p* < 0.001) remained significantly associated with the occurrence of MVO. CRPv (area under the curve [AUC] 0.76, 95% CI 0.71-0.81; *p* < 0.001) was a better predictor for MVO compared to 24 h CRP (AUC difference: 0.03, *p* = 0.002). The addition of CRPv to peak cTnT resulted in a higher AUC for MVO prediction than peak cTnT alone (AUC 0.86, 95% CI 0.82-0.90; *p* < 0.001 vs. AUC 0.84, 95% CI 0.79-0.88; *p* < 0.001. AUC difference: 0.02, *p* = 0.042).

Conclusion: In patients with STEMI treated with primary PCI, CRPv was associated with microvascular infarct pathology with a predictive value incremental to cTnT, suggesting CRPv as an early and sensitive biomarker for more severe infarct pathology and outcome.

4 CHIRURGIE

4.1

The prognostic potential of growth differentiation factor-15 on bleeding events and patient outcome after cardiac surgery—a prospective cohort study

N. Kazem¹, A. Hammer¹, L. Koller¹, F. Hofer¹, B. Steinlechner², G. Laufer³, C. Hengstenberg¹, J. Wojta¹, P. Sulzgruber¹, A. Niessner¹

¹Division of Cardiology, Department of Internal Medicine II, Medical University of Vienna, Austria, Wien, Austria

²Department of Anesthesia, General Intensive Care and Pain Management, Medical University of Vienna, Austria, Wien, Austria

³Division of Cardiac Surgery, Department of Surgery, Medical University of Vienna, Austria, Wien, Austria

Background: GDF-15 (growth/differentiation factor 15) is induced by myocardial stretch, volume overload, inflammation and oxidative stress. Its expression is tightly linked with cardiovascular events as well as the risk for major bleeding and all-cause mortality.

Objective: The objective of the present study was to elucidate the prognostic potential of GDF-15 in patients after cardiac surgery. Methods: 504 patients undergoing elective cardiac valve and/or coronary artery bypass graft surgery were prospectively enrolled. GDF-15 levels were measured prior surgery

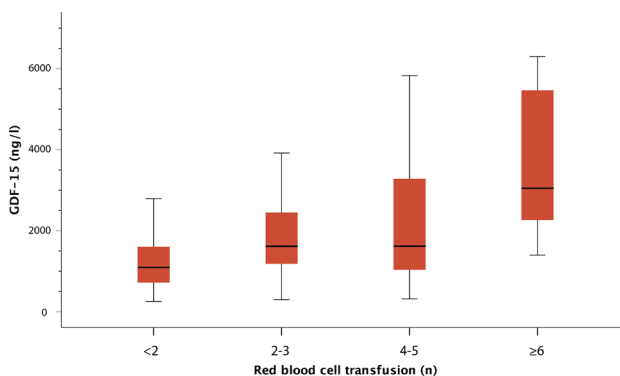


Fig. 114.1

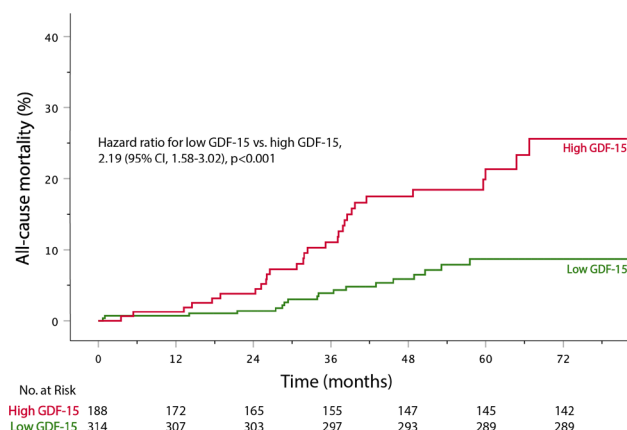


Fig. 214.1

to evaluate the impact on bleeding events, thromboembolic events and mortality.

Results: Preoperative GDF-15 was associated with the primary endpoint of intra- and postoperative red blood cell transfusion (for bleeding risk factors adjusted [adj] OR [odds ratio] per 1-SD [standard deviation] of 1.62 [95%CI:1.31-2.00]; $p < 0.001$) and postoperative atrial fibrillation (for atrial fibrillation risk factors adj. OR per 1-SD of 1.49 [95%CI:1.22-1.81]; $p < 0.001$). Higher concentrations of GDF-15 were observed in patients reaching the secondary endpoint of major or clinically relevant minor bleeding (for bleeding risk factors adj. OR per 1-SD of 1.70 [95%CI:1.05-2.75]; $p = 0.030$) during the 1st postoperative year, but not for thromboembolic events. GDF-15 was a predictor for cardiovascular mortality (for comorbidities adj. HR [hazard ratio] per 1-SD of 1.67 [95%CI:1.23-2.27]; $p = 0.001$) and all-cause mortality (for comorbidities adj. HR per 1-SD of 1.55 [95%CI:1.19-2.01]; $p = 0.001$). A combined risk model of GDF-15 and EuroSCORE II outperformed the EuroSCORE II alone for long-term survival (c-index: 0.75 [95%CI: 0.70-0.80], $p = 0.046$; net reclassification improvement: 33.6%, $p < 0.001$).

Conclusion: Preoperative GDF-15 concentration is an independent predictor for intra- and postoperative major bleeding, postoperative atrial fibrillation, major bleeding during the first year and for long-term cardiovascular or all-cause mortality after cardiac surgery.

4.2

Long-term outcome of surgical aortic valvulotomy in pediatric patients—a retrospective single center study over 30 years

J. Schlein¹, D. Wiedemann¹, H. Gabriel², C. Herbst¹, E. Kitzmüller³, M. Marx³, G. Wollenek¹, P. Simon¹, G. Laufer¹, I. Michel-Behnke³, D. Zimpfer¹

¹Universitätsklinik für Chirurgie, Abteilung für Herzchirurgie, Medizinische Universität Wien, Wien, Austria

²Universitätsklinik für Innere Medizin II, Abteilung für Kardiologie, Medizinische Universität Wien, Wien, Austria

³Universitätsklinik für Kinder- und Jugendheilkunde, Abteilung für Kinderkardiologie, Medizinische Universität Wien, Wien, Austria

Introduction: Surgical aortic valvulotomy (SAV) has been part of the armamentarium of congenital heart surgery from the early days on. SAV allows to address the individual valve pathology on a lesion specific and highly controlled manner. Additionally, to opening the zones of commissural fusion, leaflet shaving, where thickened and dysplastic leaflets are thinned can be performed. After SAV there is generally a low risk of aortic regurgitation. The study objective was to report on survival and freedom from re-operation in the third decade after SAV.

Methods: A retrospective analysis of all patients aged under 18 years at time of surgery, who underwent SAV from May 1985 until April 2020 was conducted. A complete mortality follow-up until April 30th, 2020 was obtained for 98.6% (68/69) of patients. One patient was only transferred to the center for surgery and mainly followed at a non-Austrian center. Eight closed transventricular valvulotomies, which had been performed during the study period prior to introduction of balloon aortic valvuloplasty (BAV) were not included in the study population. Time-related events were assessed using Kaplan-Meier estimator. Univariable Cox-proportional hazard modelling was used to determine risk factors for mortality.

Results: From May 1985 until April 2020 69 patients (71% male, 49/69) underwent 71 SAVs. Median age at time of surgery was 0.3 years (IQR 0-3.5 years). 67.6% (48/71) were younger than 1 year of age and 28.2% (20/71) were neonates. Aortic valve anatomy was as follows: unicuspidal (7%; 5/71), bicuspid (85.9%; 61/71) and tricuspid (7%, 5/71). In five cases (7%) a BAV had been not feasible or unsuccessful in establishing an acceptable hemodynamic situation. Median aortic cross clamp (ACCT) and cardiopulmonary bypass time (CPB) were short (ACCT: 22 (15-30) minutes; CPB: 46 (37-74) minutes). Three patients (4.3%) required extracorporeal membrane oxygenation and seven early deaths (9.9%) occurred. All early deaths occurred in neonates with critical aortic stenosis. Three patients had already undergone early aortic valve re-operation (two homografts, one Ross-Konno). There were 5 late deaths and Kaplan-Meier estimated survival was 86.8% ± 4.1% at 10 years, 83% ± 4.7% at 20 years and 78.6% ± 6.2% at 30 years. Risk factors associated with mortality identified on univariable Cox-proportional hazards analysis were neonatal period (HR 17.2, 95% CI 3.7-81.2; $p < 0.001$) and endocardial fibroelastosis (HR 8.6, 95% CI 2.8-27.1; $p < 0.001$). Freedom from aortic valve re-operation (aortic valve repair and aortic valve replacement) was 58.2% ± 6.3% at 10 years, 33.9% ± 6.4% at 20 years and 27.1% ± 7.9% at 30 years.

Conclusion: Congenital aortic valve stenosis often requires intervention in early childhood. Neonates with critical aortic stenosis, who undergo urgent intervention early after birth, represent a high-risk group with high early mortality. Endocardial fibroelastosis, which is common in neonates with critical aortic stenosis was found as a predictor for global mortality. Complications from endocardial fibroelastosis can arise also late after SAV, as patients develop diastolic left ventricular dysfunction and pulmonary hypertension in the setting of a restrictive cardiomyopathy. Valvulotomy of any kind is a palliative procedure, and the majority of patients will require repeated re-interventions over their lifetime. However, the presented 30-year freedom from re-operation rates are encouraging results in delaying and in some cases even avoiding valve replacement after SAV.

4.3

Aortic root and ascending aorta replacement in pediatric patients

J. Schlein¹, C. Pees², S. Greil², G. Wollenek¹, P. Simon¹, I. Michel-Behnke², G. Laufer¹, D. Zimpfer¹

¹Universitätsklinik für Chirurgie, Abteilung für Herzchirurgie, Medizinische Universität Wien, Wien, Austria

²Universitätsklinik für Kinder- und Jugendheilkunde, Abteilung für Kinderkardiologie, Medizinische Universität Wien, Wien, Austria

Introduction: Aortic root and ascending aorta replacements (AARs) are scarcely performed in pediatric patients and are mostly performed in patients with connective tissue disease, such as Marfan syndrome and Loeys-Dietz syndrome. In accordance with the severity of the underlying connective tissue disease and the size of the aortic root, prophylactic aortic root replacement is indicated to avoid rupture and dissection of aortic aneurysms and accompanying emergency surgeries. AAR may also become necessary in patients with aortic root dilatation after corrective surgery of congenital outflow tract lesions such as the Ross procedure or in neo-aortic position after arterial switch operation. Besides the Bentall procedure, where AAR is performed using a composite valve graft (in the vast majority a mechanical composite graft), valve sparing root replacement (VSRR) techniques gained attention in the pediatric field. VSRR allows to preserve

the native aortic valve, hence does not require anticoagulation, which is of great advantage in young patients. We present our retrospective single-center experience with AAR options in pediatric patients. The primary endpoints were re-operation and mortality.

Methods: A chart review of all patients less than 18 years of age who had AAR between May 1985 and April 2020 was conducted. During the study period 20 patients underwent 22 AARs: 11 VSSR and 11 Bentall. Mortality was cross-checked with the national health insurance data base providing a mortality follow-up until April 2020. Three from foreign countries transferred patients were censored at the last follow-up at the center. The indication for AAR was based on the severity of aortic root dilatation and/or the progression of the aortic diameter. A Bentall procedure was performed in patients with moderate to severe aortic regurgitation as a composite graft with a mechanical valve in all cases. VSRR was performed as re-implantation technique (David procedure) in which the native aortic valve is resuspended in a tubular graft (Vascutek Valsalva graft). In three cases additional valve repair was performed after resuspension of the commissures. VSRR was chosen in patients with no or minimal aortic regurgitation. There was no significant difference between the cohorts regarding aortic cross clamp time ($p=0.423$) or cardiopulmonary bypass time ($p=0.815$). In three cases arterial cannulation was performed in the right subclavian artery via an end to side sutured dacron prosthesis. Patients receiving a mechanical Bentall were anticoagulated with an INR goal range of 2–3. In recent years patients with Marfan or Loeys-Dietz syndrome received up-titrated treatment with losartan and a betablocker.

Results: From May 1985 until April 2020, 20 patients (70% male, 45% connective tissue disease, 15% complex congenital heart disease) underwent 11 VSRRs and 11 Bentall procedures. Two patients (Loeys-Dietz syndrome and Marfan syndrome) underwent a Bentall procedure 5.6 and 1.2 years after VSRR respectively. Median age at time of operation was not different ($p=0.365$) between the cohorts with 14.2 years (IQR 12.7–15.8 years) and 13.2 years (IQR 8.2–14.8 years). There were no early deaths. One patient required ECMO support after VSRR. Permanent pacemaker implantation for complete AV-block was required in three patients (VSRR: $n=2$, Bentall: $n=1$; $p>0.99$). A patient with neonatal Marfan syndrome died 5.6 years after VSRR. Kaplan-Meier estimated survival at 30 years was $90\% \pm 9.5\%$. Freedom from aortic valve re-operation was not different ($p=0.222$) between the VSRR and the Bentall cohort

with $62.5\% \pm 17.1\%$ and $66.7\% \pm 27.2\%$ at 25 years. Four VSRRs were re-operated (2 Bentall, 1 mechanical AVR, 1 decellularized homograft) and one Bentall was re-operated for pannus formation after 11.4 years (mechanical AVR). Freedom from any AAR-related re-operation was $25.7\% \pm 19.9\%$ at 30 years. Freedom from any AAR-related re-operation did not differ ($p=0.085$) between the cohorts with $37.9\% \pm 19\%$ and $66.7\% \pm 27.2\%$. One Marfan patient required early re-operation after VSRR for kinking of the RCA and another Marfan patient was re-operated 15.8 years after VSRR for coronary artery button aneurysm.

Conclusion: Composite mechanical valve graft replacement has long been standard procedure for replacement of the aortic root, but VSRR has emerged as an option in the pediatric population with aortic root dilatation including patients after repair of cono-truncal anomalies. In patients with connective tissue disease it is important to fashion the diameter of the coronary buttons as small as possible to prevent development of coronary button aneurysm.

5 COVID-19 UND HERZ

5.1

Cardiovascular disease and 6-month outcome of COVID-19 Inpatients at a tertiary referral centre

V. W. Zsilavec¹, K. Ablasser¹, L. Rech¹, V. Stangl², P. Eller³, G. Schilcher³, A. Reisinger³, K. Eller⁴, R. Krause⁵, A. Zirlik¹, M. Wallner¹, P. Rainer¹

¹Division of Cardiology, Medical University of Graz, Graz, Austria

²Diagnostic and Research Institute of Pathology, Medical University of Graz, Graz, Austria

³Intensive Care Unit, Department of Internal Medicine, Medical University of Graz, Graz, Austria

⁴Division of Nephrology, Medical University of Graz, Graz, Austria

⁵Department of Internal Medicine, Medical University of Graz, Graz, Austria

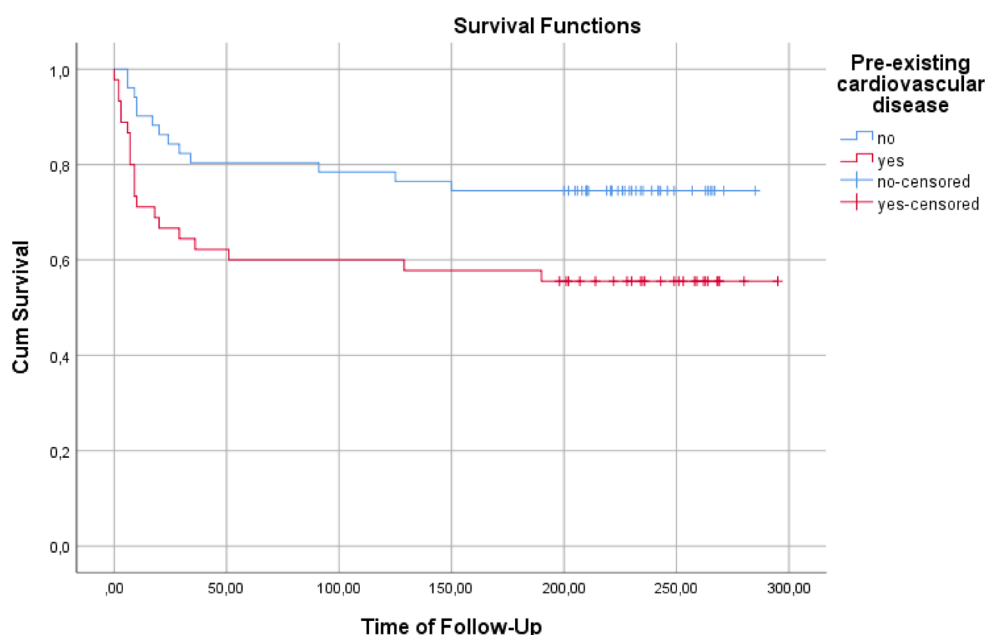


Fig. 115.1 Survival analysis from admission until end of follow-up in patients with and without manifest cardiovascular disease. Log-Rank $p=0.032$.

Introduction: Pre-existing cardiovascular disease and risk factors are common in hospitalized Sars-CoV-2 infected patients and strongly affect outcomes. Furthermore, studies suggest that a considerable proportion of hospitalized patients with COVID-19 develops symptoms that persist for more than twelve weeks and cannot be explained by an alternative diagnosis (“Post-COVID-19 syndrome”). Here, we characterize data on cardiovascular disease, risk factors and hospital outcome as well as six months outcome of COVID-19 first-wave inpatients.

Methods: Registry of 96 patients with PCR-confirmed SARS-CoV-2 infection and prospective follow-up. Patients were characterized regarding pre-existing cardiovascular disease, risk factors, other chronic diseases, laboratory results and in-hospital, 3- and 6-month outcome was determined.

Results: The majority of hospitalized patients with SARS-CoV-2 infection (77.1 %) had pre-existing cardiovascular disease (46.9 %) and/or cardiovascular risk factors (69.8 %). 25 patients (26.0 %) were admitted to the ICU and 26 patients (27.1 %) died. The adjusted (sex, age, BMI) odds ratios for in-hospital death were significantly higher in patients suffering from heart failure (OR: 13.1; 95 %-CI: 2.5–67.2; p : 0.002), ischemic heart disease (OR: 5.7; 95 %-CI: 1.6–20.1; p : 0.006) and diabetes (OR: 13.2; 95 %-CI: 3.4–51.9; p : <0.001). Of the 70 patients discharged from hospital alive 18 patients (25.7 %) were at least once re-hospitalized and 7 patients (10.0 %) died during the follow-up period. All deaths occurred in the group of cardiovascular patients and the mean age at death was 78.6 years. Telephone follow-up was possible in 56 cases (88.9 %). The most common symptoms that persisted longer than three months after discharge from hospital were dyspnoea (11 patients—19.6 %), general weakness (7 patients—12.5 %), decreased physical ability (7 patients—12.5 %), loss of memory (5 patients—8.9 %) and vertigo (5 patients—8.9 %).

Conclusion: The prevalence of cardiovascular disease and/or risk factors was high in patients with a PCR-confirmed SARS-CoV-2 infection requiring inpatient care. Heart failure, ischemic heart disease and diabetes were predictors of in-hospital mortality and cardiovascular patients were at higher risk of being treated at the ICU. 10 % of all patients that were available for follow-up died within six months after discharge from hospital and all deaths occurred in patients with pre-existing cardiovascular disease and/or risk factors.

5.2

Anxiety and depression among patients after acute myocardial infarction during COVID-19

C. K. Braun¹, H. Pagitz², A. Baranyi¹, A. Schmidt²

¹Department of Psychiatry and Psychotherapeutic Medicine, Medical University of Graz, Graz, Austria, Graz, Austria

²Division of Cardiology, Department of Internal Medicine, Medical University of Graz, Graz, Austria, Graz, Austria

Introduction: Psychological stress is an important factor that influences many somatic diseases, including myocardial infarction (MI). Depression and anxiety are of particular importance, as they increase the risk of MI and can influence its outcome [2]. Furthermore, far-reaching psychological consequences can follow as a result of a MI, as patients often experience the acute phase of a MI as traumatic and stressful, with an acute risk of death. During of the COVID-19 pandemic, an increase in anxiety disorders and depressive symptoms have already been observed [1], which makes it even more important to take a closer look at the psychological situation of myocardial

infarction patients during COVID-19. The aim of the study was to investigate patients with acute myocardial infarction (AMI) regarding their psychological situation. The focus was on anxiety and depression, as well as the influence of the COVID-19 situation on AMI patients. In particular, the psychological state of patients during lockdown should be compared to those without any lockdown restrictions, to react even better to the new demands of the COVID-19 pandemic in the future.

Methods: For analysis, differences in anxiety and depression scores at different time points of the COVID-19 pandemic in Austria (during lockdown, absence of lockdown) should be considered. 73 AMI patients were assessed for mood and anxiety symptoms after admission to the hospital using the Hospital Anxiety and Depression Scale (HADS). Furthermore, general questions about COVID-19 were asked during the survey to capture the specific anxiety situations related to COVID-19.

Results: Anxiety scores of AMI patients during lockdown were significantly higher than those who experienced an AMI during the non-lockdown period (t-Test for independent samples: $t(69) = -2.76$, $p = 0.01$). However, there were no significant differences in depression scores at different time points (t-Test for independent samples: $t(69) = -1.51$, $p = 0.14$). The analysis revealed vast but not significant differences in COVID-19 related anxiety, while a larger sample could have resulted in even more pronounced differences. AMI patients during lockdown showed higher COVID-19 related anxiety scores compared to those without any lockdown restrictions (t-Test for independent samples: $t(68) = -1.26$, $p = 0.21$). Due to the high correlation between anxiety and depression scores of AMI patients (Pearson correlation $r = 0.76$), an analysis of covariance was calculated as a consequence to investigate the anxiety situation of AMI patients in more detail, taking depression into account as a confounding variable. A significant difference in anxiety scores was found between the survey time points without and during lockdown when controlling for the influence of depression (ANCOVA: $F(1, 68) = 17.59$, $p < 0.001$). A significant effect of the confounding variable depression was found ($F(1, 68) = 91.41$, $p < 0.001$).

Conclusion: The results indicate a significant increase in anxiety scores and a considerable but not significant increase in COVID-19 related anxiety level of AMI patients during lockdown restrictions compared to patients without restrictions. There were no significantly different depression scores in AMI patients, however strong associations between anxiety symptoms and depression scores were found. Thus, varying anxiety levels in AMI patients depending on the pandemic situation could have an impact on the likelihood of developing myocardial infarction and more attention should be paid to the psychological well-being of patients. Therefore, future studies should look more closely at changes in psychological stress over even longer periods of time.

5.3

Long-term effects and cardiopulmonary outcome after Covid-19 infection

J. Niebauer¹, C. Binder-Rodriguez², A. Iscel¹, S. Klenk¹, R. Badr-Eslam², S. Cadjo², M. Kahr², S. Hoffmann¹, S. Reiter-Malmqvist¹, R. Boeck¹, R. Rettl², T. M. Dachs², A. Zoufaly³, C. Wenisch³, C. Krestan⁴, M. Lichtenauer⁵, D. Bonderman¹

¹Department of Cardiology, Klinik Favoriten, Vienna, Austria, Wien, Austria

²Department of Internal Medicine II, Division of Cardiology, Medical University of Vienna, Austria, Wien, Austria

³Department of Infectious Diseases, Klinik Favoriten, Vienna, Austria, Wien, Austria

⁴Department of Radiology, Klinik Favoriten, Vienna, Austria, Wien, Austria

⁵Department of Internal Medicine II, Division of Cardiology, University hospital Salzburg, Austria, Salzburg, Austria

Introduction: The severe acute respiratory syndrome coronavirus type 2 (SARS-CoV-2) pandemic of 2020 has an influence on people's lives worldwide, impacting global health and putting pressure on health care systems. Multiple studies have described acute effects of the Covid-19 infection on the heart, but little is known about the long-term cardiac effects and complications after recovery. The aim of this analysis was to deliver a comprehensive report of symptoms and long-term impairment after Covid-19 infection.

Methods: This study was a prospective, multicenter registry study. We included patients after verified Covid-19 infection, who have been treated at our dedicated COVID hospital (Klinik Favoriten). In all patients, testing was scheduled approximately 6 months post discharge. During each study visit the following tests and investigations were performed: detailed patient history and clinical examination, transthoracic echocardiography, electrocardiography, cardiac magnetic resonance imaging (MRI), pulmonary computed tomography (CT) scan, lung function test, spiroergometry, six-minute walk test (6MWT) and a comprehensive list of laboratory parameters including cardiac bio markers such as brain natriuretic peptide (NTpro BNP) and troponin T.

Results: In this interim analysis of an ongoing trial, we presented the first 46 patients included in our registry. Baseline values are shown in Table 1: 27 (59%) were male and the median age was 47.5 years (IQR 34.0–58.0). 83% of all patients included so far had an only mild to moderate course of disease and 17% of them had a severe course and were admitted to an intensive care unit. At the time of the study visit, the majority of patients still complained about symptoms: 47% presented with fatigue and weakness, 34% with exertional dyspnea, 24% with vertigo, 17% had an impaired taste or smell. Only 26% were completely asymptomatic (Fig. 1). From a cardiac perspective, the only abnormal findings noted in echocardiography studies were reduced left ventricular global longitudinal strains. Cardiac MRI revealed pericardial effusion in 18%, however these were only minimal up to 8 mm, not visible in echocardiography and may therefore be physiological findings. Furthermore 9% showed positive late gadolinium enhancement. It is not clear if this was a result of Covid-19 infection, as those patients had preexisting cardiac conditions for example ischemic heart disease. Cardiopulmonary function tests were abnormal in 44% of patients. The lung CT scans showed post infectious residues, mainly bilateral ground glass opacities. Exercise capacity as

Table 115.3 Baseline characteristics of the total study population

Baseline characteristics	Total study population (n=46)
Age (years)	47.5 (34.0–58.0)
Female sex (n,%)	19 (41.3)
BMI (kg/m ²)	26.8 (23.2–30.7)
Systolic blood pressure (mmHg)	130.0 (118.0–141.0)
Diastolic blood pressure (mmHg)	84.0 (76.0–96.0)
Heart rate (bpm)	72.0 (63.0–80.0)
Ventilation	
None (n,%)	22 (47.8)
O ₂ insufflation (n,%)	16 (34.8)
HFNC (n,%)	1 (2.2)
CPAP (n,%)	1 (2.2)
Invasive ventilation (n,%)	6 (13.0)
Length of hospitalization (days)	8 (4.0–14.0)
Normal care ward (n,%)	38 (82.6)
Intensive care unit (n,%)	8 (17.4)

Continuous variables are given as median and interquartile range, categorical variables are presented as numbers and percentages. BMI indicates body mass index; SpO₂, peripheral oxygen saturation; HFNC, high-flow nasal cannula; CPAP, continuous positive airway pressure

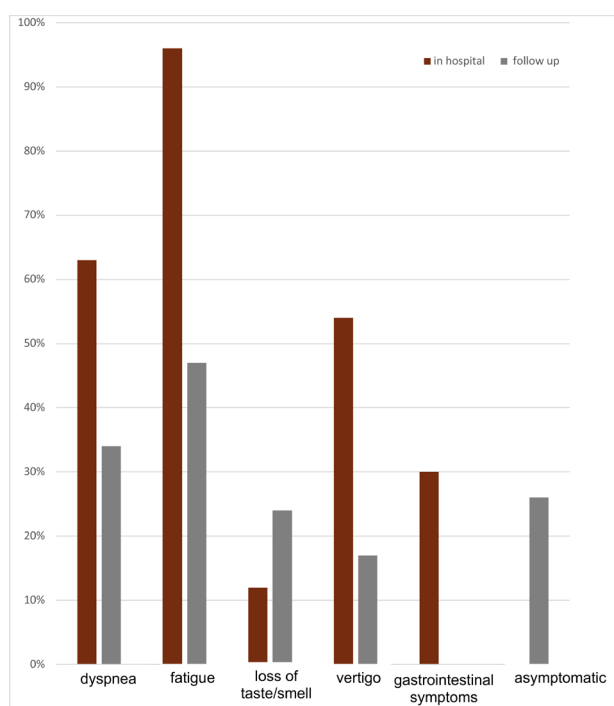


Fig. 115.3 Symptoms during initial hospital stay versus during follow up at approximately 6 months after hospital discharge

measured by the 6-minute walk test with BORG Dyspnea Score or by spiroergometry was reduced in almost 40% of study participants (Fig. 2).

Conclusion: This interim analysis of our ongoing study showed that most hospitalized patients still suffer from chronic

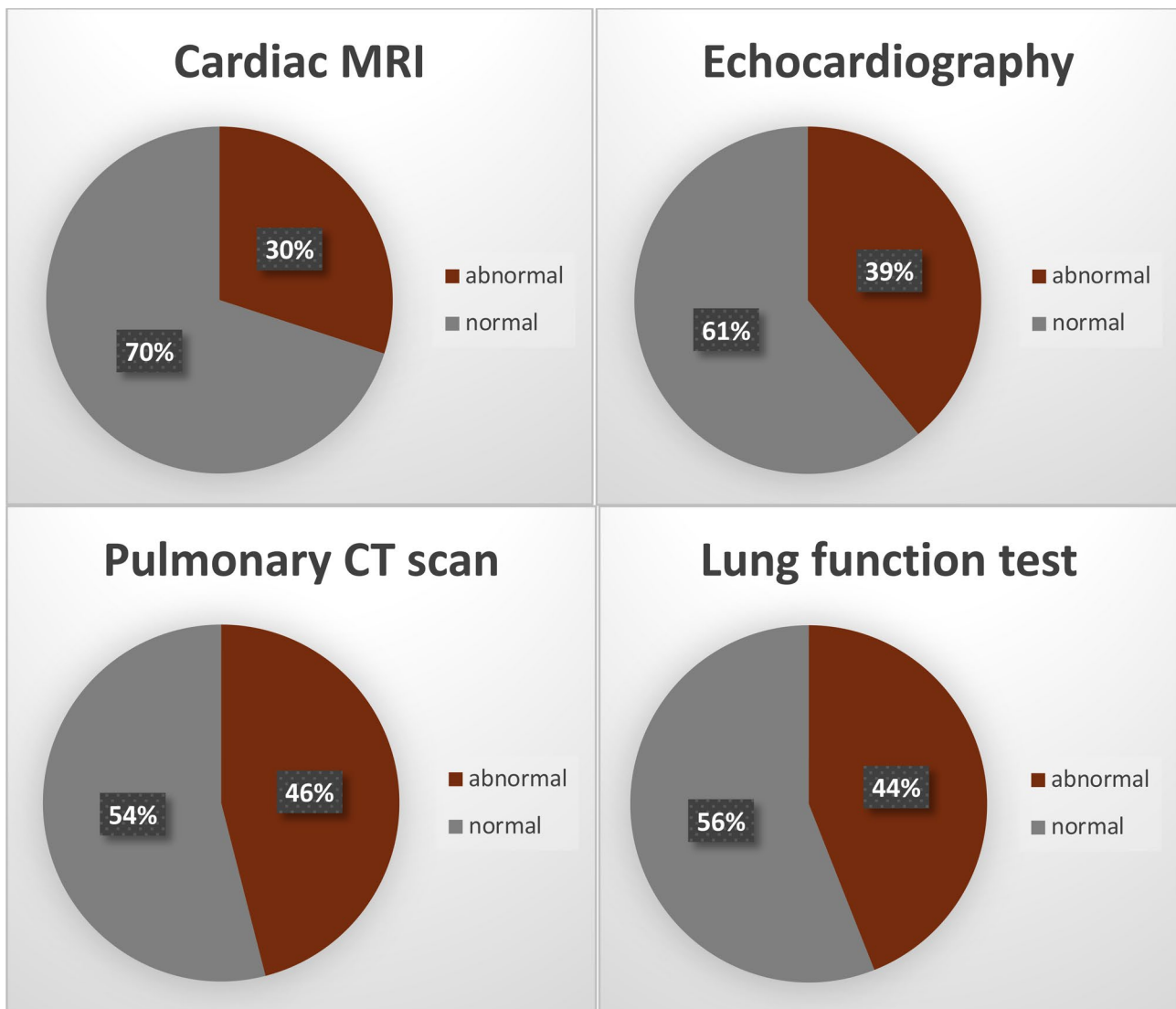


Fig. 215.3 Pathological findings approximately 6 months after hospital discharge

fatigue, exertional dyspnea and impaired cardiopulmonary function after Covid-19 infection. Furthermore, cardiac and pulmonary imaging as well as exercise capacity revealed numerous pathologic findings, however no specific correlation with the persisting symptoms was found so far. By the end of the study we aim to present more comprehensive information about how long the observed impairments persist and whether they progress over time.

5.4

Are there any long-term cardio-pulmonary limitations of hospitalized Covid-19 patients?

R. Badr Eslam¹, C. Binder-Rodriguez¹, A. Iscel², J. Niebauer², R. A. Mousavi¹, C. Kronberger¹, C. Wenisch³, D. Bonderman²

¹Department of Cardiology, Medical University of Vienna, Wien, Austria

²Department of Cardiology, Klinik Favoriten, Vienna, Austria, Wien, Austria

³Department of Infectious diseases, Klinik Favoriten, Vienna, Austria, Wien, Austria

Introduction: The Covid-19 pandemic has affected our lives for over a year and almost 500.000 people in Austria have been infected. Although many of them only had low or mild symptoms some had to be treated in the hospital. Even months after their infection some patients complain about fatigue, exercise intolerance and dyspnoea. The aim of this study was

to perform a follow-up cardiopulmonary exercise test (CPET) on those patients, at 6 months after their hospitalization to find out if there are long-term cardio-pulmonary limitations of COVID-19. We also wanted to check if there is any difference in outcome and cardio-pulmonary limitation between patients who received oxygen therapy vs. without oxygen therapy.

Methods: 40 patients were included into this study (16 women = 40%; 24 men = 60%). All patients were hospitalized during their infection with Covid-19 (5 patients at ICU) and underwent CPET 6 ± 2 month after discharge. 20 patients (50%) received oxygen therapy or ventilation during their hospitalization. CPET data were assessed at rest, during exercise and at recovery. Blood parameters including NT-pro BNP were collected and an interview and examination were performed. Cardiac limitation was defined as VO₂ % of Predicted ≤84 %, VE/CO₂ Slope ≥34 and RER at peak of exercise ≥1.1.

Results: Median age of all patients was 46 years [interquartile range (IQR): 35.3–55.8], median BMI was 26.0 m²/kg [IQR: 23.0–29.0] and the median NTproBNP was 53.1 pg/mL [IQR: 24.0–95.6]. When comparing the two groups, we found higher percentage of cardiac limitations in patients who received oxygen therapy during their hospitalization (10 % with oxygen vs. 5 % without oxygen). Notably, the number of patients with a BMI ≥25 m²/kg was higher in the oxygen therapy group than in those without oxygen (80 % vs. 45 %). The median BMI without oxygen therapy was 24.0 [IQR: 20.3–26.8] vs. 29.0 [IQR: 25.0–31.0] with oxygen therapy (*p*=0.004). There were no significant differences in NT-proBNP levels (*p*=0.545). The median VO₂ % of predicted was 88.0 % [72.5–98.0] without oxygen therapy vs. 84.5 % [IQR:70.8–91.8] with oxygen therapy (*p*=0.289), the median HR percentage of predicted was 92.5 % [IQR: 85.5–97.8] without oxygen therapy vs. 94.5 % [IQR: 88.3–103.5] with oxygen therapy (*p*=0.478), the median physical performance in watt in patients without oxygen therapy was 130.0 [IQR: 108.5–197.5] vs. 135.0 [IQR:97.0–188.3] with oxygen therapy (*p*=0.820).

Conclusion: The findings of our study did not show any statistically significant difference in long-term cardio-pulmonary limitations between patients who received oxygen therapy vs. those who didn't. Overall, only 7.5 % of the study population showed cardiac limitation. Therefore, other causes of the exercise intolerance and/or dyspnoea have to be discussed multidisciplinary.

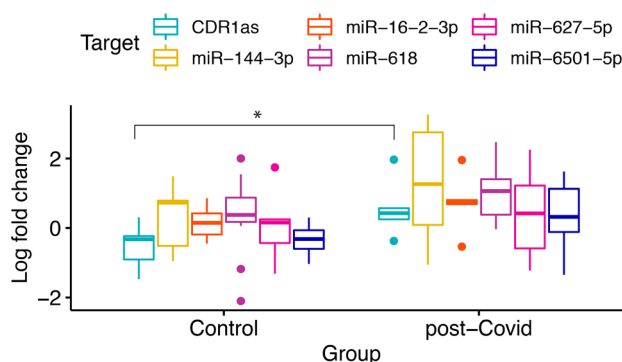


Fig. 115.5 Log fold changes of non-coding RNAs in long-COVID patients and control group

5.5

Deviated expression pattern of noncoding RNAs (microRNA and long non-coding circular RNA) in patients in the convalescent phase of post-COVID-19 disease

J. Mester-Tonczar¹, A. Spannauer¹, N. Kastner¹, D. Traxler-Weidenauer¹, E. Hasimbegovic¹, M. Gyöngyösi¹

¹Medizinische Universität Wien, Wien, Austria

Introduction: The COVID-19 disease is caused by severe acute respiratory syndrome coronavirus 2 (SARS-CoV-2), a positive-sense single-stranded RNA virus. In the convalescent phase of the virus infection, high proportion of patients (10–30 %) suffer from so-called post-COVID (or post-acute COVID-19 or long-COVID or “long-hauler”) syndrome, with cluster of diverse symptoms. Accordingly, long-COVID-19 has been recognised as a new multiorgan disease. While several large-scale multicenter studies address the clinical, cellular and molecular predictive factors, and also the role of microRNA (miRNAs) in SARS-CoV-2 infection pathogenesis, clinical development and course severity, diagnostic and therapeutic roles of non-coding RNAs (microRNAs/miRNAs/and long noncoding circular RNAs/circRNAs/) in post-COVID-19 disease have not yet been examined. The aim of our study was to investigate the differential expression of selected miRNAs and one circRNA known to be involved in inflammatory diseases.

Methods: We have measured five selected miRNAs: miR-16-2-3p, miR-6501-5p, miR-618, miR-627-5p and miR-144-3p, with proven significant de-regulation in active SARS-CoV-2 infective

Overview cardio-pulmonary limitation

Fig. 115.4

	With oxygen therapy (n=20)	Without oxygen therapy (n=20)
Female	07 (35%)	09 (45%)
Male	13 (65%)	11 (55%)
BMI ≥ 25	16 (80 %)	09 (45%)
VO ₂ ≤84 % of predicted	10 (50 %)	07 (35%)
VE/VCO ₂ -slope ≥34	03 (15 %)	01 (05%)
VO ₂ % of predicted ≤ 84 & VE/VCO ₂ -Slope ≥ 34 & RER ≥ 1.1	02 (10 %)	01 (05%)
HR % of predicted ≥ 85 at peak of exercise	17 (85%)	16 (80%)
NT-pro BNP (pg/ml) median	54.8	51.4

patients, crucial in cellular homeostasis and protease processes [1] in 12 healthy (characterized by seronegativity to SARS-CoV-2 antigen and no anamnestic infection) and 5 post-COVID-19 volunteers (EK 1008/2021). Additionally, we have assessed circulating circRNA CDR1as (with completely unexplored function in SARS-CoV-2 infection or post-COVID syndrome) for our preliminary post-COVID biomarker research. RNA was extracted using the QIAamp RNA Blood Mini Kit (Qiagen, Hilden, Germany). cDNA synthesis was done using the miScript II RT Kit and the QuantiTect Reverse Transcription Kit, respectively. The blood levels of ncRNAs were measured by qPCR of the corresponding primers, normalized to the housekeeping genes *Let-7a* for miRNAs and *beta-Actin* for CDR1as and expressed as log-fold changes.

Results: The mean age of the post-COVID volunteers and healthy controls were 36 ± 11 y and 52 ± 19 y, and there were 20 % and 33 % male individuals in the groups, respectively. The mean time after verified SARS-CoV-2 infection was 14 ± 4 weeks in the post-COVID population; two patients did not report persistent syndromes, but 3 had cough, and mild fatigue syndrome during the convalescent phase, but were symptom-free at the time of blood sampling. While the circulating level of all ncRNAs was near zero in healthy controls, a trend towards higher levels of all miRNAs ($p=0.073$ for miR162-3p), and significant upregulation of the circRNA antisense CDR1as ($p=0.019$) was observed, indicating a prolonged alteration in systemic regulation of ncRNA in response to SARS-CoV-2 infection (Fig. 1).

Conclusion: Our pilot study revealed SARS-CoV-2 associated miRNAs and a novel circRNAs (CDR1as) as possible biomarker in prediction of post-COVID-19 disease.

5.6

Frequenz und Outcome des akuten Koronarsyndroms im Covid-Jahr 2020

R. A. Mousavi¹, C. Wallmüller², P. Stratil², G. Pichler², F. Piringer², G. Delle Karth², A. Schober²

¹Medizinische Universität Wien, Wien, Österreich

²Klinik Floridsdorf, Wien, Österreich

Einleitung: Viele Studien haben sich mit dem Thema Frequenz und Outcome der PatientInnen mit akutem Koronarsyndrom (ACS) während der Covid-19 Pandemie beschäftigt. Während der Großteil einen Abfall der Häufigkeiten von ST-Hebungs-Myokardinfarkt (STEMI) und nicht-ST-Hebungs-Myokardinfarkt (NSTEMI) PatientInnen während der Pandemie beobachtet haben [1, 2], berichten andere von keinem signifikanten Unterschied im Patientenkollektiv bzw. in der Häufigkeit des STEMI [3]. Das Ziel dieser Studie war alle PatientInnen, die über die verschiedenen Lockdown Zeiträume in Österreich im „Covid Jahr 2020“ in unserem Wiener STEMI Netzwerk Zentrum im Herzkatheter behandelt wurden zu erfassen und die wechselnden Frequenzen, Komorbiditäten, sowie das Outcome zu vergleichen.

Methoden: 198 Patienten, die im Jahr 2020 mit ACS in unserem STEMI-Netzwerk-Zentrum eingeliefert wurden, wurden nach den Lockdown-Zeiträumen im Jahr 2020 in 4 Gruppen geteilt: kein Lockdown: $n=136$ -36 Wochen (01.01.2020-15.03.2020 & 07.05.2020-16.11.2020), Lockdown 1: $n=24$ -7 Wochen (16.03.2020-06.05.2020), Lockdown 2: $n=16$ -2,5 Wochen (17.11.2020-06.12.2020) und Lockdown light: $n=22$ -5,5 Wochen (03.11.2020-16.11.2020 & 07.12.2020-26.12.2020). Als Lockdown-Ende wurde die Öffnung des gesamten Einzelhandels definiert, als Lockdown light die Schließung der Schulen

und der Gastronomie, bei offenem Einzelhandel. Zur Beschreibung des Patientenkollektivs wurden Alter, Geschlecht, BMI, Komorbiditäten und Risikofaktoren erfasst. Weiteres wurden Dauer der präklinisch-symptomatischen Phase (Schmerzeintritt bis PCI), Kreatinin, Troponin, Indikation, Gefäßzugang und Zielgefäß erhoben. Als Outcome Parameter wurden Reanimation, Schock und Tod definiert.

Resultate: Im Gesamtkollektiv von 198 PatientInnen waren 126 männlich (63,6 %) und 72 weiblich (36,4 %) bei einem mittleren Alter von 65 ± 12 Jahren. Es zeigten sich keine signifikanten Unterschiede im Patientenkollektiv zwischen den Lockdown-Zeiträumen in Alter, BMI oder kardiovaskulären Risikofaktoren (siehe Abb. 1). Im Lockdown light gab es eine signifikant höhere Anzahl an Diabetikern (50 %) im Vergleich zur Zeit ohne Lockdown (25,3 %; $p=0,005$) Die STEMI Häufigkeit sank im 1. Lockdown von 2,2 Patienten/Woche in der Zeit ohne Lockdown auf 1 Patient/Woche und stieg im 2. Lockdown auf 2,8 Patienten/Woche, im Lockdown light war kein Unterschied zu beobachten (2 Patienten/Woche). Bei den NSTEMI Patienten konnte kein signifikanter Unterschied zw. kein Lockdown (1,3 Patienten/Woche), 1. Lockdown (1,4 Patienten/Woche) und Lockdown light (1,8 Patienten/Woche) beobachtet werden. Im 2. Lockdown stieg die Häufigkeit auf 3,2 Patienten/Woche. Im Outcome ließ sich ein Anstieg der Todesfälle auf 9,1 % im Lockdown Light von 4,4 % ohne Lockdown beobachten, allerdings reicht die Fallzahl nicht aus, um eine statistische Signifikanz ($\alpha=0,05$) nachzuweisen.

Schlussfolgerungen: So wie in den meisten gegenwärtigen Studien konnten wir bei einer deutlich sinkenden Anzahl an Patienten pro Woche während dem 1. Lockdown keinen statistisch signifikanten Unterschied, aber einen deutlichen Trend bei einem Signifikanzniveau $\alpha=0,05$ in der Frequenz der STEMI und NSTEMI PatientInnen beobachten. Es ließ sich keine Verlängerung des Intervalls zwischen Schmerzbeginn und PCI nachweisen. Bezüglich Komplikationen und Komorbiditäten konnten wir eine höhere Anzahl in der Lockdown light Gruppe beobachten. Außerdem zeigten sich in dieser Gruppe auffallend mehr CX Verschlüsse, sowie ein Trend zu einem schlechteren Outcome allerdings waren die Gruppengrößen nicht ausreichend, um eine statistische Signifikanz nachzuweisen. Da nur im 1. Lockdown eine Reduktion der Frequenz beobachtet werden kann, die Maßnahmen im 2. Lockdown allerdings gleich waren, postulieren wir, dass die PatientInnen im 1. Lockdown als die Unsicherheit bzgl. des Virus noch groß war, aus Angst vor einer Ansteckung mit Covid-19 trotz Beschwerden nicht ins Spital gekommen sind und die Maßnahmen an sich keinen Einfluss auf die Häufigkeit des Auftretens vom ACS hatten. Eine Untersuchung an einem größeren Kollektiv im STEMI Netzwerk wird der nächste Schritt sein, um den Trend letztendlich zu beweisen, sowie die Unterschiede in den PatientInnenkollektiven (Lockdown vs. kein Lockdown) besser definieren zu können.

	Gesamt	kein LD	LD 1	LD 2	LD light
Patientenanzahl	198 (100%)	136 (68,7%)	24 (12,1%)	16 (8,1%)	22 (11,1%)
Männer	126 (63,6%)	88 (64,7%)	17 (70,8%)	9 (56,3%)	12 (54,4%)
Frauen	72 (36,4%)	48 (35,3%)	7 (29,2%)	7 (43,8%)	10 (45,5%)
Alter	64,7 (\pm 12,2)	65,4 (\pm 12,2)	62,5 (\pm 11,8)	63,7 (\pm 11,2)	63,3 (\pm 13,5)
Gewicht	83,8 (\pm 16,4)	82,5 (\pm 17,2)	90,8 (\pm 17,0)	79,5 (\pm 15,6)	84,4 (\pm 9,7)
Raucher	122 (61,6%)	84 (61,8%)	19 (79,2%)	9 (56,3%)	10 (45,5%)
Diabetes mellitus	50 (25,3%)	29 (21,3%)	7 (29,1%)	3 (18,3%)	11 (50%)
Insult	10 (5,1%)	7 (5,1%)	1 (4,2%)	0 (0%)	2 (9,1%)
Vorhofflimmern	13 (6,6%)	11 (8,1%)	2 (8,3%)	0 (0%)	0 (0%)
frühere PCI	57 (28,8%)	34 (25%)	8 (33,3%)	5 (31,3%)	10 (45,5%)
frühere MCI	43 (21,7%)	25 (18,4%)	7 (29,2%)	4 (25%)	7 (31,8%)
Systolischer RR Aufnahme	140,8 (\pm 29,4)	140,2 (\pm 29,2)	135,8 (\pm 29,0)	142,4 (\pm 32,3)	149,4 (\pm 30,0)
Diastolischer RR Aufnahme	82,7 (\pm 17,5)	83,4 (\pm 16,0)	78,3 (\pm 15,6)	83,5 (\pm 26,7)%	83,1 (\pm 22,1)
Herzfrequenz Aufnahme	78,7 (\pm 20,8)	79,9 (\pm 22,7)	76,4 (\pm 20,6)	74,4 (\pm 10,1)	78,6 (\pm 11,0)
Troponin Erhöhung	157 (79,3%)	107 (78,7%)	21 (87,5%)	12 (75%)	17 (77,3%)
Kreatinin	1,2 (\pm 0,9)	1,2 (\pm 1,1)	1,01 (\pm 0,44)	2,0 (\pm 0,4)	1,2 (\pm 0,2)
primär Transport Rettung	134 (67,7%)	86 (63,2%)	21 (87,5%)	9 (56,3%)	18 (81,8%)
sekundär Transport Rettung	39 (19,7%)	30 (22,1%)	1 (4,2%)	5 (31,3%)	3 (13,6%)
selbst	15 (7,6%)	11 (8,1%)	2 (8,3%)	2 (12,5%)	0 (0%)
in-hospital	4 (2%)	3 (2,2%)	0 (0%)	0 (0%)	1 (4,5%)
Indikation primär PCI	116 (58,6%)	82 (60,3%)	14 (58,3%)	8 (50%)	12 (54,5%)
Indikation NSTEMI	65 (32,8%)	41 (30,1%)	7 (29,2%)	8 (50%)	9 (40,9%)
Indikation subakuter MI	17 (8,6%)	13 (9,6%)	3 (12,5%)	0 (0%)	1 (4,5%)
anteriorer STEMI	56 (28,3%)	35 (25,7%)	8 (33,3%)	4 (25%)	9 (40,9%)
posteriorer STEMI	55 (27,8%)	44 (32,4%)	6 (25,5%)	3 (18,8%)	2 (9,1%)
STEMI Summe	111 (56,1%)	79 (58,1%)	14 (58,8%)	7 (43,8%)	11 (50%)
NSTEMI	75 (37,9%)	47 (34,6%)	10 (41,7%)	8 (50%)	10 (45,5%)
radialer Gefäßzugang	147 (74,2%)	100 (73,5%)	20 (87,0%)	12 (75%)	15 (68,2%)
LAD	85 (42,9%)	54 (39,7%)	12 (50%)	9 (56,3%)	10 (45,5%)
CX	29 (14,6%)	18 (13,2%)	3 (12,5%)	3 (18,8%)	5 (22,7%)
RCA	62 (31,3%)	50 (36,8%)	7 (29,2%)	1 (6,3%)	4 (18,2%)
HS	7 (3,5%)	5 (3,7%)	1 (4,2%)	0 (0%)	1 (4,5%)
ACBP	8 (4%)	6 (4,4%)	0 (0%)	0 (0%)	2 (9,1%)
Mehrgefäß-PCI	31 (15,7%)	18 (13,2%)	4 (16,7%)	4 (25%)	5 (22,7%)
Überstellung in ein anderes KH	30 (15,2%)	22 (16,2%)	0 (0%)	4 (25%)	4 (18,2%)
Reanimation	12 (6,1%)	8 (5,9%)	2 (8,3%)	1 (6,3%)	1 (4,5%)
Schock	16 (8,1%)	10 (7,4%)	2 (8,3%)	2 (12,5%)	2 (9,1%)
Tod	9 (4,5%)	6 (4,4%)	0 (0%)	1 (6,3%)	2 (9,1%)

Fig. 115.6

Häufigkeit STEMI / NSTEMI in den Lockdownzeiträumen 2020

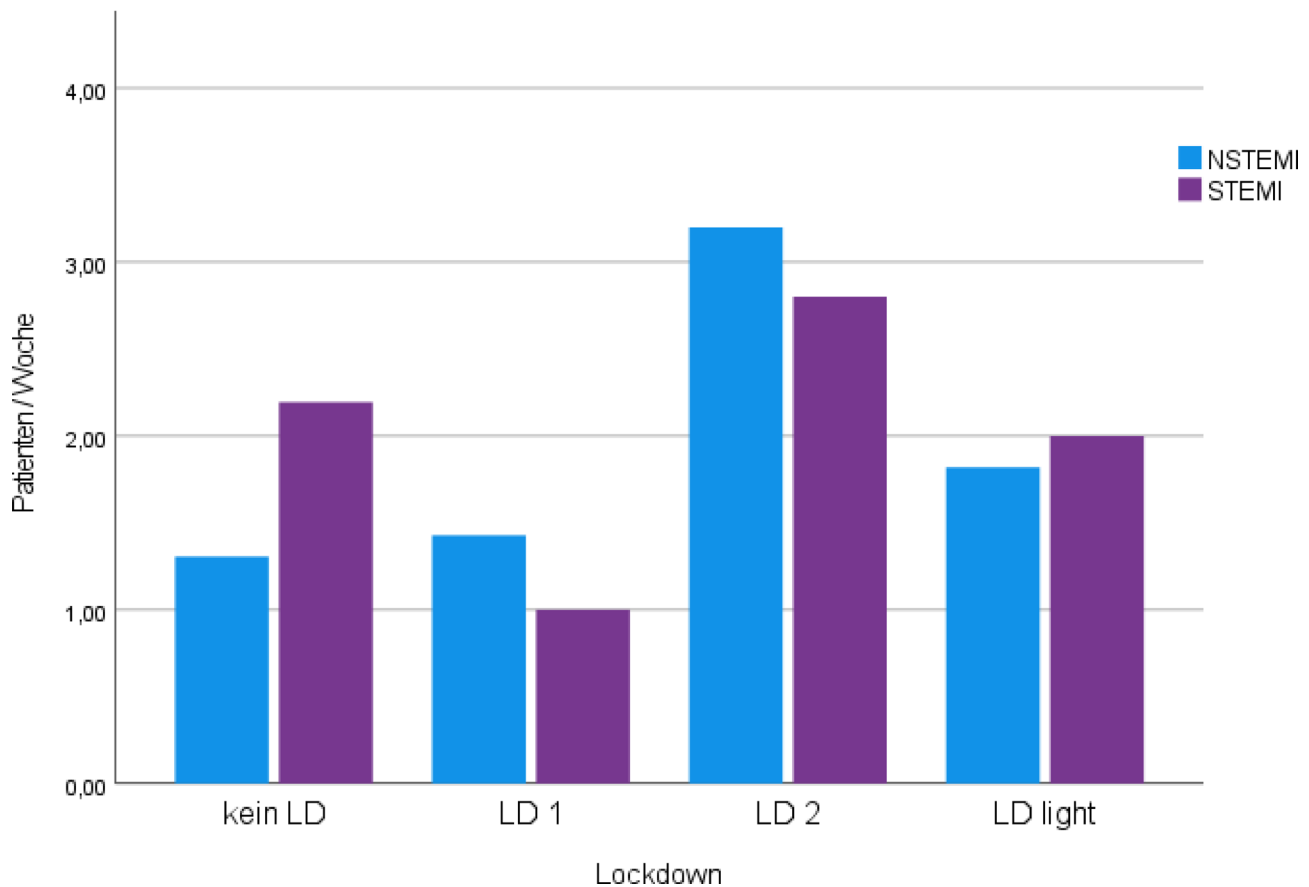


Fig. 215.6

5.7

Higher incidence of stroke in severe COVID-19 is not associated with a higher burden of arrhythmias: comparison to other types of severe pneumonia

P. Jirak¹, Z. Shomanova², R. Larbig³, D. Dankl¹, N. Frank¹, C. Seelmaier¹, D. Butkiene³, M. Lichtenauer¹, B. Strohmayer¹, J. Sackarnd², U. Hoppe¹, J. Sindermann², H. Reinecke², G. Frommeyer², R. Pistulli², L. Motloch¹

¹Uniklinikum Salzburg, Salzburg, Austria

²Universitätsklinikum Münster, Münster, Germany

³Kliniken Maria Hilf Mönchengladbach, Mönchengladbach, Germany

Introduction: Thromboembolic events, including stroke, are typical complications of COVID-19. Whether arrhythmias, frequently described in severe COVID-19, are disease-specific and thus promote strokes is unclear. We investigated the occurrence of arrhythmias, and stroke during rhythm monitoring in critically ill COVID-19, compared to severe pneumonias of other origin.

Methods: Recruited were 120 critically ill patients requiring mechanical ventilation in three European tertiary hospitals, including $n = 60$ COVID-19, matched according to risk factors for

occurrence of arrhythmias to $n = 60$ patients from a retrospective consecutive cohort of severe pneumonias of other origin.

Results: Arrhythmias, mainly atrial fibrillation (AF), were frequent in COVID-19. However, when compared to non-COVID-19, no difference was observed with respect to ventricular tachycardias (VT) and relevant bradyarrhythmias (VT 10.0 vs. 8.4 %, $p = \text{ns}$ and asystole 5.0 vs. 3.3 %, $p = \text{ns}$) with consequent similar rates of cardiopulmonary resuscitation (6.7 vs. 10.0 % $p = \text{ns}$). AF was even more common in nonCOVID-19 (AF 18.3 vs. 43.3 %, $p = 0.003$; newly onset AF 10.0 vs. 30.0 %, $p = 0.006$) which resulted in higher need for electrical cardioversion (6.7 vs. 20.0 %, $p = 0.029$). Despite these findings and comparable rates of therapeutic anticoagulation (TAC), the incidence of stroke was higher in COVID-19 (6.7 % vs. 0.0 %, $p = 0.042$). These events happened also in absence of AF (50 %) and with TAC (50 %).

Conclusion: Arrhythmias were common in severe COVID-19, consisting mainly of AF, yet less frequent than in matched pneumonias of other origin. A contrasting higher incidence of stroke independent of arrhythmias observed also with TAC, seems to be an arrhythmia-unrelated disease-specific feature of COVID-19.

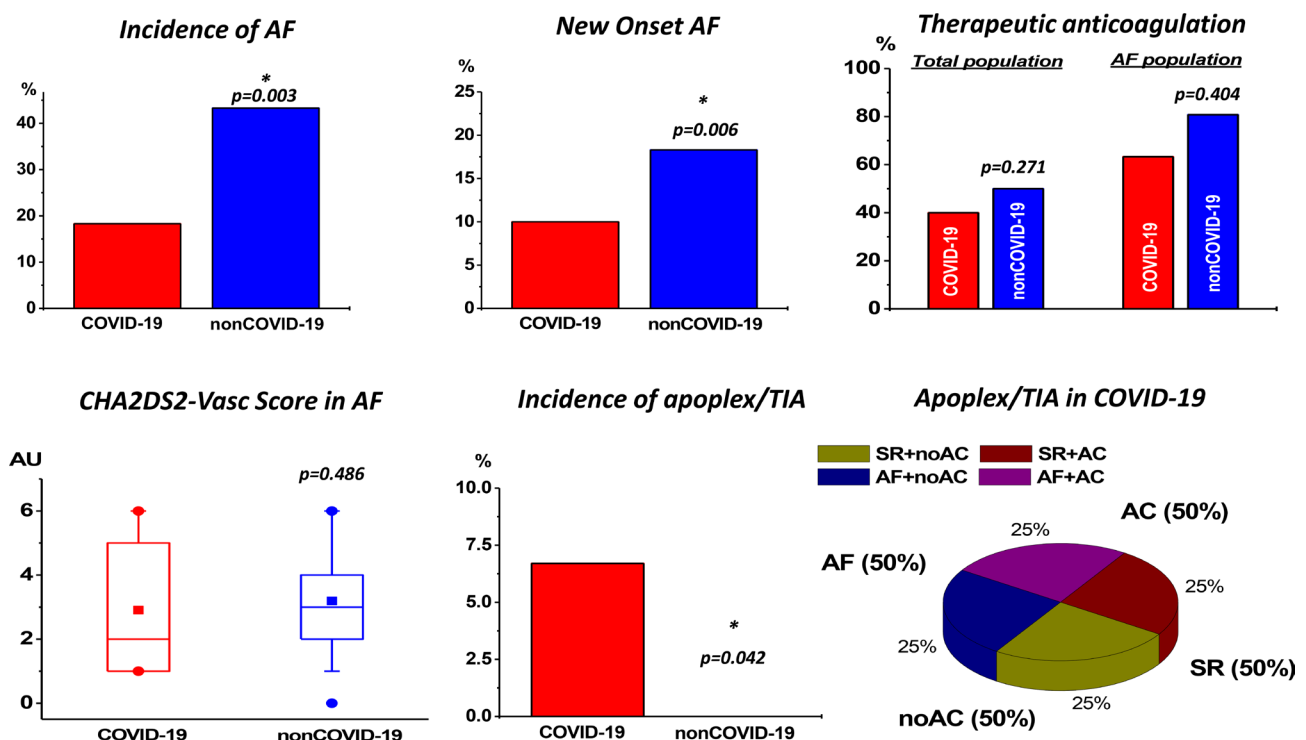


Fig. 115.7

5.8

Effects of SARS-CoV-2 infection on cardiac function—preliminary data on echocardiographic parameters after COVID-19

C. Binder-Rodriguez¹, J. Niebauer², A. Iscel², S. Klenk², M. Kahr¹, S. Cadojo¹, R. Badr Eslam¹, R. Böck², S. Reiter-Malmqvist², S. Hoffmann², A. Zoufaly³, C. Wenisch³, D. Bonderman²

¹Abteilung für Kardiologie, Medizinische Universität Wien, Wien, Austria

²Abteilung für Kardiologie, Klinik Favoriten, Wien, Austria

³Abteilung für Infektiologie, Klinik Favoriten, Wien, Austria

Introduction: Infections with the SARS-COV-2 virus are most commonly associated with respiratory symptoms ranging from a mild cough to severe pneumonia and respiratory failure. Increasing amounts of data suggest, that other organs including the heart may also be affected in patients with corona virus disease-19 (COVID-19). It has been shown, that some patients have signs of cardiac involvement, which may develop into severe myocarditis. While there is an increasing amount of data describing COVID-19 associated myocardial dysfunction in the acute phase, little is known about cardiac parameters during a post-infection follow-up. Furthermore, it is not clear, whether subclinical forms of cardiac involvement may cause remaining cardiac impairment, even in patients with only mild symptoms during COVID-19. The aim of this study was to assess subclinical myocardial dysfunction by measuring left and right ventricular strain as well as conventional echocardiographic parameters in patients after COVID-19.

Methods: We included patients after a verified infection with the SARS-CoV-2 virus, who had been discharged from the hospital. Baseline parameters including clinical history, vital

signs and symptoms were assessed. In addition, we measured laboratory parameters and a transthoracic echocardiography exam was performed in every patient. Left ventricular (LV) global longitudinal strain (LV-GLS) was measured in an apical long axis-, four- and two-chamber view. Right ventricular (RV) strain was measured in the free lateral RV-wall. In addition, standard 2-D and Doppler measurements were performed in each patient to describe cardiac dimensions as well as systolic, diastolic and valvular function. Assessed parameters were compared between two groups, which were divided by median length of hospital stay in days, which was considered as a surrogate for severity of disease.

Results: In total, 46 patients were included in this study. The median time from hospital admission to baseline visit was 29.0 weeks (IQR 23.0–33.0), and the median duration of hospitalization was 8 days (IQR 4.0–14.0). The maximum number of days in hospital was 84 days and the shortest hospital stay was 1 day. Patients who were hospitalized longer were older ($p=0.003$) and had a higher body mass index ($p=0.013$). At the performed study visit, these patients presented with higher levels of N-terminal pro brain natriuretic peptide ($p=0.016$), C-reactive protein ($p=0.005$) and gamma-glutamyltransferase ($p=0.002$).

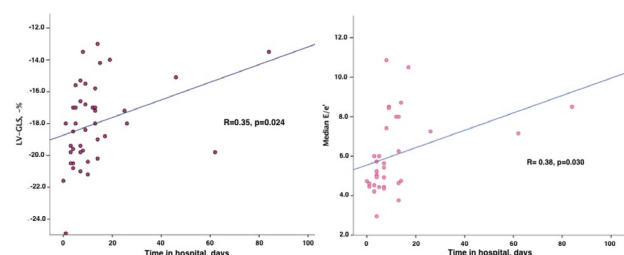


Fig. 115.8 Panel A shows the correlation between left ventricular global longitudinal strain (LV-GLS, -%) values and days of hospitalization. Panel B shows the correlation between E/e' and days of hospitalization

Table 115.8 Baseline characteristics of the total study population, as well as for patients with longer- as compared to shorter hospital stays during an acute SARS-COV-2 infection

	Total study population (n=46)	Hospital stay > 8 days (n= 22)	Hospital stay ≤ 8 days (n=24)	p-value
Baseline characteristics				
Age, years	47.5 (34.0–58.0)	54.5 (46.7–67.0)	40.0 (30.11–48.5)	0.003
Female sex	19 (41.3)	7 (31.8)	12 (50.0)	0.211
BMI, kg/m ²	26.8 (23.2–30.7)	29.3 (26.6–32.0)	25.1 (23.1–27.7)	0.013
Systolic blood pressure, mmHg	134.0 (120.0–150.0)	139.0 (124.0–150.0)	128.0 (120.0–152.0)	0.440
Diastolic blood pressure, mmHg	84.0 (76.0–96.0)	83.0 (77.0–94.0)	84.0 (73.0–98.0)	0.648
Heart rate, bpm	72.0 (63.0–80.0)	72.0 (65.0–80.0)	70.0 (62.0–79.0)	0.496
S _p O ₂ , %	98.0 (97.0–98.0)	97.0 (97.0–98.0)	98.0 (98.0–99.0)	0.137
Ventilation				<0.001
None	22 (47.8)	3 (13.6)	19 (79.2)	
O ₂ insufflation	16 (34.8)	11 (50.0)	5 (20.8)	
HFNC	1 (2.2)	1 (4.5)	0 (0.0)	
CPAP	1 (2.2)	1 (4.5)	0 (0.0)	
Invasive ventilation	6 (13.0)	6 (27.3)	0 (0.0)	
Symptoms at visit 1				
Dyspnoea	16 (34.8)	11 (50.0)	5 (20.8)	0.038
Cough	6 (13.0)	5 (22.7)	1 (4.2)	0.089
Chest pain	5 (10.9)	3 (13.6)	2 (8.3)	0.613
Fatigue	22 (47.8)	13 (59.1)	9 (37.5)	0.287
Sensory deficit	8 (17.4)	3 (13.6)	5 (20.8)	0.391
Laboratory parameters at visit 1				
CRP, mg/dl	0.07 (0.05–0.2)	0.11 (0.07–0.30)	0.05 (0.04–0.11)	0.005
eGFR, ml/min/1.732	85.4 (66.4–105.2)	79.2 (64.4–94.2)	94.0 (70.4–108.2)	0.113
NT-pro BNP, pg/ml	60.3 (28.3–123.0)	100.0 (41.0–175.0)	36.4 (22.6–89.4)	0.016
Troponin T, ng/L	5.0 (4.0–8.3)	5.0 (4.0–6.0)	5.0 (4.0–9.0)	0.925
Gamma GT, U/L	22.0 (15.8–42.3)	34.5 (19.0–85.0)	18.0 (13.0–25.5)	0.002
Echocardiography parameters at visit 1				
LVEDD, mm	45.0 (41.3–48.0)	45.5 (41.5–48.0)	44.0 (41.5–47.5)	0.653
RVEDD, mm	29.0 (28.0–32.0)	29.0 (27.0–31.0)	29.5 (28.0–32.5)	0.371
LA length, mm	45.0 (42.3–49.0)	47.0 (44.5–55.0)	44.0 (40.5–47.0)	0.014
RA length, mm	45.0 (40.5–47.0)	45.5 (39.0–51.0)	45.0 (41.0–47.0)	0.407
IVS, mm	11.0 (9.0–12.3)	11.0 (10.0–13.0)	11.0 (9.0–12.0)	0.496
LVEF, %	56.0 (52.0–63.0)	55.5 (51.5–63.0)	57.0 (52.0–62.0)	0.804
LV-GLS, -%	18.0 (19.98–16.4)	17.2 (18.8–15.5)	19.4 (20.5–17.0)	0.037
E/e', median	5.7 (4.6–8.3)	8.0 (6.3–8.7)	4.9 (4.5–5.7)	0.004
RV-LWS, -%	25.0 (26.5–22.3)	25.7 (27.0–22.0)	25.0 (26.0–22.8)	0.808
TAPSE, mm	21.0 (19.0–25.0)	21.0 (18.0–24.0)	22.0 (19.0–25.0)	0.724
RV-TDI, m/s	0.14 (0.13–0.16)	0.15 (0.13–0.16)	0.14 (0.13–0.15)	0.323
PV-AT, ms	138.0 (126.5–158.0)	138.0 (118.0–143.0)	140.5 (134.0–166.0)	0.237
sPAP, mmHg	28.0 (21.5–33.0)	32.0 (30.0–34.0)	25.0 (19.0–29.0)	0.078
Continuous variables are given as median and interquartile range, categorical variables are presented as numbers and percentages. BMI indicates body mass index; S _p O ₂ , peripheral oxygen saturation; HFNC, high-flow nasal cannula; CPAP, continuous positive airway pressure; CRP, C-reactive protein; eGFR, estimated glomerular filtration rate calculated by MDRD formula				

Echocardiographic evaluation showed that patients who had longer hospital stays also had lower left-ventricular global longitudinal strain (LV-GLS) values, as well as higher E/e' ratios, suggesting systolic as well as diastolic dysfunction (Fig. 1).

Linear regression analysis was able to show a positive correlation between LV-GLS as well as with E/e' and days in hospital (R=0.35, p=0.024 and R=0.38, p=0.030, respectively).

Conclusion: We were able to show, that during a follow-up visit after COVID-19, myocardial systolic and diastolic dysfunction as measured by LV-GLS and E/e' was more severe in patients who were hospitalized longer during the acute infection.

5.9

Mid-regional pro atrial natriuretic peptide independently predicts short-term mortality in COVID-19

C. C. Kaufmann¹, A. Ahmed¹, U. Brunner¹, B. Jäger¹, G. Aicher¹, S. Equiluz-Bruck¹, A. Spiel¹, G. Funk¹, M. Gschwantler¹, P. Fasching¹, K. Huber¹

¹Wilhelminenspital, Wien, Austria

Introduction: Mid-regional pro atrial natriuretic peptide (MR-proANP) is a strong prognostic marker in several inflammatory, respiratory and cardiovascular conditions, but has not been studied in COVID-19 yet.

Methods: This prospective, observational study of patients with COVID-19 infection was conducted from June 6th to November 26th, 2020 in different wards of a tertiary hospital. MR-proANP, N-terminal pro brain natriuretic peptide (NT-proBNP) and high-sensitive cardiac troponin I levels on admission were collected and tested for their association with disease severity and 28-day mortality.

Results: A total of 213 eligible patients with COVID-19 were included in the final analyses of whom 13.2 % (n=28) died within 28 days. Median levels of MR-proANP at admission were significantly higher in non-survivors (307 pmol/L IQR, [161–532] vs 75 pmol/L [IQR, 43–153], P < 0.001) compared to survivors and increased with disease severity and level of hypoxemia. The area under the ROC-curve for MR-proANP predicting 28-day mortality was 0.832 (95 % CI 0.753–0.912, P < 0.001). An optimal cut-off point of 160 pmol/L yielded a sensitivity of 82.1 % and a specificity of 76.2 %. MR-proANP was a significant predictor of 28-day mortality independent of clinical confounders, co-morbidities and established prognostic markers of COVID-19 (HR 2.77, 95 %

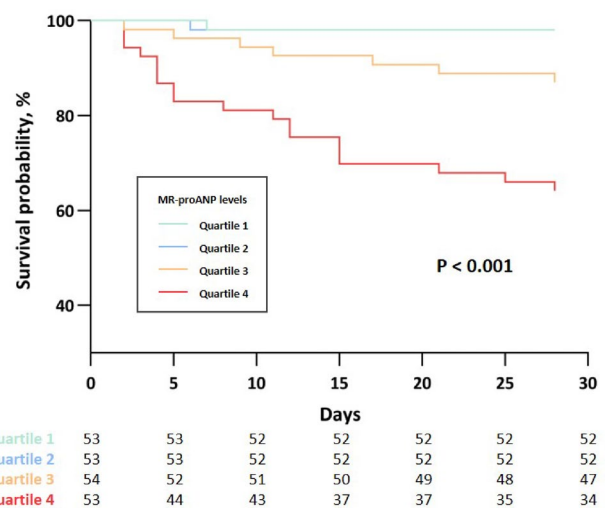


Fig. 115.9

CI 1.21–6.37; P=0.016), while NT-proBNP failed to independently predict 28-day mortality and had a numerically lower AUC compared to MR-proANP.

Conclusion: Higher levels of MR-proANP at admission are associated with disease severity of COVID-19 and act as a powerful and independent prognostic marker of 28-day mortality.

Table 115.9 Association of biomarkers of inflammation, cardiovascular disease and organ dysfunction with 28-day mortality

Biomarkers	Survivors n= 185	Non-survivors n= 28	Unadjusted P-value	Area under the receiver operating curve (95 % CI)	Adjusted P-value	
					Model 1	Model 2
Neutrophile to lymphocyte ratio	4.4 (2.8–8.0)	10.0 (7.1–13.1)	<0.001	0.754 (0.655–0.852)	0.011	0.151
Creatinine, mg/dL	1.0 (0.8–1.2)	1.4 (1.0–1.8)	<0.001	0.731 (0.615–0.847)	0.017	0.216
Blood urea nitrogen, mg/dL	15 (12–21)	31 (20–45)	<0.001	0.779 (0.686–0.873)	0.018	0.860
Lactate dehydrogenase, U/L	279 (225–370)	322 (230–516)	0.004	0.601 (0.468–0.734)	0.001	0.060
High sensitive troponin I, ng/L	11 (6–23)	62 (23–217)	<0.001	0.847 (0.778–0.917)	<0.001	<0.001
N-terminal pro-B-type natriuretic peptide, ng/L	177 (58–736)	1706 (600–7136)	<0.001	0.811 (0.728–0.895)	0.050	0.057
Mid-regional pro atrial natriuretic peptide, pmol/L	75 (43–153)	307 (161–532)	<0.001	0.832 (0.753–0.912)	0.005	0.016

Model 1 was adjusted for age, arterial hypertension, history of cardiovascular disease and chronic kidney disease; Model 2 was adjusted for Model 1 and all other biomarkers (NLR, creatinine, BUN, LDH, hs-cTnI, NT-proBNP and MR-proANP). Concentrations of biomarkers among survivors and non-survivors are reported as median with IQR. Prior to cox regression analysis all biomarkers (except for NLR) were log-transformed.

5.10

Tele-covid-monitoring tirol–fighting the pandemic with telemedical assistance

L. Pölzl¹, T. Egelseer-Bründl², T. Scheffauer², L. Brunelli², J. Hirsch¹, M. Schreinlechner², N. Vdovin², A. Bauer², G. Pölzl²

¹Universitätsklinik für Herzchirurgie Innsbruck, Innsbruck, Austria

²Universitätsklinik für Innere Medizin III Innsbruck, Innsbruck, Austria

Introduction: The Covid-19 pandemic is currently posing unprecedented challenges for the Austrian health care system. Therefore, there is a need to identify and monitor COVID-19 positive high-risk patients without compelling necessity for a hospital admission, in the home environment, in order to intensify care early in the event of progression of the disease. If the relatively short time window is not used appropriately, this can lead to a direct admission of the patient to an intensive care unit or, in the worst case, end fatally. Telemedicine enables close monitoring of affected patients and the initiation of necessary health measures from a distance without direct contact with the patient.

Methods: Covid-19 high-risk patients (age >60 years, patients with immunosuppression or oncological disease) in the greater Innsbruck area will be fitted with a Cosinuss® home monitoring system. A special earplug communicates SpO₂, respiratory rate, body temperature and heart rate to the surveillance team. Supervised by four MDs, a team of 25 medical students continuously monitor vital signs 24/7. After assessing the signal quality, a risk score is calculated based on monitored parameters. If a predefined risk score is exceeded, the patient is contacted by telephone. If this results in a deterioration of the clinical condition compared to baseline, the patient's primary care physician or, if necessary, an ambulance is alerted for therapy optimization or transport to our center.

Results: The active program was started in December 2020 and is still ongoing. Since then, 30 patients (age 75.3 ± 15.3; 43 % male) were equipped with the home monitoring system. Data quality was variable and primarily dependent on patient cooperation. In 47 % of the patients, the quality of the recorded data was excellent. Non-usable data were obtained mostly in nursing home residents. Deterioration in recorded data led to hospitalization in 12 patients (40 %), 1 of whom died because of covid-19 infection. The remaining patients recovered with no remaining limitation. Preliminary data suggest an indirect correlation between patient cooperation and hospitalization rates.

Conclusion: We introduce a telehealth system for high-risk SARS-CoV2-infected patients based on remote monitoring with the potential to care for more infected patients in safe home isolation. Measured biomarkers will allow for better understanding of the course of the disease and for the development of a self-learning algorithm for risk-stratification.

5.11

Imaging in COVID-19—a protocol for echocardiography & lung ultrasound in the follow-up

M. Altersberger¹, C. Ghesla², M. Khafaga², R. Winkler², T. Binder³, M. Genger¹

¹PEK Steyr, Kardiologie, Nephrologie und Intensivmedizin, Steyr, Austria

²Rehabilitationszentrum Hohegg, Hohegg, Austria

³MedUni Wien, Teaching Center, Wien, Austria

Introduction: The global crisis of the current pandemic of COVID-19 is holding the world hostage. Nevertheless, the follow-up after COVID-19 still holds some difficulties. There are patients after COVID-19 still suffering from symptoms such as dyspnea. In echocardiography elevated pulmonary arterial pressures, diastolic dysfunction and deterioration in regional and global strain imaging (1,2). Patients who receive a pulmonary rehabilitation after an intensive care setting after critical illnesses such as ARDS and viral infections (Influenza A) can profit with better life quality, reduction of dyspnea and better fitness levels after rehabilitation (3). Especially not only patients with chronic obstructive pulmonary disease but also patients with diffuse parenchymal lung diseases, pneumonia and after pulmonary embolism profit of a pulmonary rehabilitation (3–6). Long hospital stays and immobility lead to a reduction in strength and function of muscles (7). Long ICU stays can lead to a reduction in activities of daily living (8–10). Residual pulmonary and cardiac complications seem to dramatically improve within time. Follow-up exams might include serial echocardiographic and CT scans of the chest.

Methods: In this protocol we recommend implementing a standardized 12 zone scanning protocol (Fig. 1). Follow-up examinations, as in a rehabilitative setting, in COVID-19 patients should be consistent with the prior scans, and scanning has to be performed thoroughly to describe changes in LUS in detail. A reduction in reverberation artifacts, a reduction in size of consolidations and a reduction or vanishing of pleural effusions can be seen and should be documented (21) AUS 3.2 ÖKG In order to be able to optimally detect and follow-up ultrasound artifacts associated with COVID-19 pneumonia, a specific lung preset with a low mechanical index, single-focal point modality and no harmonic imaging or any other cosmetic filters should be chosen (22). The focal zone should be placed at the area of the pleural line. Starting with zone one in a longitudinal view followed by a transverse view, a scan of all intercostal spaces should be performed in a supine positioned patient. Posterior zones should be included always in the follow-up examinations and be performed in an upright position. A linear transducer with a specific preset should be used whenever possible. Depth setting should be adapted to patient size but will be in the range of 4–8 cm. In case of persistent larger pleural effusions or obese patients, a convex transducer should be chosen (23). The depth setting should be adapted to patients' size and will be in the range of 8–15 cm.

Results: As there are patients with a prolonged course of COVID-19 disease facing symptoms such as dyspnea with reduction in pulmonary function test, rehabilitation as proven for other pulmonary diseases, will be applicable for patients after severe and critical COVID-19 pneumonia. In case of imaging the authors recommend a 12-zone scanning protocol in LUS to visualize residual changes such as reverberation artifacts and the reduction over time. The authors recommend that consolidations in cases of bacterial superinfection, small sub-

pleural consolidations or in pulmonary embolism should be monitored. In the context of cardiac complications and possible residual findings in strain imaging, a comprehensive transthoracic echocardiography including strain imaging in rehabilitation after COVID-19 disease should be implemented (2,24). In case of pleural effusions in post COVID-19 patients' differential diagnosis such as right heart failure, kidney disease or liver disease have to be considered.

5.12

Disruption of outpatient cardiac rehabilitation during the first COVID-19 lockdown in Austria resulted in deteriorating exercise capacity

S. T. Kulnik¹, M. Sareban¹, I. Höppchen², S. Droese³, A. Egger³, J. Gutenberg¹, B. Mayr¹, B. Reich³, D. Wurhofer¹, J. Niebauer¹

¹Ludwig Boltzmann Institute for Digital Health and Prevention, Salzburg, Austria

²Institute of Nursing Science and Practice, Paracelsus Medical University, Salzburg, Austria

³University Institute of Sports Medicine, Prevention and Rehabilitation and Research Institute of Molecular Sports Medicine and Rehabilitation, Paracelsus Medical University, Salzburg, Austria

Introduction: Patients with cardiovascular disease (CVD) are at high risk of adverse outcome in case of COVID-19 [1]. Therefore, it is of crucial importance for CVD patients to observe self-preventive measures, including social distancing. But this invariably limits opportunities for physical activity and disrupts established routines for group-based exercise such as cardiac rehabilitation classes, leading to an increased risk of deterioration in modifiable CVD risk factors. The aim of this study was to explore the impact of the COVID-19-related national lockdown and the closure of group-based cardiac rehabilitation training on patients with CVD. The objectives were to investigate the impact of the first COVID-19-related lockdown in Austria during spring 2020 on patients' maintenance of physical activity, physical fitness levels, and cardiovascular risk profile; and to describe the patient experience of the closure of group-based cardiac rehabilitation training due to COVID-19.

Methods: This study employed a mixed-methods design, including quantitative (QUANT) and qualitative (QUAL) data collection. Patients were recruited from an outpatient cardiac rehabilitation centre in Salzburg, Austria, during summer 2020. Eligibility criteria were regular weekly attendance at group-based exercise training at the centre until the COVID-19-related national lockdown in March 2020; pre-lockdown completion of a maximal bicycle ergometer test at the centre; no new contraindications for maximal exercise testing; and no new pathologies limiting exercise performance. Participants underwent post-lockdown QUANT assessment of physical fitness (maximal bicycle ergometer testing, submaximal bicycle ergometer training session at individual pre-lockdown settings) and cardiovascular risk status (body weight, resting blood pressure, lipid profiles, glycaemic control). These were compared

Table 115.12 Physical fitness and cardiovascular disease (CVD) risk status in 27 cardiac rehabilitation patients pre versus post COVID-19-related lockdown in spring of 2020

Outcome	Parameter	Pre	Post	Difference	p-value
Maximal bicycle ergometer test ^a	Power (W)	165 (70)	151 (70)	-14 (12)	<0.001**
	Power (% of reference value)	112 (37)	102 (38)	-10 (10)	<0.001**
	Maximal Heart Rate (bpm)	142 (24)	135 (24)	-7 (9)	0.003**
Submaximal bicycle ergometer training session ^b	Power (W)	99 (40)	97 (40)	-2.3 (5.2)	0.038*
	Peak Heart Rate (bpm)	131 (28)	134 (28)	3.0 (22)	0.73
	Average Heart Rate (bpm)	112 (19)	115 (21)	2.4 (11)	0.30
CVD risk status	Resting Systolic Blood Pressure (mm Hg)	121 (20)	124 (18)	3 (20)	0.46
	Weight (kg)	82.5 (25.2)	82.4 (15.6)	-0.1 (3.4)	0.87
	Body Mass Index (BMI)	27.13 (4.8)	27.12 (4.8)	-0.01 (1.0)	0.94
	Cholesterol (mg/dl)	169 (53)	171 (55)	2 (28)	0.74
	Triglycerides (mg/dl)	137 (70)	145 (90)	8 (56)	0.45
	HDL Cholesterol (mg/dl)	59 (14)	65 (16)	6 (7)	<0.001**
	LDL Cholesterol (mg/dl)	88 (49)	81 (50)	-7 (23)	0.11
	Glucose (mg/dl) ^c	102 (18)	96 (10)	-6 (17)	0.11
	HbA1c (%) ^d	6.0 (0.3)	6.0 (0.2)	<0.1	0.12
CVD Risk (%) ^e	7.0 (2.8)	6.9 (2.4)	-0.1 (0.9)	0.61	

Figures are arithmetic mean (SD)

p-values were calculated by paired t-test or Wilcoxon signed rank test (2-tailed, alpha=0.05)

* statistically significant at 0.05 significance level

** statistically significant at 0.01 significance level

^an=25; median (IQR) time period between pre and post lockdown test=11 (10, 20) months

^bMedian (IQR) time period between pre and post lockdown training session=5 (5, 7) months

^cn=25

^dn=23

^eFramingham Risk Score for recurrent cardiovascular event within 2 years [3]

with pre-lockdown data from participants' medical records, using paired t-test or Wilcoxon signed rank test as appropriate (2-tailed, $\alpha=0.05$). For QUAL data collection, participants gave in-depth semi-structured interviews about their experience of lockdown and about maintaining exercise routines while group-based training had been closed. Interviews were audio-recorded, transcribed, coded, and interpreted using the framework analysis method. Ethical approval was granted from the medical ethics committee of the State of Salzburg (reference 1095/2020). [ClinicalTrials.gov](https://clinicaltrials.gov/ct2/show/study/NCT04501432) identifier: NCT04501432.

Results: Twenty-eight (57%) of 49 eligible patients were recruited, 1 withdrew, and 27 completed all study procedures. Two participants were excluded from analysis of physical fitness data, due to subsequent diagnosis of new complaints limiting exercise performance. The cohort had mean (SD) age of 69 (7.4) years. Median (IQR) time since first CVD event was 8 (5.5, 9) years. Six (22%) were female, 2 (7%) had type 2 diabetes, and none were current smokers. In QUANT analysis of maximal ergometer testing, 14 (56%) had deteriorated, 10 (40%) were unchanged, and 1 (4%) had improved post-lockdown (minimal detectable change of 13 W [2]). At group level, power was significantly reduced (maximal exercise testing, submaximal ergometer training), whereas CVD risk factors remained unchanged from pre- to post-lockdown (table 1). QUAL analysis corroborated the negative impact of the closure of cardiac rehabilitation classes. Although almost all patients had found alternatives to keep physically active during lockdown, 17 (63%) said they had not been able to maintain their exercise levels, and 15 (56%) felt their physical fitness had deteriorated. Patients regretted the lack of a weekly 'fixture' for exercise. Many missed the sense of community at the rehabilitation centre and the motivation from training together with others. Several patients stated that without professional supervision they felt less confident or unsafe to train at the same (high) intensity as at the rehabilitation centre.

Conclusion: This mixed-methods study presents a comparison of physical fitness and CVD risk before and after the COVID-19-related lockdown in spring 2020, utilising existing medical record data (pre) and prospectively collected data (post) in a cohort of outpatient cardiac rehabilitation patients at a single centre. QUAL interview data supplement and corroborate the QUANT findings. This patient cohort was heterogeneous with respect to physical activity levels and exercise capacity, yet overall motivated and experienced in exercise training, having regularly attended weekly training sessions at the centre before the lockdown. Despite individually seeking out alternative exercise options during lockdown, group average exercise capacity deteriorated even in this motivated and exercise-conscious group. This study highlights the importance of providing group-based opportunities for supervised high intensity training for patients who engage well in such a setting, and the detrimental impact of disruption to this type of rehabilitation service during the COVID-19 lockdown in spring of 2020.

5.13

Characteristics of ST-elevation myocardial infarction in COVID-19 pandemic

I. Lang¹, A. Toma¹, A. Niessner¹, B. Frey¹, K. Distelmaier¹, G. Klappacher¹, G. Goliash¹, J. Siller-Matula¹, N. Skoro-Sajer¹, C. Kopp¹, W. Speidl¹, C. Hengstenberg¹, M. Burda¹

¹Universitätsklinik für Innere Medizin II, Medizinische Universität Wien

Background/Introduction: The ongoing COVID-19 pandemic drives patients away from hospitals. Even patients suffering from ST-elevation myocardial infarction (STEMI) are reluctant to seek medical help, leading to a delay in reperfusion. Low- to no-reflow phenomenon, high peak cardiac markers, major adverse cardiac events (MACE), reduced left ventricular ejection fraction, and higher one-year all-cause mortality may be the consequence.

Purpose: To improve the quality of STEMI care, regional and current trends have to be taken into consideration. We hypothesize that the characteristics of STEMI has changed during the past year.

Methods: This is a single center prospective analysis of patients with STEMI who underwent primary percutaneous coronary intervention (pPCI) between December 15th 2020 and January 15th 2021. Data of these patients ($n=26$) are compared with STEMI patients ($n=32$) between December 15th 2019 and January 15th 2020. Cardiac markers, total ischemic time, treatment times, TIMI flow before and after intervention, thrombus characteristics, formation of collaterals and complications were recorded.

Results: During the SARS-CoV-2 pandemic total ischemic time increased from 394 (± 375) minutes to 1480 (± 1974) minutes ($p=0.020$). Time from onset of pain to first medical contact increased fourfold from 195 (± 385) minutes to 774 (± 1790) minutes ($p=0.039$). Mean creatine kinase (CK) level on admission was 830 (± 2521) U/L in 2020/2021 and 235 (± 279) U/L in 2019/2020 ($p=0.028$). Further increase in CK after admission was observed in 68.8% patients in 2020/2021 compared with 92.3% patients in 2019/2020 ($p=0.048$). Aspirated thrombus was larger and more fibrotic during the pandemic.

Conclusions: Total ischemic time and the time from onset of pain to wire crossing increased significantly during the SARS-CoV-2 pandemic. The majority of delay is caused by patient late first medical contact. Myocardial biomarkers are decreasing after admission illustrating infarcts in the recovery phase. There is a trend towards an observation of more collateralized occlusions on angiography.

One-year all-caused death and other major adverse cardiac events need to be investigated.

6 DIVERSE

6.1

Learning curve and initial experience by the implementation of a his-bundle pacing program

G. Kollias¹, M. Martinek¹, S. Sieghartsleitner¹, M. Hölzl¹, E. Sigmund¹, S. Seidl¹, J. Aichinger¹, H. Pürerfellner¹, M. Derndorfer¹

¹Ordensklinikum Linz Elisabethinen, Linz, Austria

Introduction: His-bundle pacing (HBP) has emerged in the last years as a promising alternative pacing technique. It aims to provide a more physiological pattern of ventricular activation via the native His-Purkinje system and thus to maintain contractile function, optimise atrioventricular synchrony and reduce the deleterious effects of a high percentage of right ventricular pacing. We report the initial experience of the first 10 HBP procedures in our centre.

Methods: The first 10 consecutive patients since the initiation of a His-Bundle pacing program in our institution in May 2020 were included in this analysis. All patients had an indication for permanent pacing and were expected to require ven-

tricular pacing >40 % of the time: 4 patients had a third degree atrioventricular block (AVB), 2 had a second degree AVB, 3 had atrial fibrillation with a slow ventricular response and symptomatic pauses and one patient exhibited symptomatic sick sinus syndrome with a long first degree AVB (PR interval 360 ms). Mean age was 70.3 years and 70 % were men. The lead used for HBP was a non-stylet-driven 4.1 Fr lead with an exposed helical screw (Medtronic Select Secure 3830, Medtronic, Minneapolis, MN). A range of acceptable sensing, impedance and threshold values were predefined, according to the current literature: Impedance 400-1500 Ohms, Sensing >2 mV, Threshold <3.0 V@1.0 ms. Selective HBP (sHBP) was defined as the presence of an isoelectric His-paced to QRS interval similar to native HV interval and a QRS morphology identical to the intrinsic QRS morphology, while non-selective capture (nsHBP) was defined as engagement of His along with adjacent local myocardial tissue, with pseudo-delta wave in QRS, no isoelectric interval between spike and QRS, and QRS morphology similar, but not identical to the intrinsic QRS morphology. An electroanatomical 3D mapping system (Ensite NavX, Abbott) for precise identification of His-location was used in all cases.

Results: HBP was successful with acceptable sensing, impedance and threshold values in 10/10 patients (success rate

100 %). All cases were performed by using a specially designed, non-steerable sheath with dual-plane shaping (Medtronic C315 His, Medtronic, Minneapolis, MN) and no case required the use of a deflectable sheath (Medtronic C304, Medtronic, Minneapolis, MN). Mean procedure time was 91 minutes (81-159 min.). Mean sensing, impedance and threshold values were 3.8 mV, 636 Ohms and 1.1 V@1.0 ms (0.5 V@1.0 ms-3.0 V@1.0 ms) respectively. Mean procedure duration declined from 108 min (82-159 min) in the first 5 procedures to 89 min (81-103 min) in the next 5 procedures. Similarly, the mean threshold value declined from 1.6 V@1.0 ms in the first 5 procedures to 0.6 V@1.0 ms in the next 5 ones. Selective HBP (sHBP) was achieved in 6 patients (60 %), while nsHBP was demonstrated in the rest 4 patients. No acute HBP-related complications were observed, no His-electrode dislocation has occurred. One patient underwent an early revision due to dislocation of the atrial electrode. In the 3-month follow-up of the first 5 patients, there was a loss of His-capture in one patient (who had also initially a high threshold of 3.0 V@1.0 ms at implantation); the other 4 patients exhibited a mean threshold value of 0.9 V@1.0 ms (0.5 V@1.0 ms-1.75 V@1.0 ms) at three months.

Conclusion: HBP is safe, effective and technically feasible as an alternative pacing method in patients with expected high per-

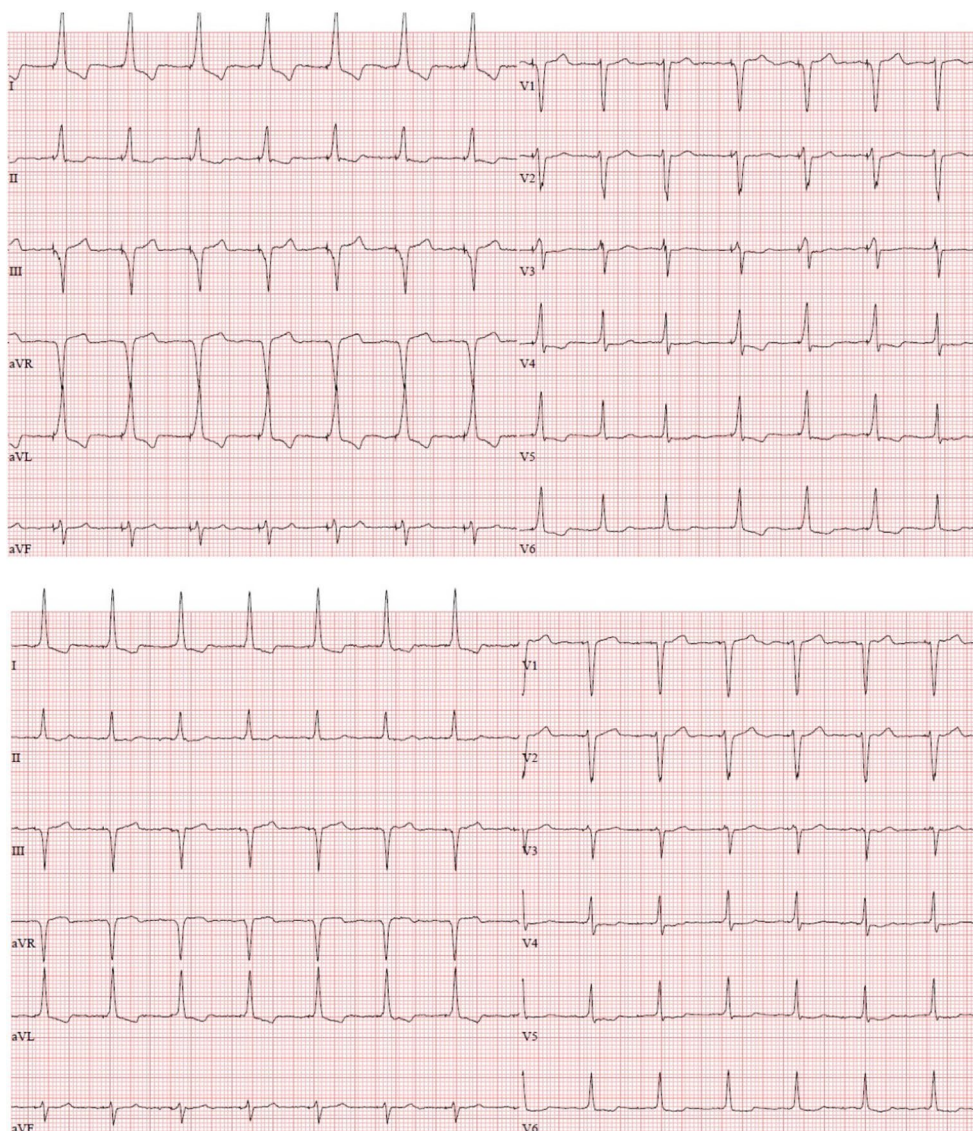


Fig. 116.1 Intermittent non-selective (above) and selective (below) His-bundle pacing

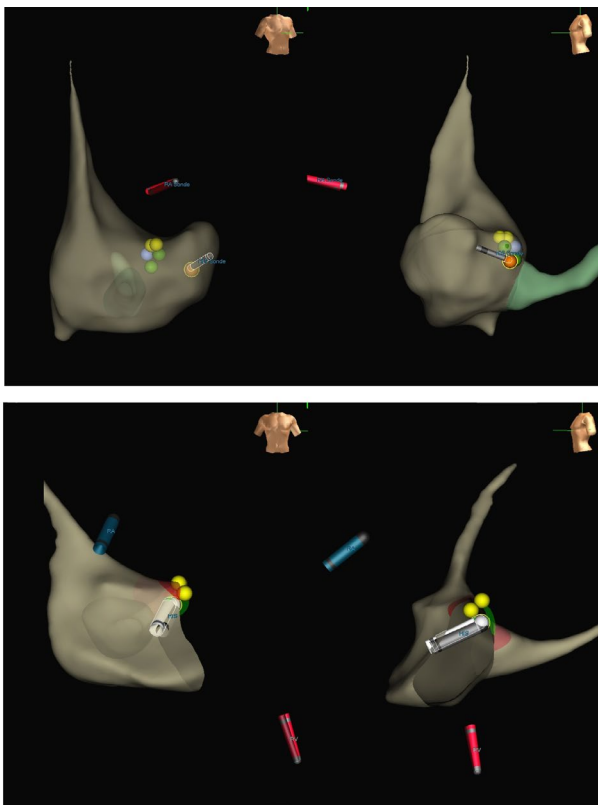


Fig. 216.1 Electroanatomical 3D mapping guidance in a HBP procedure without (above) and with (below) a back-up RV pacing-lead

centage of ventricular pacing. The procedure duration is longer at the start of the learning curve, but declines relatively fast with accumulating experience. The use of an electroanatomical 3D mapping system for accurate anatomical localisation of His-Bundle appears to accelerate the learning curve and improve the success rate of HBP at least at the initial phase of a HBP program.

6.2

Genderspezifische Unterschiede im Outcome nach kardiopulmonaler Reanimation

M. Haslinger¹, R. Rezar¹, B. Wernly¹, C. Seelmaier¹, P. Schwaiger¹, I. Pretsch¹, M. Eisl¹, C. Jung², U. C. Hoppe¹, M. Lichtenauer¹

¹Universitätsklinikum für Innere Medizin II, PMU Salzburg, Salzburg, Österreich

²Kardiologie, Universitätsklinik Düsseldorf, Düsseldorf, Deutschland

Einleitung: Genderspezifische Unterschiede sind quer durch die Medizin zu finden und erfahren zunehmende Aufmerksamkeit. Das Ziel der Studie war zu untersuchen, ob und wie stark Unterschiede im Outcome nach kardiopulmonaler Reanimation zwischen männlichen und weiblichen Patienten auftreten. Die diesbezügliche Datenlage vorhandener Studien zeigt divergente Ergebnisse – teilweise mit besserem Outcome für Männer und teilweise für Frauen.

Methoden: In dieser prospektiven Single-Center Studie wurden zwischen 2018 und 2020 PatientInnen untersucht, die

nach kardiopulmonaler Reanimation auf der Intensivstation behandelt wurden und mindestens 24 Stunden überlebten. Reanimationen infolge von Traumata wurden exkludiert. Der primäre Endpunkt war die Mortalität nach 6 Monaten. Als sekundärer Endpunkt wurde das neurologische Outcome nach 1 und 6 Monaten in 4 Kategorien eingeteilt.

Resultate: Insgesamt wurden 106 PatientInnen (76 Männer, 30 Frauen) mit einem Durchschnittsalter von 65 Jahren eingeschlossen. Männliche Patienten erreichten den primären Endpunkt, Überleben nach 6 Monaten, häufiger als weibliche Patienten, jedoch war der Unterschied nicht statistisch signifikant (68 % vs. 57 %, HR 0,68, 95 %CI 0,35–1,34, $p=0,27$). In den Subgruppen Alter $>/<65$ Jahre ($p=0,76/0,12$), Laktat $>/<2,5$ mmol/l ($p=0,35/0,14$), LVEF $>/<30$ % ($p=0,43/0,31$) und mit/ohne ACS ($p=0,18/0,73$) ergaben sich keine Überlebensbenefits, was sich auch in einer multivariaten Analyse bestätigte ($p=0,17$). Hinsichtlich des sekundären Endpunktes, dem neurologischen Outcome nach 1 und 6 Monaten, zeigten sich ebenso keine statistisch signifikanten Unterschiede zwischen den Geschlechtern. Insgesamt hatten lediglich 12 % der PatientInnen nach einem Monat ein schlechtes neurologisches Outcome (CPC 3–4) und kein Patient nach 6 Monaten.

Schlussfolgerungen: Männliche und weibliche Patienten zeigten im Gesamtüberleben keine signifikanten Unterschiede, jedoch eine Tendenz zur höheren Mortalität bei Frauen. Das neurologische Outcome der beiden Geschlechter war vergleichbar und überwiegend gut oder sehr gut. Die Gesamtmortalität lag mit ca. 35 % nach 6 Monaten unter den meisten vergleichbaren Studienkollektiven.

6.3

Risk factors associated with atrial fibrillation in hypertrophic cardiomyopathy

D. Dalos¹, T. Dachs¹, M. Srdits¹, L. Stix¹, C. Kronberger¹, R. Rettl¹, C. Binder¹, F. Duca¹, L. Schrutka¹, R. Badr Eslam¹, J. Kastner¹, D. Bonderman², M. Gwechenberger¹

¹Medizinische Universität Wien, Wien, Austria

²Klinik Favoriten, Wien, Austria

Background: Atrial fibrillation (AF) is a common arrhythmia in patients with hypertrophic cardiomyopathy (HCM) that is associated with substantial morbidity and mortality. Therefore, identifying patients at risk is of utmost importance. Objectives. To identify clinical, laboratory and imaging characteristics that are associated with the occurrence of AF.

Methods: HCM was defined as interventricular septal thickness ≥ 15 mm in the absence of abnormal loading conditions. The primary endpoint was paroxysmal, permanent or persistent AF detected on 12-lead electrocardiogram, Holter-monitoring or implantable device interrogation.

Results: Between August 2018 and February 2021 a total of 198 patients (53.5 ± 14.6 years, 35.9 % female) have been evaluated. The primary endpoint occurred in 15.2 % of patients ($n=30$). AF patients were older ($p=0.025$), had higher body mass indices ($p=0.029$), higher serum levels of troponin ($p=0.002$), larger left atrial (LA) volumes indices (LAVI, $p < 0.001$) and lower global LA strain values ($p < 0.001$) as assessed by echocardiography. A subgroup of 136 patients underwent cardiac magnetic resonance imaging and AF patients had larger LAVI ($p < 0.001$), lower LA ejection fraction ($p < 0.001$), lower ventricular longitudinal ($p=0.001$) and circumferential ($p=0.001$) but higher radial strain values ($p < 0.001$). LAVI and global LA

strain values showed a significant, albeit weak negative correlation ($r = -0.588$, $p < 0.001$). In multivariable logistic regression analysis, LAVI was independently associated with the presence of AF (OR 1.052, $p = 0.037$).

Conclusion: Resolute workup of LA size and function seems crucial in HCM patients. Close follow-up of these parameters might be beneficial in early AF detection and consecutive prevention of thromboembolic events.

6.4

Effects of SARS-CoV-2 infection on cardiac function—preliminary data on cardiac mrt parameters after COVID-19

A. Iscel¹, C. Binder², J. Niebauer¹, S. Klenk¹, R. Badr Eslam², M. Kahr², S. Cadjo², T. Dachs², R. Rettl², R. Böck¹, S. Reiter-Malmqvist¹, S. Hoffmann¹, C. Krestan³, A. Zoufaly⁴, C. Wenisch⁴, D. Bonderman¹

¹Klinik Favoriten – 5. Med. Abt. (Kardiologie), Wien, Austria

²AKH Wien – Universitätsklinik für Innere Medizin II (Kardiologie), Wien, Austria

³Klinik Favoriten – Radiologie, Wien, Austria

⁴Klinik Favoriten – 4. Med. Abt. (Infektiologie), Wien, Austria

Introduction: The SARS-CoV-2 pandemic of 2020 has an influence on people's lives worldwide, impacting global health and putting pressure on health care systems, politics and economies. There have been many studies in terms of Covid-19 describing acute cardiac involvement, but little is known about the long-term cardiac effects and complications after recovery. The aim of this study was to assess subclinical myocardial dysfunction by cardiac magnetic resonance imaging (MRI) in patients after COVID-19-infection

Methods: This study was a prospective, multicentre registry study. We included patients after a verified infection with the SARS-CoV-2 virus, who had been discharged from the hospital. Baseline parameters including clinical history, vital signs and symptoms were assessed. In addition, we measured laboratory parameters and transthoracic echocardiography and cardiac MRI were performed in each patient, for morphological and functional assessments.

Results: In this ongoing trial, we present data of the first 46 patients (27 males, 19 females; median age: 47.5 years (34.0–58.0)). 83 % of all patients included so far had an only mild to moderate course of disease and 17 % of them had a severe course being admitted to an intensive care unit. The median time from hospital discharge to clinical assessment was 29.0 weeks (IQR 23.0–33.0). In 30 of 46 patients cardiac MRI was performed. 16 patients were excluded because of panic attacks or other reasons. After 6 months, 30 % of all cardiac MRIs (10 of 30) showed abnormalities, mostly pericardial effusions up to 9 mm and late gadolinium enhancement. 3 of 4 cases with late gadolinium enhancement had a medical history of cardiomyopathy and findings were unlikely associated with SARS-CoV-2 infection. All of them had a medical history of art. hypertension, diabetes and/or hyperlipidemia. One patient with late gadolinium enhancement had no medical history of cardiomyopathy and his findings were likely associated with SARS-CoV-2-infection

Conclusion: This interim analysis of our ongoing study shows that 6 months after Covid-19 infection, 30 % of hospitalized patients showed pathologic findings in cardiac MRI. By the end of the study we shall present more comprehensive information about findings in cardiac MRI.

6.5

Of the X and the Y—sex-specific differences in patients presenting with acute myocarditis

L. Schmutzler¹, M. Mirna¹, A. Topf¹, U. Hoppe¹, M. Lichtenauer¹

¹Department of Internal Medicine II, Division of Cardiology, Paracelsus Medical University of Salzburg, Austria, Salzburg, Austria

Introduction: Biological sex has a paramount influence on the pathophysiology of diseases, and thus on clinical presentation. In this study, we provide a comprehensive analysis of sex-specific differences in patients with myocarditis, with regards to laboratory parameters, abnormalities on the electrocardiogram (ECG) and transthoracic echocardiography (TTE), as well as diagnostic procedures and outcome.

Methods: Patients with myocarditis who were admitted to our study center in the time-period of 2009 to 2019 were retrospectively enrolled in this study. Clinical data, laboratory parameters and measurements from transthoracic echocardiography were extracted from hospital records. Follow-up was acquired for 2 years after admission.

Results: 224 patients with myocarditis were enrolled in this study. Of these, 78 % were males and 22 % females. Female patients were older (median 50 years vs. 35 years, $p < 0.0001$), had a higher prevalence of respiratory tract infections and less frequently ST-segment elevations on ECG (28 % vs. 59 %, $p = 0.003$). Furthermore, C-reactive protein was lower in females (median 0.60 mg/dl vs. 3.90 mg/dl, $p < 0.0001$), but showed a less pronounced decrease within three days when compared to males (fold-change 1.00 vs. 0.80, $p = 0.002$). Cardiac MRI was conducted less often in females, whereas time to coronary angiography was significantly longer. We found no difference in LV systolic function or all-cause-mortality between the two sexes.

Conclusion: We observed sex-specific differences in laboratory parameters, abnormalities on ECG and diagnostic procedures conducted in patients with myocarditis. Understanding these differences, both at the cellular level and in regards to the clinical presentation of patients, could be helpful in the diagnosis and treatment of this disease and could further expand our understanding of its pathophysiology.

6.6

Agreement between high-sensitivity c-reactive protein and c-reactive protein assays

E. Han¹, M. Fritzer-Szekeres², T. Szekeres², A. Anvari-Pirsch¹, M. Gyöngyösi¹, J. Bergler-Klein¹

¹Universitätsklinik für Innere Medizin II, Klinische Abteilung für Kardiologie, Medizinische Universität Wien, Wien, Austria

²Klinisches Institut für Labormedizin, Medizinische Universität Wien, Wien, Austria

Introduction: High sensitivity C-reactive protein (hs-CRP) is a biomarker used for risk prediction for cardiovascular disease (CVD) by assessing low concentrations of inflammatory markers. Measurements of regular CRP assays have become very sensitive as well, with a detection limit of 0.03 mg/dL, as well as being more available and cheaper. Existing studies link chronic subclinical systemic inflammation with a higher degree

CRP	hs-CRP			Total
	Low risk; n (%)	Average risk; n (%)	High risk; n (%)	
Low risk; n (%)	191 (86.0)	4 (2.0)	0 (0.0)	195
Average risk; n (%)	31 (14.0)	180 (90.0)	0 (0.0)	211
High risk; n (%)	0 (0.0)	16 (8.0)	168 (100.0)	184
Total	222	200	168	590

91.4 % (539/590) of patients were classified into the same risk group ($\kappa = 0.87$; $p < 0.001$).

Fig. 116.6 Kappa statistic

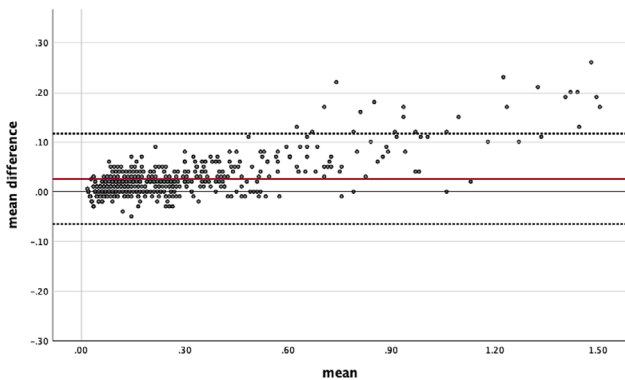


Fig. 216.6 Bland-Altman plot

of atherosclerosis, a known cause of pathogenesis for acute myocardial infarction or other CVDs. The aim of this study is to compare the association between CRP and hs-CRP.

Methods: This study compared CRP and hs-CRP serum concentrations and data acquired by medical chart review of 590 patients from 11/2017 to 10/2018 of our cardiology outpatient clinic who were divided into hs-CRP and CRP risk groups for cardiovascular events: low < 0.1 mg/dL, average 0.1–0.3 mg/dL, high > 0.3 mg/dL. Both hs-CRP and CRP were measured by automated latex-particle enhanced immunoturbidimetric assay kit (Roche Diagnostics) on a COBAS 702 analyser (Roche/Hitashi). CRP measurements used CRPL3 (C-Reactive Protein Gen.3, Roche Diagnostics), while hs-CRP measurements used CRPHS (Cardiac C-Reactive Protein (Latex) High Sensitive, Roche Diagnostics). Blood samples were centrifuged and measurements done on the same day of the sample collection, as per routine procedure. Detection limits for hs-CRP measurements were 0.015–2.0 mg/dL and for CRP measurements 0.03–35 mg/dL. The agreement of classification in hs-CRP risk groups and CRP risk groups was assessed by kappa statistic, with Kappa coefficient of < 0.20 , 0.21–0.40, 0.41–0.60, 0.61–0.80, 0.81–0.99 interpreted as slight, fair, moderate, substantial and almost perfect agreement, respectively. Bland-Altman analysis was used to assess agreement between hs-CRP and CRP by plotting the mean of the two measurements on the x-axis against the mean difference of CRP—hs-CRP on the y-axis. Statistical analyses were performed using IBM SPSS Statistics 26.

Results: Out of all 590 patients, 37.7 % were in low risk, 33.9 % in average risk and 28.5 % in high risk hs-CRP group. Some group changes occurred after reclassification of the patients according to CRP measurements. Eight percent (47/590) of patients were categorised into a higher risk group, 0.7 % (4/590) reclassified into a lower risk group, while 91.4 % (539/590) remained in the same risk group as determined by hs-CRP ($\kappa = 0.87$; $p < 0.001$) (Fig. 1). Important to note, there was a 100 % agreement between the high-risk CRP and hs-CRP group patient classification. Bland-Altman plot displayed a fixed bias with an average difference between the two laboratory tests for CRP and hs-CRP of 0.02 mg/dL \pm 0.09 SD with only sporadic

outliers. The upper limit of agreement was 0.12 and lower limit of agreement was -0.07 . In the lower range of CRP values, measurements were tightly clustered around the average difference. Greater variability could be observed at higher serum level of the inflammatory biomarker in the Bland-Altman plot with a bias to higher CRP concentrations than hs-CRP concentrations at values greater than 0.5 mg/dL. This proportional bias, which was further demonstrated by linear regression analysis, does not affect the risk predicting qualities of hs-CRP or CRP for CVD because the cut-off values for risk groups (0.1 mg/dL for low risk, 0.3 mg/dL for high risk) are all below this threshold.

Conclusion: A close agreement between measurements of hs-CRP and CRP assays was identified, therefore regular CRP assays could replace hs-CRP for cardiac risk assessment. Benefits for clinical implementation are: First, CRP assessment is routinely available in most laboratories compared to hs-CRP. Second, CRP is less costly than hs-CRP, since no further laboratory acquisitions are necessary, which is especially relevant in regions where cost efficiency is of importance.

6.7

Tests zur Diagnostik von COVID-19 – Prinzipien kommerziell verfügbarer Tests

R. Siekmeier¹, J. Hannig¹, T. Grammer², W. März³

¹Drug Regulatory Affairs, Pharmazeutisches Institut der Universität Bonn, Bonn, Deutschland

²Medical Clinic V, Mannheim Medical Faculty, University of Heidelberg, Mannheim, Deutschland

³Synlab Akademie, Mannheim, Mannheim, Deutschland

Einleitung: Im Dezember 2019 wurde auf einem lokalen Fisch- und Wildtiermarkt in Wuhan/China der Ausbruch einer neuartigen Viruserkrankung beschrieben, der am 07.01.2020 vom Chinese Center for Disease Control (CCDC) als neue Coronavirusinfektion identifiziert wurde und am 11.02.2020 von der World Health Organization (WHO) den Namen 2019-new coronavirus disease (2019-nCoV, jetzt COVID-19) erhielt. Binnen kurzer Zeit erfolgte eine weltweite Verbreitung der Erkrankung (01.08.2020: 18 Millionen nachgewiesene Infektionen, 650.000 nachgewiesene Todesfälle; 19.03.2021: 122 Millionen nachgewiesene Infektionen, 2,7 Millionen nachgewiesene Todesfälle). Aufgrund der raschen Ausbreitung der Erkrankung wurde in kurzer Zeit eine Vielzahl diagnostischer Tests zum Virusnachweis (PCR, RT-PCR und vergleichbare Methoden, Antigen tests (Labormethoden, Schnelltests (Lateral-Flow-Assays) zum Gebrauch durch professionelle und Laienanwender in Nase-Rachenabstrichen, Speichel und vergleichbaren Materialien) und Antikörpertests (IgG, IgM und/oder IgA in Serum/Plasma; Labormethoden, Lateral-Flow-Assays) entwickelt und in Verkehr gebracht. Ziel der Untersuchung war die Erstellung einer Übersicht über wesentliche im Markt befindliche Tests zur Diagnostik von COVID-19.

Material und Methoden: Zur Erstellung einer Übersicht über im Markt befindliche Tests zur Diagnostik von COVID-19 erfolgte eine Internetrecherche mit Suche entsprechender Listungen und Charakterisierungen von Tests.

Resultate: Am schnellsten entwickelt wurden als Referenz dienende molekulare Tests (PCR und vergleichbare Tests) und Antikörpertests. Es folgten Antigen tests, häufig als Schnelltests (Lateral-Flow-Assays, meist zur professionellen Anwendung), die aufgrund rascher/einfacher Durchführbarkeit in der Epidemiekontrolle von hoher Bedeutung sind. Auf der Webseite [https://www.360dx.com/coronavirus-test-tracker-launched-](https://www.360dx.com/coronavirus-test-tracker-launched)

covid-19-tests waren am 15.03.2021 520 Tests und 13 Collection devices gelistet (Stand: 31.07.2020: 280), davon 386 mit Emergency Use Authorization der Federal Drug Agency (die meisten) oder des Centers for Disease Control (CDC; wenige) der USA bzw. 204 mit CE-Kennzeichen der Europäischen Union und 34 mit Zulassung in anderen Ländern (meist Asien). Meist handelte es sich um PCR Tests (321), seltener um serologische Tests (124), Antigentests (39), isothermale Amplifikation (17), Sequenzierung (7), CRISPR (3) und andere Methoden. Eine Liste des BfArM (<https://antigentest.bfarm.de/ords/f?p=101:100:12570088148110:::and:tz=1:00>) führt 241 (Stand: 19.03.2021) Antigentests zum Gebrauch durch professionelle Anwender, meist Schnelltests, auf und stellt Informationen zur Validierung durch das Paul-Ehrlich-Institut (109 Tests), Europäischem Bevollmächtigten, Sensitivität und Spezifität (nach Herstellerangaben) sowie weitere Produktinformationen (z.B. Art des Tests (Point of Care Test (POCT) ohne Gerät (208), POCT mit Gerät (15), Labortest (3)), Gebrauchsanweisung) zur Verfügung.

Schlussfolgerungen: Zusammenfassend zeigt sich ein rascher Anstieg von Zahl und Qualität zur Verfügung stehender Tests, wobei die Entwicklung der Tests durch regulatorische Richtlinien (z.B. <https://www.gov.uk/government/publications/how-tests-and-testing-kits-for-coronavirus-covid-19-work>, <https://www.fda.gov/emergency-preparedness-and-response/coronavirus-disease-2019-covid-19/covid-19-related-guidance-documents-industry-fda-staff-and-other-stakeholders>) begleitet wird. Molekularbiologisch basierte Tests wie die PCR stellen die Referenzmethode der Virusdiagnostik dar und werden durch Antigenschnelltests (auch zur Laienanwendung) ergänzt.

6.8

The rhythmologic influence of arterial hypertension on non-obstructive hypertrophic cardiomyopathy

T. Dachs¹, L. Stix¹, C. Kronberger¹, M. Srdits¹, R. Rettl¹, C. Capelle², C. Hengstenberg¹, J. Kastner¹, D. Dalos¹, D. Bonderman¹

¹Medizinische Universität Wien, Wien, Austria

²Klinik Favoriten, Wien, Austria

Introduction: Hypertrophic cardiomyopathy (HCM) is defined by a non-dilated hypertrophic left ventricle that cannot be explained by abnormal loading conditions alone. Hypertensive heart disease represents a frequent phenocopy that remains complex to differentiate from HCM, particularly in the absence of left ventricular outflow tract obstruction (1,2). The aspect of coexistence might however be crucial regarding individual risk for arrhythmia.

Methods: Between May 2018 and January 2021, 186 patients were diagnosed with HCM according to current standard. Potential differential diagnoses were excluded accordingly (6–8). 100 (54%) patients presented without significant left ventricular outflow tract obstruction. Systemic arterial hypertension—defined by elevated blood pressure $\geq 150/90$ mm Hg at ≥ 3 distinct timepoints and/or ≥ 3 antihypertensive agents prescribed—was diagnosed in 59 (58%) patients. Rhythmologic assessment via 24-hour Holter electrocardiogram was performed on site in 59 (58%) patients.

Results: Hypertensive patients were significantly older ($p < 0.01$) and more frequently suffered from coexistent comorbidities such as diabetes ($p = 0.02$), hyperlipidemia ($p < 0.01$), coronary artery disease ($p = 0.07$), chronic obstructive pulmo-

Table 116.8 Baseline characteristics of normotensive and hypertensive non-obstructive HCM patients

	Normotensive (n=41)	Hypertensive (n=59)	p-values
Clinical characteristics			
Age, y	47 (15)	54 (12)	0.01
Female sex, %	9 (22)	12 (20)	0.85
Body surface area, m ²	2.04 (0.24)	2.07 (0.20)	0.47
Body mass index, kg/m ²	28.5 (4.7)	29.5 (4.8)	0.31
Systolic blood pressure, mm Hg	133 (18)	154 (32)	<0.01
Diastolic blood pressure, mm Hg	82 (11)	93 (17)	<0.01
Comorbidities, %			
Diabetes mellitus	3 (7)	14 (24)	0.02
Hyperlipidemia	7 (17)	25 (42)	<0.01
Coronary artery disease	6 (15)	17 (29)	0.07
Chronic obstructive pulmonary disease	0 (0)	5 (9)	0.07
Chronic kidney disease	3 (7)	22 (38)	<0.01
Atrial fibrillation	9 (22)	7 (12)	0.18
Devices, %			
Pacemaker	1 (2)	2 (3)	1.00
Implantable cardioverter defibrillator	11 (27)	4 (7)	<0.01
Functional Status			
– NYHA ≥ 2 , %	14 (34)	36 (61)	<0.01
– 6 minute walk test, m	511 (118)	461 (130)	0.10
Cardiac biomarkers			
– Median NT-proBNP, pg/mL (IQR)	357 (102–725)	341 (93–823)	0.68
Echocardiography			
Interventricular septum, mm	20 (5)	20 (4)	0.80
Interventricular septum/posterior wall thickness, mm	1.86 (0.57)	1.67 (0.44)	0.09
Left ventricular mass index, g/m ²	139 (40)	165 (58)	0.03
LVEF, %	60 (8)	57 (10)	0.24
Left ventricular end-diastolic volume index, mL/m ²	43 (14)	47 (17)	0.37
Left ventricular end-systolic volume index, mL/m ²	18 (7)	21 (10)	0.16
Global longitudinal strain, %	–16 (4)	–14 (4)	0.19
Left atrial volume index, mL/m ²	38 (20)	37 (19)	0.86
Left atrial strain, %	–23 (10)	–16 (9)	0.02

nary disease ($p = 0.07$) and chronic kidney disease ($p = 0.01$). Only atrial fibrillation, the most common sustained arrhythmia in HCM (3), occurred more often in normotensive patients ($p = 0.18$). Hypertensive patients described worse symptoms of dyspnea ($p < 0.01$) and obtained worse results in 6-minute walk test ($p = 0.10$). N-terminal prohormone of brain natriuretic peptide did not differ between groups ($p = 0.68$). Left ventricular mass index was significantly elevated in hypertensive patients ($p = 0.03$). Left atrial dimensions were balanced, however strain

Table 216.8 Parameters of 24-hour Holter electrocardiogram

Parameter	Normotensive (n=30)	Hypertensive (n=28)	p-values
Sinus rhythm	28 (93)	26 (93)	1.00
Heart rate, bpm	69 (9)	74 (9)	0.04
Supraventricular extrasystols ≥1 %	7 (23)	2 (7)	0.15
Ventricular extrasystols ≥1 %	1 (3)	4 (14)	0.19
Supraventricular tachycardia	11 (37)	12 (43)	0.54
Non-sustained ventricular tachycardia	8 (27)	2 (7)	0.08

presented significantly worse in hypertensive patients ($p=0.02$). The presence of non-sustained ventricular tachycardia as an important risk factor for sudden death was slightly elevated in normotensive patients ($p=0.08$). Accordingly, implantable cardioverter-defibrillators were present in normotensive patients with greater frequency ($p<0.01$).

Conclusion: Patients diagnosed with hypertensive, non-obstructive HCM, despite older and sicker, tend to suffer less from atrial fibrillation, non-sustained ventricular tachycardia and therefore might be at lower risk for sudden cardiac death.

6.9

Intensivmedizinische Behandlung von älteren und sehr alten PatientInnen mit Sepsis und septischem Schock: Eine Analyse aus der multizentrischen e-ICU Datenbank

B. Wernly¹, B. Mamandipoor², R. Rezar¹, B. Guidet³, D. De Lange⁴, D. Dankl⁵, A. Koköfer⁵, T. Danninger⁵, W. Szczeklik⁶, S. Sigal⁷, P. V. van Heeren⁸, M. Beil⁹, J. Fjølner¹⁰, S. Leaver¹¹, H. Flaatten¹², V. Osmani², C. Jung¹³

¹Department of Cardiology, Clinic of Internal Medicine II, Paracelsus Medical University of Salzburg, Salzburg, Österreich

²Fondazione Bruno Kessler Research Institute, Trento, Italien

³Saint-Antoine Hospital, Paris, Paris, Frankreich

⁴UMC Utrecht, Utrecht, Niederlande

⁵Department of Anesthesiology and Intensive Care, Paracelsus Private Medical University Salzburg, Salzburg, Österreich

⁶Intensive Care and Perioperative Medicine Division, Jagiellonian University Medical College, Kraków, Krakau, Polen

⁷Medical Intensive Care Unit, Hadassah University Hospital, En Kerem, Jerusalem, Jerusalem, Israel

⁸General Intensive Care Unit, Hadassah University Hospital, En Kerem, Jerusalem, Jerusalem, Israel

⁹Institute of Health Sciences at PTHV, Vallendar, Deutschland

¹⁰Department of Intensive Care, Aarhus University Hospital, Aarhus, Dänemark

¹¹Research Lead Critical Care Directorate St George's Hospital, London, London, Großbritannien

¹²Haukeland University Hospital Bergen, Bergen, Norwegen

¹³Division of Cardiology, Pulmonology, and Vascular Medicine, Medical Faculty, University Duesseldorf, Düsseldorf, Deutschland

Einleitung: Sepsis ist ein häufiges Krankheitsbild auf Intensivstationen mit sehr hoher Mortalität. Mit strikten Protokollen bis hin zur rezenten SEPSIS-3 Definition konnten einige Aspekte der Behandlung standardisiert und verbessert werden. Gerade bei älteren kritisch kranken PatientInnen stellt sich häufig die Frage inwieweit noch ein Nutzen von einer intensivmedizinischen Behandlung davongetragen werden kann oder, ob man ein Leben auf eine unwürdige Art und Weise an Maschinen beendet. Ältere Menschen (>64 Jahre) und sehr alte Menschen (>79 Jahre) weisen oftmals eine sehr hohe Mortalität an Intensivstationen auf. Vom ethischen Standpunkt aus aber auch in Zeiten der aktuellen COVID-19 Pandemie mit eventuell restriktiver Ressourcenallokation stellt sich immer wieder die Frage, ob chronologisches Alter alleine ein Triagegrund sein kann und darf. In dieser Studie sind wir dieser Frage mit einer Analyse von 9385 PatientInnen mit Sepsis aus der eICU-Datenbank weiter nachgegangen.

Methoden: Basis-Charakteristika und intensivmedizinische Maßnahmen wurden aus der Datenbank extrahiert. PatientInnen wurden in ältere (65–79 Jahre; $n=6184$) und sehr alte Menschen (ab 80 Jahren; $n=3201$) unterteilt. Für die Definition des septischen Schocks wurde die Sepsis-3-Definition herangezogen. Als primärer Endpunkt wurde Mortalität im Rahmen des Intensivaufenthaltes gewählt, als sekundäre Endpunkte dienten mechanische Beatmung und Einsatz von Katecholaminen. Eine logistische Multilevel-Regressionsanalyse wurde durchgeführt, wofür drei sequentielle Regressionsmodelle herangezogen

wurden. Im ersten Modell wurde das Patientenalter als fixer, die Intensivstation als Random-Effekt verwendet. In Modell-2 wurden verschiedene Patientencharakteristika (Geschlecht, Ethnizität, body mass index, Infektfokus, SOFA score) als unabhängige Variablen hinzugefügt. Im dritten Modell wurden intensivmedizinische Maßnahmen ergänzt. Alle Analysen wurden auf die gesamte Kohorte ($n=9385$), sowie die Subgruppe an PatientInnen mit septischem Schock ($n=1054$) berechnet. Weiters wurde anhand des ersten Modells eine stratifizierte Sensitivitätsanalyse anhand von verschiedenen Parametern ergänzt.

Resultate: Für sehr alte Menschen konnte im Median ein kürzerer Intensivstationsaufenthalt gezeigt werden (50 ± 67 Stunden versus 56 ± 72 Stunden; $p < 0,001$) und auch der Anteil an sehr kurzen Intensivaufenthalten (< 72 Stunden) war bei sehr alten Menschen größer (65% vs. 62% ; $p < 0,001$). Entsprechend war auch der Anteil an protrahierten Intensivstationsaufenthalten (> 168 Stunden) bei sehr alten Menschen kleiner (9% vs. 12% ; $p < 0,001$). Auch hinsichtlich der Mortalität aufgrund von Sepsis und bei septischem Schock zeigte sich ein Unterschied zwischen älteren und sehr alten Menschen (11% vs. 13% bzw. 36% vs. 38%). Sehr alte Menschen wiesen geringere mediane BMIs ($25 \pm 8 \text{ kg/m}^2$ vs. $27 \pm 10 \text{ kg/m}^2$) und auch SOFA-Scores (10 ± 5 Punkte vs. 9 ± 4 Punkte) auf. Hinsichtlich der Menge an Flüssigkeitssubstitution zeigten sich keine relevanten Unterschiede, wohingegen sehr alte Menschen seltener mechanisch beatmet wurden (42% vs. 55% ; $p < 0,001$).

Schlussfolgerungen: In dieser Analyse von 9385 älteren und sehr alten PatientInnen mit Sepsis zeigt sich eine geringe, jedoch statistisch signifikant höhere Mortalität bei sehr alten Menschen. Dennoch sollte trotz der statistischen Signifikanz chronologisches Alter alleine kein Grund für das Vorenthalten einer intensivmedizinischen Therapie sein. Zeit-limitierte ICU-Trials stellen eine gute Möglichkeit dar, Zeit und Informationen zu gewinnen, um auch in Zeiten von begrenzten Ressourcen eine individuelle, PatientInnen-zentrierte Intensivtherapie anbieten zu können.

6.10

sST2 als vielversprechender Indikator nach kardiopulmonaler Reanimation

B. Sipos¹, R. Rezar¹, V. Paar¹, C. Seelmaier¹, I. Pretsch¹, P. Schwaiger², K. Kopp¹, R. Kaufmann³, T. K. Felder⁴, E. Prinz¹, G. Gemes⁵, R. Pistulli⁶, U. C. Hoppe¹, B. Wernly¹, M. Lichtenauer¹

¹Universitätsklinik für Innere Medizin II, Kardiologie und internistische Intensivmedizin, Salzburg, Österreich

²Universitätsklinik für Anästhesiologie, perioperative Medizin und allgemeine Intensivmedizin, Salzburg, Österreich

³Universitätsinstitut für Radiologie, Salzburg, Österreich

⁴Universitätsinstitut für Medizinisch-Chemische Labordiagnostik – Zentrallabor LKH, Salzburg, Österreich

⁵Abteilung für Anästhesiologie und Intensivmedizin, Graz, Österreich

⁶Klinik für Kardiologie I: Koronare Herzkrankheit, Herzinsuffizienz und Angiologie, Münster, Deutschland

Einleitung: Eine der komplexesten Fragen, welche sich Intensivmediziner nach einer kardiopulmonalen Reanimation stellen, ist das prognostische Outcome des Einzelnen. Soluble suppression of tumorigenicity 2 (sST2) ist ein neuartiger Biomarker, der bei verschiedenen Krankheitsbildern, wie zum Beispiel Herzinsuffizienz, als Indikator eingesetzt wird. Ziel dieser

Studie war es, die prognostische Wertigkeit von sST2 bei Patienten nach kardiopulmonaler Reanimation zu zeigen.

Methoden: Hierbei handelte es sich um eine prospektive Beobachtungsstudie. Insgesamt konnten 106 Personen eingeschlossen werden. Die sST2-Spiegel wurden 24 Stunden nach Aufnahme an die Intensivstation mittels ELISA gemessen. Bei den Überlebenden wurde nach 6 Monaten eine Verlaufskontrolle inklusive einer Kategorisierung mittels Cerebral Performance Category (CPC) durchgeführt. Die Individuen wurden in zwei unterschiedliche Subgruppen unterteilt. Einerseits Patienten oberhalb und unterhalb der medianen Serumkonzentration der Gesamtkohorte. Primärer Endpunkt nach 6 Monaten war Tod oder CPC > 2 ; sekundärer Endpunkt war Tod nach 6 Monaten. Es erfolgte eine Regressionsanalyse mit einem uni- und multivariablen Modell.

Resultate: Patienten mit einem erhöhten Risiko für Tod oder eine CPC > 2 nach 6 Monaten hatten Intensivpatienten mit erhöhten sST2 Serumspiegel 24 Stunden nach Aufnahme (OR 1,011, 95 % CI 1,004–1,019, $p=0,004$). sST2-Spiegel, die über dem Median lagen ($> 53,42 \text{ ng/ml}$), waren mit einem erhöhten Risiko für beide Endpunkte behaftet (Tod oder CPC > 2 nach 6 Monaten: 21% vs. 49% , OR 3,59, $p=0,003$). Die Verbindung zeigte sich signifikant nach der Entfernung potenzieller Störfaktoren im multivariablen Modell.

Schlussfolgerungen: Die anhand von 106 Patienten durchgeführte prospektive Studie konnte einen Zusammenhang zwischen den sST2-Spiegeln im Serum der Probanden und der 30-Tages-Mortalität feststellen. Es korrelierte auch mit den anderen Studienendpunkten, sowie der limitierten neurologischen Prognose (CPC > 2) und der Überlebensrate nach 6 Monaten. Diese Daten zeigten, dass sST2 ein potentiell hilfreicher Marker zur Prognoseabschätzung sein dürfte.

6.11

Produktprobleme bei Tests zur Diagnostik von COVID-19 – Analyse der 2020–2021 vom BfArM veröffentlichten Kundeninformationen

R. Siekmeier¹, J. Hannig¹, T. Grammer², W. März³

¹Drug Regulatory Affairs, Pharmazeutisches Institut der Universität Bonn, Bonn, Deutschland

²Medical Clinic V, Mannheim Medical Faculty, University of Heidelberg, Mannheim, Deutschland

³Synlab Akademie, Mannheim, Mannheim, Deutschland

Einleitung: Vermarktung und Marktüberwachung von Medizinprodukten und In-vitro Diagnostika (IVD) sind in Europa durch europäische Direktiven (z.B. Verordnung (EU) 2017/745 über Medizinprodukte, Verordnung (EU) 2017/746 über In-vitro-Diagnostika) geregelt. Bei Vorkommnissen und korrekativen Maßnahmen (Field Safety Corrective Action, FSCA) müssen die Hersteller diese den zuständigen nationalen Behörden (Competent Authority (CA); in Deutschland: Bundesinstitut für Arzneimittel und Medizinprodukte (BfArM) für Medizinprodukte und die meisten IVD, in Österreich: BASG) melden und die Kunden über Kundeninformationen (Field Safety Notice, FSN) informieren, die auch den Behörden zur Verfügung gestellt werden. Seit Erstbeschreibung der Infektion auf einem lokalen Tiermarkt in Wuhan/China im Dezember 2019 und Benennung als 2019-new Coronavirus disease (2019-nCoV, jetzt COVID-19) durch die WHO am 11.02.2020 führte die Pandemie bis zum 19.03.2021 zu 122 Millionen nachgewiesenen Infektionen und 2,7 Millionen Todesfällen. Seit 2020 wurde eine Vielzahl diagnostischer Tests zum Virusnachweis (PCR,

RT-PCR und vergleichbare Methoden, Antigentests (Labormethoden, Schnelltests (Lateral-Flow-Assays)) zum Gebrauch durch professionelle und Laienanwender in Nase-Rachenabstrichen und vergleichbaren Materialien) und Antikörpertests (IgG, IgM und/oder IgA in Serum/Plasma; Labormethoden, Lateral-Flow-Assays) in Verkehr gebracht.

Material und Methoden: Für die in die Studie eingeschlossenen IVD zur Diagnose von COVID-19 erfolgte eine Analyse der vom BfArM 2020 bis 28.02.2021 auf der Homepage (<http://www.bfarm.de/DE/Medizinprodukte/riskinfo/kundeninfo/functions/kundeninfo-node.html>) publizierten FSCA und FSN.

Resultate: Es fanden sich 17 FSCA bei insgesamt 237 FSCA zu IVD im Untersuchungszeitraum, betreffend 7 molekulare Tests, 6 Tests zum Nachweis von Antikörpern (Tests für immunologische Analyser: 2, ELISA: 1, Blot: 1, Lateral-Flow-Assays: 2) und 4 Tests zum Nachweis von Virusantigenen (Tests für immunologische Analyser: 1, Lateral-Flow-Assays: 3). Berichtete Probleme waren Herstellungs-/Verpackungsfehler (4, leere, vertauschte oder falsch befüllte Flaschen, falsche Kartuschen), Kennzeichnungs-/Etikettierungsfehler (3), fehlerhafte Gebrauchsanleitungen und Werteangaben (4), Softwarefehler (2) und Stabilitätsprobleme (1), die oft zu falschen Ergebnissen/Ergebnisbeurteilungen führten sowie nicht näher bezeichnete falsch positive/negative Testergebnisse (4) (multiple entries). Typische korrektive Maßnahmen waren produkt- und fehlerabhängig Rückruf/Vernichtung der Reagenzien, Änderung der Gebrauchsanweisung bzw. Kennzeichnung, Maßnahmenempfehlung zur Testdurchführung und -wiederholung (Retestung), Software-Upgrades und Mitarbeiterschulung.

Schlussfolgerungen: Meldungen zu IVD zur Diagnostik von COVID-19 stellen eine wichtige Gruppe aller IVD dar. Betroffen sind IVD aller Testprinzipien (Analyser/Reagenzien für PCR und immunologische Verfahren, Lateral-Flow-Assays) zum Nachweis von Viren und Antikörpern, die sich in Produktproblemen und korrektiven Maßnahmen unterscheiden. FSN leisten bei FSCA einen wichtigen Beitrag zur Verminderung vom Produkt ausgehender Risiken. Das Europäische Marktüberwachungssystem leistet einen wichtigen Beitrag zur Verbesserung der Sicherheit von IVD.

7 HERZINSUFFIZIENZ

7.1

Detection of left ventricular systolic dysfunction by segmental impedance plethysmography during routine 12 lead ecg screening

K. Danninger¹, R. Binder¹, T. Weber¹

¹Klinikum Wels-Grieskirchen, Wels, Austria

Objective: Early diagnosis of impaired left ventricular systolic function may impact the course of the disease and the prognosis. We aimed to determine whether segmental impedance plethysmography, using and extending the electrodes of a conventional electrocardiography system, can detect a moderate to severe reduction of left ventricular ejection fraction.

Methods: We investigated patients with chronic heart failure as well as healthy controls, using segmental impedance plethysmography, inbuilt in a regular electrocardiography device (Combyn®, www.ac-tc.at, Graz, Austria). Parameters assessed included the area under the curve of the impedance signal measured at different parts of the body (thorax, arms, legs), specifically from the thorax (area-TH); and the time from the

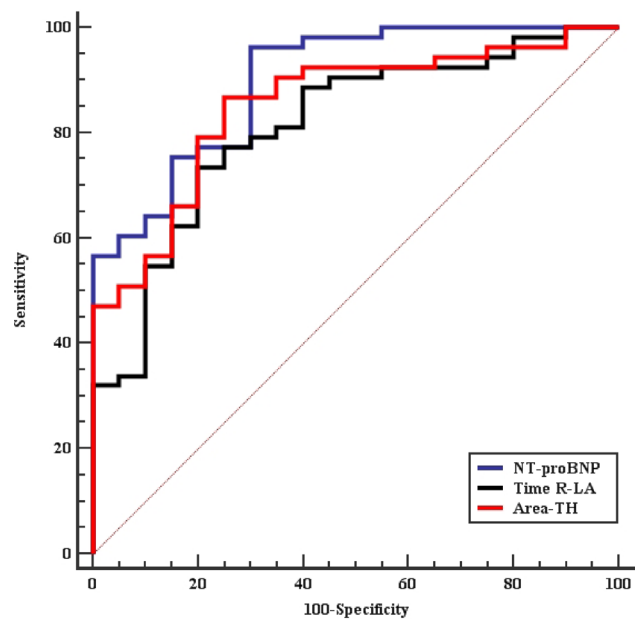


Fig. 117.1 Diagnostic performance of segmental impedance plethysmography-based measures (Time R-LA and Area-TH) and nt-proBNP to detect moderately and severely impaired LVEF. Based on z-statistics, there was no significant differences between AUCs

R wave to the beginning of the impedance signal from different parts of the body (thorax, arms, legs), specifically to the left arm (time R-LA). Comparator was left ventricular ejection fraction (LVEF), assessed by echocardiography using the biplane Simpson method. Statistics used was receiver-operating-curve (ROC) analysis for calculation of the area under the curve (AUC) for discrimination between normal/mild reduced (>45%) and moderately/severely reduced (<45%) EF.

Results: Overall, 75 participants were included, 92% of them were male, mean age was 55.9 years. The prevalence of arterial hypertension, diabetes and coronary artery disease was 32%, 23% and 35%, respectively. Mean LVEF was 39% (ranging from 9% to 75%), and EF was moderately/severely reduced in 71% of the patients.

Conclusion: Using ROC analysis, AUC for detection of moderate/severe reduction of EF was 0.841 (95% CI 0.739-0.916, p -value <0.0001) for area-TH, and 0.807 (95% CI 0.700-0.889, p -value <0.0001) for time R-LA. In comparison, AUC was 0.899 (95% CI 0.806-0.957) for NT-proBNP (Fig. 1). Based on z-statistics, both segmental plethysmography-based AUCs were not statistically different ($p=0.38$ and $p=0.17$, respectively) from NT-proBNP based AUC.

7.2

One-minute sit-to-stand test for evaluating functional exercise capacity in subjects with heart failure with preserved ejection fraction (HFpEF)

C. Kronberger¹, B. Litschauer², T. Dachs¹, R. Rettl¹, L. Camuz Ligios¹, R. Badr Eslam¹

¹Universitätsklinik für Innere Medizin II – Abteilung für Kardiologie, Wien, Austria

²Universitätsklinik für klinische Pharmakologie, Wien, Austria

Introduction: Exercise intolerance is the main chronic symptom in patients with HFpEF and leads to a reduced quality of life (QoL). Thus, exercise testing is a central tool in the clinical evaluation of HFpEF patients. Recent studies have suggested the use of the 1-min sit-to-stand test (1-min STST). In this test the patient is encouraged to stand up from a chair and sit down again as quickly and as many times as possible within one minute without using the upper limbs. The 1-min STST is shorter, requires less space and is easier to perform than the six-minute walk test (6MWT)—a test, which is already well established in the routine assessment of patients with HFpEF. Thus, it might be possible to test more patients. The 1-min STST has already been validated for patients with chronic obstructive pulmonary disease (1), but data on HFpEF patients are lacking. Project goal: Comparison of the 1-min STST with the 6MWT in subjects with HFpEF

Methods: Twenty-nine stable HFpEF patients [mean age: 70 ± 11 yrs, 41 % male, 65.5 % atrial fibrillation, median New York Heart Association (NYHA) class 3 (IQR 2–4)] were prospectively assessed for cardiorespiratory fitness with the 1-min STST and the 6MWT. The two tests were applied in a randomized order and a 10-minutes break between them was attempted. Patient-reported health-related QoL was assessed with the CAMPHOR questionnaire. The Modified Borg Dyspnea Scale was used to gauge symptoms of exertional fatigue and dyspnea.

Results: The median number of 1-min STST repetitions in the overall study sample was 16 (IQR 8–24) and the median six-minute walk distance (6MWD) was 336 m (IQR 136–536 m). We observed a strong correlation between 1-min STST performance and 6MWD ($r=0.646, p<0.001$). Furthermore, number of chair stands were highly and inversely correlated to the responses in the CAMPHOR questionnaire (relation to symptoms: $r=-0.505, p=0.009$, activities: $r=-0.433, p=0.027$, quality of life: $r=-0.581, p=0.002$). There were no statistically significant differences between men and women in both tests and symptom score for dyspnea did not differ for both tests (median value: 5 points, $t(29)=-0.818, p=0.420$). In all multiple regression models, New York Heart Association (NYHA) class provided the best explanation of 1-min STST performance, but age contributed as well.

Conclusion: Outcomes confirm that the 1-min STST is a simple and promising test to evaluate functional fitness and

exercise capacity in chronic HFpEF patients. The prognostic value of this test remains to be established in further studies.

7.3

Long-term outcome in patients with takotsubo syndrome: a single-center study from Vienna

E. Pogran¹

¹Klinik Ottakring, Wien, Austria

Introduction: There is an increasing amount of evidence suggesting multiple fatal complications in Takotsubo Syndrome. However, findings on the long-term outcome are scarce and show inconsistent evidence.

Methods: This is a single-center study of long-term prognosis in Takotsubo patients admitted to Klinik Ottakring, Vienna, Austria, from September 2006 to August 2019. We investigated the clinical features, prognostic factors and outcome of patients with Takotsubo syndrome. Furthermore, survivors and non-survivors and patients with a different cause of death were compared.

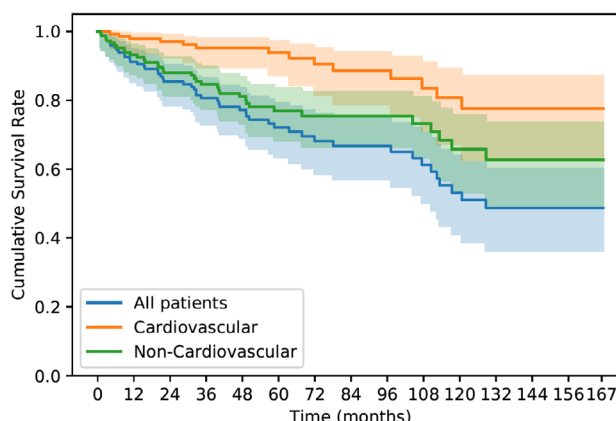
Results: Overall, 147 patients were included in the study. The mean age was 70 years (± 12.3), and 85 % of the study population were women. Forty-nine Takotsubo patients (33.3 %) died during the follow-up, with a median of 126 months. The most common cause of death was a non-cardiac cause (71.4 % of all deaths), especially malignancies (26.5 % of all deaths). Moreover, non-survivors were older and more often men with more comorbidities (chronic kidney disease, malignancy). Patients who died because of cardiovascular disease were older and more often women than patients who died due to non-cardiovascular cause. Age showed to be the only independent prognostic factor of cardiovascular mortality (HR=1.11, CI: 0.99–1.25, $p=0.05$). Female gender (HR=0.32, CI: 0.16–0.64, $p<0.001$), cancer (HR=2.35, CI: 1.15–4.8, $p=0.019$) and chronic kidney disease (HR=2.61, CI: 1.11–6.14, $p=0.028$) showed to be independent predictors of non-cardiovascular mortality.

Conclusion: Long-term prognosis of TTS patients is not favourable, mainly due to non-cardiac comorbidities. Hence,

Variable	Male (n = 12)	Female (n = 17)	p-value
Demographics			
Age, y	73.1 ± 9.4	67.9 ± 11.7	0.214
BMI, kg/m ²	27.8 ± 5.0	34.2 ± 7.7	0.019
NT-proBNP, pg/mL	1974.37 ± 2031.6	1878.2 ± 1863.2	0.896
NYHA class I or II	5 (41.7%)	5 (29.4%)	
NYHA class III or IV	7 (58.3%)	12 (70.6%)	
Comorbidities			
COPD	3 (25.0%)	5 (29.4%)	
Diabetes mellitus type II	7 (58.3%)	5 (29.4%)	
Arterial hypertension	10 (83.3%)	12 (70.6%)	
Hyperlipidemia	10 (83.3%)	13 (76.5%)	
Atrial fibrillation	8 (66.7%)	11 (64.7%)	
Trans thoracic echocardiography			
LVEF	51.89 ± 0.33	53.24 ± 3.15	0.218
sPAP, mmHg	65.8 ± 28.4	65.7 ± 22.3	0.993
Diameter of RV, cm	4.1 ± 0.7	3.8 ± 0.8	0.281
TI Vmax, m/s	3.6 ± 0.9	3.6 ± 0.7	1.000
Right heart catheterization			
mPAP, mmHg	39.7 ± 9.4	42.5 ± 14.2	0.555
PCWP, mmHg	22.1 ± 4.9	21.4 ± 5.1	0.724
PVR, dyn*s/cm ²	301.0 ± 231.6	322.3 ± 205.6	0.796
CI, L/min/m ²	2.8 ± 1.0	2.9 ± 1.0	0.683
Test performance			
6MWD, m	357.1 ± 91.3	293.2 ± 139.0	0.176
6MWD % of predicted	56.6 ± 13.1	56.1 ± 24.0	0.949
1-min STST, reps	17.9 ± 5.5	15.4 ± 7.5	0.348
1-min STST % of predicted	56.2 ± 18.6	48.4 ± 21.1	0.326

Notes. BMI indicates body mass index; NT-proBNP: N-terminal pro-brain natriuretic peptide; NYHA: New York Heart Association; COPD: chronic obstructive pulmonary disease; LVEF: left ventricular ejection fraction; sPAP: systolic pulmonary artery pressure; diameter of RV: right ventricular diameter; TI Vmax: peak trans-tricuspid flow velocity; mPAP: mean pulmonary artery pressure; PCWP: pulmonary capillary wedge pressure; PVR: pulmonary vascular resistance; CI: cardiac index; 6MWD: six-minute walk distance; 6MWD % of predicted: percent of the predicted six-minute walk distance; 1-min STST: 1-minute sit-to-stand test; 1-min STST % of predicted: percent of the predicted 1-minute sit-to-stand test repetitions.

Fig. 117.2 Patient characteristics



months	0	12	24	48	96	120	167
# of patients	154	134	115	83	39	25	2
new deaths: all causes	0	13	8	10	9	7	2
new deaths: cardiovascular	0	3	1	2	4	3	1
new deaths: non-cardiovascular	0	10	7	8	5	4	1

Fig. 117.3 Kaplan-Meier curve for long-term mortality in patients with Takotsubo syndrome

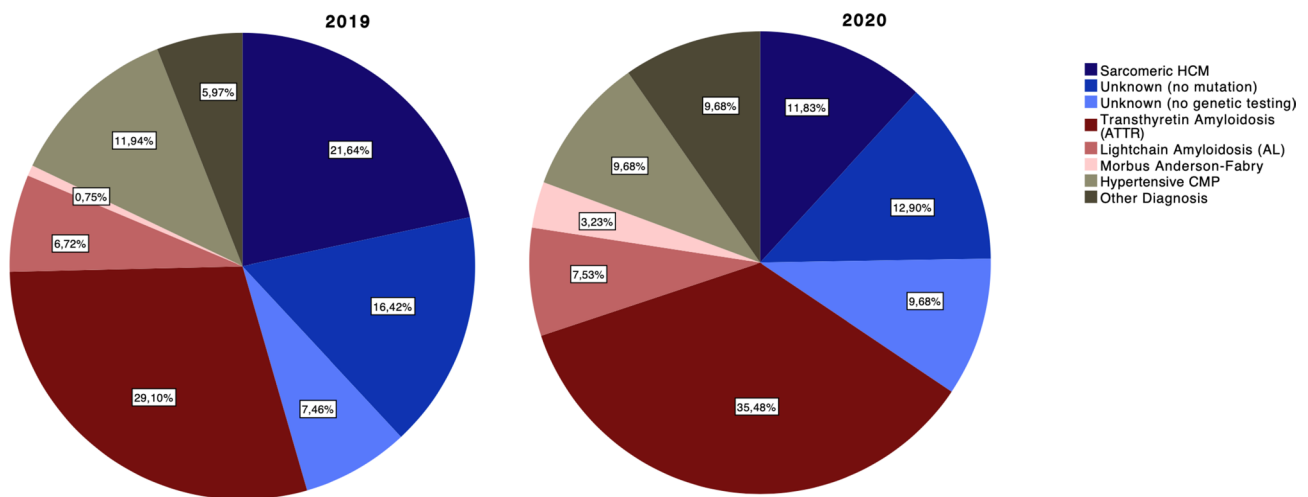


Fig. 117.4 Temporal trending and proportions of diseases leading to HCM phenotype

consequent outpatient care in relatively short time intervals after TTS event based on risk factor control and early detection of malignancies seems mandatory.

7.4

Proportions and temporal trends of diseases leading to a hypertrophic cardiomyopathy phenotype. a prospective single-center cohort study

V. Höller¹, D. Zach¹, E. Kolesnik¹, M. Wallner¹, F. Fruhwald¹, P. Rainer¹, A. Zirlik¹, N. Verheyen¹

¹Department of Cardiology, University Clinic of Internal Medicine, Medical University Graz, Graz, Austria

Introduction: Hypertrophic cardiomyopathies (HCM) are caused by genetic and non-genetic diseases leading to increased left ventricular wall thickness. Previous studies described sarcomere protein gene mutations as the most common aetiology, whereas cardiac amyloidosis was rated as a rare cause affecting an insignificant minority of HCM patients. Due to recent improvements of non-invasive diagnostic tools and novel therapeutic options, earlier epidemiological data on HCM may be outdated. We therefore aimed to investigate proportions and trends of HCM aetiologies using data derived from the Graz HCM Registry.

Methods: The Graz HCM Registry is a prospective, single-center cohort study that has been initiated in February 2019. All patients who consult our HCM outpatient clinic are invited for participation. For the present analysis, we included all participants who fulfilled echocardiographic HCM criteria. Patients underwent cardiovascular imaging and genetic testing according to international guidelines and local SOPs. Cardiac amyloidosis was diagnosed and subtyped either noninvasively using bone scintigraphy and monoclonal gammopathy assessment or invasively using endomyocardial or non-cardiac biopsy.

Results: Within 2 years 175 patients were enrolled. Mean age was 62.8 ± 16.6 years, 58 were females. Median LVEF was $56.1 \pm 11\%$ and mean E/e' was 12.7 ± 5.6 . Most common aetiologies were sarcomeric HCM in 38 patients (21.7%), cardiac amyloidosis in 59 patients (33.7%; 51 with ATTR and 8 with AL), hypertensive cardiomyopathy in 18 patients (10.2%), and

Anderson-Fabry disease in 4 patients (2.3%). Due to restrictions associated with the Covid-19 pandemia, recruitment rates were lower in 2020 compared to 2019 (106 vs 69 patients). To investigate the trending of proportions, data collected in 2019 and 2020 was compared. The proportion of patients diagnosed with cardiac amyloidosis and Anderson-Fabry disease increased from 35.8% to 43.1% and 1% to 3%, respectively. On the other hand, there was a decline of sarcomeric HCM from 21.6% to 11.8%. Proportions of hypertensive cardiomyopathy and other diseases with low prevalence did not change considerably. Proportions and trends are illustrated in Fig. 1.

Conclusion: Our data suggest that TTR amyloidosis has emerged as the most common cause of HCM-phenotype in a tertiary care setting. Moreover, its prevalence appears to increase further. Vice versa, sarcomeric HCM, as the previously most common aetiology underlying HCM, is only diagnosed in approximately one of five HCM patients.

7.5

The impact of malnutrition on the obesity paradox—fat is not enough

S. Prausmüller¹, N. Pavo¹, G. Spinka¹, H. Arfsten¹, G. Heitzinger¹, G. Goliash¹, M. Huelsmann¹, P. E. Bartko¹

¹Medical University of Vienna, Department of Internal Medicine, Division of Cardiology, Vienna, Austria

Introduction: High body mass index (BMI) is paradoxically associated with better outcome in patients with heart failure. The impact of malnutrition on the association between BMI and outcome has not been investigated yet.

Methods: In this observational study patients with heart failure classified as HF_rEF, HF_mrEF or HF_pEF according to the current guideline diagnostic criteria were included. Data was retrieved from the Viennese-community healthcare provider network between 2010 and 2020. The relationship between BMI and survival accounting for nutritional status was investigated. Nutritional status was assessed by the prognostic nutritional index (PNI) and was available in 10,005 patients. Patients were classified by the presence (PNI <45) or absence (PNI ≥45) of malnutrition.

7.6

Growth differentiation factor-15 correlates inversely with protease-activated receptor-1-mediated platelet reactivity in patients with left-ventricular assist devices

M. Tscharré¹, F. Wittmann², D. Kitzmantl³, S. Lee³, B. Eichelberger⁴, P. Wadowski³, G. Laufer², D. Wiedemann², S. Panzer⁴, T. Perkmann⁵, D. Zimpfer², T. Gremmel³

¹Wiener Neustadt, Department of Internal Medicine, Cardiology and Nephrology, Wr. Neustadt, Austria
²Medical University Vienna, Department of Surgery, Division of Cardiac Surgery, Wien, Austria
³Medical University Vienna, Department of Internal Medicine II, Wien, Austria
⁴Medical University Vienna, Department of Blood Group Serology and Transfusion Medicine, Wien, Austria
⁵Medical University Vienna, Department of Laboratory Medicine, Wien, Austria

Introduction: Growth differentiation factor (GDF)-15 inhibits platelet activation, prevents thrombus formation, and has been linked to bleeding events in patients with acute coronary syndromes and atrial fibrillation. We, therefore, investigated the association of GDF-15 with platelet reactivity and bleeding complications in patients with left ventricular assist devices (LVADs).

Methods: This was a prospective study including 51 LVAD patients on aspirin and phenprocoumon. Platelet surface expression of activated glycoprotein (GP) IIb/IIIa was assessed by flow cytometry, and platelet aggregation was measured by multiple electrode aggregometry (MEA) in response to arachidonic acid (AA), adenosine diphosphate (ADP), and thrombin receptor activating peptide (TRAP; a protease-activated receptor [PAR]-1 agonist). GDF-15 was determined by a CE-marked commercially available assay (Roche). As a clinical endpoint, we assessed bleeding complications during six months of follow-up.

Results: There was a strong trend towards an inverse correlation of GDF-15 with platelet surface expression of activated GPIIb/IIIa in response to TRAP ($r = -0.275, p = 0.0532$), but not in response to AA and ADP (both $p > 0.1$). After excluding outliers, GDF-15 correlated significantly with activated GPIIb/IIIa in response to TRAP ($r = -0.291, p = 0.0497$). Moreover, GDF-15 was inversely associated with MEA TRAP ($r = -0.326, p = 0.0194$), whereas it did not correlate with MEA ADP and MEA AA (both $p > 0.05$; Fig. 1). In a second step, GDF-15 levels in the fourth quartile were defined as high GDF-15. Accordingly, 13 patients

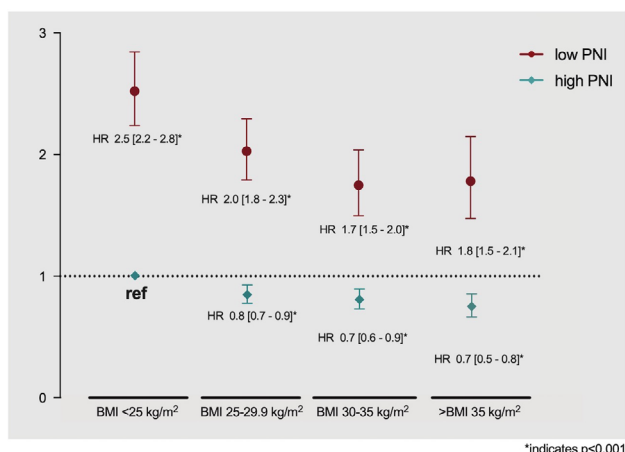


Fig. 217.5 Hazard ratios (HRs) for all-cause mortality with 95 % confidence intervals are shown for BMI in relation to low and high PNI

Results: Of the 11,995 patients enrolled, 6,916 (58 %) had HFpEF, 2,809 (23 %) HFmrEF and 2,270 HFrfEF (19 %). Median age was 70 years (IQR: 61 to 77) and the majority of patients were men (67 %). During a median follow-up time of 44 months (IQR 19–76) a total of 3,718 (31 %) deaths were observed. Across the spectrum of heart failure an inverse relationship between BMI and survival was observed (Fig. 1). Good nutritional status as indicated by high PNI was associated with improved survival (HFpEF: HR 0.93 [0.92–0.93], HFmrEF: HR 0.92 [0.91 to 0.93], HFrfEF: HR 0.93 [0.92 to 0.94], $p < 0.001$). Compared to patients with low BMI (<25 kg/m²) and high PNI, the hazard for patients with low PNI of the same BMI category was 2.5-fold higher; similarly, in patients stratified to higher BMI categories (>25 kg/m²) with low PNI, risk was up to 2.0-fold higher ($p < 0.001$ for all) (Fig. 2).

Conclusion: The obesity paradox seems to be an inherent characteristic of chronic diseases as HF regardless of phenotype. Albeit malnutrition significantly changes trajectory of outcome with regards to BMI alone: obese patients with malnutrition have a considerably worse outcome compared to their well-nourished counterparts, outweighing protective effects of high BMI alone. In this context, routine recommendation towards weight loss in patients with obesity and HF should generally be made with caution and focus should be shifted on nutritional status.

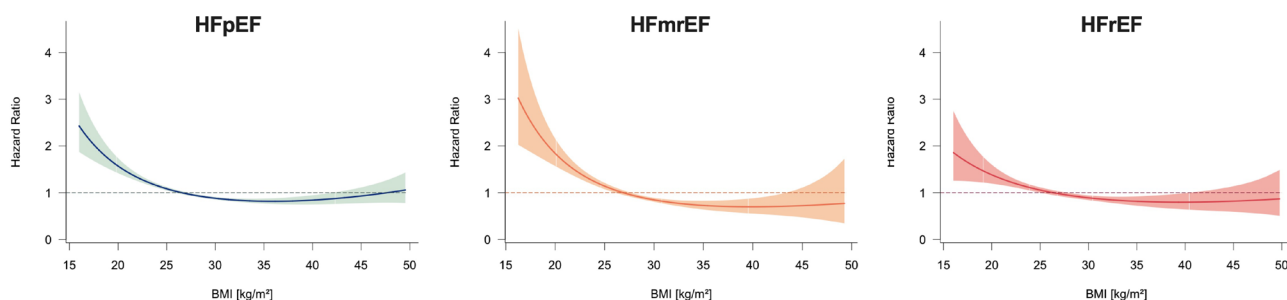


Fig. 117.5 Restricted spline curves examining the association of body-mass-index and all-cause mortality in HFpEF, HFmrEF and HFrfEF

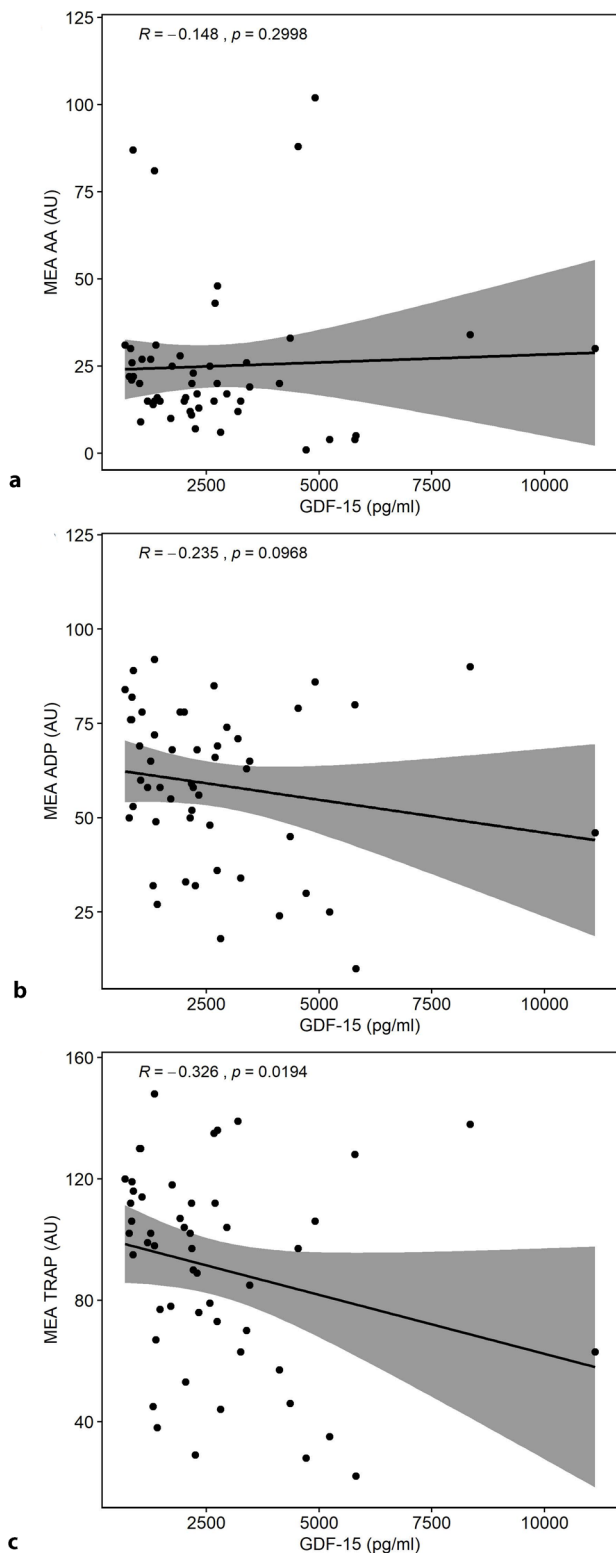


Fig. 117.6 Correlations of GDF-15 with platelet aggregation by multiple electrode aggregometry (MEA). **a** Scatter plot showing GDF-15 (x-axis) versus arachidonic acid (AA)-inducible platelet aggregation by MEA (y-axis). **b** Scatter plot showing GDF-15 (x-axis) versus adenosine diphosphate (ADP)-inducible platelet aggregation by MEA (y-axis). **c** Scatter plot showing GDF-15 (x-axis) versus thrombin receptor-activating peptide (TRAP)-inducible platelet aggregation by MEA (y-axis)

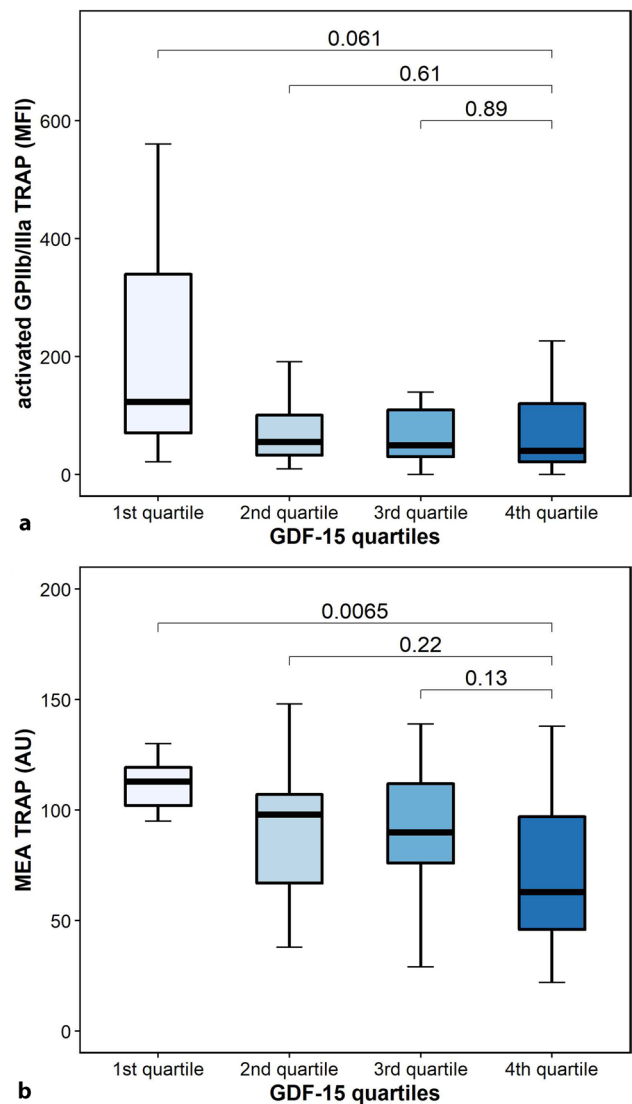


Fig. 217.6 Platelet reactivity in response to thrombin receptor-activating peptide (TRAP) according to GDF-15 quartiles. **a** Activated GPIIb/IIIa in response to TRAP according to GDF-15 quartiles. **b** TRAP-inducible platelet aggregation by multiple electrode aggregometry according to GDF-15 quartiles. The boundaries of the box show the lower and upper quartile of data, and the line inside the box represents the median. Whiskers are drawn from the edge of the box to the highest and lowest values that are outside the box but within 1.5 times the box length. The outliers are not presented

(25.5 %) had high GDF-15. Patients with high GDF-15 showed a numerically lower expression of activated GPIIb/IIIa in response to TRAP (40.5 MFI [IQR 17.6–128.6] vs. 123.6 MFI [IQR 48.4–487.1], $p=0.061$) and significantly lower TRAP-inducible platelet aggregation by MEA (63 AU [IQR 41–102] vs. 113 AU [IQR 102–120], $p=0.0065$) as compared to patients within the first quartile of GDF-15 (Fig. 2). Three patients (5.9%) experienced bleeding complications during follow-up. These patients had numerically higher GDF-15 plasma concentrations than patients without bleeding events (3843 pg/ml vs. 2176 pg/ml, $p=0.779$).

Conclusion: In LVAD patients receiving state-of-the-art antithrombotic therapy, GDF-15 was inversely correlated with residual platelet reactivity via PAR-1. Further clinical trials are

needed to investigate if GDF-15 might help to identify LVAD patients at risk of bleeding and to guide antithrombotic therapy.

7.7

Platelet activation and aggregation in different centrifugal-flow left ventricular assist devices

M. Tscharre¹, F. Wittmann², D. Kitzmantl³, S. Lee³, B. Eichelberger⁴, P. Wadowski³, G. Laufer², D. Wiedemann², B. Forstner-Bergauer⁵, C. Ay⁵, S. Panzer⁴, D. Zimpfer², T. Gremmel³

¹Wiener Neustadt, Department of Internal Medicine, Cardiology and Nephrology, Wr. Neustadt, Austria

²Medical University Vienna, Department of Surgery, Division of Cardiac Surgery, Wien, Austria

³Medical University Vienna, Department of Internal Medicine II, Wien, Austria

⁴Medical University Vienna, Department of Blood Group Serology and Transfusion Medicine, Wien, Austria

⁵Medical University Vienna, Department of Internal Medicine I, Wien, Austria

Introduction: Left-ventricular assist devices (LVADs) improve outcomes in end-stage heart failure patients. Two centrifugal-flow LVAD systems are currently approved, HeartMate 3 (HM3) and Medtronic/Heartware HVAD (HVAD). However, clinical findings suggest differences in thrombogenicity between HM3 and HVAD. We sought to compare markers of platelet activation and aggregation between HM3 and HVAD.

Methods: This was a prospective study including 59 LVAD patients (40 [67.8%] HM3, 19 [32.2%] HVAD). All patients received aspirin and phenprocoumon. Platelet expression of P-selectin and activated glycoprotein (GP) IIb/IIIa as well as monocyte-platelet aggregate (MPA) formation were assessed by flow-cytometry. Platelet aggregation was measured by light-transmission aggregometry (LTA) and multiple-electrode aggregometry (MEA). Von Willebrand factor (VWF) antigen (VWF:Ag), VWF activity (VWF:Ac), VWF multimer pattern analysis, and FVIII activity (FVIII:C) were determined. Soluble P-selectin (sP-selectin) was measured with an enzyme-linked immunoassay.

Results: P-selectin, GPIIb/IIIa and MPA levels in vivo and in response to arachidonic acid, adenosine diphosphate, and thrombin receptor activating peptide were similar between HM3 and HVAD (all $p > 0.05$; Fig. 1). Likewise, agonist-inducible platelet aggregation by LTA and MEA did not differ between HM3 and HVAD (all $p > 0.05$; Fig. 2). VWF:Ag levels and FVIII:C were similar between both systems (both $p > 0.05$), but patients with HVAD had significantly lower VWF:Ac ($p = 0.011$) and reduced large VWF multimers ($p = 0.013$). Finally, sP-selectin levels were similar in patients with HVAD and HM3 ($p = 0.845$).

Conclusion: In conclusion, on-treatment platelet activation and aggregation are similar in HM3 and HVAD patients. Potential clinical implications of observed differences in VWF profiles between both LVAD systems need to be addressed in future clinical trials.

7.8

Association of leptin serum concentration with heart adipose tissue and parameters of systolic and diastolic function in heart failure patients

B. Ohnewein¹, Z. Shomanova², E. J. Fröb², C. Pogoda², C. Granitz¹, P. Jirak¹, M. Lichtenauer¹, U. Hoppe¹, H. Reinecke², R. Pistulli², L. J. Motloch¹

¹Universitätsklinikum Salzburg, Innere Medizin II, Salzburg, Austria

²Universitätsklinikum Münster, Kardiologie, Münster, Germany

Introduction: Leptin has recently been related to myocardial remodeling in animal experimentation studies on heart failure (HF). Furthermore, leptin has been reported to be related to diastolic dysfunction, however only in healthy population. With the emergence of new medical therapies targeting cardiac remodeling, there needs to be a better understanding of the metabolic pathways involving leptin. Our study aims to investigate leptin's correlation to parameters of systolic and diastolic heart function, as well as epicardial and pericardial adipose tissue (EAT and PAT) in heart failure (HF) patients.

Methods: The study included 51 patients with chronic heart failure with reduced ejection fraction (HFrEF) of ischemic ($n = 22$) and non-ischemic ($n = 29$) origin (NYHA II-III, mean EF 29.56 %, SD 8.1; mean BMI 28.08, SD 5.8). Serum concentrations of leptin, NT-proBNP, HbA1c, LDL, and total cholesterol were also measured. Global longitudinal strain (GLS) and other LV function parameters were assessed in transthoracic echocardiography, as well as EAT and PAT in parasternal long and short-axis views.

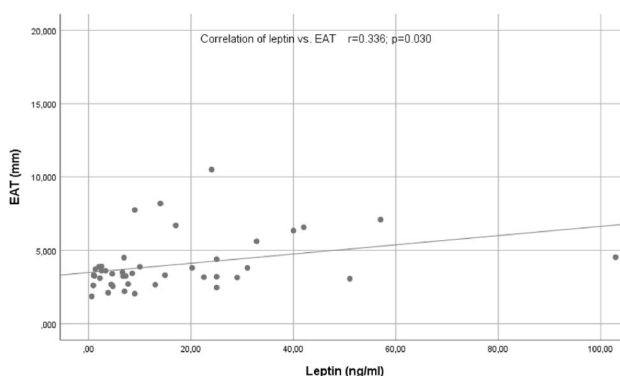


Fig. 117.8 Leptin vs. EAT

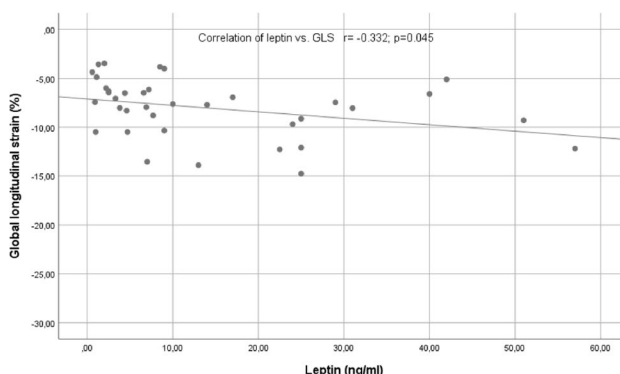


Fig. 217.8 Leptin vs. GLS

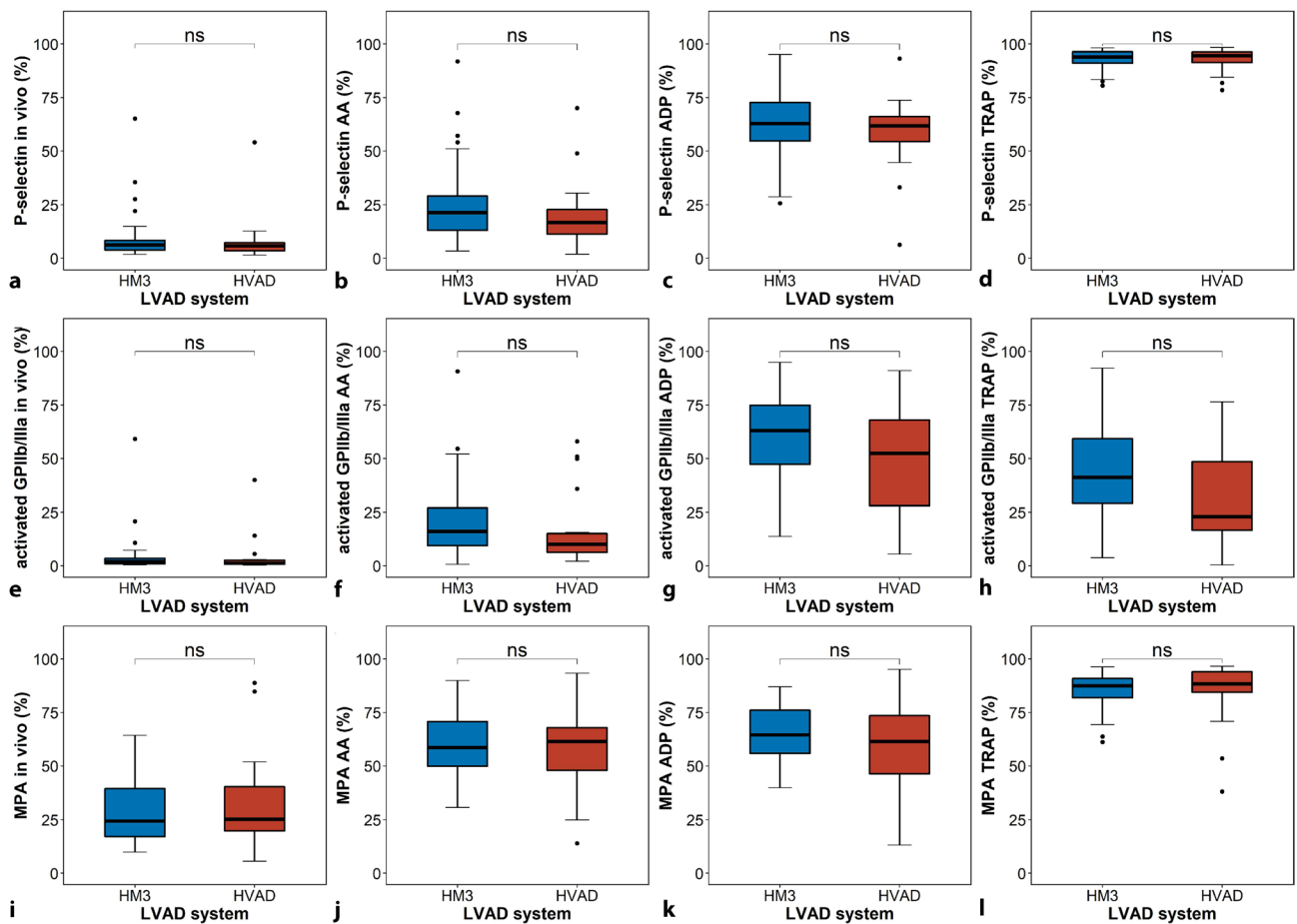


Fig. 117.7 P-selectin, activated GPIIb/IIIa positive platelets and monocyte-platelet aggregate (MPA) formation stratified for patients with HM3 and HVAD. P-selectin expression in vivo (panel a), in response to AA (panel b), in response to ADP (panel c), and in response to TRAP (panel d); activated GPIIb/IIIa in vivo (panel e), in response to AA (panel f), in response to ADP (panel g), and in response to TRAP (panel h); MPA formation in vivo (panel i), in response to AA (panel j), in response to ADP (panel k), and in response to TRAP (panel l)

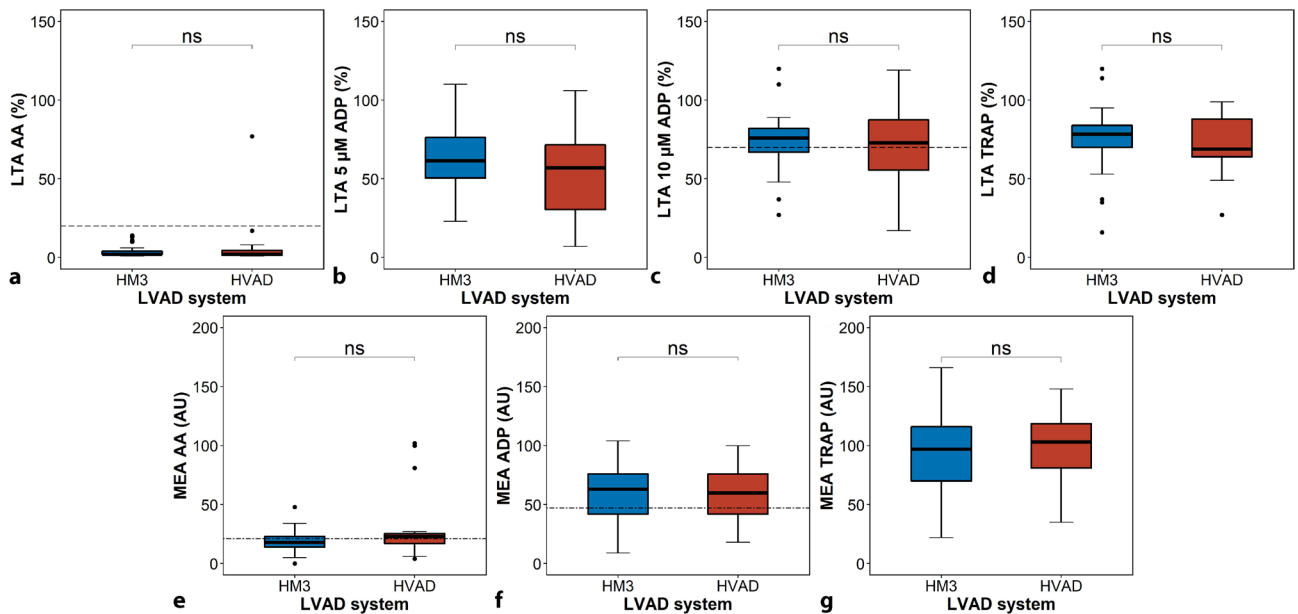


Fig. 217.7 Light-transmission aggregometry (LTA) and multiple electrode aggregometry (MEA) stratified for patients with HM3 and HVAD. Maximal aggregation % by LTA in response to AA (panel a), 5 μ M ADP (panel b), 10 μ M ADP (panel c), and TRAP (panel d). Aggregation units (AU) by MEA in response to AA (panel e), ADP (panel f), and TRAP (panel g). Cut-off values for high on-treatment residual platelet reactivity are indicated by the dashed lines

Results: We found a significant correlation between leptin serum concentration and epicardial, as well as pericardial adipose tissue (EAT $r=0.336$, $p=0.030$; PAT $r=0.565$, $p<0.001$). There was a significant negative correlation between leptin and GLS ($r=-0.332$; $p=0.045$), as well a positive correlation between Leptin and E/E' ratio ($r=0.373$; $p=0.039$). There was no significant difference between ischemic and non-ischemic HF patients.

Conclusion: We provide evidence of serum leptin correlation to remodeling parameters, as well as epicardial and pericardial fat tissue in HF patients. Whether leptin has positive effects on reversing or preventing remodeling in heart failure, needs further investigation.

7.9

Prognostic implications of a novel algorithm to grade secondary tricuspid regurgitation

M. Bannehr¹, T. Kücken¹, U. Kahn¹, C. Edlinger¹, A. Haase-Fielitz¹, C. Butter¹

¹Herzzentrum Brandenburg, Bernau, Germany

Introduction: Patients admitted for tricuspid regurgitation (TR) interventions in clinical practice often exceed the lower threshold of severe TR by far. Current cutoff values do not comprehensively reflect the true spectrum TR. Recently, Fortuni et al. proposed a novel algorithm combining vena contracta (VC) and effective regurgitant orifice area (EROA) to grade moderate and severe TR with prognostic implications (1). Applying the algorithm the authors found that it is able to capture the whole range of TR severity and identified patients with torrential TR who were characterized by a worse prognosis.

Methods: In the present study we took advantage of a recently published study evaluating functional TR and survival (2). Using this well characterized patient cohort including 362 patients with moderate and severe TR (47.9% male, mean age 75.4 ± 9.4 years) we aimed to validate findings by Fortuni et al. (1).

Results: The new classification revealed 203 patients with moderate, 107 with severe TR and 52 torrential with TR. Kaplan-

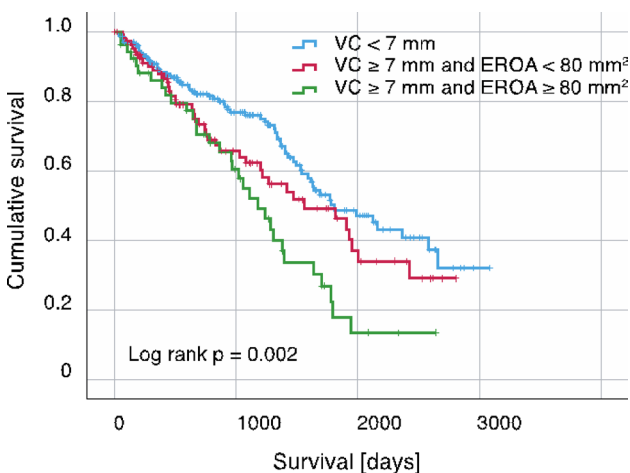


Fig. 117.9 Kaplan-Meier curves for survival in patients with moderate, severe and torrential secondary tricuspid regurgitation according to the novel algorithm proposed by Fortuni et al.; VC=vena contracta, EROA=effective regurgitant orifice area

Meier survival curves showed higher mortality rates in patients with severe and especially in those with torrential TR (Fig. 1). TR grade was associated with worsened survival in logistic regression (hazard ratio 1.44, 95 % confidence interval 1.17–1.78; $p<0.001$).

Conclusion: We found the proposed grading system was also able to reflect the range of TR severity in our cohort, thus confirming the results by Fortuni et al.. The novel algorithm may indeed help to further discriminate the spectrum of more than moderate TR and identify those patients with “torrential” TR, associated with a worse prognosis. Whether percutaneous TR interventions may represent remedy in those patients needs to be evaluated in future prospective studies.

7.10

A machine learning-derived electrocardiographic algorithm for the detection of cardiac amyloidosis

L. Schrutka¹, P. Anner¹, A. Agibetov¹, B. Seirer¹, R. Rettl¹, F. Duca¹, D. Dalos¹, T. Dachs¹, C. Binder¹, R. Badr-Eslam¹, J. Kastner¹, D. Beitzke¹, C. Löwe¹, C. Hengstenberg¹, G. Laufer¹, G. Stix¹, G. Dorffner¹, D. Bonderman¹

¹Medizinische Universität Wien, Wien, Austria

Introduction: Diagnosis of cardiac amyloidosis (CA) requires advanced imaging techniques. Typical surface ECG patterns have been described, but their diagnostic abilities are limited. The aim was to perform a thorough electrophysiological characterization in CA patients and to derive an easy-to-use tool for diagnosis.

Methods: We used recent technical innovations to develop a simple ECG-based algorithm for CA detection. We applied electrocardiographic imaging (ECGI) to acquire electroanatomical maps in CA patients and heart failure controls. A machine learning approach was then utilized to decipher the complex data sets obtained and generate a surface ECG-based diagnostic tool.

Results: Areas of low-voltage were localized in the basal inferior regions of both ventricles and the remaining right ventricular segments in CA. The earliest epicardial breakthrough of myocardial activation was visualized on the right ventricle. Potential maps revealed an accelerated and diffuse propagation pattern. We correlated the results from ECGI with 12-lead ECG recordings. Ventricular activation correlated best with R-peak timing in leads V1 to V3. Epicardial voltage showed a strong positive correlation with R-peak amplitude in the inferior leads

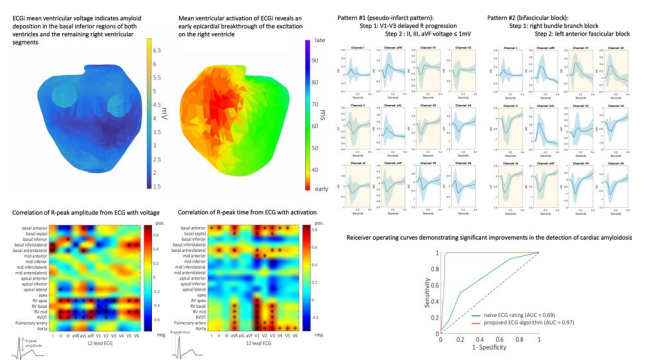


Fig. 117.10 A machine learning-derived ECG algorithm for the detection of cardiac amyloidosis

II, III, aVF. Respective surface ECG-derived leads showed characteristic patterns. Ten blinded cardiologists were then asked to detect CA patients by analyzing 12-lead ECGs before and after training on the defined ECG patterns. Training led to significant improvements in the detection rate of CA with an AUC of 0.69 before and 0.97 after training (Fig. 1).

Conclusion: Using a machine learning approach, an ECG-based tool was developed from detailed electroanatomical mapping to detect CA. The ECG algorithm is simple and has proven helpful to suspect CA without the aid of advanced imaging modalities.

7.11

Soluble neprilysin and survival in critically ill patients

M. Lenz¹, K. Krychtiuk¹, M. Brekalo¹, D. Draxler¹, N. Pavo¹, C. Hengstenberg¹, K. Huber², M. Hülsmann¹, G. Heinz¹, J. Wojta¹, W. Speidl¹

¹Innere Medizin II, Abteilung für Kardiologie, Meduni Wien, Wien, Austria

²3. Medizinische Abteilung, Klinik Ottakring, Wien, Austria

Introduction: Critically ill patients admitted to an intensive care unit (ICU) exhibit a high mortality rate irrespective of the initial cause of hospitalization. Neprilysin is a neutral endopeptidase degrading an array of vasoactive peptides and became a drug target within the treatment of heart failure with reduced ejection fraction. The aim of this study was to analyze whether circulating levels of neprilysin at ICU admission are associated with 30-day mortality.

Methods: In this single-center prospective observational study, 222 consecutive patients admitted to a tertiary ICU at a

university hospital were included. Blood was drawn at admission and soluble neprilysin levels were measured using ELISA.

Results: Median simplified acute physiology score II (SAPS II) was 44 and 30-day mortality was 35.1 % in medical patients ($n=151$) and 7.1 % in patients after surgery and heart valve interventions ($n=71$). Soluble neprilysin levels did not differ according to survival status after 30 days as well as type of admission in the total cohort. However, when assessing neprilysin and survival according to admission type, no association was found in medical patients, while in patients after surgery or heart valve intervention, 30-day survivors exhibited significantly lower circulating neprilysin levels as compared to those who died within 30 days (660.2, IQR: 156.4–2512.5 pg/ml versus 6532.6, IQR: 1840.1–10000.0 pg/ml; $p=0.02$). Soluble neprilysin predicted mortality independently from age, gender, NT-proBNP, and SAPS II (hazard ratio (HR) per 1-standard deviation (SD) increase of neprilysin: 2.52, 95 %CI 1.01–6.32; $p < 0.05$). Additionally, soluble neprilysin was markedly elevated in patients with sepsis and septic shock ($p < 0.05$).

Conclusion: At the time of ICU-admission, circulating levels of neprilysin independently predicted 30-day mortality in patients following cardiac surgery or heart valve intervention, but not in critically ill medical patients. Furthermore, patients suffering from sepsis and septic shock displayed significantly increased circulating neprilysin levels.

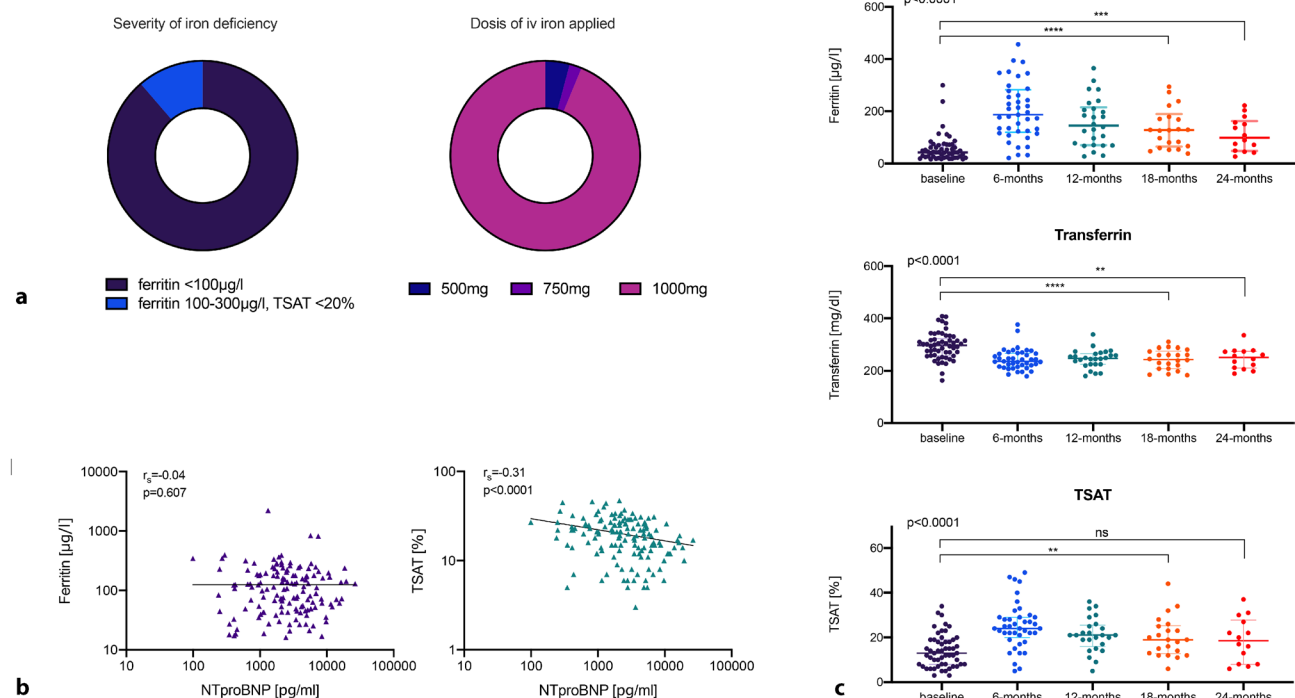


Fig. 117.12

7.12

Long term effects of intravenous iron therapy on iron status of patients with heart failure with reduced ejection fraction (HFrEF)

B. Sakar¹, S. Prausmüller¹, G. Spinka¹, H. Arfsten¹, G. Goliash¹, P. E. Bartko¹, M. Hülsmann¹, N. Pavo¹

¹Abteilung für Kardiologie, Universitätsklinik für Innere Medizin II, Universitätsklinikum AKH Wien, Wien, Austria

Introduction: Iron deficiency (ID), both absolute and functional, is prevalent in chronic diseases, particularly in patients with heart failure with reduced ejection fraction (HFrEF). Intravenous iron (i.v.) administration results in beneficial effects on physical status, NYHA class, quality of life, NT-proBNP and reduces risk of heart failure hospitalizations and currently holds a IIa recommendation in the ESC guidelines. [2-7] Concomitant amelioration of iron status has been documented up to 52 weeks after i.v. iron supplementation, however long-term data are lacking. The aim of this study was to follow the iron status of patients with HFrEF after intravenous iron application up to 36 months.

Methods: Patients with HFrEF who received i.v. iron infusion (Ferriccarboxymaltose) were included from a prospective registry of the Heart Failure Unit of the Medical University of Vienna between 01.01.2015 and 31.04.2020. Demographic and laboratory data including iron parameters (i.e. plasma ferritin, transferrin concentration, transferrin saturation (TSAT), red cell distribution width (RCDW), mean corpuscular volume (MCV), NTproBNP and hemoglobin (Hb)) as well as clinical follow-up was documented. Baseline was defined as the last laboratory test before i.v. iron supplementation and follow-up timepoints were defined at 6±3, 12±3, 18±3 and 24-36 months, respectively. Parameters of iron status were compared between timepoints by non-parametrical tests. The association between iron status and outcome was investigated in an exploratory manner.

Results: 55 Patients with at least one-time i.v. iron were included into the analysis. 29% of patients were female, median age 68 (IQR: 56-78) and patients were well-treated by HF therapy. 92% of patients have a baseline ferritin <100 ug/

ml, the iron need calculated by Ganzoni's formula was 984 mg (IQR: 797-1148) and most patients (94%) received 1000 mg iron (Fig. 1A). Interestingly 9 patients underwent a second i.v. infusion during FUP, whereas only 2 of them received 1000 mg instead of 1500 mg as an optimum iron dose. Heart failure severity reflected by NT-proBNP was not correlated to ferritin but to TSAT values (Fig. 1). Hemoglobin was comparable at long-term FUP to baseline values (not shown). Iron status improved after i.v. iron supplementation as expected, whereas improvement in ferritin, transferrin and TSAT levels were robust even after 18 months and longer (Fig. 1). Over time, however, a trend to re-worsening towards values compatible with iron deficiency was observable for all parameters. Out of 13 patients with FUP data longer than 2 years, 11 (85%) fulfilled the criteria of iron deficiency and i.v. iron supplementation.

Conclusion: The results demonstrate that patients with HFrEF and iron deficiency receiving intravenous iron supplementation show a subsequent marked improvement in iron status, however a re-worsening is observable after a follow-up as short as 2-3 years with most patients again fulfilling the indication for i.v. iron. The mechanisms of iron redistribution as well as the significance or multiple iron supplementation needs to be elucidated in further studies.

7.13

Effects of tafamidis on quantification of myocardial amyloid deposits in patients with transthyretin amyloid cardiomyopathy

R. Rettl¹, T. Wollenweber¹, C. Mann¹, F. Duca¹, T. Dachs¹, C. Binder¹, M. Stojanovic¹, L. Camuz Ligios¹, L. Schrutka¹, D. Dalos¹, S. Charwat-Resl², C. Hengstenberg¹, R. Badr Eslam¹, J. Kastner¹, M. Hacker¹, D. Bonderman²

¹Medizinische Universität Wien, Wien, Austria

²Klinik Favoriten, Wien, Austria

Introduction: Tafamidis is a kinetic stabilizer of transthyretin (TTR) that prevents tetramer dissociation and amyloidogen-

	Ferritin (n=39) Transferrin (n=40) TSAT (n=40)			Ferritin (n=24) Transferrin (n=25) TSAT (n=24)			Ferritin (n=20) Transferrin (n=21) TSAT (n=21)			Ferritin (n=14) Transferrin (n=14) TSAT (n=14)			Ferritin (n=5) Transferrin (n=5) TSAT (n=5)			Ferritin (n=4) Transferrin (n=4) TSAT (n=4)		
	0 mo	6 mo	p	0 mo	12 mo	p	0 mo	18 mo	p	0 mo	24 mo	p	0 mo	30 mo	p	0 mo	36 mo	p
Ferritin	42 (25,05-71,25)	186,6 (119,6-282,25)	<0,0001	42 (25,05-71,25)	145,45 (70,15-215,48)	0,0001	42 (25,05-71,25)	128,2 (64,78-189,9)	0,002	42 (25,05-71,25)	98,8 (48,2-162,85)	0,026	42 (25,05-71,25)	161,4 (122,85-211,9)	0,043	42 (25,05-71,25)	161,4 (143,85-226,35)	0,068
Transferrin	296,5 (257,75-321,75)	236 (215,5-267)	<0,0001	296,5 (257,75-321,75)	247,5 (225-266)	<0,0001	296,5 (257,75-321,75)	243 (208-275,75)	0,0002	296,5 (257,75-321,75)	251 (210,5-275,75)	0,001	296,5 (257,75-321,75)	228 (201-233)	0,063	296,5 (257,75-321,75)	238 (196,5-262,25)	0,125
TSAT	12,95 (7,57-18,88)	24,1 (19,6-28,9)	<0,0001	12,95 (7,57-18,88)	20,6 (16-25,6)	0,0001	12,95 (7,57-18,88)	18,5 (12,8-25,23)	0,005	12,95 (7,57-18,88)	18,35 (8,18-27,63)	0,135	12,95 (7,57-18,88)	26,60 (14,35-28,5)	0,125	12,95 (7,57-18,88)	18,4 (14,43-25,07)	0,125
	Baseline n= 53			6 mo (+/- 3mo) n=41			12 mo (+/- 3mo) Ferritin (n=26) Transferrin (n= 26) TSAT (n=25)			18 mo (+/- 3mo) n=22			LZ-FUP (2-3a) Ferritin (n=13) Transferrin (n= 14) TSAT (n=14)			overall p-value		
Ferritin ng/ml	42,8 *#~ (23,95-71,25)			186 * (119,6-282,25)			145,45 # (70,15-215,48)			128,2 + (64,78-189,9)			138,2 ~ (62,2-168,7)			<0.0001		
TSAT %	13,10 *# (7,75-18,95)			24,10 * (19,6-28,9)			20,6 # (16-25,6)			18,5 + (12,8-25,23)			16,0 (8,18-23,33)			<0.0001		
Transferrin mg/dl	294 *#~ (257,5-324,5)			236 * (215,5-267)			247,5 # (225-266)			243 + (208-275,5)			253 ~ (230-274,75)			<0.001		

Fig. 217.12

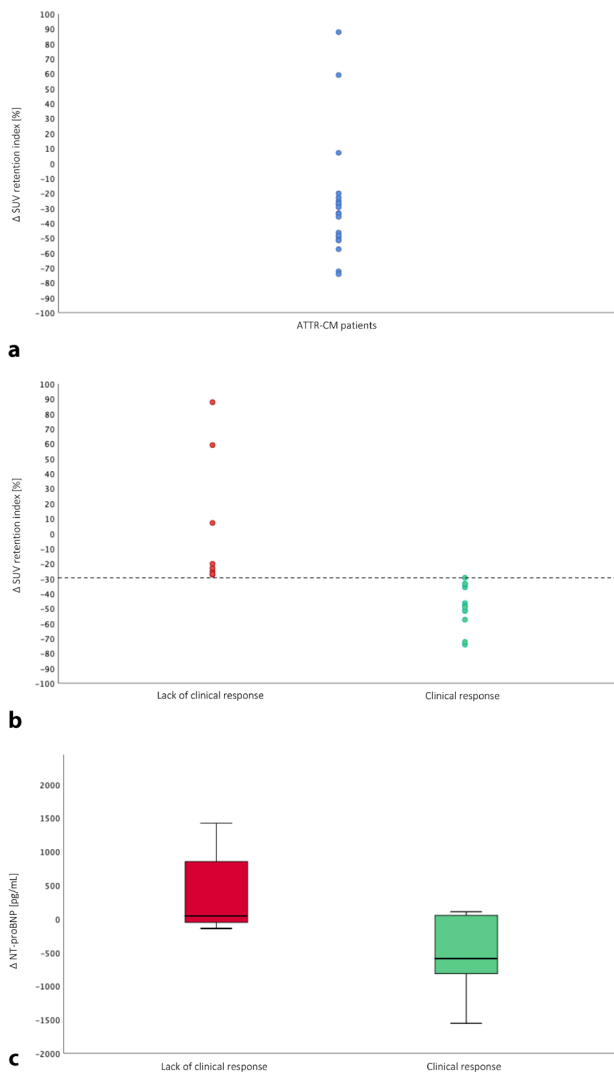


Fig. 117.13 **a** Percent change from baseline in standardized uptake value (SUV) retention index in ATTR-CM patients after tafamidis treatment. **b** Classification based on clinical response: a threshold of -30 % distinguishes between ATTR-CM patients who respond clinically and those who do not respond. **c** Change in serum NT-proBNP level from baseline for each cohort

esis in patients with TTR amyloid cardiomyopathy (ATTR-CM), resulting in delayed disease progression. However, the endomyocardial effects of tafamidis are still unknown.

Methods: Twenty patients with ATTR-CM were treated with tafamidis 61 mg for a period of six months. In our explorative analysis, we aimed to investigate the effects of tafamidis on the quantification of myocardial amyloid deposits measured by myocardial standardized uptake value (SUV) peak and SUV retention index by quantitative single-photon emission computed tomography/computed tomography (SPECT/CT) of the thorax, and to observe their association with clinical parameters.

Results: Main results are summarized in Table 1. In brief, we observed a significant reduction of myocardial SUV peak (mean, baseline (BL): 15.50 vs. follow-up (FU): 11.61, $p < 0.001$) and SUV retention index (mean, BL: 5.64 vs. FU: 3.58, $p = 0.001$) after tafamidis treatment (Fig. 2A). In addition, a higher percentage decrease in the SUV retention index is more likely to be

associated with clinical benefit, with a threshold of -30 % differentiating between patients who respond clinically ($n = 12$) and those who do not respond ($n = 8$, Fig. 2B). Clinical response is reflected in improvement of exercise capacity (6MWD, mean, BL: 349.5 m vs. FU: 356.7 m, $p = 0.736$). Cardiac biomarkers showed a conclusive reduction in serum NT-proBNP levels (median, BL: 2765.0 pg/mL vs. FU: 1904.0 pg/mL, $p = 0.041$) in the responder cohort compared to an increase (median, BL: 1825.0 pg/mL vs. FU: 1944.0 pg/mL, $p = 0.208$) in the non-responder cohort (cohort comparison: $p = 0.026$, Fig. 2C). Echocardiographic findings revealed an improvement of LV strain (mean, BL: -12.0 % vs. FU: -13.5 %, $p = 0.049$) and the LVEF (mean, BL: 48.5 % vs. FU: 52.7 %, $p = 0.287$) in the responder cohort, while a significant deterioration of the LV function (LV strain, mean, BL: -13.9 vs. FU: -10.5, $p = 0.035$; LVEF, mean, BL: 53.2 % vs. FU: 46.5 %, $p = 0.012$) was observed in the non-responder cohort, with an additional substantial worsening of the RV function as measured by TAPSE (mean, BL: 19.2 mm vs. FU: 12.6 mm, $p = 0.037$) in those patients.

Conclusion: Treatment with tafamidis in patients with ATTR-CM leads to significant reductions of myocardial amyloid deposits as measured by SUV retention index, with a threshold of -30 % differentiating between patients who respond clinically and those who do not respond. However, a larger patient sample is required to verify these results.

7.14

Mode of action and effects of a multidimensional post-discharge disease management programme for heart failure patients on morbidity and mortality: the herzmobil tirol programme

T. Egelseer-Bründl¹, B. Pfeifer², R. Modre-Osprian³, S. Welte³, B. Fetz², S. Krestan², B. Haselwanter², M. Zaruba¹, J. Dörler¹, C. Rissbacher⁴, E. Ammenwerth⁵, A. Bauer¹, G. Pözl¹

¹Clinical Division of Cardiology and Angiology, Medical University of Innsbruck, Innsbruck, Austria

²Landesinstitut für Integrierte Versorgung Tirol, Innsbruck, Austria

³Center for Health & Bioresources, AIT Austrian Institute of Technology, Graz, Austria

⁴University Hospital Innsbruck, Tirol Kliniken, Innsbruck, Austria

⁵Institute of Medical Informatics, UMIT – Private University for Health Sciences, Medical Informatics and Technology, Hall in Tirol, Austria

Introduction: It remains unclear whether transitional care management outside of a clinical trial setting provides benefits for patients with acute heart failure (AHF) after hospitalization. We evaluated the efficacy of a multidimensional post-discharge disease management programme (HerzMobil Tirol, HMT).

Methods: The study included 508 AHF patients that were managed in HMT ($n = 251$) or usual care (UC, $n = 257$) after discharge from hospital from 2016 to 2019. The primary endpoint was time to HF readmission and all-cause mortality within six months. Multivariable Cox proportional hazard models were used to assess the treatment effect.

Results: The primary endpoint occurred in 48 patients (19.1 %) in HMT and 89 (34.6 %) in UC. Compared with UC, management by HMT was associated with a 46 %-reduction in the primary endpoint (adjusted HR 0.54; 95 % CI 0.37-0.77;

Table 117.13 Baseline and follow-up characteristics of ATTR-CM patients after six months of tafamidis treatment

Characteristic	Overall (n = 20)			Clinical response (n = 12)			Lack of clinical response (n = 8)		
	Baseline	Follow-up	p-Value	Baseline	Follow-up	p-Value	Baseline	Follow-up	p-Value
Clinical parameters									
Age—years (SD)	79.7(5.5)			80.6(6.5)			78.3(3.5)		
Male—n(%)	16(80.0)			9(75.0)			7(87.5)		
NYHA functional class III—n(%)	14(70.0)	8(40.0)	0.009	10(83.3)	5(41.7)	0.047	4(50.0)	3(37.5)	0.082
6-min walk distance—m (SD)	379.2(82.3)	385.6(107.2)	0.678	349.5(79.2)	356.7(94.4)	0.736	428.7(65.9)	433.7(118.2)	0.836
Laboratory parameters									
Hemoglobin—g/dL (SD)	13.9(1.6)	13.2(1.8)	0.067	13.2(1.7)	13.3(1.8)	0.957	14.9(0.9)	13.2(1.8)	0.025
Creatinine—mg/dL (SD)	1.43(1.00)	1.42(0.96)	0.951	1.60(1.26)	1.52(1.22)	0.037	1.17(0.31)	1.27(0.35)	0.188
Troponin T—ng/L (SD)	56.7(24.0)	61.3(30.5)	0.091	57.8(24.5)	60.6(31.6)	0.452	54.9(24.8)	62.4(30.9)	0.094
NT-proBNP—pg/mL (IQR)	2341.0 (1395–3164)	1904.0 (1353–2865)	0.398	2765.0 (1510–3164)	1904.0 (1504–2865)	0.041	1825.0 (1364–4573)	1944.0 (1261–6898)	0.208
Myocardial SUV parameters									
SUV peak (SD)	15.50(4.20)	11.61(2.96)	<0.001	15.77(3.80)	11.95(3.37)	<0.001	15.09(4.98)	11.11(2.33)	0.012
SUV retention index (SD)	5.64(2.60)	3.58(1.54)	0.001	6.37(2.68)	3.13(1.27)	<0.001	4.56(2.20)	4.26(1.75)	0.654
Echocardiographic parameters									
LA length—mm (SD)	58.6(9.2)	57.1(6.2)	0.471	58.7(12.0)	56.3(7.0)	0.457	58.4(4.6)	58.1(5.2)	0.916
RA length—mm (SD)	58.3(10.9)	56.3(7.0)	0.294	55.5(13.1)	54.1(7.4)	0.668	61.9(6.4)	59.1(5.8)	0.120
Interventricular septum—mm (SD)	19.9(6.0)	21.5(5.6)	0.091	16.9(3.3)	18.7(3.7)	0.283	23.3(6.7)	24.6(6.0)	0.147
LV end-diastolic diameter—mm (SD)	42.9(7.5)	41.2(8.1)	0.379	44.1(6.7)	42.6(8.1)	0.576	41.5(8.5)	39.6(8.3)	0.531
RV end-diastolic diameter—mm (SD)	34.9(5.5)	35.1(4.2)	0.865	37.3(5.2)	35.8(5.3)	0.174	32.1(4.5)	34.3(2.8)	0.231
LV ejection fraction—% (SD)	50.6(9.1)	50.4(12.3)	0.929	48.5(10.3)	52.7(15.3)	0.287	53.2(7.0)	47.5(7.2)	0.012
LV strain—% (SD)	−12.9(3.3)	−12.2(4.4)	0.449	−12.0(3.7)	−13.5(4.2)	0.049	−13.9(2.6)	−10.5(4.3)	0.035
TAPSE—mm (SD)	17.5(4.5)	14.9(4.4)	0.025	16.6(4.6)	16.0(4.5)	0.168	19.2(4.3)	12.6(3.4)	0.037
CMR parameters									
	n = 11			n = 6			n = 5		
LV ejection fraction—% (SD)	44.0(10.4)	42.5(11.4)	0.579	41.9(11.2)	45.7(8.1)	0.250	46.5(10.1)	38.7(14.5)	0.053
RV ejection fraction—% (SD)	40.5(11.3)	38.4(12.6)	0.626	36.2(6.8)	40.1(9.1)	0.159	45.7(14.1)	36.4(16.8)	0.296
MOLLI-ECV—% (SD)	47.4(10.2)	52.4(15.0)	0.101	47.3(12.8)	53.4(20.4)	0.181	47.5(7.4)	51.2(6.4)	0.437
T1 relaxation time—ms (SD)	1127.8(48.8)	1106.4(47.7)	0.323	1105.2(37.4)	1122.1(46.0)	0.456	1155.0(50.1)	1087.6(47.2)	0.064

NHYA indicates New York Heart Association; NT-proBNP, N-terminal pro-hormone of brain natriuretic peptide; SUV, Standardized uptake value; LA, Left atrium; RA, Right atrium; LV, Left ventricle; RV, Right ventricle; TAPSE, Tricuspid annular plane systolic excursion; CMR, Cardiac magnetic resonance imaging; MOLLI-ECV, Modified look-locker inversion recovery sequence derived extracellular volume. Values are given as mean ± standard deviation (SD), or median and interquartile range (IQR), or total numbers (n) and percent (%). Bold indicates $p < 0.05$.

$P < 0.001$). Subgroup analyses revealed a consistent treatment effect. The composite of recurrent HF hospitalization and death within six months per 100 patient-years was 64.2 in HMT and 108.2 in UC (adjusted HR 0.41; 95% CI 0.29–0.55; $P < 0.001$ with death considered as a competing risk). After one year, 25 (10%) patients died in HMT compared with 66 (25.7%) in UC (HR 0.38; 95% CI 0.23–0.61, $P < 0.001$).

Conclusion: A multidimensional post-discharge disease management programme, comprising a telemedical monitoring system incorporated in a comprehensive network of specialized heart failure nurses and resident physicians, is feasible and effective in clinical practice by means of a reduction of 6-months HF readmissions and all-cause mortality.

7.15

Elevation of circulating dipeptidyl peptidase (CDPP3) is associated with worse outcome in stable heart failure with reduced ejection fraction

n. pavo¹, s. Prausmüller¹, G. Spinka¹, H. Arfsten¹, P. Bartko¹, G. Golasch¹, M. Hülsmann¹

¹Medical University Vienna, Wien, Austria

Background: Dipeptidyl dipeptidase (DPP3) is a protease involved in the degradation of cardiovascular mediators. [1] Increased levels of circulating DPP3 (cDPP3) have been shown to be associated with impaired myocardial contraction whereas inhibition may restore cardiac function in preclinical models.

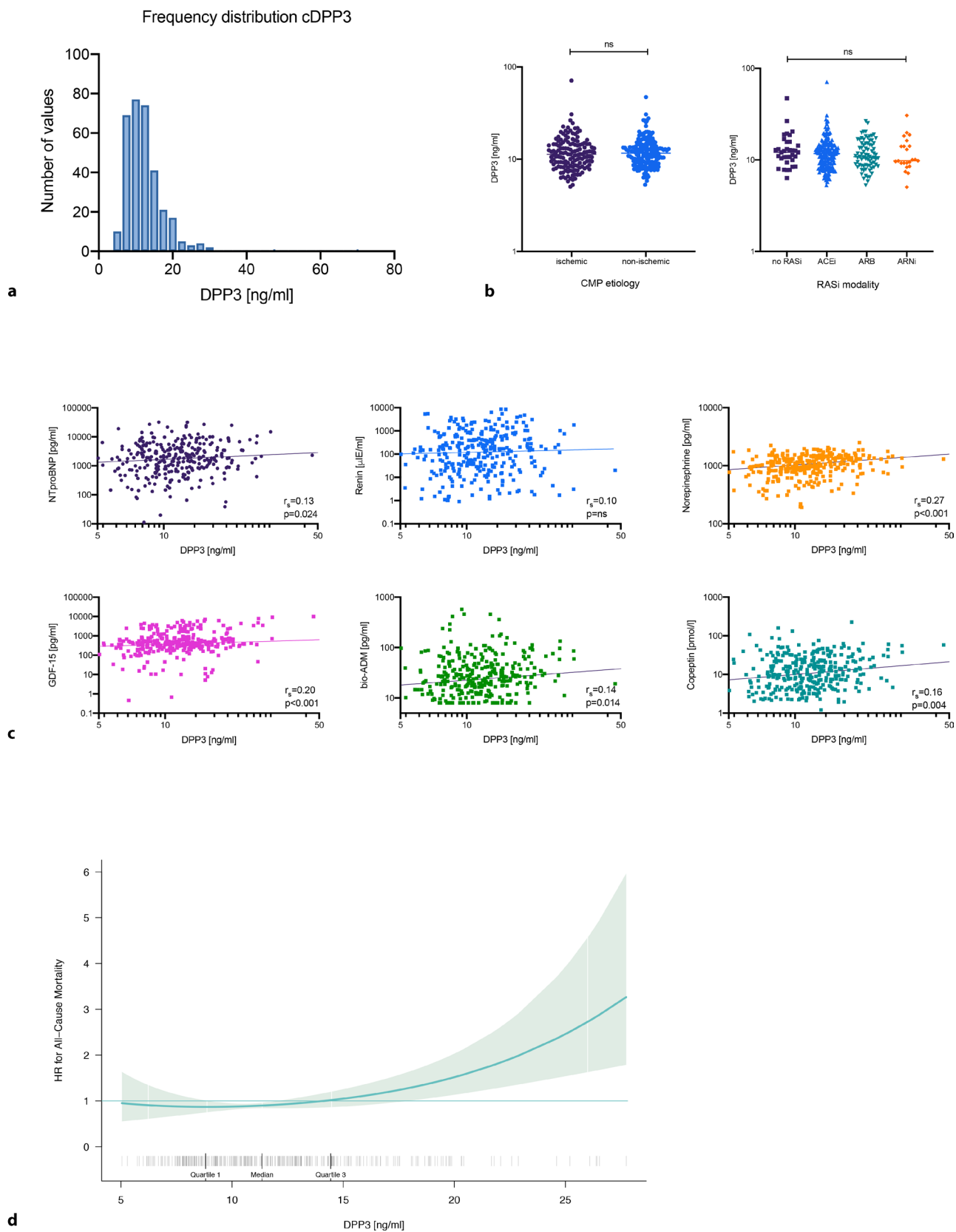


Fig. 117.15 cDPP3 levels in stable HFrEF. A. Frequency distribution, B. levels according to CMP etiology and RAS-inhibitor modality strata, C. correlation with heart failure biomarkers and D. cubic spline curve analysis for all-cause mortality are shown. For B. groups were compared by non-parametric tests (mann-Whitney-U and Kruskal-Wallis test), for C. regression lines were constructed using robust regression (least square model) for the log x log models without special handling for outliers, the Spearman's correlation coefficient and p -values for correlation analysis are indicated within each plot

[2] Elevated DPP3 is similarly associated with therapy refractoriness in cardiogenic shock.[3] In contrast, data on cDPP3 levels in stable heart failure with reduced ejection fraction (HFrEF) are lacking. Purpose. The present study aims to evaluate the impact of cDPP3 in patients with chronic HFrEF.

Methods: Consecutive patients with stable chronic HFrEF and optimal medical therapy have been enrolled prospectively from the outpatient unit of heart failure at the Medical University of Vienna between February 2016 and December 2017. Routine laboratory parameters including NT-proBNP and additionally other heart failure biomarkers as active plasma renin concentration (ARC), norepinephrine (NE), GDF-15 and copeptin have been measured by specific immunoassays. Bioadrenomedullin (bio-ADM) and DPP3 have been determined by the sphingotest® assay. All-cause mortality was assessed as the primary outcome.

Results: A total of 365 patients were included into the study. Samples were hemolytic in 40 cases, so that cDPP3 measurements were analyzed for a total of 325 patients. The distribution of DPP3 is displayed in Fig. 1A, median cDPP3 was 11.36 ng/ml (IQR: 8.87–14.48). cDPP3 levels were comparable for ischemic and non-ischemic etiology of HF and also for different RAS-inhibitors (Fig. 1B). DPP3 showed a modest correlation with NT-proBNP ($r_s=0.13$, $p=0.024$), GDF-15 ($r_s=0.20$, $p<0.001$), NE ($r_s=0.27$, $p<0.001$), copeptin ($r_s=0.16$, $p=0.004$) and bio-ADM ($r_s=0.14$, $p=0.014$) shown in Fig. 1C. Increasing DPP3 was associated with worse outcome as shown by spline analysis in Fig. 1D and univariate Cox regression [crude HR 1.15 (95% CI: 1.03–1.28), $p=0.011$ for an increase of 5 ng/ml cDPP3]. The association remained as a trend after adjustment for NT-proBNP [adj. HR 1.12 (95% CI: 1.00–1.25), $p=0.058$], suggesting an independent additional value.

Conclusion: cDPP3 levels in stable HFrEF are lower compared to patients with sepsis or cardiogenic shock. cDPP3 shows a modest correlation with other heart failure biomarkers and is a risk factor for worse outcome in stable HFrEF as shown for other more critical conditions. The source of cDPP3 in stable HFrEF as well as its cardiodepressive potential/potentially related pathophysiological mechanisms have to be investigated in further studies.

7.16

Psychocardiological assessment in the acute phase of the takotsubo syndrome. somatic and depressive disorders, resilience and illness perception

V. Weihs¹, E. Pogran¹, E. Kunschitz², W. Weihs³, E. Prinz⁴, C. Eichenberg⁵, J. Fiegl⁶, O. Friedrich⁷, K. Huber¹

¹3rd Medical Department, Cardiology and Intensive Care Medicine, Wilhelminenhospital (Klinik Ottakring), Wien, Austria

²II. Medical Department for Cardiology, Takotsubo-Ambulanz, Hanusch Krankenhaus, Wien, Austria

³Hospital Graz II, Department of Cardiology, Graz, Austria

⁴Clinic of Internal Medicine II, Department of Cardiology, Paracelsus Medical University, Salzburg, Austria

⁵Institute for Psychosomatic, Sigmund Freud University Vienna, Medical Faculty, Wien, Austria

⁶Faculty of Psychotherapy Science, Sigmund Freud University Vienna, Wien, Austria

⁷Karl Landsteiner Institute for Scientific Research in Clinical Cardiology, II. Medical Department for Cardiology, Hanusch Krankenhaus, Wien, Austria

Introduction: To analyse the clinical characteristics and the psychocardiological profile in Takotsubo Syndrome (TTS) patients in the acute phase of the syndrome.

Methods: Prospective multi-center cohort study on TTS patients with regard to clinical characteristics, prevalence of somatic, depressive, panic, stress and anxiety disorders. Assessment of illness perception and resilience.

Results: The evaluated 27 TTS patients were female with a mean age of 68 years (± 11.4). Main clinical symptom leading to hospital admission was chest pain in 78% of patients. Main ECG finding was ST-segment elevation (44%) followed by T wave inversion (26%). The apical type of TTS was found in 60% of patients, followed by the combined type of TTS in 30% of patients. In 11.1% of patients ($n=3$) no stress event could be found, in the remaining 24 patients (88.9%) a stress event could be evaluated: an endogenous (emotional) stress event was found in 17 patients (63.0%), an exogenous (physical) stress event in 5 patients (18.5%) and a combined stress-event in 2 patients (7.4%). Somatic disorders were found in half of the patients (56%) followed by depressive disorders in 26% of patients. Moderate to high levels of illness threatening were found in 48% of patients and low to moderate resilience scores were found in 40% of patients.

Conclusion: In summary it can be said, that patients with TTS present in the acute phase with a high prevalence of somatic disorders and relatively high prevalence of depressive disorders. Moderate to low resilience scores and moderate to high levels of illness threatening can be seen in the acute phase of TTS, reflecting the severity of the experience as an adverse life event. Level of Evidence: Level III Key words: Takotsubo syndrome; psychosomatic disorders; resilience; illness perception

7.17

Post-processing measurement of left ventricular ejection fraction compared to direct measurement in patients with heart failure with reduced ejection fraction

N. Schwegel¹, E. Kolesnik¹, G. Toth-Gayor¹, A. Zirlik¹, D. von Lewinski¹, K. Ablasser¹, N. Verheyen¹

¹Division of Cardiology, Department of Internal Medicine, Medical University Graz, Graz, Austria

Introduction: Evaluation of left ventricular ejection fraction (LVEF) derived from transthoracic echocardiography is routinely used to guide therapeutic decisions in patients with heart failure with reduced ejection fraction (HFrEF). However, TTE-based quantification of LVEF is limited by low diagnostic accuracy and poor agreement with gold-standard methods which may be improved by application of post-processing analysis tools. In our study, we aimed to compare different methods of LVEF quantification, using direct and image post-processing techniques, and their correlations to NT-proBNP plasma concentrations in patients with a previous diagnosis of HFrEF.

Methods: A total of 205 clinically stable patients diagnosed with HFrEF were enrolled in a prospective cohort study. They underwent a standardized echocardiographic examination using a GE Vivid E9 ultrasound machine performed by two investigators with the experience of more than 5.000 performed echocardiographic examinations. Biplane LVEF according to Simpson's method was evaluated directly during the examination. Images and echo loops were digitally saved. Post-processing evaluation of biplane and triplane LVEF (pp LVEF) using the vendor-independent software TomTec was performed by a blinded investigator who underwent comprehensive training in post-processing analysis but was otherwise unexperienced in transthoracic echocardiography. For correlation analyses

patients were subdivided according to the underlying etiology of HF into ischemic and non-ischemic HF.

Results: Post-processing analysis was feasible in 164 patients. Mean direct biplane LVEF was 36.0 ± 9.1%, mean pp biplane LVEF was 35.8 ± 8.2%, mean pp triplane LVEF was 34.2 ± 8.8%, and median NT-proBNP was 978 (IQR 332-2279) pg/mL. All LVEF parameters had strong and comparable correlations to NT-proBNP (direct biplane: $r = -0.352$; pp biplane: $r = -0.412$, pp triplane: $r = -0.426$; $p < 0.01$ for each). Bland Altman Plot revealed a high variability between direct and pp biplane LVEF values, with a mean difference of 0.15 ± 6.2%. Linear regression analysis indicated proportional bias between both measurements across all LVEF ranges ($\beta = 0.154$, $p = 0.049$). Among 83 patients with direct biplane LVEF >35%, a total of 16 had a pp biplane LVEF ≤35% (mean pp biplane 43.3 ± 4.5% vs 32.0 ± 2.3%, $p < 0.001$; median NT-proBNP 511 [IQR 179-1421] vs. 1205 [IQR 457-3706] pg/mL, $p = 0.055$). On the other hand, out of 81 patients with direct biplane LVEF ≤35%, 16 patients had pp biplane LVEF >35% (mean pp biplane 28.2 ± 4.8 vs 39.2 ± 3.4%, $p < 0.001$; median NT-proBNP 1644 [IQR 711-3113] vs. 543 [IQR 297-3015] pg/mL, $p = 0.1$). Furthermore, the correlation between biplane LVEF and NT-proBNP was more pronounced in patients with ischemic HF ($n = 65$) using post-processing than direct measurement (pp: $r = -0.443$, $p < 0.001$; direct: $r = -0.314$, $p = 0.01$). We did not observe such a signal in patients with non-ischemic HF ($n = 99$) where both measurements showed comparable correlations to NT-proBNP (pp: $r = -0.367$; direct: $r = -0.380$, $p < 0.001$ for each).

Conclusion: Direct biplane LVEF measurement shows low agreement with pp biplane LVEF in patients with HFrEF. Moreover, application of post-processing analyses leads to a reclassification from LVEF >35% to LVEF ≤35% in one out of five patients. In conclusion, pp biplane LVEF analysis appears to provide more accurate values and should be preferred in examinations with therapeutic implication, particularly in patients with HFrEF of ischemic origin.

7.18

Inflammation-based scores as a common tool for prognostic assessment in patients with heart failure or cancer

H. Arfsten¹, A. Cho¹, S. Prausmüller¹, G. Spinka¹, J. Novak¹, G. Goliash¹, P. E. Bartko¹, M. Raderer², H. Gisslinger³, G. Kornek², W. Köstler², G. Strunk⁴, M. Preusser², C. Hengstenberg¹, M. Hülsmann¹, N. Pavo¹

¹Medical University of Vienna, Department of Internal Medicine II/Division of Cardiology, Wien, Austria

²Medical University of Vienna, Department of Internal Medicine I/Division of Oncology, Wien, Austria

³Medical University of Vienna, Department of Internal Medicine I/Division of Hematology and Hemostaseology, Wien, Austria

⁴Complexity Research, Wien, Austria

Introduction: Comparable to cancer, evidence emerges that heart failure with reduced ejection fraction (HFrEF) can be triggered and fueled by individual inflammatory host response. Inflammation-based scores are widely tested in cancer, but have not been evaluated in a well-defined population of chronic HFrEF patients. We aimed to investigate the link between inflammatory status reflected by established inflammation-based scores and disease severity and impact on survival in

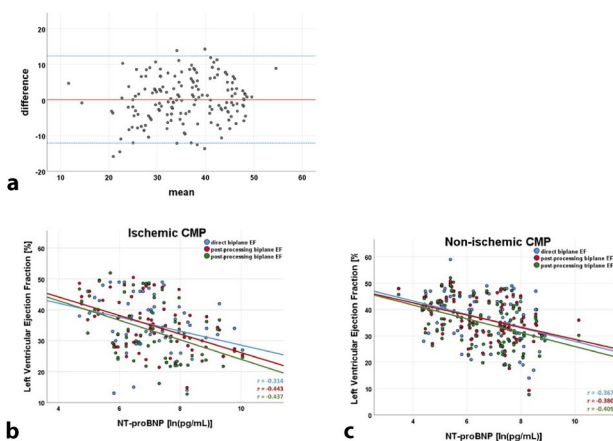


Fig. 117.17 A: Bland Altman plot; *difference: direct–post-processing biplane measurement. B: Scatterplot; significant correlations between NT-proBNP and direct biplane EF ($r = -0.314$, $p = 0.01$), post-processing biplane EF ($r = -0.443$, $p < 0.001$), and post-processing triplane EF ($r = -0.437$, $p < 0.001$) in patients with ischemic CMP. C: Scatterplot; significant correlations between NT-proBNP and direct biplane EF ($r = -0.367$), post-processing biplane EF ($r = -0.380$), and post-processing triplane EF ($r = -0.409$, $p < 0.001$ for each) in patients with non-ischemic origin of CMP

patients with stable HFrEF. In parallel, the study investigated an intra-institutional cohort of treatment naïve cancer patients and compared the prognostic value of each score between the cohorts.

Methods: Registry-based chronic HFrEF patients undergoing routine ambulatory care and treatment naïve cancer patients have been prospectively enrolled. Comorbidities and

laboratory data at baseline were assessed. All-cause mortality was defined the primary endpoint. The neutrophil-to-lymphocyte ratio (NLR), the monocyte-to-lymphocyte ratio (MLR), the platelet-to-lymphocyte ratio (PLR) as well as the prognostic nutritional index ($PNI = \text{albumin (g l}^{-1}) \times \text{total lymphocyte count} \times 10^9 \text{ l}^{-1}$) were calculated. Association of scores with disease

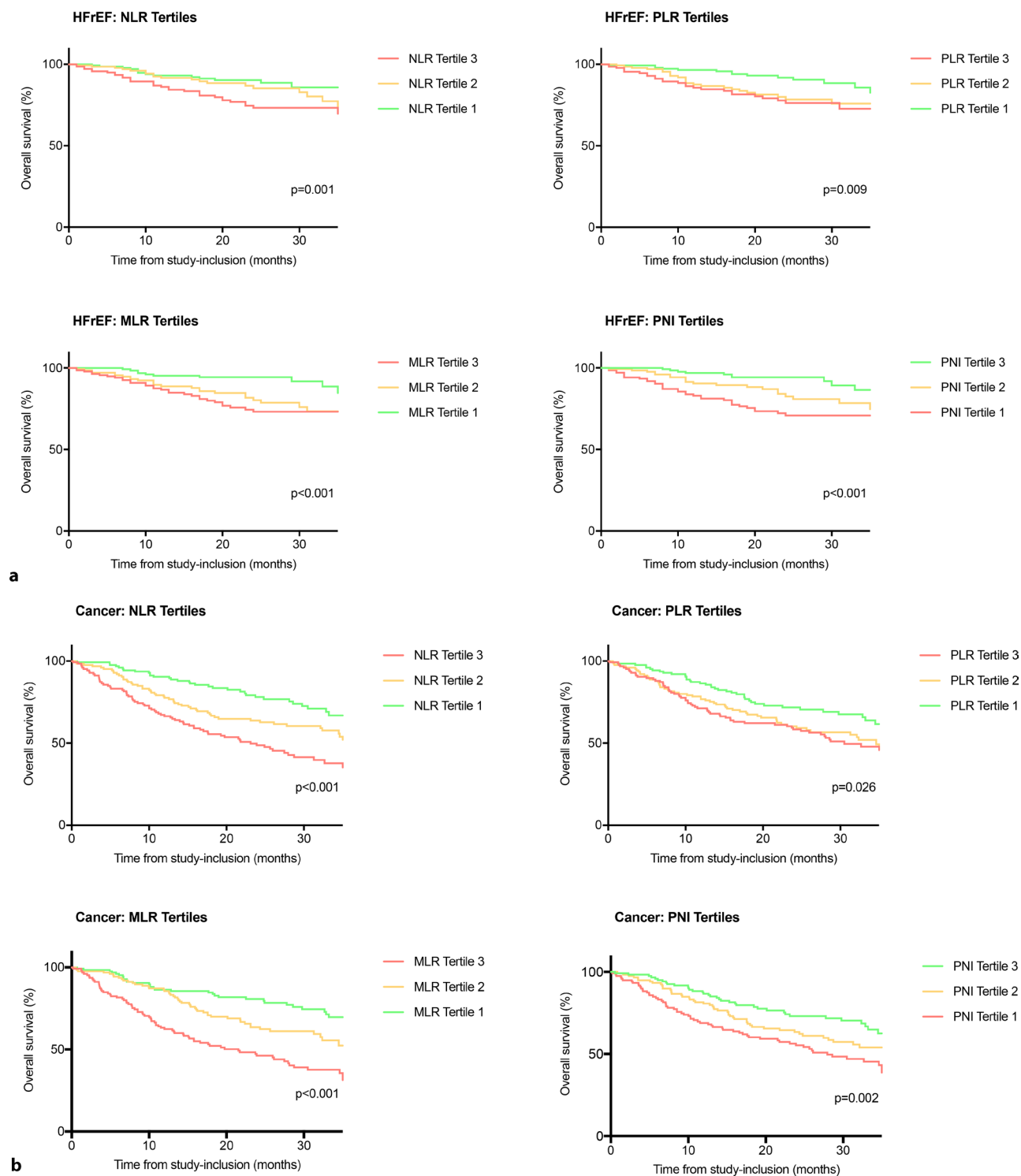


Fig. 117.18 Kaplan Meier estimates for overall survival in stable HFrEF(A) or treatment naïve cancer (B) according to prognostic scores, NLR, PLR, MLR, and PNI. Curves were compared by the log-rank test

severity and impact on overall survival were determined. Interaction analysis was performed for the different populations.

Results: A total of 818 patients (443 HFrEF and 375 cancer patients) were enrolled. Median age was 63 years (IQR: 53–72 years), and 474 (58 %) were male. In the HFrEF study-cohort, there was a strong association between all scores and disease severity reflected by NT-proBNP and NYHA class ($p \leq 0.001$ for all). In the oncologic study-cohort, association with tumor stage was significant for the MLR and the PNI only ($p \leq 0.029$, for both). In both cohorts, all scores were associated with all-cause mortality in Cox regression analysis ($p \leq 0.014$ for all scores). Kaplan Meier analysis confirmed the discriminatory power of all scores in the HFrEF and the oncologic study-population, respectively (log-rank $p \leq 0.026$ for all scores) (Fig. 1A&B). A significant interaction with disease (HFrEF vs. cancer) was observed for PNI or PLR respectively, with higher increase in risk per inflammatory score increment for HFrEF ($p(\text{interaction}) \leq 0.013$). This was not observed for NLR, or MLR ($p(\text{interaction}) \geq 0.192$).

Conclusion: The inflammatory scores NLR, MLR, PLR and PNI are associated with severity of disease and survival in heart failure similarly to cancer patients. For the PNI and PLR even a stronger association with HFrEF than with malignant disease could be shown. This relationship underscores the significance of proinflammatory response on prognosis and reaffirms similarities between systemic diseases heart failure and cancer.

7.19

Imaging and circulating biomarkers—a united approach for secondary tricuspid regurgitation

G. Spinka¹, P. E. Bartko¹, G. Heitzinger¹, E. Teo², S. Prausmüller¹, H. Arfsten¹, N. Pavo¹, M. Winter¹, J. Mascherbauer¹, C. Hengstenberg¹, M. Hülsmann¹, G. Goliash¹

¹Medizinische Universität Wien, Innere Medizin II, Kardiologie, Wien, Austria

²Royal Melbourne Hospital, Melbourne, Australia

Introduction: Secondary tricuspid regurgitation (sTR) is frequent among patients with heart failure with reduced ejection fraction (HFrEF), however inheres considerable diagnostic challenges. The assessment of circulating biomarkers reflecting neurohumoral activation may constitute a valuable supplement to the current imaging-based diagnostic process. This study therefore sought to investigate (i) the expression of a set of complementary biomarkers in sTR, (ii) to evaluate their association with sTR severity, and (iii) to analyse whether the combination of neurohormone measurement and echocardiographic grading improves the individual patient risk assessment.

Methods: We included 576 HFrEF patients under guideline-directed therapy recording functional, echocardiographic, invasive hemodynamic and biochemical measurements, i.e. (N-terminal pro-B-type natriuretic peptide, mid-regional proatrial natriuretic peptide (MR-proANP), mid-regional pro-adrenomedullin, C-terminal pro-endothelin-1 (CT-pro-ET1), and copeptin).

Results: Plasma levels of aforementioned neurohormones were significantly rising with increasing sTR severity (for all $P < 0.001$). Among all measured biomarkers, CT-pro-ET1 and MR-proANP were closest related to severe sTR, even after multivariate adjustment for established clinical confounders (adj. OR 1.46; 95 %CI 1.11–1.91, $P = 0.006$ and adj. OR 1.45, 95 %CI 1.13–1.87, $P = 0.004$, respectively). By means of individual outcome in patients with moderate to severe sTR, adding the selected

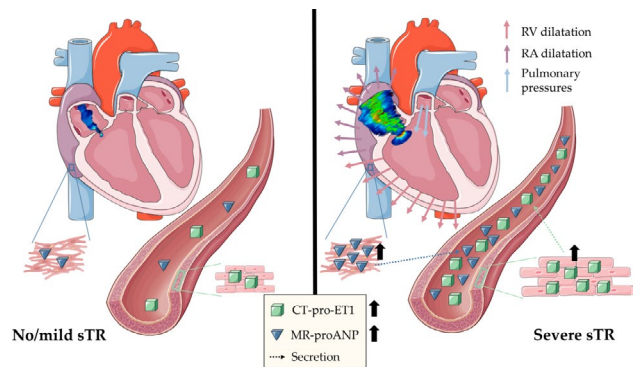


Fig. 117.19

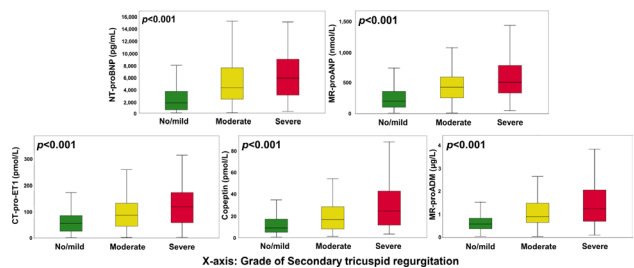


Fig. 217.19 Neurohumoral profiles in HFrEF patients with no/mild, moderate or severe tricuspid regurgitation. Levels are displayed as Tukey boxplots. Comparisons between different degrees of tricuspid regurgitation were analysed by the Kruskal-Wallis test

biomarkers (i.e. CT-pro-ET1 and MR-proANP) resulted in a substantial improvement of the discriminatory power regarding long-term mortality (C-statistic: 0.54 vs. 0.65, $P < 0.001$; continuous NRI 57 %, $P < 0.001$).

Conclusion: Circulating biomarkers closely relate to sTR severity and correlate with hemodynamic and morphologic mechanisms of sTR. Specifically, MR-proANP and CT-pro-ET1 are closely related to the presence of severe sTR and a combined assessment with the guideline recommended echocardiographic grading leads to a significant improvement of individual risk stratification.

7.20

MicroRNA assessment in secondary mitral regurgitation—evidence for remodelling mechanisms at a cellular level

G. Spinka¹, P. E. Bartko¹, N. Pavo¹, C. Freitag¹, K. Zlabinger¹, S. Prausmüller¹, H. Arfsten¹, G. Heitzinger¹, J. Mascherbauer¹, C. Hengstenberg¹, M. Gyöngyösi¹, M. Hülsmann¹, G. Goliash¹

¹Medizinische Universität Wien, Innere Medizin II, Kardiologie, Wien, Austria

Introduction: Secondary mitral regurgitation (sMR) is associated with adverse outcome in patients with heart failure with reduced ejection fraction (HFrEF), possibly driven through malignant cardiac remodelling. MicroRNAs (miRNA/miR), small non-coding RNAs involved in post-transcriptional gene regulation, have recently been associated with the development of fibrosis and hypertrophy. This study therefore sought to

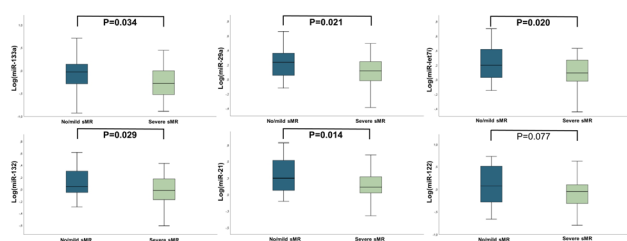


Fig. 117.20 MicroRNA profiles in HFref patients with either severe sMR or no/mild sMR (matched controls). MicroRNA-profiles are displayed as Tukey Boxplots, comparisons between patients with severe sMR and matched controls were analysed by an independent t-test

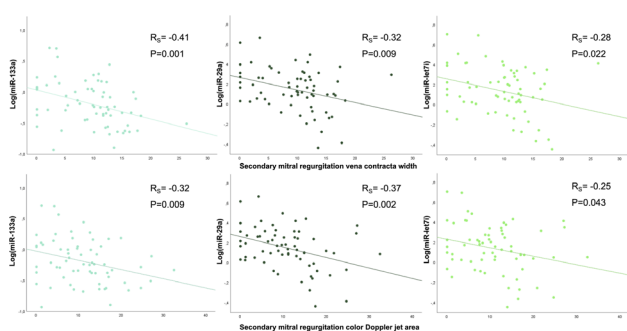


Fig. 217.20 Scatter plot displaying the association between quantified surrogates of sMR (i. e. sMR vena contracta width and sMR regurgitant jet area) and microRNA-levels in patients with HFref and severe sMR (matched controls). The correlation between the aforementioned variables was assessed using Spearman rho correlation analysis

assess the differences in miRNA-profiles in patients with severe sMR compared to matched disease controls, the correlation of circulating miRNAs with sMR severity as well as the prognostic implications of miRNA-levels in patients with HFref and severe sMR.

Methods: Sixty-six patients with HFref were included in this pilot study. Forty-four patients with severe sMR were matched to disease controls with no/mild sMR in a 2:1 ratio. A comprehensive panel of miRNAs (miR-21, miR-29a, miR-122, miR-132, miR-133a, and miR-let7i) was measured using real time polymerase chain reaction and related to echocardiographic assessment of sMR severity.

Results: The profiles of miR-21, miR-29a, miR-132, miR-133a, and miR-let7i differed significantly between patients with severe sMR and HFref controls (for all $P < 0.05$). Moreover, we observed significant correlations between circulating miR-133a ($r = -0.41, P = 0.001$), miR-29a ($r = -0.32, P = 0.009$), and miR-let7i ($r = -0.28, P = 0.022$) and sMR vena contracta width. Elevated levels of miR-133a conveyed an increased risk for cardiovascular death and/or heart failure hospitalisations with an adjusted HR of 1.85 (95 % CI 1.24–2.76, $P = 0.003$). Furthermore, Kaplan-Meier-Analysis revealed a significantly higher risk for the above-mentioned outcome in patients with severe sMR and miR-133a-levels above the median.

Conclusion: This study unveils distinct pathophysiologic mechanisms at a cellular level in patients with severe sMR compared to patients with no/mild sMR. We observed significant differences in miRNA-profiles and strong correlations of miRNAs with surrogates of sMR severity, supporting the concept that sMR drives adverse cardiac remodelling in heart failure. Finally, elevated levels of miR-133a convey an increased risk for

morbidity and mortality in patients with HFref and severe sMR, potentially implying advanced myocardial damage.

7.21

Influence of diabetes, heart failure, and NT-proBNP on cardiovascular outcomes in patients with atrial fibrillation—insights from a cohort study of 7850 patients with extended follow-up

F. Hofer¹, U. Pailer², P. Sulzgruber¹, C. Gerges¹, M. P. Winter¹, M. Gottsauner-Wolf¹, M. Hülsmann¹, N. Kazem¹, L. Koller¹, R. Schönbauer¹, A. Niessner¹, C. Hengstenberg¹, T. A. Zelniker¹

¹Medizinische Universität Wien, Wien, Austria

²Wiener Gesundheitsverbund, Wien, Austria

Introduction: Diabetes and heart failure (HF) promote atrial fibrillation (AF) and are associated with an increased risk of adverse cardiovascular (CV) events in patients with AF. Because of effective anticoagulation options, AF patients are now more likely to develop HF than a stroke or a systemic embolic event. Appropriate risk stratification of patients with AF should therefore not only consider the risk for stroke but also for HF events.

Methods: Patients with AF admitted to a tertiary academic center between 07/2000 and 07/2019 were identified through a search of electronic health records. The primary outcome of interest was CV death or hospitalization for HF (HHF). We used Cox regression models adjusted for age, sex, estimated glomerular filtration rate, diabetes, HF, body mass index, prior myocardial infarction, hypertension, CRP, LDL-C, and smoking.

Results: In total, 7,850 patients (median age 70 years, 39.6 % female) were included in the present analysis and followed over a median of 4.7 years. Both diabetes (Adjusted (Adj.) hazard ratio (HR) 1.87, 95 % confidence interval (CI) 1.58 to 2.21) and HF (Adj. HR 2.43, 95 % CI 2.10 to 2.82) were significantly associated with CV death/HHF after multivariable adjustment. Compared to patients with diabetes, HF patients had a higher risk of HHF but a similar risk of CV and all-cause death. There was a robust relationship between CV death/HHF and NT-proBNP

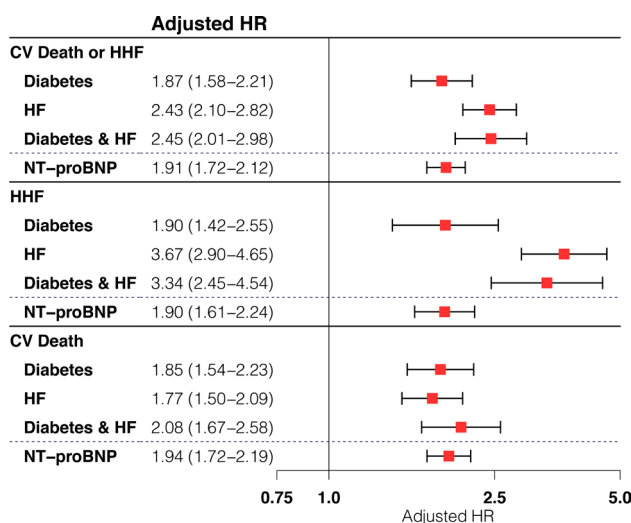


Fig. 117.21 Relationship between diabetes, heart failure, and NT-proBNP and cardiovascular outcomes

(Adj. HR for 1-unit increase in standardized log-transformed biomarker 1.91, 95 % CI 1.72 to 2.12). NT-proBNP showed good discriminatory performance (AUC 0.78, 95 % CI 0.77–0.80), and the addition of NT-proBNP to the covariates used for adjustment resulted in a significant AUC improvement ($\Delta=0.04$, $P < 0.001$). With least absolute shrinkage and selection operator logistic regression, the strongest associations for CV death/HHF were obtained for NT-proBNP (OR 2.83 per 1-SD in log-transformed biomarker), diabetes (OR 2.17), and HF (OR 2.14).

Conclusion: These findings suggest that the influence of diabetes and HF expand beyond the risk of stroke and systemic embolic events to CV death/HHF in an unselected AF patient population. NT-proBNP may provide improved risk assessment in AF patients.

7.22

Correlation between invasive and non-invasive quantification of myocardial amyloid load in cardiac transthyretin amyloidosis

M. Ungericht¹, V. Groaz¹, M. Messner¹, M. Zaruba¹, J. Doerler¹, D. Lener¹, E. Stocker¹, A. Mayr², A. Kroiss³, G. Poelzl¹

¹Department of Internal Medicine III, Cardiology & Angiology, Medical University of Innsbruck, Innsbruck, Austria

²Department of Radiology, Medical University of Innsbruck, Innsbruck, Austria

³Department of Nuclear Medicine, Medical University of Innsbruck, Innsbruck, Austria

Introduction: Cardiac transthyretin (ATTR) amyloidosis is an infiltrative disease caused by the extracellular deposition of misfolded ATTR protein in the myocardium. Early disease recognition and accurate description of cardiac involvement are fundamental, as cardiac ATTR amyloidosis is associated with poor prognosis. Although endomyocardial biopsy (EMB) remains the gold standard in amyloid detection and typing, non-invasive imaging can provide an accurate diagnostic tool. Bone scintigraphy enables early disease detection with high accuracy. However, it remains to be determined whether the degree of cardiac tracer uptake on bone scintigraphy correlates with the extent of histologic amyloid burden in EMB. This single centre observational study aimed to compare the histological amyloid load in endomyocardial biopsies with the quantification of cardiac tracer uptake on 99mTechnetium-3,3-diphosphono-1,2-propanodicarboxylic acid (99mTc-DPD) scintigraphy in cardiac ATTR amyloidosis.

Methods: 23 patients with cardiac ATTR amyloidosis were enrolled. Diagnosis was obtained with a combination of invasive and non-invasive methods. Perugini score, mean left ventricular tracer uptake (LV uptake) and left ventricular to corpus sterni uptake ratio (LV/CS ratio) on 99mTc-DPD-scintigraphy were measured, while histological amyloid load was quantified as percentage of the analysed myocardial tissue using Sulfated Alcian Blue staining and the Fiji-ImageJ programme. Bivariate correlation and Pearson correlation coefficient were used to study the relationship between EMB and 99mTc-DPD-scintigraphy findings.

Results: We found a statistically significant correlation between histological amyloid load and Perugini score ($r=0.47$ $p=0.02$), as well as between Perugini score and LV/CS ratio ($r=0.31$ $p=0.046$). Mean LV tracer uptake showed a trend for correlation with histological amyloid load ($r=0.37$ $p=0.08$), without reaching statistical significance.

Correlation between Perugini score by 99mTc-DPD-scintigraphy and histological amyloid load in ATTR CA
 $r=0.47$ $p=0.02$ $n=23$

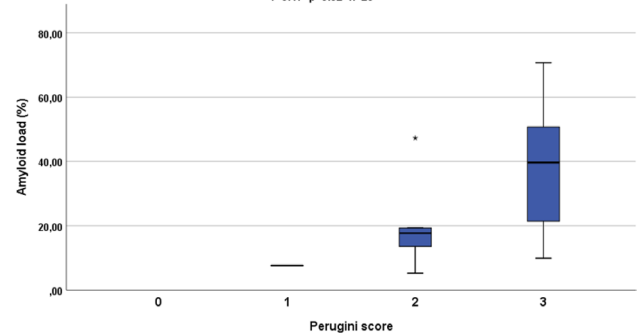


Fig. 117.22

Correlation between LV / CS ratio and Perugini score by 99mTc-DPD-scintigraphy in ATTR CA
 $r=0.31$ $p=0.046$ $n=23$

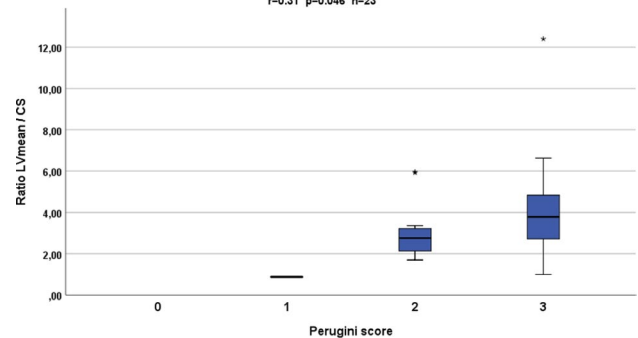


Fig. 217.22

Conclusion: We found a correlation between the extent of histologic amyloid burden in EMB and the degree of cardiac tracer uptake on 99mTc-DPD-scintigraphy. Our results underline the reliability of 99mTc-DPD-scintigraphy as a surrogate of histological amyloid load in the diagnosis of cardiac ATTR amyloidosis. Possible implications for the assessment of prognosis are subject to future studies with a larger number of patients.

7.23

Recurrent heart failure hospitalizations in patients with preserved ejection fraction: predictors and outcome

L. Schrutka¹, B. Seirer¹, F. Frommlet¹, R. Rettl¹, T. Dachs¹, C. Binder¹, F. Duca¹, D. Dalos¹, R. Badr-Eslam¹, J. Kastner¹, C. Hengstenberg¹, D. Bonderman¹

¹Medizinische Universität Wien, Wien, Austria

Introduction: Heart failure with preserved ejection fraction (HFpEF) is the most common form of HF and its prevalence is approaching epidemic proportions. Current treatment strategies aim to improve clinical status and reduce mortality rates. Episodes of acute HF are one of the main reasons for hospitalization in people over 65 years; however, they have not been well studied in HFpEF patients yet. The aim of this study was to investigate the impact of recurrent HF hospitalizations on long-term outcomes and to find predictors for subsequent events.

Methods: Between December 2010 and December 2019, 422 patients with confirmed HFpEF were enrolled in this study and prospectively followed.

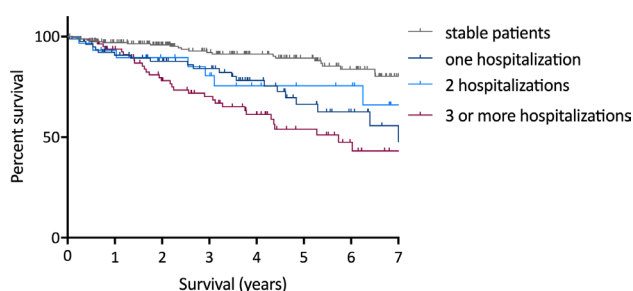


Fig. 117.23

Results: During follow-up, 190 HFpEF patients (45 %) experienced HF hospitalizations with a median frequency of 2 (IQR: 1–4). Those presenting with acute HF had higher body mass indices ($p=0.018$), worse performance in 6-minute walking tests ($p<0.001$), higher levels of N-terminal prohormone of brain natriuretic peptide (NT-proBNP, $p<0.001$) and, compared to stable patients, a larger proportion suffered from New York Heart Association functional class \geq III ($p<0.001$). Furthermore, baseline left ventricular diastolic dysfunction (early mitral inflow velocity/early diastolic mitral annular velocity; $p=0.002$) as well as right ventricular afterload (pulmonary artery wedge pressure; $p<0.001$) were more pronounced in patients with acute deteriorations. Over the observation period 107 patients (25 %) died. Kaplan-Meier curves revealed increasingly worse survival in patients with recurrent HF events (5-years survival: 1 HF event 66 % vs ≥ 3 HF events 53 %, $p<0.001$; Fig. 1). Time to last hospitalization was a strong predictor of survival with an adjusted HR of 2.5 (95 % CI 1.63–3.98; $p<0.001$) in multivariate Cox regression analysis. Predictors of recurrent HF hospitalization were 6-minute walking distance (OR: 0.07, CI 0.02–0.22; $p=0.001$), systolic pulmonary artery pressure (OR: 1.05, CI 1.03–1.07, $p=0.001$) and NT-pro BNP (OR: 4.92, CI: 2.68–9.04, $p=0.001$)

Conclusion: HFpEF patients experiencing recurrent HF hospitalizations have worse long-term outcome. Intensive efforts should be made to maintain HFpEF patients compensated over time.

7.24

Tafamidis treatment in patients with transthyretin amyloid cardiomyopathy

R. Rettl¹, M. Christopher¹, F. Duca¹, T. Dachs¹, C. Binder¹, C. Kronberger¹, F. Dusik¹, L. Camuz Ligios¹, L. Schrutka¹, D. Dalos¹, S. Charwat-Resl², R. Badr Eslam¹, C. Hengstenberg¹, J. Kastner¹, D. Bonderman²

¹Medizinische Universität Wien, Wien, Austria

²Klinik Favoriten, Wien, Austria

Introduction: Tafamidis is a kinetic stabilizer of transthyretin (TTR) that prevents tetramer dissociation and amyloidogenesis in patients with TTR amyloid cardiomyopathy (ATTR-CM), resulting in delayed disease progression.

Methods: Patients with ATTR-CM were treated with tafamidis 61 mg ($n=64$) or tafamidis 20 mg ($n=23$) for a period of six to nine months. In our explorative analysis, we aimed to evaluate the effects of tafamidis based on changes in exercise capacity, cardiac biomarkers, as well as cardiac structure and function, and to compare tafamidis-treated patients with an untreated control cohort ($n=54$).

Results: Main results are summarized in Fig. 1. In brief, we observed an improvement in exercise capacity as measured by the 6-minute walking distance (6MWD, mean, baseline (BL): 377.1 m vs. follow-up (FU): 383.2 m, $p=0.678$) in tafamidis 61 mg treated patients compared to a significant decrease in 6MWD (mean, BL: 388.1 m vs. FU: 336.4 m, $p=0.002$) in untreated patients (cohort comparison: $p=0.005$). Cardiac biomarkers showed a conclusive reduction in serum NT-proBNP levels (median, BL: 2633.0 pg/mL vs. FU: 2244.0 pg/mL, $p=0.366$) in tafamidis 61 mg treated patients, while a significant increase (median, BL: 2798.0 pg/mL vs. FU: 3422.0 pg/mL, $p<0.001$) was observed in untreated patients (cohort comparison: $p<0.001$). Echocardiographic findings revealed almost stabilization of the left ventricular (LV) strain (mean, BL: -11.75 % vs. FU: -11.58 %, $p=0.534$) and the right ventricular (RV) strain (mean, BL: -14.18 % vs. FU: -13.72 %, $p=0.377$) in the tafamidis 61 mg treatment cohort compared to a significant deterioration in the longitudinal function of the LV (mean, BL: -11.71 % vs. FU: -10.59 %, $p=0.001$) and RV (mean, BL: -14.36 % vs. FU: -12.99 %, $p=0.038$) in the non-treatment cohort (cohort comparison: $p=0.030$ and $p=0.269$). In addition, structural cardiac magnetic imaging parameters demonstrated a significant increase in LV mass (mean, BL: 199.1 g vs. FU: 214.3 g, $p=0.040$) and extracellular volume (ECV, mean, BL: 50.52 % vs. FU: 55.96 %, $p=0.026$) in the untreated cohort.

Conclusion: Treatment with tafamidis in patients with ATTR-CM leads to significant improvements in exercise capacity (6MWD), biomarkers (NT-proBNP), and shows substantial advantages in terms of functional (LV strain, RV strain), as well as structural (LV mass, ECV) imaging parameters compared to an untreated control cohort.

7.25

Seasonal variation in decompensated heart failure in the emergency unit according to LVEF category—a retrospective analysis

Hermann Riepl¹, Markus Wallner¹, Ewald Kolesnik¹, Klemens Ablasser¹, Peter Rainer¹, Friedrich Fruhwald¹, Andreas Zirlik¹, Philipp Kreuzer², Andreas Lueger², Nicolas Verheyen¹

¹Division of Cardiology; ²Emergency Unit; Department of Internal Medicine, Medical University of Graz, Graz, Austria

Background: Observational studies suggest that heart failure decompensations follow a seasonal trend, with increased prevalence during the winter months. Whether this trend differs by heart failure aetiology is unknown. We therefore aimed to assess the seasonality of decompensated heart failure in an emergency unit of a tertiary care hospital, categorizing patients into heart failure with preserved ejection fraction (HFpEF), mid-range ejection fraction (HFmrEF), and reduced ejection fraction (HFrEF).

Methods: We performed a systematic retrospective chart review of patients presenting in the Emergency Unit of the Department of Internal Medicine of the University Hospital of Graz (Graz, Austria). Records of patients were individually analysed for signs of cardiac decompensation. Age, gender, LVEF, NT-proBNP and eGFR were included in the dataset when available. According weather data were acquired from the National Institute of Meteorology and Geodynamics.

Results: Between August 2018 and July 2019, 32,028 patients presented in the emergency unit, and 1248 fulfilled the criteria of cardiac decompensation (3.9 %). Mean age was 79.6 ± 9.8

Table 117.24 Comparison of baseline and follow-up characteristics between tafamidis-treated and untreated ATTR-CM patients.

Characteristics	Tafamidis 61 mg (n = 62)			Tafamidis 20 mg (n = 21)			Not treated (n = 54)			ΔTaf. 61 mg ΔUntreated	ΔTaf. 20 mg ΔUntreated	ΔTaf. 61 mg ΔTaf. 20 mg
	Baseline	FollowUp	<i>p</i>	Baseline	FollowUp	<i>p</i>	Baseline	FollowUp	<i>p</i>	<i>p</i>	<i>p</i>	
Functional capacity												
6-min walk distance – m (SD)	381.2 (118.9)	386.3 (137.8)	0.764	408.4 (121.0)	397.3 (141.1)	0.486	388.1 (148.9)	336.4 (141.2)	0.002	0.006	0.124	0.479
Laboratory parameters												
NT-proBNP – pg/mL (IQR)	2633 (1445–5185)	2244 (1353–4784)	0.488	2740 (1355–4419)	2533 (1271–3975)	0.614	2798 (1803–4634)	3422 (2060–9065)	<0.001	<0.001	0.053	0.741
Echocardiographic parameters												
LA length – mm (SD)	60.9 (8.3)	60.2 (7.3)	0.429	63.7 (5.4)	63.0 (5.8)	0.652	63.0 (6.4)	64.2 (6.1)	0.209	0.143	0.294	0.988
RA length – mm (SD)	59.5 (8.9)	59.5 (7.5)	0.957	59.4 (6.8)	61.9 (6.5)	0.065	61.8 (7.5)	62.7 (8.2)	0.279	0.450	0.276	0.137
Interventricular septum – mm (SD)	19.6 (4.2)	20.0 (4.4)	0.067	21.3 (3.8)	22.0 (3.5)	0.004	18.8 (3.7)	19.9 (3.7)	<0.001	0.006	0.068	0.411
LV end-diastolic diameter – mm (SD)	42.4 (6.7)	41.4 (6.9)	0.227	40.0 (6.3)	39.8 (6.6)	0.841	41.6 (6.6)	41.6 (7.2)	0.918	0.358	0.838	0.575
RV end-diastolic diameter – mm (SD)	35.4 (5.8)	34.8 (4.8)	0.414	32.7 (7.1)	34.3 (6.0)	0.193	34.7 (5.3)	36.4 (7.0)	0.067	0.048	0.951	0.125
LV strain – % (SD)	–11.75 (3.16)	–11.58 (3.14)	0.534	–10.61 (2.76)	–10.12 (2.50)	0.309	–11.71 (3.17)	–10.59 (3.00)	0.001	0.030	0.274	0.568
RV strain – % (SD)	–14.18 (4.86)	–13.72 (5.07)	0.377	–14.53 (6.22)	–13.99 (5.73)	0.452	–14.36 (5.37)	–12.99 (5.21)	0.038	0.269	0.440	0.939
CMR parameters												
LA area – cm ² (SD)	31.5 (7.1)	31.6 (6.6)	0.955	31.4 (6.8)	32.8 (6.1)	0.334	33.7 (6.3)	33.2 (5.4)	0.666	0.754	0.306	0.542
RA area – cm ² (SD)	31.0 (7.6)	29.5 (6.3)	0.156	29.9 (5.8)	29.6 (6.5)	0.753	32.2 (7.7)	35.0 (8.4)	0.050	0.060	0.198	0.715
Interventricular septum – mm (SD)	19.0 (4.0)	20.2 (6.7)	0.198	21.1 (2.9)	22.3 (4.1)	0.136	19.4 (3.5)	20.8 (3.3)	<0.001	0.914	0.707	0.943
LV end-diast. vol. index – mL/m ² (SD)	93.6 (22.3)	97.0 (20.3)	0.124	86.2 (12.7)	89.0 (14.9)	0.361	76.8 (14.4)	86.9 (15.9)	0.003	0.078	0.074	0.699
RV end-diast. vol. index – mL/m ² (SD)	98.2 (23.8)	106.8 (28.2)	0.014	81.8 (16.1)	91.8 (23.6)	0.054	82.4 (17.1)	94.8 (22.9)	0.005	0.483	0.698	0.809
LV ejection fraction – % (SD)	47.6 (10.9)	47.5 (12.0)	0.935	52.4 (11.0)	52.1 (11.7)	0.930	53.3 (11.5)	45.7 (10.9)	0.031	0.035	0.120	0.971
RV ejection fraction – % (SD)	42.4 (11.8)	42.3 (10.7)	0.962	48.8 (13.9)	46.6 (9.7)	0.475	47.9 (11.5)	42.5 (10.1)	0.119	0.130	0.501	0.526
LV mass index – g/m ² (SD)	110.2 (25.9)	106.2 (24.2)	0.304	114.5 (19.0)	115.4 (29.3)	0.900	98.9 (22.8)	106.9 (22.7)	0.027	0.036	0.287	0.525
MOLLI-ECV – % (SD)	47.5 (12.3)	47.7 (10.0)	0.861	56.7 (14.0)	57.5 (11.8)	0.759	49.3 (9.5)	54.6 (11.0)	0.023	0.030	0.158	0.834

NT-proBNP indicates N-terminal prohormone of brain natriuretic peptide; LA, Left atrium; RA, Right atrium; LV, Left ventricle; RV, Right ventricle; CMR, Cardiac magnetic resonance imaging; MOLLI-ECV, Modified look-locker inversion recovery sequence derived extracellular volume. Values are given as mean ± standard deviation (SD), or median and interquartile range (IQR), or total numbers (n) and percent (%). Bold indicates *p*<0.05.

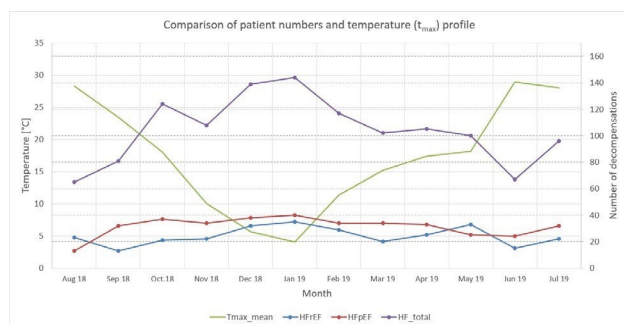


Fig. 117.25

years and 625 (50.1 %) were females. Among those with available LVEF ($n=866$, 69 %), the prevalence of HFpEF, HFmEF and HFrEF was 43 %, 23 % and 34 %, respectively. Compared with HFrEF, patients with HFpEF were older (mean age \pm SD 78.6 ± 9.4 vs 76.3 ± 9.4 years), more often females (57 % vs 25 %, $P < 0.001$) and had lower NT-proBNP levels (median 2982 [IQR, 1388–6702] pg/ml vs 7216 [3502–16.485] pg/ml, $P < 0.001$). Most patients decompensated in January ($n=144$) and least patients in August ($n=65$). When stratifying maximal daily temperature by deciles, there were significantly more heart failure decompensations on coldest days (1st decile vs. 10th decile: 102 vs 73 decompensations, $P=0.025$). We found a significant inverse association between temperature and prevalence of decompensations both in patients with HFpEF (P for linear-by-linear = 0.002) as well as in patients with HFrEF (P for linear-by-linear = 0.003).

Conclusion: These data reconfirm a prevalence for HFpEF of approximately 50 % among patients with decompensated heart failure, and a seasonal trend of heart failure decompensations. The prevalence of cardiac decompensation is indirectly proportional to temperature, regardless of the underlying heart failure aetiology. One may speculate that mechanisms underlying the adverse effect of cold temperature are similar between HFpEF and HFrEF. The fact that decompensations rise in winter months might lead to an adaptation of preventive strategies in patients with chronic heart failure during the cold season.

8 INTERVENTIONELLE KARDIOLOGIE

8.1

Tumor necrosis factor alpha—an underestimated risk predictor in patients undergoing transcatheter aortic valve replacement (TAVR)?

M. Mirna¹, V. Paar¹, J. Kellermair², H. Blessberger², J. Kammler², L. Motloch¹, C. Jung³, U. Hoppe¹, C. Steinwender², M. Lichtenauer¹

¹Department of Internal Medicine II, Division of Cardiology, Paracelsus Medical University of Salzburg, Austria., Salzburg, Austria

²Department of Cardiology, Kepler University Hospital, Medical Faculty, Johannes Kepler University Linz, Linz, Austria, Linz, Austria

³Division of Cardiology, Pulmonology, and Vascular Medicine, Medical Faculty, University Duesseldorf, Germany, Düsseldorf, Germany

Introduction: Although systemic inflammation has been identified as a major cardiovascular risk factor, it is currently not adequately portrayed in scores for pre-interventional risk assessment in patients undergoing transcatheter aortic valve replacement (TAVR). The aim of this study was to investigate the predictive ability of tumor necrosis factor alpha (TNF- α) in TAVR.

Methods: A total of 431 patients undergoing transfemoral TAVR were enrolled in this study. Blood samples were drawn pre-interventionally, after 24 hours, after 4, 5 and 7 days and after 1, 3 and 6 months post TAVR. Biomarker concentrations were analyzed by ELISA.

Results: TAVR resulted in a 1.6-fold increase of the concentrations of TNF- α after 5 days (mean 26.8 ± 115.0 pg/ml vs. 42.0 ± 151.3 pg/ml, $p=0.269$). In univariate Cox proportional hazards analysis, plasma concentrations of TNF- α after 24 h and after 5 days were associated with mortality after 12 months (after 24 h: HR 1.002 (1.000–1.004), $p=0.028$; after 5d: HR 1.003 (1.001–1.005), $p=0.013$). This association remained significant even after correction for confounders in a multivariate Cox regression analysis. Additionally, cut-offs were calculated. Patients above the cut-off for TNF- α after 5d had a significantly worse 12-month mortality than patients below the cut-off (18.8 % vs. 2.8 %, $p=0.046$).

Conclusion: Plasma levels of TNF- α after 24 h and 5 days were independently associated with 12-month mortality in patients undergoing TAVR. Thus, TNF- α could represent a novel inflammatory biomarker for enhanced peri-interventional risk stratification in these patients.

8.2

Prospective registry of cardiogenic shock patients in cath-lab patients of a tertiary centre

L. Herold¹, G. Toth-Gayor¹, A. Schmidt¹, R. Zweiker¹, R. Gasser¹, S. Pätzold¹, F. Fruhwald¹, S. Altmanninger-Sock¹, C. Sourij¹, K. Ablasser¹, A. Zirlik¹, D. von Lewinski¹

¹Klinische Abteilung für Kardiologie, LKH-Univ. Klinikum Graz, Graz, Austria

Tab. 118.2 Results

	Overall (n=171)	nodevice (n=139)	ECMO (n=13)	IMPELLA (n=17)	ECMELLA (n=2)
Age (years), median (IQR)	69(58-76)	70(58-77)	65(54-72)	71(61-74)	60(52-67)
male gender, n (%)	121(70.8)	99(71.2)	9(69.2)	12(70.6)	1(50)
BMI, median (IQR)	27.1(24.5-30.4)	27(24.3-30.4)	28.3(26.2-29.4)	27(25.3-30.5)	22.8(21.7-23.7)
no CPR, n (%)	61(35.7)	45(32.3)	2(15.4)	13(76.5)	1(50)
—discharged alive, n (%)	43(70.5)	32(71.1)	0	9(69.2)	1(100)
CPR, n (%)	110(64.3)	94(67.6)	11(84.6)	4(23.5)	1(50)
—discharged alive, n (%)	50(45.5)	45(47.9)	2(18.2)	2(50)	1(100)
—OHCA, n (overall%)	77(45.0)	70(50.4)	5(38.5)	2(11.8)	0
—discharged alive, n (%)	37(48.1)	35(50.0)	1(20)	1(50)	0
—IHCA, n (overall%)	33(19.3)	24(17.3)	6(46.2)	2(11.8)	1(50)
—discharged alive, n (%)	13(39.4)	10(41.7)	1(16.7)	1(50)	1(100)
under lying disease, n (%):					
—STEMI	93(54.4)	73(52.5)	9(69.2)	9(52.9)	2(100)
—NSTEMI	28(16.4)	23(16.5)	2(15.4)	3(17.6)	0
—others (arrhythmia, valvular,...)	50(29.2)	43(30.9)	2(15.4)	5(71.4)	0
initial lactate (mmol/L), median (IQR)	3.3(1.7-7.0)	3.1(1.55-6.35)	10(5.1-12.4)	2.6(1.2-5.0)	2.3(2.2-2.5)
initial pH, median (IQR)	7.27(7.13-7.39)	7.26(7.14-7.37)	7.13(7.07-7.27)	7.34(7.25-7.42)	7.40(7.37-7.43)
ventilation duration (days), median (IQR)	1(0-7)	1(0-7)	7(1-16)	1(0-5)	16(13-18)
total CCU stay after surviving day ofshock (days), median (IQR)	6(3-14)	6(3-14)	15(7-23)	5(4.5-7)	40(27-52)
first-day-mortality, n (%)	39(22.8)	33(23.7)	4(30.8)	2(11.8)	0
7-day-mortality, n (%)	59(34.5)	49(35.3)	7(53.8)	5(29.4)	0
28-day-mortality, n (%)	77(45.0)	60(43.2)	11(84.6)	6(35.3)	0
in-hospital-death, n (%)	78(45.6)	61(43.9)	11(84.6)	6(35.3)	0

Tab. 218.2 Contraindications for MCS

	CPR	noCPR
biological age (years)	>60	>70
pH	<6.8	<7.1
initial lactate (mmol/L)	>20	>15
co-morbidities	COPD>III; neurological, internal or oncological diseases with palliative treatment	COPD>III; neurological, internal or oncological diseases with palliative treatment
Furthermore	nobystander-CPR/no-flow-time>10 min; CPR>45 min without ROSC; contraindication for full anticoagulation (bleeding, trauma, hemothorax, ...)	–

Introduction: Cardiogenic shock (CS) is a high-acuity and challenging situation for which temporary and long-term outcomes are less than ideal. Studies have figured out that mechanical circulatory support (MCS) systems such as VA-ECMO, IMPELLA or a combination of these two are capable of improving the prognosis of patients in refractory CS. However, it is recommended to define criteria to decide on the use of MCS based on the prognosis of the patients.

Methods: A total of 171 patients with CS were enrolled in a large, open prospective mono-centre registry study within 16 months. The inclusion criteria was the administration of vasopressors in the catheter laboratory in patients with suspected CS aged between 18 and 99 years. After therapy in the catheter laboratory, patient data such as demographic data, need of CPR, underlying disease, laboratory analyses et cetera

were acquired and registered in a case report form (CRF). The outcome was analyzed with regard to the possibility of discharging alive, total duration of hospital stay and complications as, for instance, bleeding events. Centre-defined contraindications for implantation of MCS-devices are shown in Fig. 2.

Results: Of the 171 patients analyzed, 78 died during their hospital stay. Mortality was highest in ECMO patients, but those were significantly sicker indicated by higher rate of CPR, lactate and initial pH, whereas patients with IMPELLA-use were characterized by better baseline values compared to the overall cohort. Two patients were treated with ECMELLA and were discharged alive. Outcome as measured by 1-, 7- and 28-days mortality was comparable between patients getting device support and the ones without, but depended mainly on baseline clinical characteristics such as lactate and initial pH.

Conclusion: Cardiogenic shock is characterized by a poor prognosis. The use of MCS-devices can help to reach an improved outcome in very severe patients but patients characteristics strongly determine that outcome. Therefore, patient selection is crucial to achieve good outcomes in this vulnerable group.

8.3

Improved protection for operator and assistant from occupational scatter radiation in interventional cardiologic procedures with a suspended radiation protection system—a per-procedure live-dosimetry analysis

M. C. Brandt¹, E. Prinz¹, W. Wintersteller¹, C. Schernthaler¹, M. Hammerer¹, J. Kraus¹, F. Danmayr¹, B. Strohmayer¹, I. Pretsch¹, M. Lichtenauer¹, L. J. Motloch¹, U. C. Hoppe¹, O. Nairz²

¹Uniklinik II für Innere Medizin, PMU Salzburg, Salzburg, Austria

²Uniklinik Salzburg, Strahlenschutzdienst, Salzburg, Austria

Introduction: Interventional cardiologists (IC) are exposed to the highest doses of radiation compared to all other medical specialties. Although head and eyes are exposed to a significant dose of scatter radiation (SCR), precise per-procedure data is sparse. Taking effect in 2021, the federal guidelines for maximum eye lens SCR doses have been reduced from 150 mSv to 20 mSv per year. It is still unclear, how these stricter values can be met in current cathlab setups. A ceiling suspended operator radiation protection system (Zero Gravity, CFI Medical Solutions, MI, USA), which was developed to reduce weight for the interventionalists' spine and shoulders, has shown additional benefits with respect to SCR protection. Up to now, most publications with ZG are based on selected radiologic interventional procedures [1]. Individual per-procedure SCR data including a representative array of cardiologic procedures is still lacking.

Methods: The purpose of this study was (A) to measure realistic per-procedure SCR doses at critical anatomical locations of the IC (frontal head at eye level, left lateral head, left shoulder) and sterile assistant (Left head/neck) and (B) to study the impact of the ZG system on IC and sterile assistant (SA) SCR exposure when used in addition to the current standard of X-ray protection (SXP) in unselected all-comers cardiologic procedures. Methods: IC and SA were equipped with Unfors RaySafe i3 live-dosimeters at prespecified locations. 151 consecutive cardiac procedures were recorded, in which either both IC and SA were using SXP (lead apron, thyroid shield) or the IC was using the ZG system and the SA was wearing SXP. In all procedures a suspended lead shield, patient lead cover and an adjustable lead side-shield were present. Diagnostic angiographies (DA) and interventions (PCI) were grouped separately. Within both groups, the IC's and SA's SCR doses were compared. Statistic averages are shown as Mean±SEM. Groups were compared with the two-sample t-test, $p < 0.05$ was considered statistically significant.

Results: SCR doses were recorded in 82 DA and 69 PCI procedures. Compared to SXP, the use of the ZG device reduced the average SCR doses per procedure of the IC recorded at the left lateral head from $4.68 \pm 0.80 \mu\text{Sv}$ to $0.66 \pm 0.08 \mu\text{Sv}$ in DA (-86%; $n=36/42$, $p < 0.0001$) and from $19.63 \pm 3.71 \mu\text{Sv}$ to $1.11 \pm 0.33 \mu\text{Sv}$ for PCI (-94%; $n=46/21$, $p=0.002$). The IC's average frontal dose at eye level was reduced from $1.27 \pm 0.32 \mu\text{Sv}$ to $0.40 \pm 0.05 \mu\text{Sv}$ in DA (-69%; $n=36/41$, $p=0.0070$) and from $3.48 \pm 0.61 \mu\text{Sv}$ to $0.93 \pm 0.23 \mu\text{Sv}$ in PCI (-73%; $n=46/21$, $p=0.0074$). Consistently, the dose recorded immediately under the IC's left shoulder were reduced from $42.82 \pm 11.60 \mu\text{Sv}$ to $1.25 \pm 0.33 \mu\text{Sv}$ in DA (-97%; $n=25/32$, $p=0.0002$) and from $77.26 \pm 13.14 \mu\text{Sv}$ to $2.78 \pm 0.78 \mu\text{Sv}$ in PCI (-96%; $n=35/21$, $p=0.0004$). Furthermore, when the IC used the ZG system, the average SCR dose recorded at the SA's head was reduced from $5.29 \pm 1.38 \mu\text{Sv}$ to

$2.25 \pm 0.34 \mu\text{Sv}$ in DA (-57%, $n=31/40$, $p=0.019$) and from $18.59 \pm 2.76 \mu\text{Sv}$ to $6.12 \pm 1.63 \mu\text{Sv}$ in PCI (-67%, $n=45/21$, $p=0.0051$). With the exception of the IC frontal dose, all SCR dose effects remained significant after correction for total radiation time ($\mu\text{Sv/s}$) and dose-area product ($\mu\text{Sv/Gy}\cdot\text{cm}^2$). Procedure duration, contrast use and patient radiation dose were not affected by ZG use.

Conclusion: Analysis of individual procedural data for IC and SA SCR exposure showed a substantial degree of dose variation depending on procedure complexity and numerous other factors. These variations are poorly represented in conventional cumulative dose measurements. Consistent with previous phantom-studies, the frontal dosimeter underestimated the SCR eye dose compared to the left lateral dosimeter position. In a representative all-comers cohort of cardiac procedures, the ZG X-ray protection system demonstrated an impressive potential for SCR reduction. ZG provided significant protection for ICs in critical anatomical areas—even in a state-of-the-art cathlab inventory with multiple SCR reduction measures already in place. Remarkably, the protective effect also included the sterile assistant at the table wearing SXP. The implementation of additional X-ray protection systems like ZG may be a viable approach to reach the new federal goal to drastically reduce cathlab staff SCR exposure at the head and eye level.

8.4

Impact of Transcatheter Edge-to-edge Mitral Valve Repair On Echocardiographic Parameters

S. Koschatko, M. Koschutnik, C. Donà, V. Dannenberg, C. Nitsche, A. Kammerlander, G. Goliash, P. Bartko, M. Schneider, C. Hengstenberg, J. Mascherbauer

Department of Internal Medicine II, Division of Cardiology, Medical University of Vienna, Austria, Wien, Austria

Introduction: Previous studies examining echocardiographic changes in patients undergoing transcatheter edge-to-edge mitral valve repair (TMVR) show discrepant results regarding the efficacy of the intervention. We aimed to investigate changes in echocardiographic parameters, routine biomarkers, and clinical presentation after TMVR.

Methods: We prospectively enrolled consecutive patients with severe symptomatic mitral regurgitation scheduled for TMVR. Transthoracic echocardiography and assessment of clinical and laboratory parameters were performed prior intervention and at follow-up.

Results: 112 patients ($75.6 \pm 8.2\%$ female, EuroSCORE II: $9.4 \pm 8.6\%$, mean follow-up time: 10.1 ± 7.5 months) were prospectively included. Following TMVR, left ventricular (LV) function remained unchanged (LV ejection fraction: 47.4 vs. 48.2%, $p=0.608$). Right ventricular (RV) function significantly improved (TAPSE: 17.1 vs. 18.2 mm, $p < 0.001$), alongside with a reduction in estimated pulmonary artery systolic pressure (PASP: 56.7 vs. 49.2 mm Hg, $p < 0.001$). Tricuspid regurgitation (TR) severity decreased after TMVR (TR \geq grade II: 52 vs. 39%, $p=0.023$). Furthermore, both left atrial (67.7 vs. 64.0 mm, $p=0.024$) and right atrial size (62.9 vs. 60.2 mm, $p=0.009$) declined. At baseline, patients presented with worse renal function (eGFR: 52.0 vs. 54.1 ml/min/1.73 m², $p=0.701$) and higher NT-proBNP serum levels (5875 vs. 4769 pg/mL, $p=0.219$), when compared to follow-up. NYHA functional status significantly improved (NYHA \geq III: 84 vs. 26%, $p=0.006$) after TMVR.

Conclusion: RV function significantly improved after TMVR, alongside with a reduction in estimated PASP and TR severity. In addition, a significant improvement in the clinical presentation was observed at 10 months follow-up.

8.5

Transcatheter versus surgical valve repair in patients with severe mitral regurgitation

M. Koschutnik¹, V. Dannenberg¹, C. Donà¹, C. Nitsche¹, A. Kammerlander¹, S. Koschatko¹, B. Mora², A. Bartunek², D. Wiedemann³, D. Zimpfer³, M. Hülsmann¹, M. Schneider¹, P. Bartko¹, G. Goliasch¹, C. Hengstenberg¹, J. Mascherbauer¹

¹Universitätsklinik für Innere Medizin II – Kardiologie, AKH Wien, Wien, Austria

²Universitätsklinik für Anästhesie – Herz-Thorax-Gefäßchirurgische Anästhesie und Intensivmedizin, AKH Wien, Wien, Austria

³Universitätsklinik für Herzchirurgie, AKH Wien, Wien, Austria

Introduction: Background. Transcatheter edge-to-edge mitral valve repair (TMVR) is increasingly performed, however, its efficacy in comparison with surgical MV treatment (SMV) is unknown.

Methods: Consecutive patients with severe mitral regurgitation (MR) undergoing TMVR (68 % functional, 32 % degenerative) or SMV (9 % functional, 91 % degenerative; 23 % MV replacement) were enrolled. To account for differences in baseline characteristics, propensity score-matching including age, EuroSCORE-II, left ventricular ejection fraction, and NT-proBNP was performed. A composite of heart failure (HF) hospitalization/death was defined as primary endpoint. Kaplan-Meier curves and Cox-regression analyses were used to investigate associations between baseline, imaging, and procedural parameters and outcome.

Results: Between July 2017 and April 2020, 245 patients were enrolled, of which 102 patients could be adequately

matched (73y/o, 61 % females, EuroSCORE-II: 5.7 %, $p > 0.05$ for all). Despite matching, TMVR patients were sicker at baseline (higher rates of prior myocardial infarction, coronary revascularization, pacemakers/defibrillators, and diabetes mellitus, $p < 0.009$ for all). Patients were followed for 28.3 ± 27.2 months, during which 27 events (17 deaths, 10 HF hospitalizations) occurred. Postprocedural MR reduction (MR grade < 2 : TMVR vs. SMV: 88 % vs. 94 %, $p = 0.487$) and freedom from HF hospitalization/death (log-rank: $p = 0.221$, Fig. 1) were similar at two years. By multivariable Cox analyses, EuroSCORE-II (adj. HR 1.07 [95 %CI: 1.00–1.13], $p = 0.027$) and postprocedural MR severity (adj. HR 1.85 [95 %CI: 1.17–2.92], $p = 0.009$) emerged as independent predictors of outcome.

Conclusion: In this propensity matched, all-comers cohort, 2-year outcomes after TMVR versus SMV were similar. Given the reported favorable long-term durability of TMVR, the interventional approach emerges as valuable alternative for a substantial number of patients with functional and degenerative MR at high/prohibitive surgical risk.

8.6

Low haemoglobin is associated with increased risk of complications in left atrial appendage closure patients

D. Zweiker¹, R. Sieghartsleitner¹, G. Toth¹, G. Stix², P. Vock³, A. Schratte⁴, L. Fiedler⁵, J. Aichinger⁶, C. Steinwender⁷, R. K. Binder⁸, F. Barbieri⁹, K. Ablasser¹, N. Verheyen¹, A. Zirlik¹, D. Scherr¹

¹Division of Cardiology, Medical University of Graz, Graz, Austria

²Division of Cardiology, Medical University of Vienna, Vienna, Austria

³Department of Internal Medicine III, Karl Landsteiner University Hospital St. Pölten, St. Pölten, Austria

⁴Department of Cardiology, Hospital North (Klinikum Floridsdorf), Vienna, Austria

⁵Department of Internal Medicine, Hospital Wiener Neustadt, Wiener Neustadt, Austria

⁶Department of Internal Medicine 2, Elisabethinen Hospital Linz, Linz, Austria

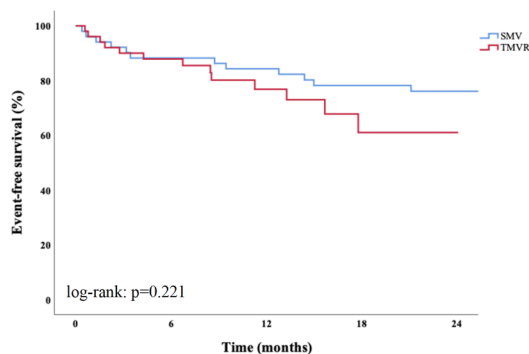
⁷Division of Cardiology, Kepler University Hospital Linz, Linz, Austria

⁸Department of Internal Medicine 2, Hospital Wels-Grieskirchen, Wels, Austria

⁹Division of Internal Medicine III, Medical University of Innsbruck, Innsbruck, Austria

Introduction: Left atrial appendage closure is associated with a relevant procedural complication rate. Baseline risk factors, such as pre-procedural lab results, may identify patients that develop acute complications.

Methods: We performed a retrospective analysis of the impact of baseline characteristics and preprocedural lab results on the acute procedural outcome in patients undergoing left atrial appendage closure from the Austrian Left Atrial Appendage Closure Registry between 2010 and 2019. The endpoint for procedural complications was defined as death, stroke, major bleeding, necessity for intensive care, other complications requiring invasive interventions or failure to implant the device. We also evaluated a modified endpoint with the exclusion of bleeding events. Logistic regression was performed using step-



Number at risk:	0	6	12	18	24
SMV:	51	45	43	40	39
TMVR:	51	45	41	38	38

Fig. 118.5 Kaplan-Meier estimators demonstrating differences in time to the primary composite endpoint (heart failure hospitalization/death) between surgical treatment (SMV) and transcatheter mitral valve repair (TMVR) in the matched study population ($n = 102$).

Table 118.6 Univariate and multivariate analysis for major procedural complications after left atrial appendage closure.
*: $p < 0.05$

Parameter	Univariate analysis			Multivariate analysis	
	Complications	No complications	P value	OR (95% CI)	P value
Age	76 (72–79)	75 (70–78)	0.233	1.02 (0.97–1.04)	0.544
LVEF <35 %	4.1 %	9.2 %	0.399	0.55 (0.08–2.07)	0.443
LVEF 35–50 %	18.4 %	16.2 %	0.680	1.01 (0.42–2.22)	0.985
eGFR (MDRD, ml/min)	75 (69–82)	75 (70–79)	0.500	1.02 (0.99–1.04)	0.119
Haemoglobin (g/dL)	11.9 ± 2.0	12.8 ± 2.0	0.005*	0.83 (0.70–0.97)	0.017*
History of intracerebral haemorrhage	8.2 %	23.6 %	0.013*	0.36 (0.10–0.96)	0.065
APTT	23 (30–36)	35 (31–41)	0.010*		
Liver disease	12.2 %	4.1 %	0.031*		
Aortic stenosis	4.1 %	0 %	0.023*		

wise approach (backward method with $p[\text{out}] = 0.1$) and forced inclusion of age, left-ventricular function and kidney function.

Results: A total of 320 consecutive patients from 9 centres with a median age of 75 years (36.6 % female) were included. Seventy-eight percent had a history of bleeding and 35 % had a history of stroke. Median CHA2DS2-VASc score was 5 (interquartile range, 3–5) and median HAS-BLED score was 3 (2–4). Procedural complications occurred in 15.3 % of cases. Low haemoglobin and low activated partial thromboplastin time were associated with an increased complication rate. Other significant baseline factors were liver disease, absence of intracranial haemorrhage and severe aortic stenosis. In multivariate analysis, low haemoglobin remained a significant predictor, even after adjustment for age, left-ventricular function and kidney function (Table). In the modified procedural complication endpoint excluding major bleeding events (14.1 %), low haemoglobin remained a significant predictor (haemoglobin 11.9 ± 2.0 vs. 12.8 ± 2.0 g/dL in patients with vs. without modified endpoint, $p = 0.013$). A baseline haemoglobin lower than 12 g/dL was present in 39.4 % and it increased relative risk of procedural complications by 89 % (21.4 vs. 11.3 % in patients with reduced vs. normal haemoglobin), and risk of complications without bleeding by 92 % (19.8 vs. 10.3 %).

Conclusion: Low baseline haemoglobin is independently associated with a higher complication rate after left appendage closure compared to patients with normal haemoglobin levels, even in a modified endpoint excluding bleeding and requirement for transfusion.

8.7

Right ventricular longitudinal strain on cardiovascular magnetic resonance imaging predicts outcome in patients undergoing transcatheter mitral valve repair

M. Koschutnik¹, C. Donà¹, C. Nitsche¹, V. Dannenberg¹, S. Koschatko¹, D. Beitzke², C. Loewe², M. Hülsmann¹, M. Schneider¹, P. Bartko¹, G. Goliash¹, C. Hengstenberg¹, A. Kammerlander¹, J. Mascherbauer¹

¹Universitätsklinik für Innere Medizin II – Kardiologie, AKH Wien, Wien, Austria

²Universitätsklinik für Radiologie und Nuklearmedizin – Kardiovaskuläre und Interventionelle Radiologie, AKH Wien, Wien, Austria

Introduction: The prognostic value of left and right ventricular global longitudinal strain (LV and RV GLS) derived from cardiovascular magnetic resonance (CMR) feature tracking in patients with severe mitral regurgitation (MR) undergoing transcatheter mitral valve repair (TMVR) is unknown.

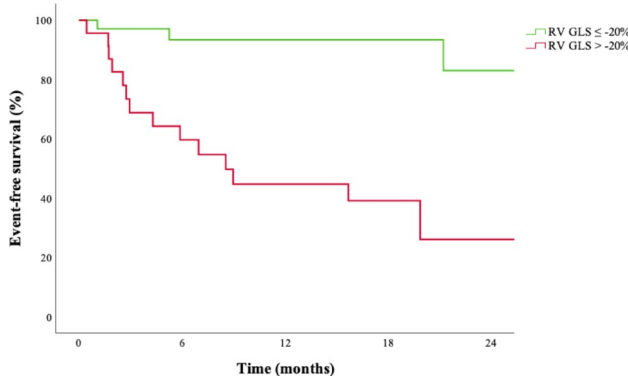


Fig. 118.7 Kaplan-Meier estimators demonstrating differences in time to the primary composite endpoint (heart failure hospitalization/death) stratified by right ventricular global longitudinal strain (RV GLS) on cardiovascular magnetic resonance (CMR) imaging (log-rank: < 0.001)

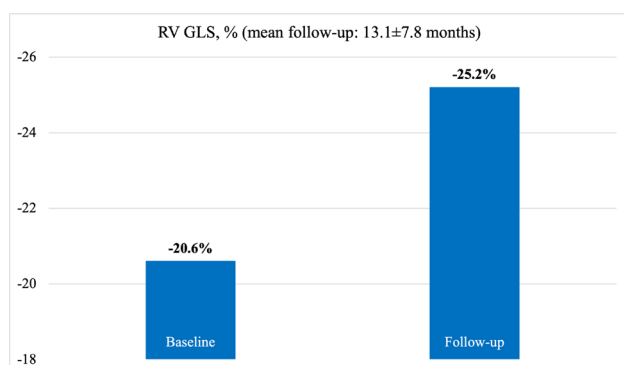


Fig. 218.7 Comparison between right ventricular global longitudinal strain (RV GLS) on cardiovascular magnetic resonance (CMR) imaging at baseline and after transcatheter mitral valve repair (TMVR; $n=21$, $p=0.016$)

Methods: Consecutive patients scheduled for TMVR underwent pre-procedural and follow-up CMR imaging including feature tracking strain analysis. Kaplan-Meier estimates and multivariate Cox-regression analyses were used to identify the prognostic impact of LV and RV GLS on CMR using a composite of heart failure hospitalization and death.

Results: A total of 62 patients (78.3 ± 7.0 y/o, 45 % female, EuroSCORE II: 9.7 ± 7.2 %) with severe MR underwent CMR prior to TMVR. 23 (37 %) patients presented with right ventricular dysfunction (RVD) defined by RV GLS >-20 % on CMR. At baseline, RVD was associated with NT-proBNP levels (9510 vs. 4064 pg/mL, $p=0.030$). On CMR, RVD was associated with reduced left and RV ejection fraction (LVEF: 39.2 vs. 48.7 %, $p=0.011$, RVEF: 35.1 vs. 46.7 %, $p<0.001$), as well as increased LV GLS (-14.0 vs. -19.5 %, $p=0.003$). A total of 18 events (12 deaths, 6 hospitalizations for heart failure) occurred during follow-up (mean 11.4 ± 9.1 months). While LV GLS was not significantly associated with outcome (HR 0.95 , 95 % CI: $0.90-1.01$, $p=0.082$), RV GLS showed a strong and independent association with event-free survival by multivariate Cox-regression analysis (adj. HR 0.91 , 95 % CI: $0.83-0.99$, $p=0.033$) after adjustment for relevant baseline and procedural data (EuroSCORE II, postprocedural residual MR), imaging parameters (TAPSE, LV and RVEF on CMR), and cardiac biomarkers (NT-proBNP). When compared with the “gold standard” RVEF on CMR (RVEF <45 %: adj. HR 0.86 , 95 % CI: $0.23-3.20$, $p=0.825$) and TAPSE on echo (TAPSE <17 mm: adj. HR: 2.77 , 95 % CI: $0.72-10.70$, $p=0.140$), only RVD (RV GLS >-20 %: adj. HR 5.05 , 95 % CI: $1.23-20.63$, $p=0.024$) was significantly associated with the composite endpoint (Fig. 1). Follow-up CMR was performed in 21 (34 %) patients. RV GLS significantly improved after TMVR (-20.6 to -25.2 %, $p=0.016$, Fig. 2).

Conclusion: RV rather than LV GLS, as determined on CMR, is an important predictor of outcome in patients undergoing TMVR. At 1 year follow-up, RV function significantly improved, and thus might add useful prognostic information on top of established risk factors.

8.8

Covered stents treatment for coronary artery aneurysms: a systematic review

M. Will¹, C. S. Kwok², T. Weiss¹, J. Mascherbauer¹, K. Schwarz¹

¹3. Medizinische Abteilung für Kardiologie, Universitätsklinikum Sankt Pölten, Sankt Pölten, Austria

²Department of Cardiology, Royal Stoke University Hospital, Stoke-on-Trent, UK, Stoke on Trent, United Kingdom

Objectives: To evaluate the current practice and outcomes of elective treatment of coronary aneurysms (CAA) using covered stents. Background: CAAs are reported in up to 5 % of patients undergoing coronary angiography. Treatment of CAAs with covered stents has been reported in several case reports, however, limited evidence supports the effectiveness and safety of this anecdotal interventional practice.

Methods: We conducted a systematic review of published case reports and case series of patients presenting with CAA that have been treated with covered stents in a non-emergency setting.

Results: A total of 63 case reports and 3 case series were included in the final analysis comprising data from 81 patients. The proportion of patients with arterial hypertension, history of smoking, diabetes and previous myocardial infarction were 59.3, 28.8, 15.3, and 34.4 %, respectively. The treated CAA was situated in a native coronary artery in 91.4 %, and in a saphenous vein graft in 8.6 %. The size of CAAs ranged from 7 to 60 mm diameter and 8 to 70 mm length. Procedural success was achieved in 95.1 %. The types of stents used were mainly polytetrafluoroethylene (75.3 %) and Papyrus (11.1 %). In 11.0 % of cases additional abluminal drug eluting stents (DES) and in 6.8 % additional adluminal DES were implanted. After a medium follow up of 6 months (range 1–84 months) overall MACE, mortality, myocardial infarction, stroke, stent thrombosis and target lesion revascularization were reported in 26.2, 0.0, 7.6, 0.0, 4.6 and 18.5 % of cases, respectively.

Conclusion: The use of covered stents for elective treatment of CAA appears to be safe and effective. Nevertheless, it is associated with increased MACE rates, which are driven mainly by higher target lesion revascularization. Further studies, particularly randomized trials and controlled registries, are warranted.

8.9

Rate, correlates, and outcomes of hemodynamic valve deterioration after transcatheter aortic valve replacement

C. Nitsche¹, D. Mutschlechner¹, L. Sinnhuber¹, M. Koschutnik¹, C. Dona¹, V. Dannenberg¹, A. Kammerlander¹, M. Winter¹, G. Goliash¹, C. Hengstenberg¹, J. Mascherbauer¹

¹Medical University of Vienna – AKH of Vienna – Cardiology Clinic, Wien, Austria

Objektives: Treatment expenditure of transcatheter aortic valve replacement (TAVR) to younger individuals may potentially be limited by valve durability. Long-term hemodynamic performance of transcatheter aortic valves is not well documented. This study sought to determine the incidence, predis-

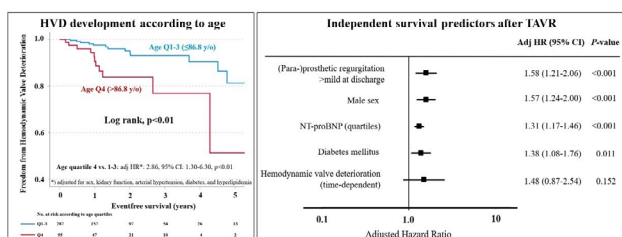


Fig. 118.9 Determinants and outcomes of hemodynamic valve deterioration (HVD) after transcatheter aortic valve replacement (TAVR). Rate, correlates, and outcomes of hemodynamic valve deterioration after transcatheter aortic valve replacement

posing factors and outcomes of hemodynamic valve deterioration (HVD) after TAVR.

Methods: Consecutive patients undergoing TAVR between May 2007 and December 2018 (67.0 % Sapien, 14.6 % Evolut, 6.8 % Acurate, 6.8 % Portico, 4.8 % other) were prospectively studied. Baseline assessment included echocardiography, laboratory, and clinical assessment. Echocardiographic and laboratory follow-up after TAVR was performed prior to discharge, at 3 and 12 months, and yearly thereafter. HVD was defined by Doppler assessment according to Valve Academic Research Consortium 3 criteria as a ≥ 10 mm Hg increase in mean gradient to ≥ 20 mm Hg OR worsening of (para-)prosthetic regurgitation $\geq 1/3$ class to \geq moderate. The primary endpoint was the incidence of HVD. All-cause mortality served as secondary endpoint. Multivariate cox regression was used for outcome analysis.

Results: 649 patients (82.2 ± 6.7 y/o, 55.5 % female, EuroSCORE II 4.4 ± 1.0) were analyzed. Among survivors with available echo data from ≥ 2 follow-ups ($n=382$), the incidence of HVD was 6.8 % ($n=26$; 4.1 % per valve-year), with no difference between valve types. Modes of HVD were stenosis ($n=8$), regurgitation ($n=14$), and both ($n=4$). Median time to HVD was 14.2 months (interquartile range, 9.4 to 35.0 months), and was significantly shorter in patients in the highest age quartile (Q4 vs. Q1-3: log-rank, $p < 0.01$, Fig. 1). Also, increased age was the only factor that independently predisposed for HVD (Q4 vs. Q1-3: adjusted hazard ratio [adj HR]: 2.86, 95 % confidence interval [CI]: 1.30-6.30, $p < 0.01$). Following TAVR, 355 patients (54.7 %) had died after 64.2 ± 31.9 months. Independent predictors of mortality were (para-)prosthetic regurgitation >mild at discharge (HR: 1.58, 95 % CI: 1.21-2.06, $p < 0.001$), male sex (HR: 1.57, 95 % CI: 1.24-2.00, $p < 0.001$), baseline NT-proBNP serum levels (graded into quartiles, HR: 1.31, 95 % CI: 1.17-1.46, $p < 0.001$), and diabetes (HR: 1.38, 95 % CI: 1.08-1.76, $p = 0.011$), but not time-dependent HVD ($p > 0.05$, Fig. 1).

Conclusion: This study reports good hemodynamic performance of transcatheter aortic valves up to 8 years following intervention. The incidence of HVD, which may develop over time-especially in the elderly-, is low and does not impact survival. Conversely, (para-)prosthetic regurgitation early after TAVR conveys detrimental prognostic implications and needs to be avoided-particularly in younger patients.

8.10

Cerebral protection in TAVR—can we do without? impact on stroke rate, length of hospital stay and 12-month mortality

C. Donà¹, M. Koschutnik¹, C. Nitsche¹, M. Winter¹, M. Mach², M. Andreas², P. Bartko¹, A. Kammerlander¹, G. Goliash¹, I. Lang¹, C. Hengstenberg¹, J. Mascherbauer¹

¹Medizinische Universität Wien – Innere Medizin II, Klinik für Kardiologie, Wien, Austria

²Medizinische Universität Wien – Chirurgie, Klinik für Herzchirurgie, Wien, Austria

Introduction: Stroke associated with transcatheter aortic valve replacement (TAVR) is a potentially devastating complication. Until recently, the Sentinel[®] Cerebral Protection System (CPS; Boston Scientific) has been the only commercially available device for mechanical prevention of TAVR-related stroke. However, its effectiveness is still undetermined.

Methods: Between January 2019 and August 2020 consecutive patients were randomly assigned to TAVR with or without Sentinel[®] in a 1:1 fashion. We defined as primary endpoint clinically detectable cerebrovascular events within 72 hours after TAVR, and as secondary endpoints LOS and 12-month mortality. Logistic and linear regression analyses were used to assess associations of Sentinel[®] use with endpoints.

Results: Of 411 patients (80 ± 7 y/o, 47.4 % female, EuroSCORE II 6.3 ± 5.9 %), Sentinel[®] was used in 213 (51.8 %), with both filters correctly deployed in 189 (46.0 %). 20 (4.9 %) cerebrovascular events were recorded, 10 (2.4 %) of which were disabling strokes. Sentinel[®] reduced cerebrovascular events in univariate analysis by 71 % (OR 0.29, 95 % CI 0.11-0.82; $p = 0.02$) and after multivariate adjustment by 75 % (adj. OR 0.25; 95 % CI 0.08-0.80; $p = 0.02$). Sentinel[®] use was also significantly associated with shorter LOS (8.4 ± 9.6 versus 6.7 ± 6.1 days; $p = 0.03$) and lower 12-month all-cause mortality (15.7 % versus 7.5 %, $p = 0.01$).

Conclusion: In the present prospective all-comers TAVR cohort, Sentinel[®] significantly 1) reduced cerebrovascular events, 2) shortened LOS, and 3) improved 12-month survival. These data promote the use of a CPS when implanting TAVR valves.

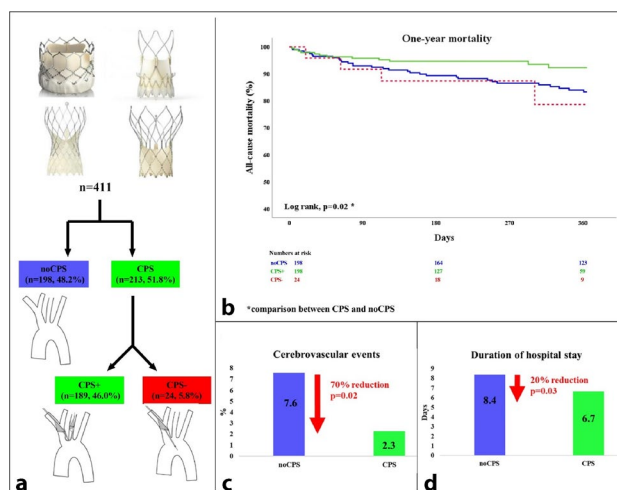


Fig. 118.10 Overview

8.11

Comprehensive Analysis of TMVRs

M. Bruckner¹, W. Mohl¹¹AVVie, Wien, Austria

Introduction: The first footsteps in Transcatheter Valve Technology was made with pulmonary valvuloplasty (1982) and mitral valvuloplasty (1984), followed by percutaneous aortic balloon valvuloplasty in 1986. Since then there was an immense evolving process in Transcatheter procedures. [1], [2], [3] Mitral Regurgitation (MR) is the second most frequent native valve disease [4], for example in the adult western population the prevalence of MR is 1.5–1.9%, up to 9.3% in patients older than 75 years. [5] The prevalence of significant MR leads to poorer survival, especially in elderly respectively comorbid patients. [6], [7], [8] Surgical repair yet is the first-line in therapy of MR, but patients with high surgical risk (advanced age, restricted left ventricular function and comorbidities) are not referred to open-heart surgery. [9] Especially in the last decade MR therapies were revolutionised by many different devices, so that these group of patients can get treated. The aim of this article is to show established MR transcatheter procedures, as well as newer developments.

Methods: To present a systematic overview about the current study situation on transcatheter mitral valve repair (TMVR), the clinical database “clinicaltrials.gov” was used. We used the keyword “mitral regurgitation” in the tab “condition or disease”. The search identified 436 studies. We included only 106 studies, which were based on TMVR.

Results: Showed current clinical evidence of TMVR devices, focussing there on edge-to-edge and chordal repair. We showed also the current aspects, what current studies are investigating and in which areas there are still gaps.

Conclusion: Due to the ageing population and the increasing number of associated comorbidities, the development of further minimally invasive products for mitral valve repair is of major importance. Advances in fluoroscopic and echocardiographic visualisation are also leading to increased safe and better use of these products. Nevertheless, one of the most important decision makers at present is the local “heart team”, which decides on the best possible therapy through a multidisciplinary group of specialists.

9 KARDIOLOGISCHES ASSISTENZ- UND PFLEGEPERSONAL

9.1

Generelle Herausforderungen in der Versorgung kardiologischer Patientinnen und Patienten während der COVID-19-Pandemie

J. Kappel¹, K. J. Wild¹¹KFN, Wien, Austria, Wien, Österreich

Einleitung: Die steigenden Zahlen der bereits mit COVID19 infizierten Personen und die damit verbundene Pflege, Betreuung beziehungsweise Versorgung dieser Menschen während und nach einer Sars-CoV2 Infektion stellt die Organisation

der betroffenen Abteilungen vor neue Herausforderungen, die durch strukturelle Veränderungen bewältigt werden müssen.

Methoden: Für die vorliegende Arbeit wurde eine systematische Literaturrecherche durchgeführt, um wissenschaftlich relevante Literatur zu finden. Das Ziel dieser Arbeit ist es, die neu aufgetretenen Herausforderungen, mit denen Gesundheits- und Krankenpflegerinnen und -pfleger aufgrund der COVID-19 Pandemie konfrontiert sind, aufzuzeigen.

Resultate: Die Ergebnisse zeigten, dass es zu verschiedenen Herausforderungen bei der Versorgung von isolierten Patientinnen und Patienten, die aufgrund ihrer Erkrankung eine invasive Blutdrucküberwachung (z. B.: einen arteriellen Zugang) oder eine nicht invasive Beatmung (z. B.: High-Flow Therapie oder CPAP-Therapie) benötigen, kommt. Aufgrund der Durchführung dieser Tätigkeiten unter strikten Sicherheitsmaßnahmen kommt es zu einem erhöhten Pflegeaufwand. Was wiederum dazu führt, dass diese Pflegetätigkeiten besonders bei isolierten Patientinnen und Patienten mehr Zeit in Anspruch nehmen als bei nicht-isolierten Patientinnen und Patienten.

Schlussfolgerungen: Es konnte aufgezeigt werden, dass sich Gesundheits- und Krankenpflegepersonen verschiedenen Herausforderungen, sowohl bei der Versorgung von kardiologischen Patientinnen und Patienten während einer COVID-19 Pandemie als auch persönlichen Herausforderungen und Belastungen stellen müssen.

10 KORONARE HERZKRANKHEIT – CHRONISCH

10.1

Predictive value of clinical parameters in relation to the effectiveness of therapy in anemic patients with chronic heart failure and chronic kidney disease

G. Tytova¹, O. Liepieieva², N. Ryndina¹¹Kharkiv National Medical University, Kharkiv, Ukraine²Kharkiv City Hospital #27, Kharkiv, Ukraine

Introduction: Anemia and renal dysfunction are common comorbid conditions associated with poor prognosis in patients with chronic heart failure (CHF).[1] Purpose: To analyze the predictive value of clinicoanamnestic indicators due to therapy effectiveness of anemia with CHF and CKD using an oral form of Fe(III)hydroxide complex polymaltose for optimization and providing an individual approach to every patient.

Materials and methods: 68 pts with CHF II-IV FC due to IHD and CKD II-III st. were examined. Among the causes of CKD were: chronic pyelonephritis in 50 pts, diabetic nephropathy in 18 pts. [2] All pts with CHF and CKD had anemia. Hb level was within 78–91 g/l. Diagnosis of anemia was determined by criteria of the Medical Committee of Standards of Hematology (ICST,1989). CHF FC was established by NYHA. Availability and stage of CKD was determined according to the National Kidney Foundation USA (NKF) K/DOQ classification. Pts with CHF and CKD were treated according to the standards.[3] Pts with anemic syndrome received Fe(III)hydroxide polymaltose complex 100 mg orally 1–2 times a day. Hb target level was within 110–120 g/l. The observation period was 3 months. Evaluation of prognostic properties was performed using non-uniform procedures Wald-Genkina. All signs were distributed by gradient with subsequent calculation of prognostic factors (PF) and the general informative features (I).

Results: To assess the prognostic value of clinicoanamnesic parameters, pts ($n=68$) that received Fe(III) hydroxide polymaltose complex, at the end of treatment were divided into 2 groups: a) with good antianemic effect ($n=50$)-achieved the target level of Hb;b) a satisfactory effect ($n=18$)-Hb levels approach to the target one. Very high informational content ($I \geq 6.0$) is given to the duration of CHF($I=9.55$), CHF FC ($I=8.03$),cardiac cachexia syndrome ($I=7.16$). High predictive value ($6.0 > I \geq 1.0$) to the severity of anemia ($I=5.88$),lower extremities edema and dyspnea ($I=5.60$), acute myocardial infarction ($I=1.94$),post-infarction left ventricular aneurysm ($I=2.82$),patient age ($I=2.50$),severity of CKD ($I=3.28$) and the presence of type 2 diabetes mellitus ($I=1.16$). Moderate predictor properties ($1.0 > I \geq 0.50$) identified in relation to BMI ($I=0.82$),history of stroke ($I=0.76$) and the presence of permanent atrial fibrillation ($I=0.50$).

Conclusion: Clinicoanamnesic indicators revealed a high predictive informational content about the effectiveness of therapeutic correction of anemia with CHF and CKD using an oral form of Fe(III)hydroxide polymaltose complex that allows to include them into predictive algorithms. Most informative criteria: the duration and severity of CHF, cardiac cachexia formation on a background of biventricular cardiac decompensation, progression of renal dysfunction, severity of anemia, which leads to the desirability and feasibility of application of these criteria at all levels of preventive and curative care with the aim of stratification effectiveness of treatment strategies.

11 PULMONALE HYPERTENSION

11.1

Cardiac amyloidosis—a significant blind spot of the H2FPEF score

F. Duca¹, S. Aschauer¹, R. Rettl¹, A. Snidat¹, C. Binder¹, H. Agis², R. Kain³, T. Dachs¹, C. Hengstenberg¹, R. Badr Eslam¹, D. Bonderman¹

¹Division of Cardiology, Department of Internal Medicine II, Medical University of Vienna, Wien, Austria

²Division of Oncology, Department of Internal Medicine I, Medical University of Vienna, Wien, Austria

³Clinical Institute of Pathology, Medical University of Vienna, Vienna, Wien, Austria

Introduction: Approximately half of all heart failure (HF) patients present with a preserved ejection fraction (HFpEF). However, correctly diagnosing HFpEF is challenging, even for experienced physicians. Therefore, Reddy and colleagues developed a score, consisting of clinical as well as echocardiographic parameters aiming to assess the probability of HFpEF in patients presenting with dyspnea. The score can be calculated in a categorical way [body mass index (BMI) $>30 \text{ kg/m}^2$ (yes/no), intake of ≥ 2 antihypertensive drugs (yes/no), presence of atrial fibrillation (yes/no), systolic pulmonary arterial pressure (sPAP) $>35 \text{ mm Hg}$ (yes/no), >60 years of age (yes/no), $E/E' > 9$ (yes/no); Fig. 1][1] resulting in scores between 0 and 9 points. Scores of 0–1 points are considered low and HFpEF can be ruled out. Patients in the intermediate score range (2–5 points) should be referred to further diagnostic testing. In patients with scores of 6–9 points HFpEF can be diagnosed with a high probability. Complicating the diagnostic work-up, it has been shown that a significant proportion of HFpEF patients suffer from cardiac amyloidosis (CA). We therefore aimed to investigate the applicability of the H2FPEF score in patients with HFpEF cardiac

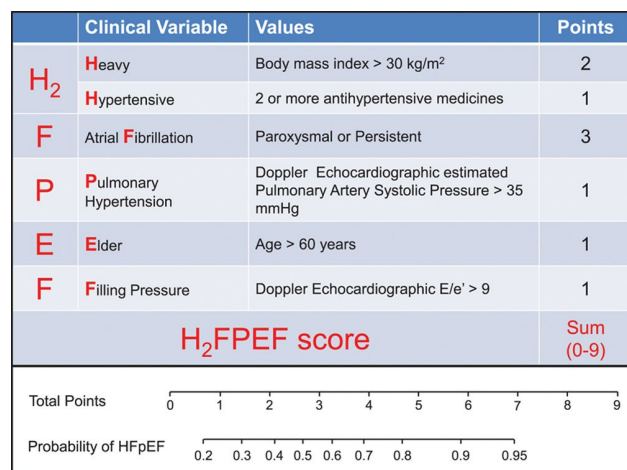


Fig. 1][1.1

transferrin (ATTR), as well as light chain (AL) amyloidosis and its accuracy in ruling in the correct diagnosis in HFpEF patients, as well as ruling it out in CA patients.

Methods: The presents study was performed within the framework of a prospective HF registry. HFpEF was diagnosed according to current guidelines by the European Society of Cardiology. ATTR CA was diagnosed in accordance with the diagnostic algorithm by Gillmore and co-workers. AL CA was diagnosed either with endomyocardial biopsy or in the case of extracardiac biopsy, cardiac involvement was determined according to current recommendations. In order to achieve the highest level of comparability between our study cohorts and the study cohort by Reddy et al. HFpEF patients without an invasive confirmation (pulmonary artery wedge pressure $<15 \text{ mm Hg}$) and CA patients with a left ventricular ejection fraction $>50\%$ were excluded from our study.

Results: Between December 2010 and October 2020, 685 patients (427 HFpEF, 258 CA) were included in our prospective registry, of whom 187 (100 HFpEF, 87 CA) were available for final analyses (Fig. 2). Categorical H2FPEF scores and respective parameters for HFpEF, ATTR and AL CA patients differed significantly between cohorts. The highest median H2FPEF score was found among our HFpEF cohort with 5.0 points, compared to ATTR CA with 4.0 points and AL CA with 3.0 points ($p < 0.001$). We could also detect differences with respect to H2FPEF score ranges (low: 0–1 points, medium: 2–5 points, high: 6–9 points). Albeit 29.4 % of the AL CA cohort were in the low score range, neither HFpEF nor ATTR CA patients were ($p < 0.001$, Fig. 2). The highest percentage of patients in the medium score range were found in the ATTR CA (94.3 %) cohort followed by HFpEF (80 %) and AL CA (67.9 %) patients ($p=0.006$). The remaining 20.0 % of HFpEF, 5.7 % of ATTR CA, and 2.9 % of AL CA patients ($p=0.007$) were in the high H2FPEF score ranges (Fig. 2). True positive rates of high-probability H2FPEF scores (6–9 points) in HFpEF, ATTR, and AL CA were 20.0 % (95 % CI: 12.7–29.2), 5.7 % (95 % CI: 1.2–15.7), and 29.4 % (95 % CI: 0.7–15.3), respectively. Contrary to HFpEF as well as ATTR CA patients in whom false negative rates of low-probability H2FPEF scores (0–1 points) were 0.0 % (95 % CI: 0.0–3.6) and 0.0 % (95 % CI: 0.0–6.7), FNR were as high as 29.4 % (95 % CI: 15.1–47.5) in the AL CA cohort.

Conclusion: Our study suggests H2FPEF scores should be used with caution in the diagnostic work-up of patients with preserved ejection fraction as on the one hand the majority of ATTR and AL CA patients are in the medium and high HFpEF probability range and on the other hand a significant proportion of AL CA patients would be ruled out from having HF.

H2FPEF score in patients with HFpEF and cardiac amyloidosis

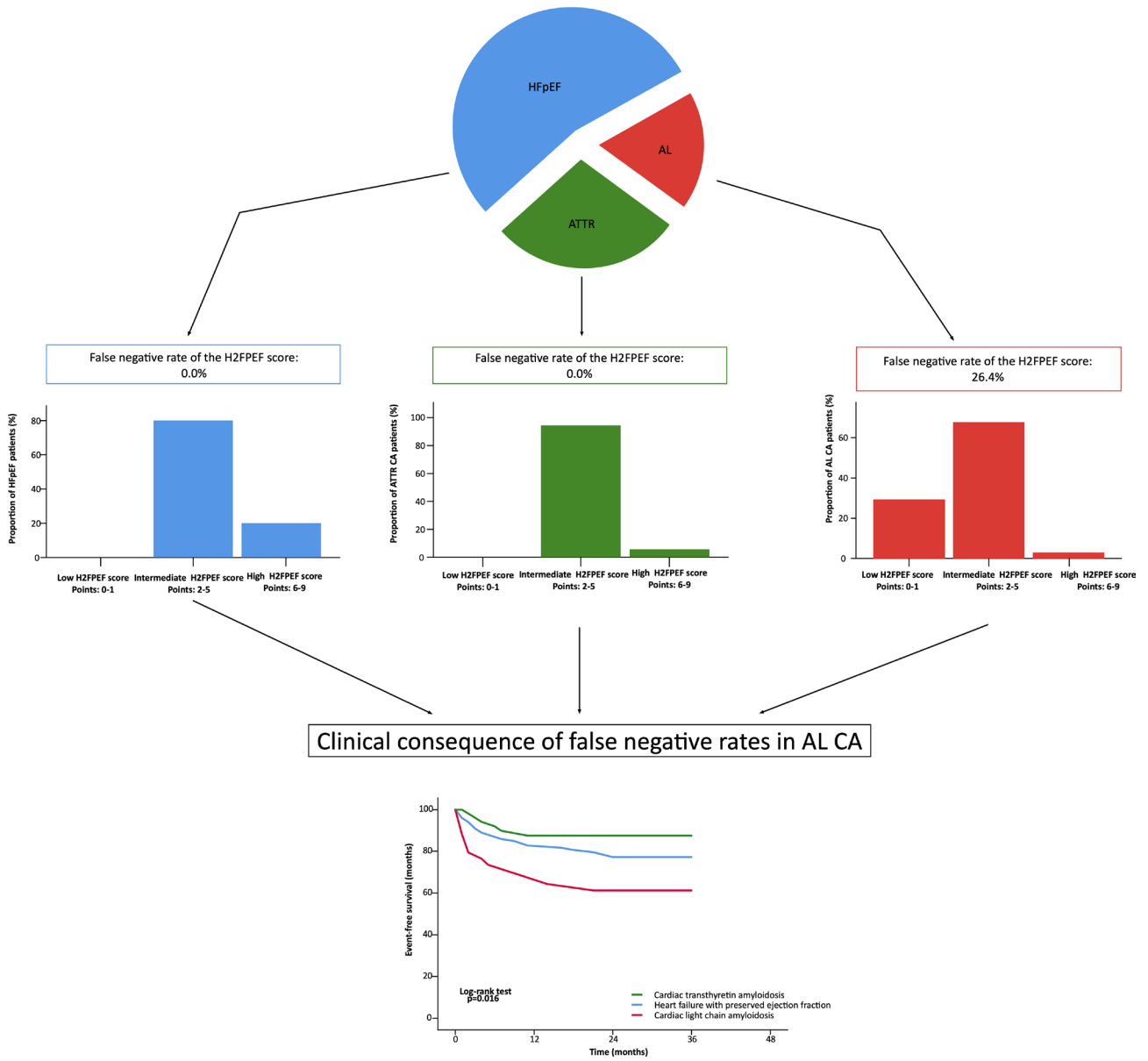


Fig. 2|11.1

12 RHYTHMOLOGIE

12.1

A new mapping tool for catheter ablation of persistent atrial fibrillation: high density mapping using a grid shaped catheter

F. Lukas¹, F.X. Roithinger², I. Roca-Luque³, F. Lorgat⁴, A. Roux⁵, J. Lacotte⁶, A. Miller⁷, D. Steven⁸

¹Landeskrankenhaus Wiener Neustadt, Wiener Neustadt, Austria

²2. Medizinische Abteilung Kardiologie/Nephrologie/Intensivmedizin, Wiener Neustadt, Austria

³Hospital Clínic de Barcelona · Arrhythmia Unit. ICCV, Barcelona, Spain

⁴Christiaan Barnard Memorial Hospital, Cape Town, South Africa

⁵SANTE REPUBLIQUE CENTRE, Clermont-Ferrand, France

⁶Institut Cardiovasculaire Paris Sud, Paris, France

⁷Abbott, Minneapolis, United States

⁸University hospital Köln, Cologne, Germany

Introduction: Catheter ablation (CA) of persistent atrial fibrillation (persAF) remains a challenge with respect to outcomes, and pulmonary vein isolation (PVI) is the cornerstone of interventional treatment. Thus far, mapping has mainly been performed using circular mapping catheters. We present the first registry data in patients undergoing CA for persAF using the novel grid shaped high density (HD) mapping catheter.

Methods: The novel Advisor™ HD Grid mapping catheter consists of four splines with four 1 mm equidistant electrodes mounted on each spline. The splines are attached at the tip to also maintain a fixed distance between the splines. The Advisor™ HD Grid mapping catheter was used to (1) assess the geometry (2) acquire electrical substrate information and (3) to assess pulmonary vein isolation. The aim of the registry was to evaluate procedural parameters as well as outcome with respect to freedom from AF during the follow-up

Results: The Advisor™ HD Grid mapping catheter was used in 333 PersAF ablation procedures (age: 64.1 yr, 76.0 % male, 25.2 % with history of AF ablation). A PVI approach was used in 93.1 % of all ablation procedures; ablation strategy was limited to only PVI in 197 (59.2 %) subjects. Ablation of the left atrial roof was performed in 66 (19.8 %) subjects, posterior wall isolation in 41 (12.3 %) subjects, targeting of CFE in 24 (7.2 %) subjects, and of isolation of fibrotic areas in 16 (4.8 %) subjects. The mean procedure duration was 134.4 ± 51.4 minutes with 14.5 ± 11.3 minutes of fluoroscopy use. An average of 9779.1 ± 8655.4 mapping points were collected in 12.5 ± 9.1 minutes per map. The procedure was considered successful in 98.8 % of cases (329). Peri-procedural adverse events were experienced in 4.4 % of subjects, with only 1 event considered related to the Advisor™ HD Grid mapping catheter.

Conclusion: CA procedures of persAF can safely be performed using the Advisor™ HD Grid mapping catheter. Left atrial substrate maps can be performed in relatively short time acquiring high resolution maps. Acute outcome results are comparable to other substrate-based approaches.

12.2

Very high-power short-duration (HPSD) ablation for pulmonary vein isolation—comparison of a 90 w 4 seconds approach to a HPSD-CLOSE strategy

S. Seidl¹, H. Pürerfellner¹, G. Kollias¹, M. Derndorfer¹, M. Meisinger², M. Martinek¹

¹Ordensklinikum Linz GmbH Elisabethinen, Linz, Austria

²Biosense Webster, Wien, Austria

Introduction: Circumferential pulmonary vein isolation (PVI) using radiofrequency ablation (RFA) is a standard of care intervention for patients with symptomatic atrial fibrillation (AF). During follow up a substantial amount of patients needs a redo procedure due to reconnections on the basis of insufficient ablation lesions. High-power short-duration ablation (HPSD) is expected to create efficient lesions while causing less complications. The aim of this study was to compare intraprocedural duration—a surrogate parameter for intraprocedural safety—as well as the complication rate of very HPSD (90 Watt, 4 sec) to a strategy using 50 W guided by the CLOSE-protocol using the Ablation Index (AI), an arbitrary unit composed of power, contact force and ablation time.

Methods: We retrospectively analyzed intraprocedural duration from 46 patients that were scheduled for first-do-PVI. A very HPSD ablation protocol with 90 W and a 4 second duration cut-off was compared to a HPSD-CLOSE approach (50 Watts; AI 550 at the anterior LA wall; AI 400 at the posterior LA wall, roof and floor) in terms of ablation time, left-atrial dwell time, fluoroscopy- and total procedure time and complication rate.

Results: As expected, the very HPSD group ($n=22$) showed significantly shorter ablation times (mean ablation time 8.3 min ± 4.1 min vs 23.2 min ± 10.0; $p < 0.001$) with non-significant trends of time-saving for the other measured parameters (mean left atrial dwell time 77 min ± 28.4 min vs 90 min ± 31.9 min; $p 0.162$; fluoroscopy-time 13.1 min ± 6.9 min vs 14.7 ± 11.7 min; $p 0.588$; total procedure time 112.7 min ± 30.1 min vs. 126.6 min ± 35.8 min; $p 0.167$). There was no significant difference concerning the complication rate (very HPSD group $n=2$: 1 × pseudoaneurysm with the need of thrombin-injection and 1 × pericardial tamponade requiring pericardial puncture; HPSD-CLOSE group $n=1$: pericardial tamponade requiring pericardial patch repair; $p=0.499$) compared to the HPSD-CLOSE approach.

Conclusion: Very high-power short-duration ablation (90 W, 4 sec) for PVI significantly shortens ablation times thereby reducing radiation exposure without significantly increasing the

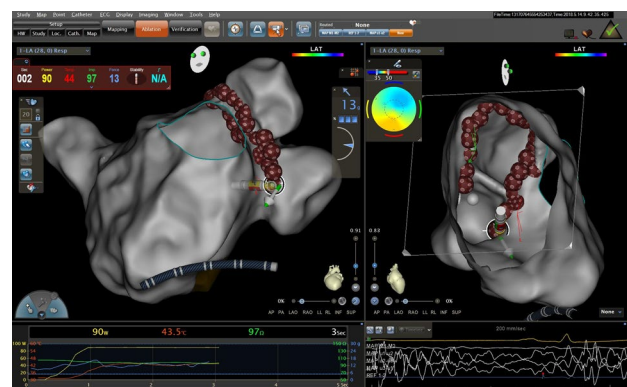


Fig. 112.2

rate of relevant intraprocedural complications. The clear trend of time-saving across other measured parameters (left atrial dwell time, total procedure time and fluoroscopy time) will most likely show significance with a raising number of cases in the future.

12.3

Unexpected turn in a thought to be crystal clear arrhythmia—a case for the FBI

S. Seidl¹, M. Martinek¹, M. Derndorfer¹, G. Kollias¹, H. Pürerfellner¹

¹Ordensklinikum Linz GmbH Elisabethinen, Linz, Austria

Introduction: An otherwise healthy woman at the age of 53 years presented at a regional hospital due to nausea and palpitations. As part of the initial work-up an electrocardiogram (ECG) was recorded, which showed a regular wide complex tachycardia of around 200 beats per minute (bpm). Because of hemodynamic instability an urgent electrocardioversion needed to be done. Afterwards the patient was transferred to our hospital for further diagnostic investigations. The basic clinical assessment (ECG, transthoracic echocardiogram, blood tests) were inconspicuous. Coronary artery disease could be ruled out by coronary computed tomography angiography (CCTA). In the complementary cardiac magnetic resonance imaging (MRI) signs of late enhancement could be found at the peak of the posteromedial papillary muscle. Taking everything together a scar related ventricular tachycardia was the most likely differential diagnosis. Prior to implantation of an implantable cardioverter-defibrillator (ICD) an antiarrhythmic medication (betablocker and class IC antiarrhythmic) was established and the patient was assigned for catheter ablation of ventricular tachycardia.

Methods: In expectation of a papillary muscle related ventricular tachycardia an intracardiac echocardiography (ICE) catheter was placed in the right atrium (RA), as were EP catheters in the apex of the right ventricle (RV) and the coronary sinus (CS). Under echocardiographic and fluoroscopic guidance a transeptal puncture was performed and a multipolar navigational diagnostic catheter (CARTO PENTARAY) was put forward into the left ventricle. Via programmed ventricular stimulation (PVS) non-decremental ventriculoatrial (VA) conduction with a short VA interval and the earliest atrial activation nearby the CS entrance could be detected. Shortly after atrial fibrillation (AF) with rapid ventricular response was triggered by ventricular extrastimulus testing (VET) and quickly degenerated into an almost regular wide complex tachycardia mirroring the initial ECG at the emergency admission. Persistence of the rhythm disorder after administration of an intravenous 10 mg

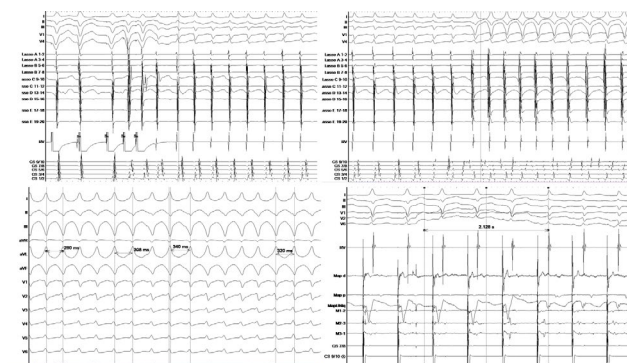


Fig. 1 | 12.3

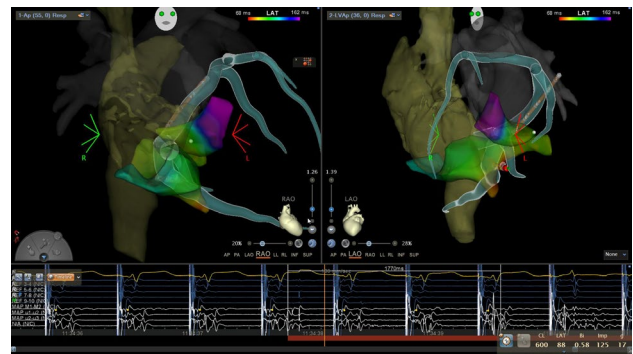


Fig. 2 | 12.3

Adenosin bolus-injection accompanying maximum pre-excitation proved the concept of an FBI tachycardia—the combination of atrial fibrillation and a malignant accessory pathway. Immediately prior planned electrocardioversion the rhythm disorder stop spontaneously. Thereafter the accessory pathway could be located at the entrance from the middle cardiac vein where it was successfully treated by temperature guided radiofrequency ablation. Preinterventional imaging served as a valuable tool to delineate CS anatomy and branches.

Results: So far the patient's follow-up is unremarkable. The ICD implantation procedure was canceled as was the antiarrhythmic medication.

12.4

Long-term follow-up data reveal the micra™ leadless cardiac pacemaker to be a safe therapeutic option for octo- and nonagenarians

J. Maier¹, H. Blessberger¹, D. Kiblböck¹, J. Bötscher¹, J. Ebner¹, K. Saleh¹, A. Nahler¹, M. Savci¹, A. Fellner¹, C. Reiter¹, T. Lambert¹, C. Steinwender¹

¹Department of Cardiology, Kepler University Hospital, Medical Faculty, Johannes Kepler University, Linz, Austria

Introduction: In an aging population with increasing life expectancy, safe treatment options for octo- and nonagenarians in need of cardiac pacing are becoming increasingly relevant. While conventional pacemaker implantations have been shown to be safe for the elderly, the rate of complications is higher than after leadless cardiac pacemaker (LCP) implantation. In the elderly, the occurrence of peri-procedural complications has been demonstrated to be an important predictor of post-implant death. Large post-approval registry studies have proven the Micra™ to be a safe option for a younger (75 years-old, on average) population. This study is the first to provide long-term data for nonagenarians who received an LCP and offers a comparison to long-term octogenarian and younger patient data.

Methods: 283 patients who received a Micra™ LCP at our department between 12/2013 and 07/2020, were included in this retrospective data analysis. Patients were grouped according to their age at the date of implantation (90+, n = 19; 80-90, n = 134; <80-year-olds, n = 130). Categorical variables are given as frequencies and percentages and group comparisons conducted with Pearson's chi-square test. Post-hoc multiple comparisons were done with the chi-square test and Bonferroni correction was applied. Continuous variables are presented as mean values (±SD) when normally distributed or medians (with IQR) and compared with the Kruskal-Wallis test. Multiple testing was

performed with the Mann-Whitney U test and Bonferroni corrected. Survival analyses were conducted with Kaplan-Meier curves and the log-rank test was employed to test for differences between groups. Cox regression analyses were performed to determine predictors of all-cause death in the investigated population. For a subanalysis, patients were matched concerning sex and comorbidities, employing a modified r2-cha2ds2-vasc score. Except for post-hoc analyses where Bonferroni correction was applied and the value lowered accordingly, *p*-values <0.05 were considered statistically significant.

Results: The median age of patients was 80.00 years (76.00–85.00; for nonagenarians: 91.00 [90.00–93.00], octogenarians: 84.00 [82.00–86.00] and younger patients: 76.00 [71.75–77.25]). The median length of follow-up was 25.00 (13.25–47.00) months. Complications were rare (*n* = 12, 4.24 %, with no significant differences between groups). In the nonagenarian group, BMI was significantly decreased and oral anticoagulant use significantly increased compared to the other groups. Interestingly, while the Charlson Comorbidity Index (CCI) significantly differed between the groups, a modified CCI without the variable age, yielded no significant differences. To further investigate the influence of age on outcomes, we matched the nonagenarians according to sex and comorbidities (determined with a modified r2cha2ds2-vasc score) 1:1 with patients from the other groups. Kaplan-Meier analyses revealed significant differences in all-cause (log-rank: *p* = 0.009) but not cardiovascular mortality (*p* = 0.84) between the groups. Similar results were seen in the full, unmatched, patient cohort. Cox regression analyses demonstrated age (HR: 1.34, *p* = 0.003) and NT-pro BNP concentrations (HR: 1.0002, *p* = 0.031) to be the most relevant predictors of all-cause death. No significant differences between the groups were found in periprocedural and device-related parameters.

Conclusion: Taken together with previous findings, LCP are a viable alternative to conventional pacemakers for octo- and nonagenarians in need of pacing. The low rates of complications and severe adverse device effects associated with the Micra™ LCP pacemaker render it an enticing treatment option for octo- and nonagenarians.

12.5

Long-term electrical performance of the Micra™ leadless cardiac pacemaker

J. Ebner¹, D. Kiblböck¹, J. Bötscher¹, J. Maier¹, J. Kellermair¹, C. Reiter¹, K. Saleh¹, J. Kammler¹, A. Fellner¹, T. Lambert¹, C. Steinwender¹, H. Blessberger¹

¹Department of Cardiology, Kepler University Hospital, Medical Faculty, Johannes Kepler University, Linz, Austria

Background: Leadless cardiac pacemakers (LCPs) have become an established treatment option for patients with an indication for single chamber pacing since 2013, when the first in men implantation of a Micra™ was performed. AV-synchronous pacing has become a new therapeutic option with the Micra™ AV LCP. Whereas short- and mid-term stability of electrical device parameters and battery voltage of the Micra™ system have already been confirmed, long-term data are still limited.

Methods: In this retrospective analysis we included all patients with a Micra™ LCP implanted at our center since December 2013. We analyzed electrical device parameters over time that were assessed during routine follow-up visits at our outpatient clinic (pacing threshold, sensing, impedance, battery voltage and proportion of ventricular pacing after 3, 12, 24, 36, 48, and 60 months, respectively). A descriptive statistical analysis and a regression analysis were performed.

Results: Since 2013 a Micra™ LCP was implanted in 283 patients (age [mean ± SD]: 79.2 ± 9.6 years, female: 36.4 %, CHA2DS2-Vasc [median, IQR] (4; 3–5) at our center. The most frequent indications for pacing were atrial fibrillation with slow AV conduction (41.3 %), third degree AV-block (30.4 %) and sick sinus syndrome (14.5 %), respectively. Overall implantation success rate was 99.3 % and 73.1 % of pacemakers were implanted in a septal position. During a median follow-up of 25 months (IQR 14–47) battery voltage and impedance decreased

Table 1|12.5

Time point	Baseline	3 Months	12 Months	24 Months	36 Months	48 Months	60 Months
n	273	218	158	118	76	48	14
Battery Voltage (V) Mean ± SD	not measured	3.11 ± 0.04	3.02 ± 0.25	3.01 ± 0.02	3.00 ± 0.03	3.0 ± 0.02	2.99 ± 0.01
Proportion of Pacing (%)							
Median	not measured	42.3	54.5	62.7	90.7	85.2	95.9
IQR		(6.0–93.2)	(11.1–95.3)	(8.5–96.5)	(35.4–97.4)	(33.0–99.4)	(30.2–99.4)
Sensing (mV)	10.67 ±	13.76 ±	13.95 ±	14.27 ±	14.60 ±	14.27 ±	14.01 ±
Mean ± SD	4.74	4.90	5.15	5.20	4.58	4.91	5.23
Impedance (Ω)	773.72 ±	588.67 ±	563.05 ±	543.9 ±	535.6 ±	538.33 ±	521.4 ±
Mean ± SD	234.27	125.71	108.34	93.91	87.13	89.89	82.0
Pacing Threshold (V)	0.53 ±	0.54 ±	0.59 ±	0.58 ±	0.57 ±	0.57 ±	0.59 ±
Mean ± SD	0.31	0.38	0.31	0.27	0.22	0.20	0.27

Table 2|12.5

Parameter	Regression Coefficient	95 % Confidence Interval	p-value
Battery Voltage (V)	−0.003 V/month	−0.003 to −0.003	<i>p</i> < 0.001
Proportion of Pacing (%)	+0.17 %/month	+0.07 to +0.26	<i>p</i> < 0.001
Sensing (mV)	+0.05 mV/month	+0.03 to +0.07	<i>p</i> < 0.001
Impedance (Ω)	−4.55 Ω/month	−5.24 to −3.87	<i>p</i> < 0.001
Pacing Threshold (V)	+0.001 V/month	+0.03 to +0.07	<i>p</i> = 0.095

significantly ($p < 0.001$), while sensing and the proportion of pacing showed a significant increase ($p < 0.001$). Pacing threshold remained stable over the follow-up period ($p = 0.095$) (see Table 1 and 2). The median percentage of ventricular pacing varied between 42.3 % and 95.9 %. The complication rate at implantation procedure was 4.2 % and pacemaker dysfunction was detected in 1.4 % of patients (increase in pacing threshold $n = 2$, pacemaker induced cardiomyopathy $n = 1$, sensing defect $n = 1$) during follow-up. The mortality of the Micra™ LCP population was 21.2 % during the follow-up period.

Conclusion: Electrical parameters were stable in Micra™ over a median follow-up of 25 months, except for the expected small decline in battery voltage. However, prospective studies have to prove its performance in the long-term.

12.6

Mid-term outcome after ablation of paroxysmal and persistent atrial fibrillation using the close protocol

F. Gallob¹, U. Rohrer¹, M. Manninger¹, D. Jenny¹, E. Bisping¹, T. Geczy¹, P. Lercher¹, G. Prenner¹, M. Sereinigg¹, D. Zweiker¹, L. Andrecs¹, B. Prati¹, S. Trummer¹, A. Zirlik¹, D. Scherr¹

¹Medizinische Universität Graz, Graz, Austria

Introduction: Catheter ablation of atrial fibrillation is (AF) an established second line therapy for patients with symptomatic paroxysmal (PAF) and persistent AF (persAF). The novel ablation tool Ablation Index (AI) combines information of contact force sensing, stability and energy output monitoring to predict lesion formation. Standardisation of inter-lesion distance (ILD) and differential AI threshold for the anterior and posterior wall within the CLOSE protocol have shown to increase procedural outcome in single centre studies. We aimed to describe mid-term outcome of CLOSE protocol guided ablation.

Methods: 324 consecutive patients (233 PAF and 91 persAF) underwent pulmonary vein isolation (PVI) using a contact force sensing catheter targeting an ILD ≤ 6 mm and AI ≥ 380 at the posterior and ≥ 500 at the anterior wall.

Results: Mean age was 60 ± 10 years, 30 % were female, mean BMI was 27 ± 4 kg/m², median CHA2DS2-VASc Score 1 (0;6), median HAS-BLED Score 1 (0;3), history of AF was 27 (2;444) months, mean left ventricular ejection fraction was

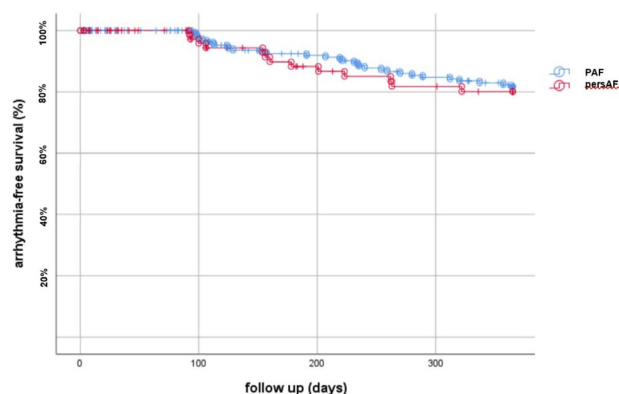


Fig. 112.6 Arrhythmia-free survival in patients with paroxysmal (PAF) and persistent atrial fibrillation (persAF) after CLOSE-guided PVI

58 ± 8 %. 37 % of PAF and 24 % of persAF patients had additional ablation of typical right atrial flutter ($p = 0.034$). Age (59 ± 11 years in PAF patients vs. 60 ± 10 years in persAF patients, $p = n.s.$), gender distribution (32 % vs. 24 % females, $p = n.s.$), CHA2DS2-VASc score (1 [0;6] vs. 2 [0;6], $p = n.s.$), HAS-BLED score (1 [0;3] vs. 1 [0;2], $p = n.s.$) and AF duration (28 [2;444] vs. 24 [2;204] months, $p = n.s.$) did not differ between both groups. Patients with PAF had lower BMI (27 ± 4 kg/m² vs. 28 ± 5 kg/m², $p < 0.05$), and higher left ventricular ejection fraction (60 ± 7 vs. 55 ± 9 %, $p < 0.001$). Primary success rate to meet CLOSE protocol criteria as well as pulmonary vein isolation was achieved in all patients. 201/233 PAF (86 %) and 78/91 persAF (86 %, $p = n.s.$) patients were arrhythmia-free after the first procedure, while 32 patients with PAF and 8 patients in persAF underwent a re-do procedure during the mean follow up duration of 298 ± 99 days. The arrhythmia-free survival did not differ between both groups (logrank $p = 0.7$, Fig. 1). There were no procedure-related complications or complications during follow-up.

Conclusion: Strict application of criteria for contiguity and ablation index using the CLOSE protocol is safe and results in a high success rate after PVI. A randomized controlled multicentre trial is needed to compare outcome to conventional PVI approaches.

12.7

Causes of death after Micra™ leadless cardiac pacemaker implantation: a single centre, long-term experience

J. Maier¹, H. Blessberger¹, J. Bötscher¹, J. Ebner¹, K. Saleh¹, S. Schwarz¹, A. Fellner¹, M. Savci¹, S. Rechberger¹, T. Lambert¹, C. Steinwender¹, D. Kiblböck¹

¹Department of Cardiology, Kepler University Hospital, Medical Faculty, Johannes Kepler University, Linz, Austria

Introduction: Due to the decreased complication rate compared to conventional cardiac pacemaker implantation, leadless cardiac pacemakers (LCP) have become an important clinical alternative during the last decade. Long-term follow-up data of Micra™ LCPs revealed high success and low peri-procedural complication rates. This study aims to investigate and describe the major causes of death in a long-term follow-up cohort of patients who received a Micra™ pacemaker.

Methods: 283 patients who received a Micra™ LCP at our department, between 12/2013 and 07/2020, were included in this retrospective data analysis. Follow-up was conducted 3 and 12 months post-implant and yearly afterwards. Patients were grouped in alive and deceased. Categorical variables are given as frequencies and percentages and group comparisons conducted with Pearson's chi-square test. Continuous variables are presented as mean values (\pm SD) when normally distributed or medians (with IQR) and compared with the Mann-Whitney U test. During a median follow-up of 25 (13.25–47.00) months, 60 (21.20 %) patients died. The median time to death was 19.50 (11.25–35.00) months. Statistical analyses were performed with R Studio Version 01.02.5003 (R Studio Inc., Boston, Massachusetts) and SPSS Statistics version 26.0 (IBM, Armonk, New York). P-values < 0.05 were considered statistically significant.

Results: While deceased patients were on average older than alive patients, the difference was not statistically significant (84.00 years [77.25–87.00] vs. 79.00 [76.00–84.00], $p = 0.09$). 19 (31.67 %) of the deceased died due to a cardiovascular event (12 due to heart failure, 2 to myocardial infarction, 5 to cardio-respiratory failure).

6 (10 %) succumbed to cancer and another 6 patients died due to marasmus senilis. 4 (6.67 %) patients' cause of death was renal failure. 5 (8.33 %) died to pulmonary geneses, 3 (5 %) to neurological events or infections, respectively. One died of trauma and for 13(21.67 %) patients the cause of death could not be determined. The deceased cohort suffered more frequently from atrial fibrillation at the time of the index procedure ($p=0.025$). In addition, patients who later died had a prolonged length of hospital stay compared to the other group (median 3.00 [2.00–5.75] vs. 2.00 [1.00–4.00] days, $p=0.006$). Deceased patients had a significantly decreased ejection fraction (55.00 [50.00–60.00] vs. 60.00 % [55.00–65.00], $p=0.005$), a higher incidence of coronary artery disease (46.67 % vs. 30.49 %, $p=0.019$) and increased NT-pro BNP concentrations (3950.50 [1146.75–5307.75] vs. 1093.00 pg/ml [545.00–2613.50], $p < 0.001$). In addition, the renal function of patients who died was significantly worse ($p < 0.001$). No significant group differences were found concerning the rate of complications and device related parameters.

Conclusion: The main causes of death after Micra™ implantation in our cohort were cardiovascular events unrelated to periprocedural events, followed by cancer and marasmus senilis. This distribution appears to be in line with the main causes of death of the elderly in general, who constitute the main patient population receiving an LCP.

12.8

Ertugliflozin to reduce arrhythmic burden in ICD/CRT patients (ERASe-Trial) – a phase III study

D. von Lewinski¹, N.J. Tripolt², H. Sourij², A. Oulhaj³, H. Alber⁴, M. Gwechenberger⁵, M. Martinek⁶, M. Nürnberg⁷, F.X. Roithinger⁸, C. Steinwender⁹, M. Stühlinger¹⁰, U. Rohrer¹, M. Manninger-Wünscher¹, D. Scherr¹

¹Abteilung für Kardiologie, Medizinische Universität Graz, Graz, Austria

²Medical University of Graz, Department of Internal Medicine, Division of Endocrinology and Diabetology, Graz, Austria

³College of Medicine and Health Sciences, United Arab Emirates University, United Arab Emirates, Al-Ain, United Arab Emirates

⁴Klinikum Klagenfurt, Abteilung für Innere Medizin und Kardiologie, Klagenfurt, Austria

⁵Medical University of Vienna, Department of Cardiology, Wien, Austria

⁶Ordensklinikum Linz Elisabethinen, Innere Medizin 2 mit Kardiologie, Angiologie und Intensivmedizin, Linz, Austria

⁷Klinik Ottakring, Abteilung für Kardiologie, Wien, Wien, Austria

⁸Landesklinikum Wiener Neustadt, Abteilung für Innere Medizin, Kardiologie und Nephrologie, Wiener Neustadt, Austria

⁹Kepler University Hospital Linz, Department of Cardiology and Intensive Care Medicine, Linz, Austria

¹⁰Medical University of Innsbruck, Univ. Clinic of Internal Medicine III/Cardiology and Angiology, Innsbruck, Austria

Background and aim: Sodium glucose cotransporter 2 (SGLT2) have proven profound positive effects in heart failure with reduced ejection fraction (HFrEF). These effects are independent from the presence of diabetes. Since SGLT2 receptors are not expressed in human myocardium, these cardioprotective effects be indirect or pleiotropic. Besides metabolic effects anti-inflammatory anti-fibrotic properties are discussed. Despite a strong correlation of ventricular arrhythmias with

HFrEF, the impact of ertugliflozin on the arrhythmic burden has not been investigated, yet. Therefore, the Ertugliflozin to Reduce Arrhythmic burden in ICD/CRT patients (ERASe) trial was designed to investigate the efficacy and safety of ertugliflozin in diabetic and non-diabetic HFrEF patients.

Methods: Within a multicentre, national, randomized, double-blind, placebo-controlled, phase 3b trial we aim to enrol a total of 402 patients across Austria. Patients with HFrEF or HFmrEF and ICD±CRT therapy >3 months and previous ventricular tachycardia (at least 10 documented non-sustained VT episodes within the last 12 months) are randomized in a 1:1 ratio to ertugliflozin (5 mg once daily orally administered) or matching placebo. The primary endpoint of the ERASe trial is to investigate the impact of Ertugliflozin on total burden of ventricular arrhythmias. Further objectives will be the number of therapeutic interventions of implanted devices, atrial fibrillation, heart failure biomarker and changes in physical function quality of life, stress and anxiety.

Results: 1:

Conclusion: The ERASe trial will be the first trial to test ertugliflozin in heart failure patients with non-preserved ejection fraction and ongoing ICD/CRT therapy regardless of their diabetic status. The ERASe trial may therefore extend the concept of SGLT2 inhibition to improve cardiac reverse remodeling, including reduced arrhythmic burden.

12.9

Fluoroscopy use during different arial fibrillation ablation

M. Manninger¹, U. Rohrer¹, K. Hartmann¹, T. Geczy¹, E. Bisping¹, P. Lercher¹, G. Prenner¹, M. Sereinigg², B. Prati¹, S. Trummer¹, L. Andrecs¹, D. Zweiker¹, A. Zirlik¹, D. Scherr¹

¹Abteilung für Kardiologie, Universitätsklinik für Innere Medizin, Medizinische Universität Graz, Graz, Austria

²Abteilung für Transplantationschirurgie, Universitätsklinik für Chirurgie, Medizinische Universität Graz, Graz, Austria

Introduction: Catheter ablation of atrial fibrillation is (AF) an established therapy for patients with symptomatic paroxysmal (PAF) and persistent AF (persAF). The cornerstone of AF ablation is pulmonary vein isolation (PVI), which can be achieved by different techniques including radiofrequency (RF) and cryoablation. It has been previously demonstrated that procedure times using single shot devices such as cryo-balloons are shortened. We aimed to test, whether radiation exposure differed between both ablation techniques.

Methods: We reviewed retrospectively procedural data from first ablation of AF with PVI only using RF and cryoablation. Primary endpoints were fluoroscopy time and dose area product.

Results: A total of 242 patients underwent PVI only, 54 patients underwent cryoablation (93 % PAF, 7 % pers AF) and 188 patients (63 % PAF, 31 % persAF, $p=0.03$) underwent RF ablation. Age (61 ± 11 in Cryo vs. 59 ± 10 years in RF), female gender (37 vs. 31 %), BMI (27 ± 6 vs. 28 ± 4 kg/m²), left ventricular ejection fraction (59 ± 4 vs. 59 ± 8 %), AF duration (36 (IQR 60) vs. 24 (IQR 57) months), rate of diabetes mellitus (4 vs. 6 %) and arterial hypertension (56 vs. 53 %) were comparable between both groups. Fluoroscopy times were significantly longer when using cryo ablation (1632 ± 568 vs. 1142 ± 1034 s, $p=0.02$) while dose area product was comparable (57 (IQR 87) vs. 56 (IQR 73) Gycm²).

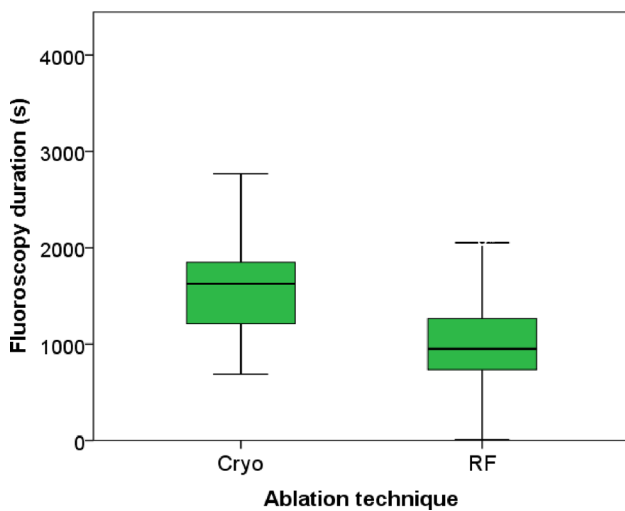


Fig. 1112.9 Fluoroscopy times using radiofrequency (RF) and cryo ablation

Conclusion: Shorter procedure durations come at the price of greater radiation exposure during cryo ablation. Single shot devices using electroanatomic mapping systems may overcome this limitation.

12.10

Initial experience with very high-power short duration ablation for atrial fibrillation

M. Manninger¹, T. Geczy¹, U. Rohrer¹, E. Bisping¹, P. Lercher¹, G. Prenner¹, M. Sereinigg², B. Pratl¹, S. Trummer¹, L. Andrecs¹, D. Zweiker¹, A. Zirlik¹, D. Scherr¹

¹Abteilung für Kardiologie, Universitätsklinik für Innere Medizin, Medizinische Universität Graz, Graz, Austria
²Abteilung für Transplantationschirurgie, Universitätsklinik für Chirurgie, Medizinische Universität Graz, Graz, Austria

Introduction: Catheter ablation of atrial fibrillation (AF) is an established therapy for patients with symptomatic paroxysmal (PAF) and persistent AF (persAF). Novel catheters using thermocouples to regulate irrigation during ablation allow safe radiofrequency application with very high power during pul-

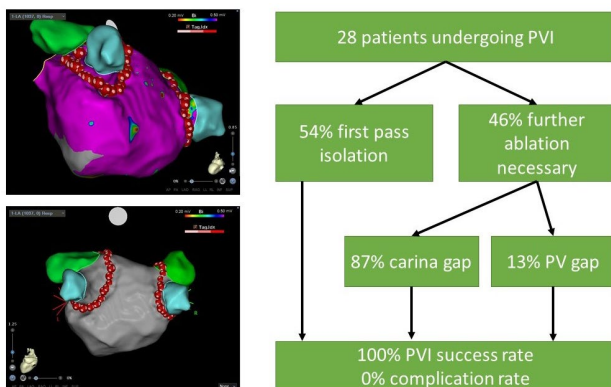


Fig. 1112.10 Left panels, map and voltage map of left atrium with ablation lesions. Right panels, procedural success rates

monary vein isolation (PVI). Real life procedural data using these novel technologies is scarce.

Methods: We report a single centre experience of the first 28 consecutive patients undergoing PVI using QMODE+ (90 W, 4s) by three different operators. Target inter-lesion distance was 6 mm on the posterior wall and 4–5 mm on the anterior wall. Pulmonary vein entrance and exit block were checked after 20 min waiting time. In case of documented typical right atrial flutter, ablation of the cavotricuspid isthmus (CTI) was performed in the same session using the CLOSE protocol (target ablation index 500, inter-lesion distance ≤6 mm).

Results: Mean age was 61 ± 10 years, 32 % were female, median CHA2DS2-VASc Score 2 (0, 5), 50 % of patients had PAF, 43 % had persAF and 7 % longstanding persAF. Concomitant ablation of typical atrial flutter was performed in 36 % of patients. Primary success rate to meet pulmonary vein isolation was achieved in all patients. First pass isolation was achieved in 54 % of patients. 87 % of patients without first pass isolation required ablation of either the left (33 %) or right (66 %) carina. Mean procedure time was 1:12 h in case of PVI only and 1:39 h in case of PVI+CTI ablation. Mean radiofrequency time was 4:32 min. There were no procedure-related complications.

Conclusion: Very high-power short duration ablation using QMODE+ is safe and allows quick PVI. However, further ablation of the carina is often necessary which might be overcome by peanut-shaped ablation lines.

12.11

Early recurrences after atrial fibrillation ablation—insights from the TeleCheck-AF Study

M. Manninger¹, L. Andrecs¹, S. Trummer¹, U. Rohrer¹, B. Pratl¹, J. Hendriks², N. Pluymaekers³, D. Linz³, A. Zirlik¹, D. Scherr¹

¹Abteilung für Kardiologie, Universitätsklinik für Innere Medizin, Medizinische Universität Graz, Graz, Austria
²Centre for Heart Rhythm Disorders, University of Adelaide and Royal Adelaide Hospital, Adelaide, Australia
³Department of Cardiology, Maastricht University Medical Centre and Cardiovascular Research Institute Maastricht, Maastricht, Netherlands

Introduction: Recently, multiple widely available wearable devices have been developed that can assess heart rate and rhythm using photoplethysmography (PPG). We previously implemented a remote on-demand mobile health (mHealth) infrastructure based on a mobile phone app using photoplethysmography (PPG) technology allowing monitoring of patients with atrial fibrillation (AF). Catheter ablation of AF is an established therapy for patients with symptomatic paroxysmal (PAF) and persistent AF (persAF). The cornerstone of AF ablation is pulmonary vein isolation (PVI). While early recurrences within a three-month blanking period are not considered an ablation failure, early recurrences predict long term success. We aimed to study the impact of early symptomatic recurrences on long-term ablation outcome using PPG monitoring.

Methods: Patients undergoing scheduled PVI were given the opportunity to monitor their rhythm using “FibriCheck” within the “TeleCheck-AF” initiative for seven days. They received a QR code for installation of the software on their smartphone and were connected to the clinician’s telemedicine portal. Patients were told to measure their heart rate three times per day and in case of symptoms. Clinicians assessed the tracings and contacted the patients if therapeutic steps were indicated.

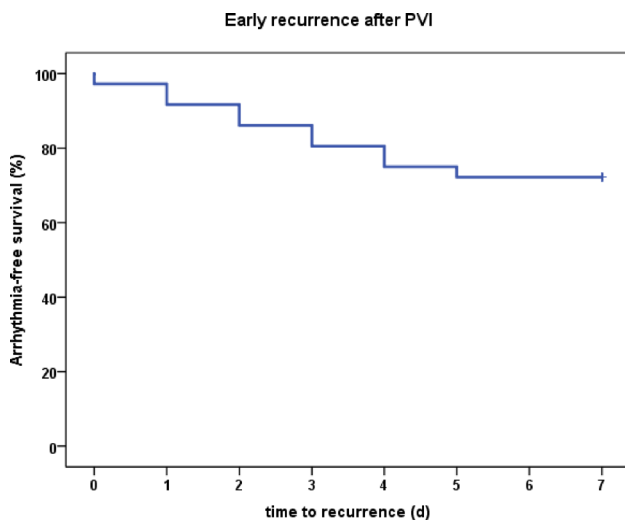


Fig. 1112.11 Arrhythmia-free survival of patients undergoing AF ablation

Results: Thirty-six patients were included in this retrospective analysis. Median age was 57 ± 12 years, 33 % were female, median CHA2DS2-VASc-Score was 2 (0–4). The majority of patients (72 %) had paroxysmal AF, 25 % had persistent AF and 3 % had longstanding persistent AF. Within one week, patients recorded 20 ± 1 PPGs. 771 tracings were analysed, early AF recurrences were detected in 32 % of patients. However, only 60 % of these patients experienced symptomatic recurrences after a three-month blanking period. 11 % of the patients with recurrences had recurrences of persistent AF and were scheduled for cardioversion.

Conclusion: Rhythm monitoring with a PPG-based mHealth application helps to detect early recurrences after PVI and helps in identifying patients at risk of recurrences after the blanking period.

12.12

Electroanatomic mapping system guided his bundle pacemaker implantation: experience of a high volume center

U. Rohrer¹, G. Prenner¹, M. Sereinigg¹, M. Manninger¹, E. Bisping¹, T. Geczy¹, P. Lercher¹, A. Zirlik¹, D. Scherr¹

¹Medical University of Graz, Graz, Austria

Introduction: Patients with bradyarrhythmia in need for pacemaker implantation and ventricular pacing often suffer from pacing-induced heart failure due to unphysiological pacing by the right ventricular lead. His bundle pacing allows to overcome this common issue with a more physiologic approach but real-life procedural data using this technology is scarce.

Methods: We report a single centre experience of the first 23 consecutive patients being implanted with a His-bundle-based pacemaker between 09/2020 and 02/2021 due to different types of bradyarrhythmia, or for cardiac resynchronisation therapy in heart failure combined with a left-ventricular lead (HOT-CRT) ± a right ventricular defibrillator lead. The positioning of the His-bundle-lead was done by identifying the His-bundle-location with a 3D electroanatomic mapping system via an introducing sheath that is provided with electrodes at its tip (Abbott Agilis HisPro™ catheter).

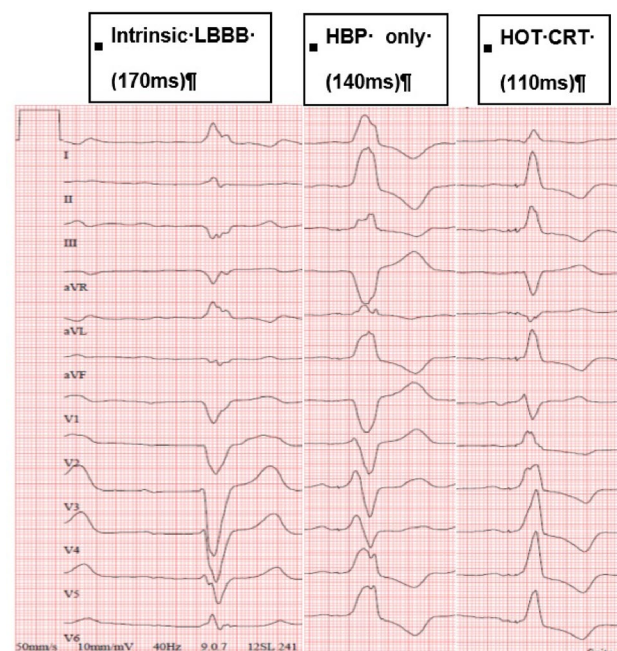


Fig. 1112.12

Results: Mean age was 72 ± 14 years, 5/23 (22 %) patients were female, mean baseline LVEF was 43 ± 15 %. Baseline ECG was captured before implantation: QRS width was 126 ± 31 ms, with typical LBBB in 6/23 (26 %), typical RBBB in 4/23 (17 %), alternating BBB in one patient (4 %) and either no BBB or ventricular escape rhythm in 12/23 (52 %). Indications for implantation were AV-block II°-III in 12/23 (52 %), heart failure with reduced ejection fraction in 7/23 (30 %), asystole 3/23 (13 %) and atrial fibrillation with bradycardic conduction in one patient (4 %). Therefore, 8 dual-chamber-pacemaker, 2 single-chamber-pacemaker, 7 single-chamber CRT-pacemaker, 3 dual-chamber CRT-pacemaker and 3 single-chamber CRT-defibrillator were implanted. Primary success rate to pace at the his-position was 100 %. Median skin-to-skin procedure time was 97 (50–147) min in his-bundle-device-implantation. The paced QRS width at the post-implantation follow up was 120 ms (60;196 ms) with a change in QRS width of -8 ms (+72; -92 ms). The mean his-bundle threshold was 1.1 ± 0.8 V over 0.5 ms (0.5;1.5 ms). The proportion of ventricular pacing was 97 % (1;99 %). There was one post-procedural pneumothorax that needed drainage, no major procedure-related complications occurred. In one patient the his-bundle-lead dislocated shortly after implantation and showed complete exit block. In this case due to narrowing of QRS complex (intrinsic LBBB with 150 ms to paced QRS with 120 ms) excellent improvement of the LVEF (baseline 20 % to follow-up 50 %)

Conclusion: with conventional CRT-pacing the his-bundle-lead was extracted and not re-implanted. Electroanatomic-guided His bundle pacing is feasible, with high implantation success rate and electric impact, both regarding QRS width and pacing threshold.

12.13

Prognose nach VT-Ablation bei Ischämischer Kardiomyopathie

S. Sieghartsleitner¹, M. Derndorfer¹, G. Kollias¹, M. Martinek¹, S. Seidl¹, E. Sigmund¹, J. Aichinger¹, H. Pürerfellner¹

¹Ordensklinikum Linz Elisabethinen, Linz, Österreich

Einleitung: Die ischämische Kardiomyopathie (ICM) ist mit dem Auftreten von potenziell lebensbedrohlichen ventrikulären Tachykardien (VT) assoziiert. Zur Behandlung der Rhythmusstörungen spielt neben der Therapie der zugrunde liegenden Erkrankung und der Devicetherapie die Katheterablation eine zunehmende Rolle. Diese steht als komplexe elektrophysiologische Prozedur meist nur in einem spezialisierten Zentrum zur Verfügung. In ausgewählten Fällen ist der perkutanen epikardiale Zugangsweg vorteilhaft, jedoch mit potenziellen Komplikationen behaftet. In der Literatur konnte bereits gezeigt werden, dass mit Hilfe einer Katheterablation eine signifikante Reduktion der VT-Episoden erreicht werden konnte, zusätzlich gibt es Hinweise für eine Mortalitätsreduktion. Welche Parameter in der Nachsorge (inkl. einer stattgehabten epikardialen Prozedur) für die weitere Prognose der Pat. eine Rolle spielen, ist dennoch nicht völlig geklärt.

Methoden: Mit Hilfe eines Registers ($n=78$) wurden seit 03/2016 Parameter zur Ablationsbehandlung bei ischämischer Kardiomyopathie erfasst und zusätzlich Sterbedaten abgeglichen.

Resultate: Das Prognose im Follow-up ist signifikant mit dem Alter und dem Auftreten einer periprozeduralen Perikardtamponade ($n=6$) verknüpft. Hinsichtlich des epikardialen Zugangswegs ($n=8$) konnte kein Zusammenhang mit dem Auftreten von Perikardtamponaden und keine negative Beeinflussung der Prognose gefunden werden. Nach einer Gesamtsterblichkeit von 15 % in den ersten 9 Monaten kommt es zu einer nachfolgenden Stabilisierung (Plateaubildung in der Kaplan-Meier Kurve).

Schlussfolgerungen: Alter und eine komplikative Perikardtamponade sind die hauptsächlichen Faktoren für eine reduzierte Überlebenswahrscheinlichkeit nach einer VT-Ablation. Eine perkutane epikardiale Prozedur war per se nicht mit einer erhöhten Rate an Tamponaden oder einer gesteigerten Mortalität assoziiert. Das Auftreten einer Perikardtamponade steigert die Mortalität nicht nur akut, sondern auch im weiteren Verlauf. Dies ist möglicherweise auf den vorzeitigen Abbruch der Prozedur und somit den nicht erreichten Endpunkt zurückzuführen.

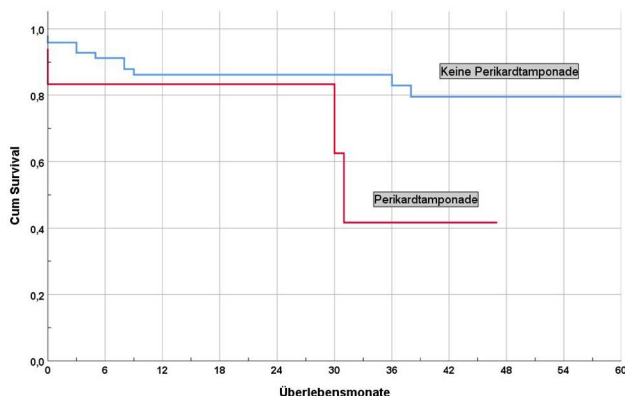


Fig. 1112.13 Kaplan-Meier-Kurve

12.14

Simultaneous orthogonal bipole mapping compared to conventional electrode configurations and impact on ablation strategies: results from a real world observational study

L. Fiedler¹, F. X. Roithinger¹, I. Roca-Luque², F. Lorgat³, A. Roux⁴, J. Lacotte⁵, A. Miller⁶, D. Steven⁷

¹12. medizinische Abteilung Landesklinikum Wiener Neustadt, Wiener Neustadt, Austria

²Hospital Clínic de Barcelona · Arrhythmia Unit. ICCV, Barcelona, Spain

³Christiaan Barnard Memorial Hospital, Cape Town, South Africa

⁴SANTE REPUBLIQUE CENTRE, Clermont-Ferrand, France

⁵Institut Cardiovasculaire Paris Sud, Paris, France

⁶Abbott, Minneapolis, United States

⁷University Hospital Köln, Köln, Germany

Introduction: 3D mapping systems are pivotal to identify low voltage areas and to define ablation strategies. In this context, high-density (HD) multipolar mapping catheters with varying electrode configurations are used for accurate myocardial substrate definition. High density mapping using a grid shaped catheter allows for use of simultaneous analysis of adjacent orthogonal bipole signals that may assist in more accurate substrate characterization and ablation strategy decisions. This was a prospective, multicenter observational study to characterize the utility of electroanatomical mapping with the Advisor™ HD Grid mapping catheter in subjects undergoing catheter ablation for persistent atrial fibrillation (PersAF) or ventricular tachycardia (VT) in real-world clinical settings.

Methods: Mapping was performed with Ensite Precision cardiac mapping system (Abbott, MN) and Advisor™ HD Grid catheter to generate high-density maps of cardiac chambers in order to assess the potential influence of the simultaneous orthogonal bipole analysis using HD Wave Solution™ software configuration on PersAF and VT ablation strategies. Differences in substrate identification between simultaneous orthogonal bipole configuration and standard along-the-spline electrode

Example of Case Maps

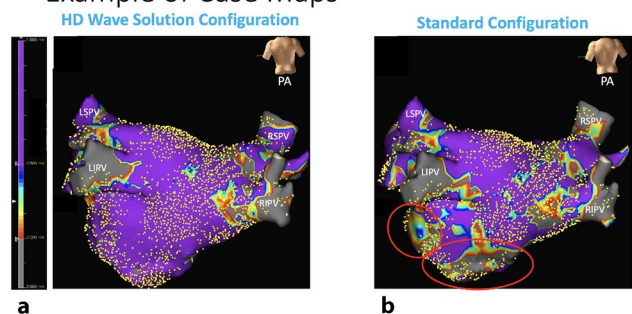


Fig. 1112.14 **a** left atrial high density voltage map from posterior anterior view (PA) during sinus rhythm in HD Wave Solution configuration. **b** left atrial high density voltage map from posterior anterior view (PA) during sinus rhythm in standard configuration, along the spline. Depicting Scar area <0.2mV in gray and healthy myocardium >0.5mV in purple in both maps. 6789 Yellow dots depict recorded local atrial signal. LSPV left superior pulmonary vein; LIPV left inferior pulmonary vein, RSPV left posterior pulmonary vein, RIPV left posterior pulmonary vein

configuration, and potential effects on ablation strategies were investigated.

Results: During the study period (January 2019 through April 2020), the study enrolled 367 subjects patients undergoing catheter ablation for PersAF ($N=333$, average age 64.1 yr, 75 % male) or VT ($N=34$, average age = 64.3 yr, 85.3 % male). In total, 494 maps were generated to treat patients undergoing PersAF ablation and 57 to treat patients undergoing VT ablation. Compared to standard along-the-spline configuration, mapping with the simultaneous orthogonal bipole configuration showed differences in 57.8 % (178/308) of maps generated, with the greatest difference noticed in surface area of low voltage (62.9 %) and location of low voltage (55.6 %). In comparisons performed live during the procedure ($n=50$), the Advisor™ HD Grid catheter assisted in identification of ablation targets in 70.0 % of cases, changing the ablation strategy compared to that identified with along-the-spline configuration in 34.3 %. In comparisons performed retrospectively after the procedure ($n=258$), the ablation strategy identified with simultaneous orthogonal bipole configuration differed from an along-the-spline configuration in 21.7 %. Even compared to a higher-density electrode configuration using all-bipoles rather than along-the-spline bipoles, use of the simultaneous orthogonal bipole configuration identified differences in 57.1 % of maps.

Conclusion: The Advisor™ HD Grid catheter combined with HD Wave Solution™ software mapping configuration can define myocardial substrate more accurately compared to standard along-the-spline configuration. The difference in substrate identification has potential impact on ablation strategy. Further clinical trials are needed to elucidate the role of orthogonal bipole configuration mapping and improved ablation success rates.

12.15

Comparison of patients managed by drug therapy vs. PVI in an upper austrian atrial fibrillation cohort

M. Martinek¹, H.J. Crijns², B.A. Essers², J. Schatzl³, R. Wiesinger³, G. Pruckner³

¹Department of Internal Medicine II with Cardiology, Angiology, and Intensive Care Medicine, Ordensklinikum Linz Elisabethinen, Linz, Austria

²Maastricht University, CARIM – Cardiovascular Research Institute Maastricht, Maastricht, Netherlands

³Institute of Health Economics, JKU Linz, Linz, Austria

Introduction: This is the first part of a PhD project at CARIM with the scope of a direct comparison of true healthcare expenditure and outcomes of drug therapy (non-PVI) vs. catheter ablation therapy (PVI) for atrial fibrillation (AF) in an Upper Austrian cohort.

Methods: We included all patients who were first diagnosed with AF (LKF-codes I48.*) in the years 2005 to 2018 and were insured via the Upper Austrian Health Insurance Fund (OÖGKK). PVI patients were identified by the MEL-codes 6546 (2005–2007, 6547 (2008), and DE060 (from 2009 on). We aimed to describe the socio-demographic characteristics and the health care expenditure in both patient groups.

Results: The final dataset includes 21,791 patients-identified by their first hospitalization due to AF between Q1/2005 and Q4/2018. Of these, 1,624 (7.5 %) were treated with at least one PVI (1,222 had one PVI and 404 individuals had up to 5 re-dos), the rest received other treatment. We observe significant differences in health care expenditure and all demographic and socio-economic characteristics between non-PVI and PVI patients (Fig. 1

	Ø Non-PVI	Ø PVI	Diff.	95 % CI		Sign.
Female	0.520	0.316	-0.204	-0.229	-0.179	***
Age†	71.557	58.267	-13.290	-13.926	-12.654	***
Age < 55†	0.095	0.337	0.241	0.226	0.257	***
Age 55 – 65†	0.176	0.395	0.219	0.199	0.239	***
Age > 65†	0.728	0.268	-0.460	-0.483	-0.438	***
Deceased until 2018 (HV)	0.314	0.081	-0.233	-0.256	-0.210	***
Employed†	0.164	0.531	0.366	0.346	0.387	***
Unemployed†	0.016	0.030	0.014	0.007	0.021	***
Retired†	0.838	0.466	-0.372	-0.392	-0.351	***
AF at Elisabethinen Linz	0.143	0.542	0.400	0.381	0.418	***
AF at AKH Linz/KUK	0.160	0.471	0.311	0.292	0.330	***
AF at Klinikum Wels	0.178	0.128	-0.050	-0.069	-0.031	***
Heart Failure	0.259	0.142	-0.118	-0.139	-0.096	***
Hypertension	0.148	0.123	-0.026	-0.044	-0.008	***
Diabetes	0.064	0.034	-0.030	-0.042	-0.018	***
TIA/Stroke	0.154	0.091	-0.064	-0.082	-0.046	***
Myocardial Infarction	0.237	0.280	0.044	0.022	0.065	***
Peripheral Artery Disease	0.076	0.033	-0.043	-0.056	-0.030	***
Hyperlipidemia	0.003	0.011	0.008	0.005	0.011	***
Renal Failure	0.067	0.023	-0.045	-0.057	-0.032	***
Dementia	0.044	0.009	-0.036	-0.046	-0.026	***
Four Quarters Before First AF						
Hospital Days	1.683	0.907	-0.776	-0.923	-0.630	***
LKF Points	750.880	429.658	-321.222	-398.021	-244.424	***
LKF Turnover	976.135	549.943	-426.192	-526.452	-325.932	***
Drug Expenditure	218.872	137.542	-81.330	-108.562	-54.099	***
Outpatient Medical Care	172.055	160.098	-11.957	-18.593	-5.321	***
Sick Leave Days	0.840	2.600	1.761	1.492	2.029	***
Quarter of First AF						
Hospital Days	8.538	6.311	-2.227	-2.668	-1.787	***
LKF Points	3,195.315	4,268.696	1,073.381	836.560	1,310.201	***
LKF Turnover	4,159.938	5,503.132	1,343.193	1,033.377	1,653.010	***
Drug Expenditure	308.309	222.561	-85.747	-138.807	-32.687	***
Outpatient Medical Care	226.005	212.559	-13.446	-26.165	-0.728	**
Sick Leave Days	2.116	7.786	5.670	4.996	6.343	***
Four Quarters After First AF						
Hospital Days	2.620	1.910	-0.710	-0.891	-0.530	***
LKF Points	1,103.234	1,417.350	314.116	222.959	405.273	***
LKF Turnover	1,441.653	1,836.759	395.105	275.492	514.719	***
Drug Expenditure	301.364	206.549	-94.815	-127.811	-61.819	***
Outpatient Medical Care	198.874	182.281	-16.593	-23.416	-9.770	***
Sick Leave Days	1.448	5.189	3.741	3.340	4.141	***

Fig. 1112.15

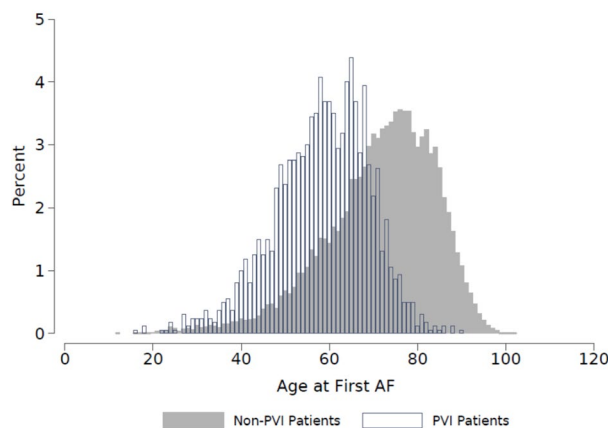


Fig. 2112.15

Demographics). PVI patients are substantially younger (Fig. 2) and show different mortality rates after first AF diagnosis.

Conclusion: As expected, non-PVI and PVI patients in an AF cohort differ substantially in all characteristics. As a further step, we conduct propensity score matching and a differences in differences approach (DiD) to provide (some) comparability between the groups for a cost effectiveness analysis. Still a substantial selection bias between non-PVI and PVI patients may remain.

12.16

Assessment of the Micra™ leadless pacemaker system in patients after TAVI (MITAVI)—a case-control study

H. Blessberger¹, D. Kiblböck¹, H. Rohringer², J. Ebner¹, J. Bötscher¹, J. Maier³, K. Saleh¹, S. Schwarz¹, C. Reiter¹, T. Lambert¹, M. Grund¹, C. Steinwender¹

¹Department of Cardiology, Kepler University Hospital, Medical Faculty, Johannes Kepler University, Linz, Austria

²Sigmund Freud University Vienna, Wien, Austria

³Institute of Pharmacology, Medical University of Vienna, Wien, Austria

Introduction: The incidence of newly developed AV conduction disturbances is higher after transfemoral aortic valve implantation (TAVI) than after conventional surgical valve replacement. Radial forces exerted by the TAVI help to secure the valve prosthesis in the left ventricular outflow tract but also compress adjacent AV conduction tissue. Patients with permanent atrial fibrillation or with an anticipated low rate of ventricular pacing (back-up pacing only) are eligible for single chamber pacing with a leadless cardiac pacemaker (LCP). As conventional single-chamber pacemakers have been the systems of choice in TAVI patients up to now, data about the safety and performance of LCPs in this setting are still scarce. Several considerations have to be taken into account in TAVI patients: Implantation itself may be more challenging as the access site in the right groin has previously been used for the TAVI implantation. Moreover, severe left ventricular hypertrophy and distorted geometry of the left ventricular outflow tract by the TAVI prosthesis may complicate the LCP implantation into the right ventricle or impair proper LCP function (pacing threshold, impedance, sensing). Oral anticoagulation therapy in TAVI patients with atrial fibrillation combined with mandatory antiplatelet therapy in the weeks after TAVI may put patients at higher risk for access site bleedings. The aim of this investigation was to systematically assess the safety and performance of LCP after TAVI.

Methods: In this single-center, retrospective case-control study patients who had received a Micra™ LCP within 4 weeks after TAVI (group 1=G1) due to a new onset AV conduction disturbance were compared with sex and age-matched (± 2.5 years) controls who had received an LCP, but no TAVI (group 2=G2). Device parameters (R wave sensing, pacing threshold, impedance, battery life), as well as serious adverse device effects (SADEs), were compared between the groups at implant and until 12 months thereafter. Furthermore, baseline characteristics, implant complications, procedure, and fluoroscopy times were assessed in both groups. Continuous variables are described as median and interquartile range. An unpaired Mann-Whitney U-test or a chi-square test was applied to compare baseline characteristics, as appropriate. Device parameter changes between different time points were evaluated using a mixed-effects linear regression model.

Results: Thirty-one patients received an LCP after a median of 5 days after TAVI implantation (indications complete AV block [$n=6$], afib with slow conduction [$n=6$], and SR with intermittent AV block [$n=19$]). LCP implant time was longer in G1 as compared with G2 (G1: 45 [30–55] min., G2: 30 [20–45] min., $p=0.003$). The same trend could be found for fluoroscopy time (G1: 7 [4–11] min., G2: 5 [4–8] min., $p=0.052$). 32 % of patients in G1 were on oral anticoagulation vs. 65 % in G2 ($p=0.203$). Bridging regimens and the rate of suspension for LCP implantation were not different between groups. Subjects in G1 were

more often on a concomitant antiplatelet therapy (G1: 100 %, G2: 16 %, $p < 0.001$). Overall, only one complication occurred in G1 which was not related to the LCP implant procedure (death due to myocardial infarction during the index stay after LCP implantation, $p=0.492$ for inter-group difference). Baseline device parameters, as well as the length of stay after LCP implantation, did not significantly differ between both groups. During 12 months of follow-up, the ventricular pacing rate was persistently higher in G2 (3 months: G1: 1.2 [0.3–7.3]%, G2: 44.9 [14.8–84.0]%, $p < 0.001$; 12 months: G1: 1.0 [0.2–5.8]%, G2: 69.9 [25.1–90.2]%, $p < 0.001$). R wave sensing significantly increased in both groups over time (0.24 mV per month on average for G1 and G2, $p=0.952$ for inter-group difference), whereas the pacing threshold remained stable ($p=0.791$ for inter-group difference). No SADEs were identified.

Conclusion: Micra™ LCP implantation for treatment of AV conduction disturbances after a TAVI procedure is safe but associated with slightly longer procedure durations. Immediate implantation complication rate, as well as device baseline parameters, were not different as compared with matched patients who received a Micra™ LCP without a prior TAVI procedure. During a 12-month follow-up period, pacing thresholds remained stable and R wave sensing increased in a similar fashion in both groups.

12.17

Characteristics of patients managed by PVI in an upper austrian atrial fibrillation cohort

M. Martinek¹, H. J. Crijns², B. A. Essers², J. Schatzl³, R. Wiesinger³, G. Pruckner³

¹Department of Internal Medicine II with Cardiology, Angiology, and Intensive Care Medicine, Ordensklinikum Linz Elisabethinen, Linz, Austria

²Maastricht University, CARIM – Cardiovascular Research Institute Maastricht, Maastricht, Netherlands

³Institute of Health Economics, JKU Linz, Linz, Austria

Introduction: This analysis is part of a PhD project at CARIM with the scope of a direct comparison of true health care expenditure and outcomes of drug therapy vs. catheter ablation therapy (PVI) for atrial fibrillation (AF) in an Upper Austrian cohort.

Methods: We included all patients who were first diagnosed with AF (LKF-codes I48.*) in the years 2005 to 2018 and

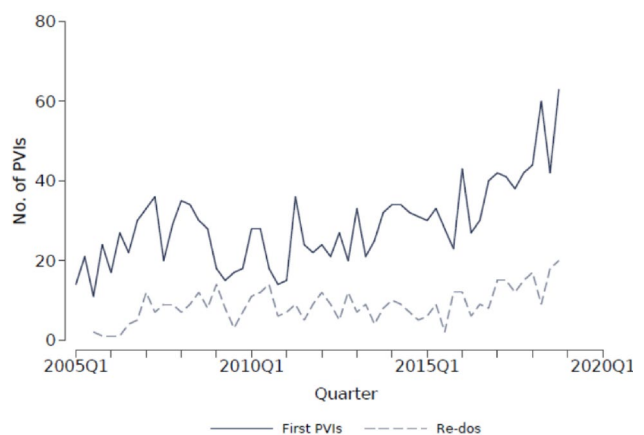


Fig. 112.17

Different patterns of inflammation after leadless cardioac pacemaker implantation—an autopsy study

H. Blessberger¹, D. Kiblböck¹, C. Grosse², P. Noack², J. Ebner¹, J. Bötscher¹, J. Maier³, K. Saleh¹, T. Lambert¹, J. Kellermair¹, J. Kammler¹, C. Steinwender¹

¹Department of Cardiology, Kepler University Hospital, Medical Faculty, Johannes Kepler University, Linz, Austria
²Institute of Pathology and Microbiology, Kepler University Hospital, Medical Faculty, Johannes Kepler University, Linz, Austria
³Institute of Pharmacology, Medical University of Vienna, Wien, Austria

Introduction: Leadless cardiac pacemakers (LCPs) have fundamentally changed the field of device therapy. Lead and pacemaker pocket-related complications—that affect between 2 % and 12 % of individuals with conventional pacemaker systems—can be effectively avoided with this new technology. The introduction of an LCP with VDD capabilities in 2020 will likely further increase the implantation rate of these devices in the future. However, there are certain drawbacks of LCP that have to be considered. Namely, the mode of extraction of LCP, especially years after implantation, in the case of a device infection or after battery depletion are issues that are still being debated. For extraction purposes, the Micra™ LCP has a knob on its tail that enables catching the device with a snare. Until now, there is still a lack of data on how much the Micra™ tends to be overgrown with tissue over time. Overgrowth with cardiac tissue may influence both the resistance to infection with blood-borne bacteria and the ability to grasp the device with a snare if extraction is needed. On the one hand, tissue could shield the device from bacteria, on the other hand, this very tissue could cover the extraction knob and thus prevent a successful interventional extraction.

Methods: We followed up on all patients who received a Micra™ LCP at our department. Survival status was determined by searching the hospital information system and by contacting the patients, relatives or their treating physicians. If no patient contact could be established, survival status was determined by contacting local registration authorities. If patients had deceased, efforts were made to identify the exact cause of death. As all pacemaker systems have to be removed before burial in Austria, we tried to find out whether the Micra™ LCP with the adjacent cardiac tissue block had been preserved and was still amenable to a thorough histopathological examination. If available, the following histological features were evaluated by two experienced pathologists in consensus: fibrin exudates on the LCP surface as well as fibrosis, inflammatory infiltrates, vascular proliferation, and hemosiderin deposits in the myocardium adjacent to the LCP and its fixation tines. These findings were semi-quantitatively assessed as mild, moderate, and marked depending on the degree and extent of histopathological changes. In addition to routine hematoxylin and eosin stains, Elastica-van-Gieson stainings were used to evaluate the extent of fibrosis, and immunohistological stainings for CD3, CD20 and CD34 were used to identify T- and B-lymphocytes as well as endothelial cells, respectively.

Results: Between December 2013 and July 2020, a Micra™ LCP was implanted in 283 patients (36.0 % female) with a median age of 80.6 years (IQR: 76.5–85.1 years). During a

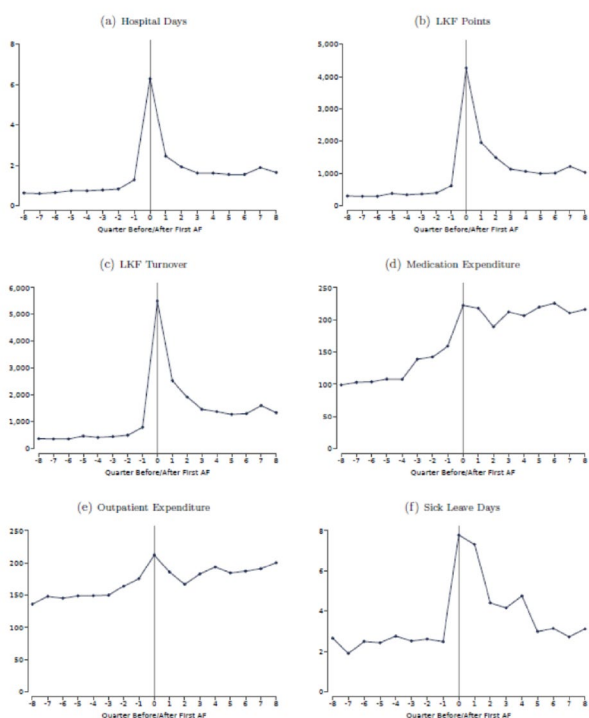


Fig. 2 | 12.17

were insured via the Upper Austrian Health Insurance Fund (OÖGKK). PVI patients were identified by the MEL-codes 6546 (2005–2007, 6547 (2008), and DE060 (from 2009 on). We aimed to describe demographic, socio-economic, and health care expenditure characteristics of PVI patients.

Results: The final dataset includes 1,624 patients—identified by their first hospitalization due to AF between Q1/2005 and Q4/2018 and the MEL-Code for PVI. In our sample, 1,222 had only one PVI and 404 individuals had multiple procedures (up to 5). PVI numbers in Upper Austria are steadily increasing (Fig. 1). Less than 30 % of eligible AF patients are treated by PVI in the first quarter after first hospitalization due to AF. PVI patients are on average 60 years old, roughly 50 % belong to the working force, and only 31.6 % are female. After PVI a slight increase in hospital days, inpatient costs, medication expenditure, and outpatient costs remain, whereas sick leave days tend to decrease to levels before AF diagnosis (Fig. 2).

Conclusion: While the absolute number of PVIs in Upper Austria increases over time, only less than 30 % of eligible patients undergo the PVI within the first three months after AF diagnosis. To assess the cost effectiveness of the procedure, in- and outpatient costs must be compared to a matched cohort not undergoing PVI in the next step of the project.

median follow-up of 2.16 years (IQR: 1.17–3.96 years), sixty patients (21.2 %) had died, predominantly from cardiovascular causes. The median survival time from implantation to death was 1.70 years (IQR: 1.02–2.98 years). Tissue blocks for histological analysis were available in eight patients (8/60, 13.3 %) with a median survival time after LCP implantation of 379 days (IQR: 232–637 days; range: 18–1428 days). Fibrin capsules coating the LCP as a whole or in part were identified in six (6/8, 75.0 %) patients who had a median implant duration of 295 days (IQR: 228–403 days, range: 18–576 days, septal position of the LCP in 2, apical position in 4 patients). In two (2/8, 25.0 %) patients who died 697 and 1428 days after implantation, no fibrin coating was present (septal position of the LCP in both). Fibrin exudates were admixed with a few neutrophils and lymphocytes, and in one patient few endothelial cells could be identified lining the fibrin coating. In all patients, fibrosis was found in the myocardium adjacent to the LCP and its tines. The degree of fibrosis ranged from mild ($n=1$) to moderate ($n=7$). Within the fibrotic areas, CD3-dominant inflammatory infiltrates and vascular proliferation were seen in all patients. Hemosiderin deposits were detected in four (4/8, 50.0 %) patients.

Conclusion: After Micra™ LCP implantation, a fibrotic tissue response with varying degrees of inflammation in the surrounding right ventricular implant area can be expected. Thereby, CD3-positive T-lymphocytes could predominantly be found. We could show that the LCP was covered with a fibrin capsule in many cases. The extent of overgrowth substantially varied between individuals but could be found as early as 18 days after implantation. Innovative physical methods of surface treatment might help to prevent the deposition of a fibrin cover on the Micra™ LCP. This would allow snaring of the LCP in all scenarios where extraction is required.

12.19

CRT 2.0: erste österreichische klinische Erfahrungen mit Left-Branch Pacing

M. Derndorfer¹, H. Pürerfellner¹, M. Martinek¹, S. Sieghartsleitner¹, J. Aichinger¹, G. Kollias¹

¹Ordensklinikum Linz GmbH Elisabethinen, Linz, Österreich

Einleitung: Rechtsventrikuläre (RV) Stimulation stellt den aktuellen Goldstandard der Herzschrittmacher-Therapie dar. Allerdings wird hierunter – je nach Studie – bei ca. 5 bis 15 % der Patienten die Entwicklung einer schrittmacherinduzierten Herzinsuffizienz (HI) beobachtet, besonders dann, wenn bereits eine leicht- bis mittelgradige HI vorbesteht und der RV-Stimulationsanteil >20 % liegt. Auch Sonden-Platzierungen im RV-Ausflusstrakt bzw. am RV-Septum konnte bislang keine eindeutige Verbesserung klinischer Endpunkte verglichen zu apikalem RV-Pacing erbringen. Die kardiale Resynchronisationstherapie (CRT) mittels Koronarsinussonde (CS) ist eine gut etablierte Therapieoption bei HI. Der Wert der CRT-Therapie bei erhaltener LVEF bleibt vorerst im Fokus von Studien. Rezent finden nun Methoden zur Stimulation des intrinsischen Reizleitungssystems (engl. Conduction System Pacing, CSP) zunehmend Einzug in die tägliche Praxis. HIS-Bündel-Stimulation (engl. HIS Bundle Pacing, HBP) gehört bereits zum fixen Repertoire der täglichen Schrittmacherroutine. Jedoch können hier hohe Stimulationsreizschwellen (bei Implantation oder im zeitlichen Verlauf), niedriges Sensing und fallweise die fehlende Korrektur eines bestehenden Schenkelblockes die Anwendbarkeit limitieren. Ergänzend wird an unserer Klinik seit 06/2020 die noch junge Methode der Linksschenkelstimulation (engl. Left

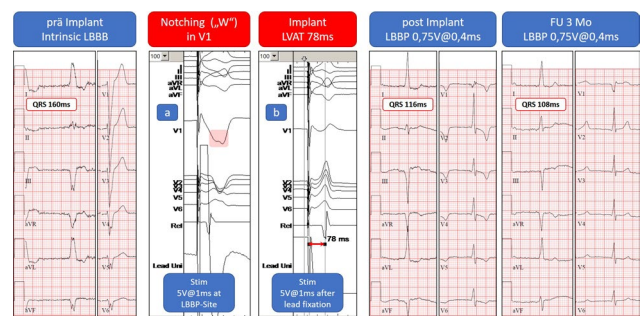


Abb. 1 | 12.19 Prozedur

	n	%	mean	min	max
männlich	7	58%			
Alter			73	59.7	84.3
art HT	5	42%			
Diabetes	4	33%			
KHK	5	42%			
VHF	6	50%			
SD-Dysfunktion	3	25%			
GFR (ml/min)			56	25	82
BMI			29	21.4	39.3
LVEF prä(%)	12		41	15	60
LVEF FU-3Mo (%)	6		55	42	65
QRS präOP (ms)	12		144	80	194
QRS postOP (ms)	12		117	90	130
QRS FU-3Mo (ms)	6		113	94	126
LVEDD prä (mm)	12		48	44	54
LVEDD FU-3Mo (mm)	6		45	40	52
LBBP-Reizschwelle (V@1ms)	12		0.6	0.3	1.25
LBBP-Reizschwelle-3Mo (V@1ms)	6		0.6	0.5	0.75
Device: 2-Kammer-SM	7	58%			
Device: CRT	5	42%			
OP-Dauer (min)			164	96	227

Abb. 2 | 12.19 Demographie, Prozedurdaten

Bundle Branch Pacing, LBBP [1]) angewandt, deren Technik hier anhand erster klinischer Erfahrungen beschrieben wird.

Methoden: Grundvoraussetzung für LBBP ist die Beherrschung von HBP. Nach üblichem Venenzugang über die V cephalica, axillaris oder subclavia wird an unserer Abteilung ein Elektrophysiologie-Katheter (EP) eingebracht und damit ein grobes 3D-Map des rechten Atriums, CS und RV angefertigt. Darin werden HIS-Signale markiert und nun mit einer speziell vorgeformten HIS-Schleuse und Schrittmachersonde fluoroskopiefrei diese Stelle angesteuert. Primär wird HBP versucht. Bei fehlendem Erfolg (siehe Einleitung) wird nun selbiges Equipment an das proximale RV-Septum herangeführt und hier unipolar mit 5V@1 ms stimuliert. Bei positiver Antwort (sog. „Notching“ in Ableitung V1, Abb. 1, a) erfolgt unter ständigem Impedanz-Monitoring das Einschrauben der Sonde in das interventrikuläre Septum (IVS). An korrekter Stelle kann nun ein Wandern des Notch mit allmählicher RSB-Morphologie, sowie eine sprunghafte Verkürzung der linksventrikulären Aktivierungszeit (LVAT) auf meist <90 ms mit Schmälerung des QRS-Komplexes beobachtet werden (Abb. 1, b). Das EKG kann selektives oder nichtselektives LBBP sowie anodales Capture zeigen. Ein Linksschenkel-Potential ist nicht immer vorhanden. Mittels Schleusen-Angiographie kann die tiefe Lage der Sonde im IVS dokumentiert werden. Dokumentiert wurden QRS-Breite, LVEF und der linksventrikuläre enddiastolische Durchmesser (LVEDD) vor/nach der OP sowie zum 3-Monats FU (soweit bereits verfügbar).

Resultate: Demographische, Prozedur- sowie Follow-UP-Daten finden sich in Abb. 2. Bei 12 von bisher 13 Patienten, wo LBBP versucht wurde, konnte LBBP erfolgreich durchgeführt werden. Alle Patienten hatten zuvor mehrere Versuche von HBP in derselben Sitzung, was sich letztlich auch in der OP-Dauer

von durchschnittlich 164 min widerspiegelt. 1 Patient erhielt aufgrund einer diffusen Erregungsleitungsstörung mit unzureichender Verbesserung der QRS-Breite durch HBP oder LBBP letztlich ein herkömmliches CRT-System. Relevante Komplikationen traten keine auf. Einmalig wurde beim Schrauben der Sonde das IVS perforiert, was das erneute Fixieren der Sonde an benachbarter Stelle nötig machte. Alle Prozeduren wurden im EPU-Labor unter Verwendung eines 3D-Mapping-Systems durchgeführt. Üblich waren ein sehr gutes Sensing (bei allen >8V), sehr gute Reizschwellenwerte (meist <1V@1 ms) sowie initiale T-Wellen-Negativierungen nach Korrektur des Schenkelblockes im Sinne eines „Cardiac Memory“ (Abb. 1). Bei allen Patienten mit breitem Schenkelblock konnte eine deutliche Schmälerung des QRS (Abb. 1), bei jenen mit schmalen intrinsischen Komplexen ein annähernd unveränderter QRS erzielt werden. In nahezu allen Fällen wurden stabile Sonden-Werte innerhalb von 3 Monaten sowie eine Verbesserung der LVEF beobachtet (siehe Abb. 2). Häufigste Indikation war jene einer kardialen Resynchronisation, teils nach frustriertem CRT-Versuch in der Vergangenheit, gefolgt von AV-Blockierungen und pace&ablate-Indikationen.

Schlussfolgerungen: Linksschenkelstimulation/Left Bundle Branch Pacing ist neben HBP eine aufstrebende Methode zur Stimulation des spezifischen Reizleitungssystems und konnte in globalen, multizentrischen Studien bereits sehr günstige klinische Daten mit Schmälerung des QRS-Komplexes durch Korrektur des vorliegenden Schenkelblockes, sowie eine Verbesserung der LVEF und des NYHA-Stadiums, weiters eine Abnahme des LVEDD beweisen [2]. Die Beherrschung beider Methoden (HBP und LBBP) erhöht die Erfolgchancen der Prozedur deutlich, da Probleme des HBP (erhöhte Reizschwellen, hoher Stromverbrauch, manchmal fehlenden Korrigierbarkeit eines Schenkelblockes, Sensing-Probleme) mittels LBBP meist gut überwunden werden können. 3D-Mapping war äußerst hilfreich zum Verständnis und Erlernen der Technik, die grundsätzlich auch ohne 3D-System, dann aber unter Inkaufnahme längerer Fluoroskopie-Zeiten, erfolgen kann. LBBP wird zukünftig neben der klassischen CRT-Therapie und HBP eine zunehmend bedeutsame Rolle einnehmen. Wir präsentieren hier die ersten österreichischen Daten zu LBBP, das durch gute Durchführbarkeit und fehlend relevante Komplikationen überzeugen konnte. Eine erste Auswertung deutet einen ähnlich positiven klinischen Verlauf für die Patienten wie in oben genannten Studien an (Abb. 1, Abb. 2). Bis zum ÖKG verfügbare, aktualisierte Follow-UP-Daten werden präsentiert werden.

12.20

Sex-based differences in patients with Micra™ leadless cardiac pacemakers

J. Bötscher¹, H. Blessberger¹, K. Saleh¹, J. Ebner¹, J. Maier¹, M. Savci¹, G. Buchmayr¹, B. Wichert-Schmitt¹, S. Schwarz¹, C. Reiter¹, A. Fellner¹, C. Steinwender¹, D. Kiblboeck¹

¹Department of Cardiology, Kepler University Hospital, Medical Faculty, Johannes Kepler University, Linz, Austria

Introduction: Following the tendency towards individualized therapy in all disciplines of medicine, sex-specific differences are receiving more and more attention in cardiology in general and also in the field of pacemaker therapy.

Methods: The aim of this study was to identify commonalities and differences between sexes in terms of baseline data, indication and outcome parameters of patients with the Micra™

leadless cardiac pacemaker (LCP) system. In this retrospective, single-center study, we analyzed data from all patients with LCP implantation between December 2013 and July 2020.

Results: Out of 283 patients with Micra™ LCP, 103 were female (F: 36.4 %) and 180 were male (M: 63.6 %). Baseline data did not differ significantly between both sexes: mean age (F: 79.7 ± 7.7 years, M: 78.8 ± 10.5 years), atrial fibrillation (F: n = 70, 68.0 %, M: n = 138, 76.2 %), CHA2DS2-VASc-score (F: 4.6 ± 1.3 including 1 point for female sex, M: 3.6 ± 1.4). The most frequent indications were atrial fibrillation with slow conduction, third degree AV-block and sick sinus syndrome for both sexes. There were no significant differences with respect to mean implantation procedure time (F: 42.3 ± 17.7 min, M: 44.7 ± 19.2 min), number of deployments (F: 1.7 ± 1.5, M: 1.8 ± 1.9), sensing values (F: 10.6 ± 5.0 mV, M: 10.7 ± 4.6 mV), pacing thresholds (F: 0.49 ± 0.3 V/0.24 ms, M: 0.56 ± 0.31 V/0.24 ms) or impedance (F: 786 ± 233 Ω, M: 767 ± 236 Ω). Overall, 12 complications (4.2 %) were reported: 6 (2.1 %) during implantation, 6 (2.1 %) during the index stay after implantation. While the rate of complications did not differ significantly between both sexes (F: n = 6, 5.8 %, M: n = 6, 3.3 %, p = 0.32), there were significantly more major complications in women (F: n = 4, 3.9 %, pericardiocentesis: n = 2, unsuccessful LCP implantation: n = 1, intraprocedural death due to severe sepsis after device extraction: n = 1) compared to men (M: n = 1, 0.6 %, stroke: n = 1, p = 0.04). Long-term mortality did not significantly differ between women and men (F: n = 21, 20.4 %, M: n = 39, 21.7 %, log-rank p = 0.43) over a median follow-up of 25 months (IQR 14–47 months).

Conclusion: Our study revealed no significant differences in baseline and procedural data between women and men receiving Micra™ LCP therapy. However, more major complications occurred in women compared to men. Survival analysis did not demonstrate a difference in all-cause mortality.

12.21

Type of arrhythmia recurrence predicts long-term success after stepwise ablation of persistent atrial fibrillation

M. Manninger¹, U. Rohrer¹, P. Khairy², S. Miyazaki³, P. Pascale⁴, Y. Komatsu⁵, L. Roten⁶, A. Shah⁷, S. B. Wilton⁸, A. Jadidi⁹, S. Knecht¹⁰, A. Denis⁷, H. Cochet⁷, M. Hocini⁷, N. Derval⁷, F. Sacher⁷, A. Zirikli¹, M. Haissaguerre⁷, P. Jais⁷, D. Scherr¹

¹Abteilung für Kardiologie, Universitätsklinik für Innere Medizin, Medizinische Universität Graz, Graz, Austria

²Montreal Heart Institute, Montreal, Canada

³Department of Cardiovascular Medicine, University of Fukui, Fukui, Japan

⁴Arrhythmia Unit, Cardiovascular Department, Centre Hospitalier Universitaire Vaudois and University of Lausanne, Lausanne, Switzerland

⁵Department of Cardiology, Faculty of Medicine, University of Tsukuba, Tennodai, Tsukuba, Ibaraki, Japan

⁶Department of Cardiology, Inselspital, Bern University Hospital, University of Bern, Bern, Switzerland

⁷Electrophysiology Department, Hôpital Cardiologique du Haut-Lévêque and, Université de Bordeaux, Bordeaux, France

⁸Department of Cardiac Sciences, Libin Cardiovascular Institute of Alberta, University of Calgary, Calgary, Canada
⁹Department of Electrophysiology, University-Heart-Center Freiburg-Bad Krozingen, Bad Krozingen, Germany
¹⁰Division of Cardiology, AZ Sint-Jan, Brugge, Belgium

Introduction: Catheter ablation for persistent atrial fibrillation (AF) is a well-established therapy. However, results of randomized controlled multi-centre trials on ablation techniques other than pulmonary vein isolation (PVI) have not demonstrated superiority. We previously presented the “stepwise approach” aiming at AF termination resulting in sinus rhythm (SR) maintenance in most patients. In this retrospective analysis, we investigated, whether the type of recurrence determined arrhythmia-free survival.

Methods: One hundred nine patients (age 57 ± 9 years, 15 % female) underwent repeat ablation after “stepwise approach” ablation. Patients were classified according to their type of recurrence: paroxysmal AF (PAF), atrial tachycardia (AT) and persistent AF (persAF). Patients with persAF recurrence had larger atria, longer continuous AF duration and converted less frequently to SR during the initial procedure as compared to patients with PAF or AT recurrence. Success was defined as atrial tachyarrhythmia-free survival during follow-up by means of serial Holter-ECG monitoring.

Results: Single procedure success during a median follow-up duration of 59 (47–69) months, was achieved in 46.9 % if the initial recurrence was an AT, 36.4 % in case of PAF and 20.6 % in case of persAF (logrank $p=0.129$). In case of redo procedures, multiple procedure success during a median follow-up duration of 47 (30–60) months was achieved in 90.9 % of patients, if the initial recurrence was PAF, 72.9 % in case of AT recurrence and 47.9 % in case of persAF recurrence (logrank $p=0.022$). Non-termination of AF during the first ablation procedure, continuous AF duration ≥18 months, LA diameter ≥50 mm were independent predictors of multiple re-do-procedure failure in multivariate analysis.

Conclusion: In patients with persAF undergoing stepwise ablation, the type of recurrence after first ablation impacts long-term maintenance of SR after repeat ablations.

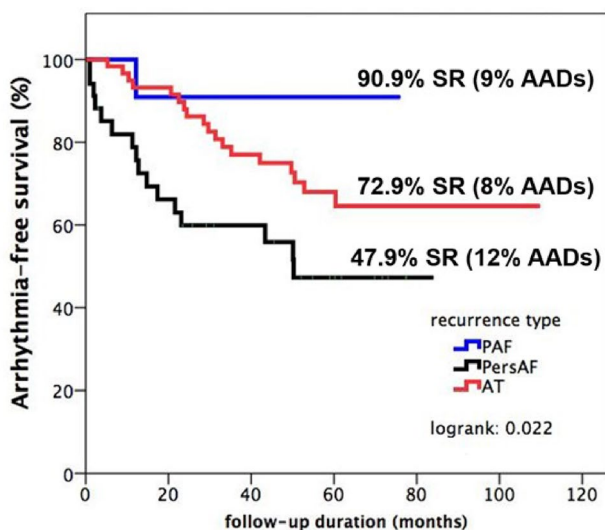


Fig. 112.21 Multiple procedure outcome grouped by type of recurrence (blue: paroxysmal AF–PAF; black: persistent AF–persAF; red: atrial tachycardia–AT)

12.22

Micra™ leadless cardiac pacemaker implantation in patients with cardiac implantable electronic device extraction

D. Kiblböck¹, H. Blessberger¹, J. Ebner¹, J. Bötscher¹, J. Maier¹, M. Savci¹, S. Schwarz¹, C. Reiter¹, G. Buchmayr¹, B. Wichert-Schmitt¹, C. Steinwender¹, K. Saleh¹

¹Department of Cardiology, Kepler University Hospital, Medical Faculty, Johannes Kepler University, Linz, Austria

Introduction: Several studies have demonstrated adverse outcomes in patients requiring extraction of infected or dysfunctional cardiac implantable electronic devices (CIED). Micra™ leadless cardiac pacemaker (LCP) may be a beneficial option for patients requiring permanent pacemaker therapy after CIED extraction, especially due to infection.

Methods: The aim of this study was to assess the feasibility, safety and outcome of Micra™ LCP implantation in patients with CIED extraction because of infection or dysfunction. We reviewed retrospectively the local LCP registry for LCP implantation and CIED extraction.

Results: CIED extractions (DDD: $n=25$, VVI: $n=9$, CRT-P: $n=1$, ICD: $n=1$) were performed in 36 patients (76.6 ± 9.9 years, female: $n=15$). Twenty-seven CIED (75 %) were extracted because of infection (pocket infection: $n=13$, lead infection: $n=7$, pocket perforation: $n=7$) with 13 positive microbiological cultures (48.1 %, Staph. aureus: $n=7$, MRSA: $n=1$, Staph. epidermidis: $n=1$, Staph. hominis: $n=1$, beta-hemolytic Streptococcus: $n=1$, Pseudomonas aeruginosa: $n=1$, Arthrobacter sp.: $n=1$) and 14 negative microbiological cultures (51.9 %). Nine CIED (25 %) were extracted because of dysfunction (severe tricuspid regurgitation due to CIED lead: $n=5$, lead failure: $n=3$, chronic pain due to CIED: $n=1$). Twenty-one Micra™ LCP (58.3 %) were implanted with the CIED extraction procedure on the same day, while 3 LCP (8.3 %) were implanted prior and 12 LCP (30.6 %) after the CIED extraction. Implantation success rate was 97.2 % ($n=35$). During a median follow-up of 23.1 months (IQR 6.7–45.8 months), no reinfections of the LCP occurred. Survival rates at 30 days, 90 days and 1 year after device extraction were 94.4 %, 90.9 % and 89.7 %, respectively.

Conclusion: Micra™ LCP implantation in patients requiring extraction of infected or dysfunctional CIED was feasible and safe in patients requiring permanent pacemaker therapy. No reinfections were detected during follow-up. Long-term follow-up demonstrated high survival rates.

12.23

Atrial sense or atrial nonsens?

E. Gatterer¹, T. Yoshida¹, H. Keller¹, M. Lassnig², M. Grabenwöger³, F. Weidinger¹

¹Klinik Landstraße, Wien, Österreich

²Fa. Abbott, Wien, Österreich

³Klinik Floridsdorf, Wien, Österreich

Einleitung: Fallbericht eines 87-jährigen Patienten: 2005 Zweikammer-SM wegen eines AV-Block II. 2012 Generatortausch und Implantation einer neuen Ventrikelsonde, die alte Sonde wurde belassen. Wenige Tage nach der Revision erstmals

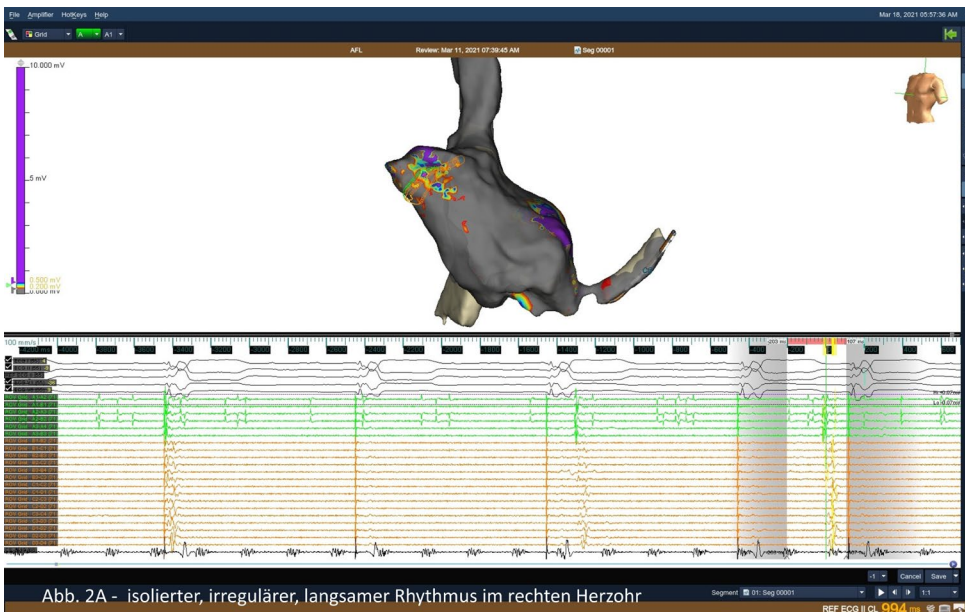
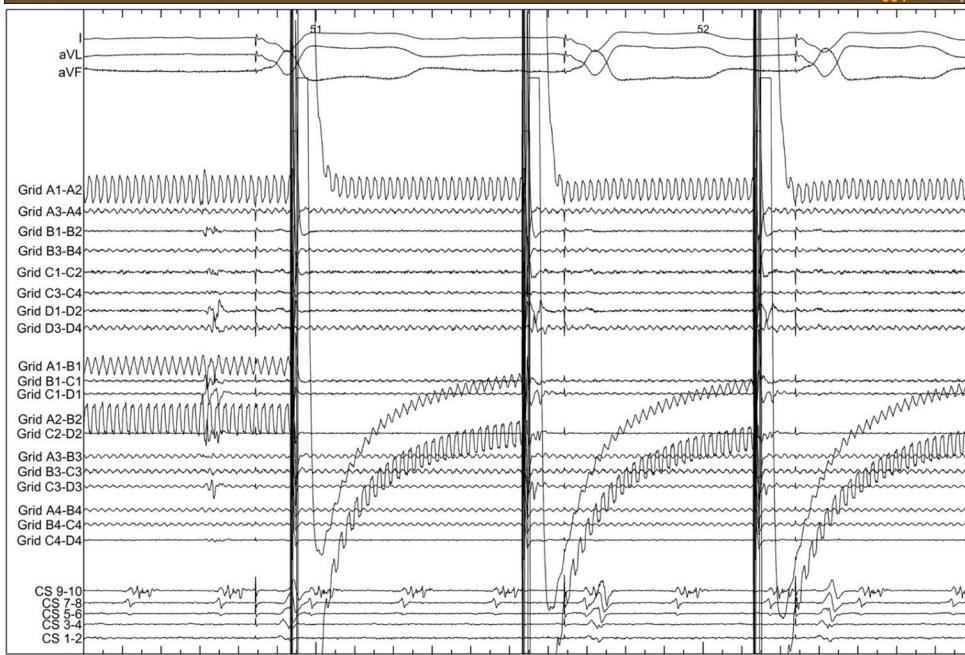


Abb. 2A - isolierter, irregulärer, langsamer Rhythmus im rechten Herzohr



Page: Vorhofflimmern Speed: 100 mm/s

11 Mar 2021 13:04:10

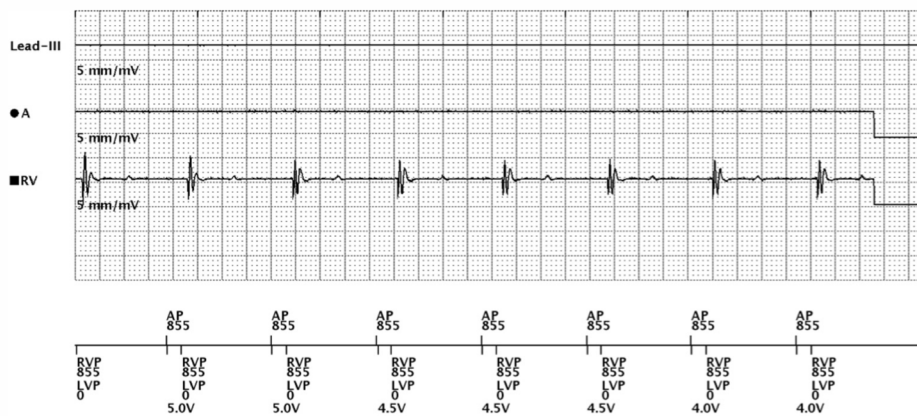


Abb. 2112.23 a isolierter, irregulärer, langsamer Rhythmus im rechten Herzohr. b isoliertes Signal im linken Herzohr, intermitt. lokales Capture vom hdM. c Kein atriales Capture bei Pacing mit 5,0 Volt

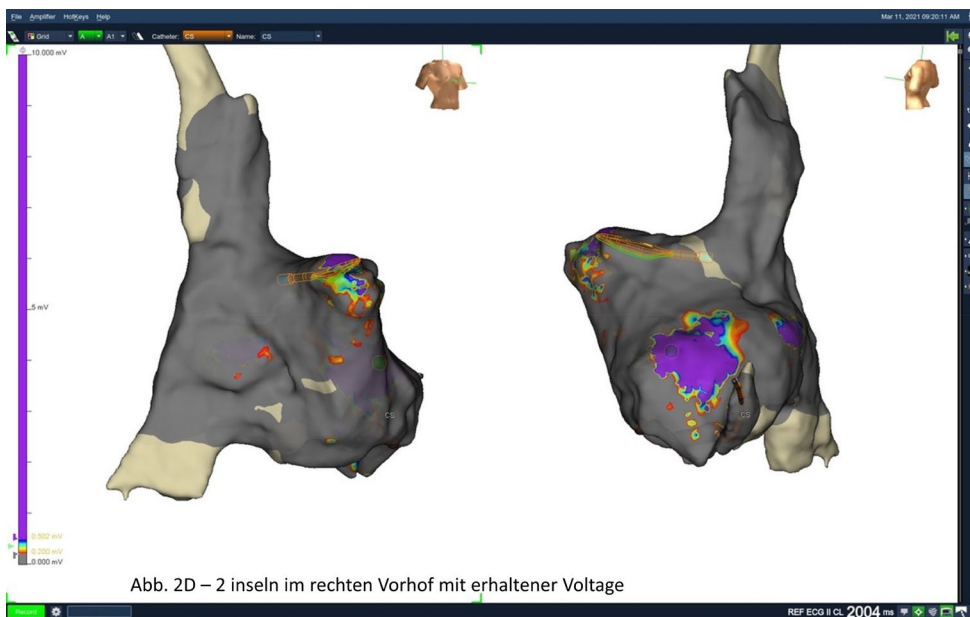


Abb. 2112.23 Fortsetzung d 2 Inseln im rechten Vorhof mit erhaltener Voltage

Methoden: Das Sensing ging offensichtlich schon 2017 verloren (Abb. 1A). 2019 bezog sich die automatische Messung wohl auf das isolierte Potential im rechten Herzohr (Abb. 1B). Die Vorhoffarrhythmie wurde vom Schrittmacher nicht mehr erkannt, der AT-Burden war 0 % und der Pat. wurde fälschlicherweise im Atrium stimuliert. Dass die Vorhoffarrhythmie aber weiterhin persistierte, wäre leicht aus dem Oberflächen-EKG zu diagnostizieren gewesen. Im September 2021 klagt der Pat. über Atemnot bei Belastung und wird zur elektrischen Cardioversion aufgenommen, weil auswärts im Oberflächen-EKG Vorhofflattern zu erkennen ist (Abb. 1C) und die Vermutung bestand, dass die „neuaufgetretene Arrhythmie“ die Ursache für die klinische Verschlechterung ist. Die CV wird nicht durchgeführt, weil man rätselt, wie die EGMs zu interpretieren sind (Abb. 1D.) Da der Schrittmachergenerator sich ERI nähert (5 Mo) Entschluss zur elektrophysiologische Untersuchung (EPU) mit 1. hochauflösendem Mapping des rechten Atriums (RA) zur Klärung des Tachykardiemechanismus mit Option auf Ablation, sollte ein rechtsatrialer Reentrykreis vorliegen. 2. Versuch die Frage zu klären, welches Signal bei fehlendem Sensing immer wieder erkannt wird, 3. um die Frage zu beantworten, warum es zum loss of capture kam. 4. Einen Ortes im rechten Atrium festzulegen, wo gegebenenfalls adäquates Sensing und Pacing möglich wäre.

Resultate: Elektrophysiologische Untersuchung am 11.03.2021: Im stark vergrößerten rechten Vorhof finden sich trotz des hochauflösenden Maps (45.000 Punkte) mit dem high density-Mappingkatheter (hdM) nur mehr an 3 kleinen Stellen Signale: Im rechten Herzohr Nachweis eines isolierten, niedrigamplitudigen Signals mit einer Frequenz von 22–33/min (Abb. 2A). Bei Pacing von den Bipolen mit den höchsten Signalamplituden (SA) intermitt. lokales Capture (Abb. 2B). Bei atrialer Stimulation von der SM-Sonde (Abb.) kein lokales Capture (Abb. 2C). Anteriorseptal Nachweis eines umschriebenen Arealen von ca. 3 cm² mit SA bis zu max. 2 mV (Abb. 2D) In diesem Bereich Ableitung der linksatrialen Makroreentry-tachykardie LAMRT und posterior zwischen Mündung der V. Cava superior und inferior ein zweites kleineres, ca. 1 cm² großes Areal ebenfalls mit SA von ca. 2 mV ebenfalls Ableitung der LAMRT. Obwohl lokales Capture bei Stimulation vom hdM in beiden Arealen möglich ist, gelingt es nicht, die Makroreentry-tachykardie zu terminieren. Eine Positionierung einer atrialen Schraubsonde in dieses Areal wäre prinzipiell möglich.

Schlussfolgerungen: Aufgrund des EPU-Befundes, des NT-Pro BNP-Wertes und der milden Symptomatik des Patienten, nahmen wir nach frustrierten Versuch die Arrhythmie mit Ibutilid i. v. zu terminieren, von einer elektrischen Cardioversion Abstand und trafen die Entscheidung, beim anstehenden Generatorwechsel auf die Revision der atrialen Sonde zu verzichten. Differentialdiagnostisch könnte das isolierte Signal im RAA am ehesten einem langsamen Fokus aus dem RAA (komplett umringt von Narbe) oder der Ableitung des kranken Sinusknotens, erregt über epikardiale Fasern, entsprechen. Bei Auftreten von atrialen Sensingproblemen und Diskrepanzen zwischen Oberflächen-EKG und Schrittmacher-EGMs kann ein hochauflösendes Mapping des rechten Vorhofs zur Problemlösung sehr nützlich sein. Wenn Schrittmacher- oder ICD-Kontrollen in der Klinik stattfinden, sollte ein 12-Ableitungs-EKG nicht fehlen.

12.24

Ventricular tachyarrhythmias in patients with Micra™ leadless cardiac pacemakers—a safety study with implantable loop recorders

D. Kiblböck¹, K. Saleh¹, S. Schwarz¹, C. Reiter¹, A. Fellner¹, J. Ebner¹, J. Bötscher¹, J. Maier¹, J. Kellermair¹, A. Nahler¹, C. Steinwender¹, H. Blessberger¹

¹Department of Cardiology, Kepler University Hospital, Medical Faculty, Johannes Kepler University, Linz, Austria

Introduction: Several studies have demonstrated high implantation success rates and low device-related complication rates with stable pacing thresholds and sensing values for Micra™ leadless cardiac pacemakers (LCP). However, malignant ventricular tachyarrhythmias caused by suspected proarrhythmic effects of LCP leading to life-threatening critical conditions were recently described in case reports.

Methods: The aim of this single-center study was to investigate the incidence of ventricular tachyarrhythmias in patients with Micra™ LCP during the index stay and after hospital discharge with implantable loop recorders (ILR).

Results: No sustained ventricular tachyarrhythmias occurred in 283 patients with Micra™ LCP during the index stay after implantation. Eleven of these patients were monitored with an ILR over a median follow up duration of 22.9 months (IQR 5.7–31.5 months). ILR interrogations revealed no ventricular tachyarrhythmias (nsVT: $n=0$, VT: $n=0$, VF: $n=0$). Pacing thresholds and sensing values of the LCP remained stable, whereas battery capacity and electrode impedance declined over time. The ILR did not detect any malfunctions of the LCP (asystole >3 seconds: $n=0$, bradycardia <40/min: $n=0$). No serious adverse events (syncope, stroke, pericardial effusion) occurred during the follow-up period.

Conclusion: In this single-center study no episodes of ventricular tachyarrhythmias were detected in patients with Micra™ LCP during the index stay after implantation and after hospital discharge by ILR. Further large-scale prospective studies are warranted to exclude pro-arrhythmogenic effects of LCP.

12.25

coolloop® cryoablation for treatment of atrial fibrillation

F. Hintringer¹, T. Senoner¹, F. Barbieri¹, A. Adukauskaitė¹, A. Rubatscher¹, W. Dichtl¹, D. Simon²

¹Medizinische Universität Innsbruck, Universitätsklinik für Innere Medizin III/Kardiologie & Angiologie, Innsbruck, Austria

²afreeze GmbH, Innsbruck, Innsbruck, Austria

Introduction: The coolloop® cryoablation system for treatment of atrial fibrillation (AF) is designed for wide area circumferential lesions at the pulmonary veins (PV) without interruption of the blood flow. Due to cryogenic temperatures below -80 °C in the loop, very fast adherence to the tissue and extremely fast thawing are achieved. This study evaluated for the first time safety and procedural parameters of the coolloop® cryoablation system in a routine setting. The second objective

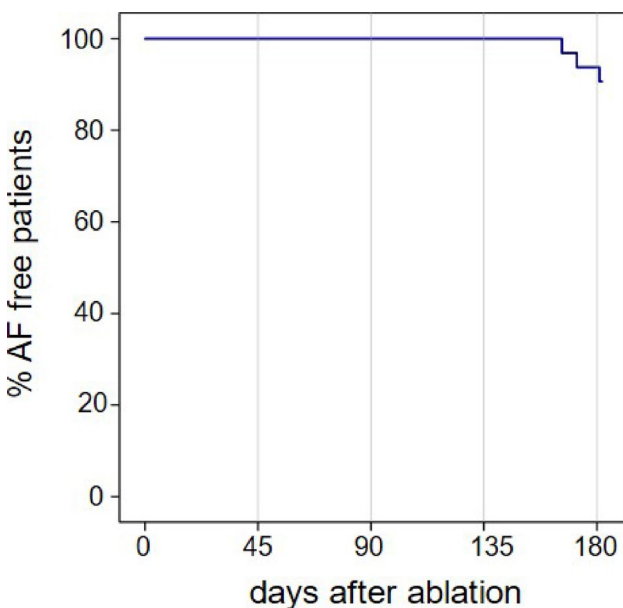


Fig. 112.25 Freedom from atrial fibrillation after 6 months of follow up

Measure	% (n)
Adverse Events (AEs)	13.5 (5)
coolloop® related	0.0 (0)
procedure related	5.4 (2)
Serious Adverse Events (SAEs)	8.1 (3)
coolloop® related	0.0 (0)
procedure related	2.7 (1)

Fig. 212.25 Adverse events

of the study was to evaluate the freedom from atrial arrhythmias over a 6-month follow-up period.

Methods: After establishing the coolloop® cryoablation system as one of the routine treatment regimens at our institution, 37 consecutive patients with paroxysmal AF were treated as part of the Cool-TreatS study. Three freezes of 180 seconds each were applied per vein. For each application, the cryo-loop was rotated by approx. 120°. If the PV was not isolated, additional freezes of 90 to 180 seconds were applied. 6-months follow-up data are available for a total of 32 patients.

Results: Out of 144 treated PVs, 135 PVs (94%) could be isolated with the coolloop®. The median total procedure time was 161 min [range 97–275 min]. Mean coolloop® procedure time was 122.6 ± 25 min, mean fluoroscopy time was 25.8 ± 6.8 min. There were 2 adverse events and 1 serious adverse event that were classified as procedure related, but without relation to the coolloop® cryoablation system. After a follow-up period of 6 months, 27 out of 32 patients (84%) were AF-free after a single procedure.

Conclusion: Treatment of atrial fibrillation with the coolloop® catheter is safe. Procedural efficacy, procedural parameters, and 6-months follow-up data are comparable to similar devices and very promising for an ablation system that has just recently been introduced to clinical practice.

12.26

C-reactive protein is a promising indicator of ventricular arrhythmias in pacemaker patients

P. Jirak¹, B. Wernly¹, L. Hinterbuchner¹, V. Paar¹, L. Hauptmann¹, D. Fejzic¹, A. Topf¹, U. Hoppe¹, M. Lichtenauer¹, J. Kraus¹, C. Scherthaner¹, B. Strohmer¹, L. Motloch¹

¹Uniklinikum Salzburg, Salzburg, Austria

Background: Ventricular tachyarrhythmias are the main reason for sudden cardiac death to date. Accordingly, tools for risk stratification for ventricular arrhythmias are paramount. Non-sustained ventricular tachycardia (nsVT) represents a predictor of malignant rhythm disorders. Recently, low grade chronic inflammation was shown to predict ventricular arrhythmic events in high risk patients.

Aims: This study aims to investigate, if inflammatory markers may predict higher arrhythmia burden in a low risk population.

Methods: We prospectively analyzed ventricular arrhythmia burden in pacemaker records of 166 patients (age 79.2 ± 9.3; male 60.2%, 38 with coronary artery disease (CAD)) with preserved ejection fraction (left ventricular ejection fraction ≥ 50%)

during a annually pacemaker follow up in a single center. To evaluate potential predictive factors, associations of laboratory values including inflammatory markers (CRP and interleukin 6) with occurrence of nsVT was evaluated using logistic regression. Sensitivity analysis in patients with and without established CAD was performed.

Results: The cumulative incidence of nsVT was 12.7%. Concentrations of BNP (OR 1.00 95 %CI 0.99-1.01; $p=0.46$), troponin (OR 0.98 95 %CI 0.95-1.02; $p=0.43$) or interleukin-6 (OR 1.03 95 %CI 0.99-1.07; $p=0.16$) were not associated with the occurrence of nsVTs. However, the concentration of CRP was associated with increased odds of nsVT (OR 1.26 95 %CI 0.97-1.64; $p=0.09$) in trend. In sensitivity analysis in CAD patients, CRP was associated with increased likelihood of nsVT (OR 3.89 95 %CI 1.14-13.29; $p=0.03$), whereas in patients without CAD there was no association between CRP and rates of nsVTs (OR 1.16 95 %CI 0.88-1.54; $p=0.30$).

12.27

Nachweis von verzögert auftretendem AV-Block III° nach transfemoralem Aortenklappenersatz mittels Loop-Recorder

C. Reiter¹, T. Lambert¹, J. Kellermair¹, H. Blessberger¹, A. Fellner¹, A. Nahler¹, M. Grund¹, J. Ebner¹, J. Bötscher¹, S. Rechberger¹, C. Steinwender¹

¹Kepler Universitätsklinikum Linz, Linz, Österreich

Einleitung: Bei älteren PatientInnen mit hochgradiger symptomatischer Aortenklappenstenose ist der transfemorale Aortenklappenersatz (TAVI) eine etablierte Therapieoption. Dieser ist allerdings mit einem weiterhin beträchtlichen Risiko für das Auftreten höhergradiger AV-Blockierungen assoziiert. Im Rahmen eines Konsensus-Papiers wurde der verzögert-auftretende komplette AV-Block (DT-AVB) mit einem Auftreten >48 h nach TAVI definiert.

Methoden: Im Zuge einer prospektiven klinischen Single-Center-Studie wurde bei PatientInnen, die sich einer TAVI unterzogen und bei welchen es bis zu 48 Stunden nach der Intervention nicht zum Auftreten eines anhaltenden bzw. rezidivierenden kompletten AV-Blocks kam, eine Loop-Recorder-Implantation zum kontinuierlichen EKG-Monitoring durchgeführt. Zur Evaluation möglicher Prädiktoren erfolgte im Rahmen der TAVI-Prozedur auch eine simultane elektrophysiologische Messung der AH- und HV-Intervalle mittels Platzierung eines His-Katheters über eine Femoralvene.

Resultate: Im Zuge der Studie wurden insgesamt 59 PatientInnen (36 Frauen, 23 Männer) mit einem mittleren Alter von 80,3 Jahren rekrutiert. Im Rahmen des einjährigen Follow-Up konnte bei 7 (11,9%) PatientInnen ein DT-AVB dokumentiert werden, welcher bei allen eine Schrittmacherimplantation zur Folge hatte. Bei 5 (71,4%) dieser PatientInnen konnte der AV-Block nur mittels Loop-Recorder und nicht mittels 12-Kanal-EKG nachgewiesen werden. Jene PatientInnen mit DT-AVB zeigten hierbei eine fast 4-mal höhere Zunahme der PQ-Dauer bzw. eine knapp 3-mal höhere Zunahme des HV-Intervalls als jene ohne dokumentiertem DT-AVB. Sowohl die Zunahme der PQ-Dauer zwischen dem EKG vor der Prozedur und 48 Stunden nach TAVI (OR 1,04 (95 % CI 1,01-1,09), $p=0,032$) als auch die intraprozedurale Zunahme des HV-Intervalls (OR 1,07 (95 % CI 1,02-1,14), $p=0,015$) erwiesen sich als signifikante Prädiktoren für das Auftreten eines DT-AVB.

Schlussfolgerungen: Innerhalb von 12 Monaten nach TAVI zeigte sich mit 11,9% ein erheblicher Anteil an verzögert aufgetretenen kompletten AV-Blöcken, welcher in 71,4% der Fälle lediglich mittels Loop-Recorder dokumentiert werden konnte. Die intraprozedurale Zunahme des HV-Intervalls und die Zunahme der PQ-Dauer im Vergleich zwischen jenem EKG am Tag vor bzw. 48 Stunden nach der Klappenintervention erwiesen sich als signifikante Prädiktoren.

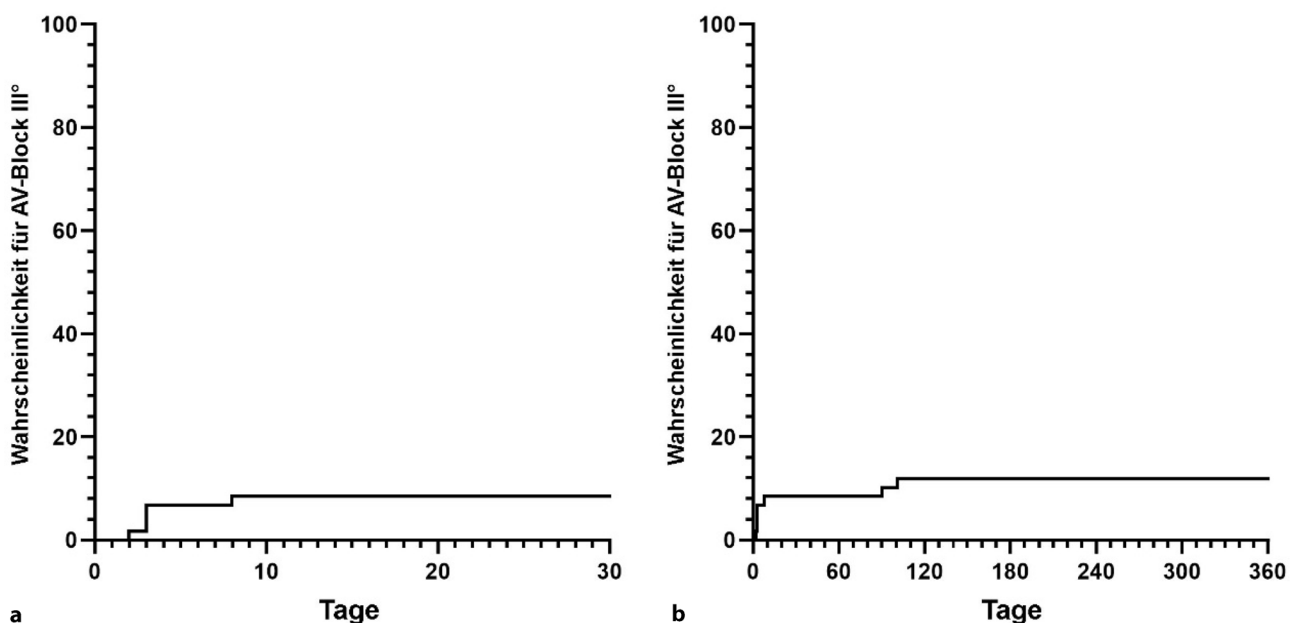


Abb. 112.27 Kaplan-Meier-Kurve mit Darstellung der Wahrscheinlichkeit des Auftretens eines DT-AVB im zeitlichen Verlauf der ersten 30 Tage nach TAVI (a) bzw. des gesamten 12-Monats-Follow-Ups (b)

Tab. 1112.27 Vergleich von PatientInnen mit aufgetretenem DT-AVB vs. jenen ohne DT-AVB

Parameter	Kein DT-AVB (n=52)	DT-AVB (n=7)	p
Alter (Jahre)	80,27 ± 4,25	80,43 ± 5,03	0,979
Euro Score (Punkte)	5,13 ± 3,62	4,10 ± 3,78	0,341
Klappenöffnungsfläche (cm ²)	0,65 ± 0,18	0,60 ± 0,14	0,492
Prothesengröße (mm)	28,4 ± 2,98	28,3 ± 3,04	0,943
Mittlerer Durchmesser des Aortenanus (mm)	23,72 ± 2,51	24,30 ± 1,77	0,464
Mittlerer LVOT-Durchmesser (mm)	23,61 ± 2,77	23,58 ± 2,80	0,841
Calciumscore (Einheiten)	3033 ± 1584	4059 ± 1664	0,081
Implantationstiefe (mm)	0,65 ± 0,39	0,69 ± 0,36	0,841
PQ BL (ms)	179,5 ± 31,4	198,0 ± 42,7	0,254
PQ PT (ms)	188,3 ± 32,0	221,7 ± 45,4	0,049
PQ +2 (ms)	192,1 ± 27,1	243,1 ± 77,1	0,045
PQ Delta +2 vs. BL (ms)	12,3 ± 22,0	45,1 ± 44,9	0,015
AH BL (ms)	100,5 ± 29,3	136,1 ± 36,5	0,017
AH PT (ms)	100,8 ± 25,4	142,9 ± 45,7	0,019
AH Delta PT vs. BL (ms)	1,1 ± 15,7	6,7 ± 19,9	0,715
HV BL (ms)	55,7 ± 16,6	50,9 ± 10,5	0,436
HV PT (ms)	66,1 ± 15,2	78,7 ± 22,9	0,135
HV Delta PT vs. BL (ms)	10,3 ± 13,9	27,9 ± 21,1	0,049
QRS BL (ms)	107,0 ± 27,8	104,3 ± 28,2	0,868
QRS PT (ms)	137,1 ± 29,4	143,6 ± 38,1	0,619
QRS Delta PT vs. BL (ms)	29,8 ± 23,4	39,3 ± 25,1	0,471

12.28**Impact of high density mapping using a grid shaped catheter with orthogonal signal analysis on ventricular tachycardia ablation strategy**

I. Roca-Luque¹, F. Lorgat², J. Lacotte³, H. Haqqani⁴, F. X. Roithinger⁵, L. Fiedler⁵, A. Miller⁶, D. Steven⁷

¹Hospital Clínic de Barcelona · Arrhythmia Unit. ICCV, Barcelona, Spain

²Christiaan Barnard Memorial Hospital, Cape Town, South Africa

³Institut Cardiovasculaire Paris Sud, Paris, France

⁴The Prince Charles Hospital, Brisbane, Australia

⁵2. Medizinische Abteilung Kardiologie/Nephrologie/Intensivmedizin, Wiener Neustadt, Austria

⁶Abbott, Minneapolis, United States

⁷University Hospital Köln, Köln, Germany

Introduction: Ventricular tachycardia (VT) in patients with structural heart disease (SHD) is related to scar and slow conduction areas. Substrate-based ablation has become the gold standard treatment in patients with SHD-related refractory VT. A new high-density grid shaped catheter that allows simultaneous analysis of adjacent orthogonal bipolar signals can allow better understanding of these slow conduction areas with the potential to improve ablation results. This was a prospective, multicenter observational study to characterize the utility of electroanatomical mapping with a high density grid-style mapping catheter (HD Grid) in subjects undergoing catheter ablation for ventricular tachycardia (VT) in real-world clinical settings.

Methods: During the study period, patients who underwent VT ablation using the HD Grid catheter as the primary mapping

catheter were included. Comparisons both during the procedure and retrospectively were performed between conventional electrode configuration maps and simultaneous orthogonal bipole electrode configuration maps. The influence of these different configurations on ablation strategy was analyzed.

Results: During study period (January 2019–April 2020) 57 maps were performed in 34 VT subjects (average age: 64.3 yr, male: 85.3 %, ischemic cardiomyopathy: 70.6 %). The left ventricle was mapped in 94.1 % of subjects, including left ventricular outflow tract and papillary muscles in 20.6 % and 8.8 % respectively, reporting minimal or no ectopic beats in 97.1 % of the subjects. The total number of mapping points collected was 14172.0 ± 15174.8 in 24.3 ± 17.9 min per map. Simultaneous orthogonal bipole mapping identified differences in 67.6 % of maps compared to linear along-the-spline electrode configurations. The differences consisted mainly in the surface area (92 %) and location of low voltage (40 %). When compared during the procedure, simultaneous orthogonal bipole mapping was used to identify ablation strategy in 100 % of cases. When compared to a standard along-the-spline configuration retrospectively, the ablation strategy identified with simultaneous orthogonal bipoles was different in 30.1 % of cases. The ablation strategy used in these subjects was mainly substrate ablation (late potentials and low voltage areas in scar regions) with an acute success rate of 97.1 %.

Conclusion: The use of the HD Grid catheter with the ability to analyze orthogonal signals is feasible and has the potential to change the ablation strategy in one third of VT patients with a high acute success rate.

12.29

Incidence and risk factors for acute kidney injury in patients with cardiac implantable electronic devices undergoing transvenous lead removal

C. Edlinger¹, M. Bannehr¹, T. Kücken¹, A. Haase-Fielitz¹, C. Butter¹

¹Herzzentrum Brandenburg; Bernau/Berlin, Berlin, Germany

Introduction: Patients with cardiac implantable electronic devices (CIED) carry several risk factors for acute kidney injury (AKI). However, little is known about the incidence of AKI and whether there are procedure-related or potential modifiable risk factors for the development of AKI after transvenous lead removal. This study aimed to investigate the incidence and risk factors of AKI in patients with CIED admitted for transvenous lead removal.

Methods: In this observational cohort study, data from 147 consecutive patients undergoing transvenous lead removal were analyzed. Primary endpoint was AKI according to KDIGO criteria. Multivariable logistic regression analysis was performed to identify independent risk factors for AKI.

Results: Lead removal was performed due to isolated pocket infection (34.7%), systemic infection (49.3%), pocket or lead perforation without infection (13.9%) and endocarditis (2.1%). Out of 147 patients 34 (23.1%) developed AKI (82.4% stage 1, 8.8% stage 2 and 8.8% stage 3). In-hospital mortality was 8.2%. Defibrillator lead type (HR 24.55, CI 2.41–249.97, $p=0.007$), necessity to perform laser-assisted lead removal (HR 5.41, CI

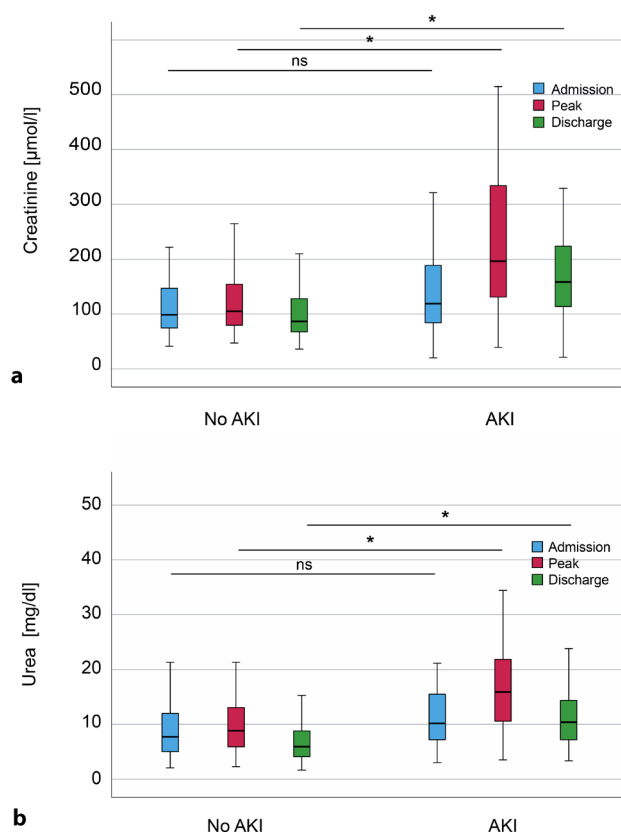


Fig. 112.29 Serum creatinine and urea levels (at admission, peak and at discharge) in patients with and without acute kidney injury (AKI). ns=non-significant, *= p -value ≤ 0.05

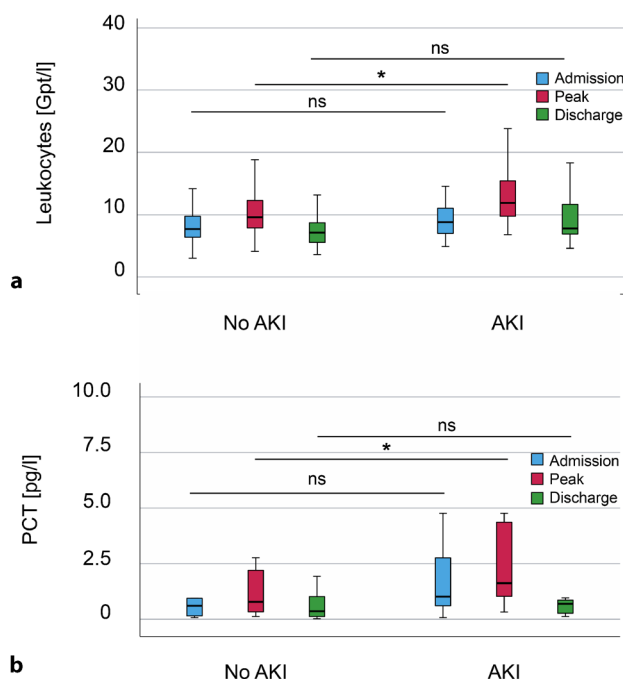


Fig. 212.29 Leukocytes and procalcitonin (PCT) values (at admission, peak and at discharge) in patients with and without acute kidney injury (AKI). ns=non-significant, *= p -value ≤ 0.05

1.12–26.13, $p=0.035$) and time from initial implantation to lead removal (HR 1.01, CI 1.00–1.02, $p=0.013$) were independent risk factors for AKI. Also, AKI was independently associated with in-hospital mortality (HR 8.439, CI 2.08–34.33, $p=0.003$).

Conclusion: Almost a quarter of patients undergoing transvenous lead removal developed AKI. Defibrillator lead type, necessity to perform laser-assisted lead removal and time from initial implantation to lead removal were risk factors for AKI, while AKI itself was associated with increased in-hospital mortality.

12.30

Working on the dirty side—the ipsilateral subclavian access for temporary pacing after lead extraction

D. Zweiker¹, F. Melillo², G. D’Angelo¹, A. Radinovic¹¹, A. Marzi¹, C. Lorenzo³, S. Altizio⁴, L. R. Limite¹, G. Paglino¹, A. Frontera¹, K. Nakajima¹, P. Della Bella¹, P. Mazzone¹

¹Department of Cardiac Electrophysiology and Arrhythmology, IRCCS San Raffaele Scientific Institute, Vita-Salute University and San Raffaele Hospital, Milan, Italy

²Department of Cardiovascular Imaging, IRCCS San Raffaele Scientific Institute, Vita-Salute University and San Raffaele Hospital, Milan, Italy

³Cardiac Rehabilitation Unit, IRCCS San Raffaele Scientific Institute, Milan, Italy

⁴Department of Anesthesia and Intensive Care, IRCCS San Raffaele Scientific Institute, Vita-Salute University and San Raffaele Hospital, Milan, Italy



Fig. 1 | 12.30

Introduction: Temporary pacing is necessary in pacemaker-dependent patients after transvenous lead extraction (TLE) for cardiac implantable electronic device infection. We propose to use the ipsilateral subclavian access (ISA) combined with a standard permanent active fixation lead for the temporary pacemaker (Fig. 1).

Methods: We consecutively enrolled patients undergoing TLE that received a temporary pacemaker using the ISA between August 2016 and April 2020 at our centre.

Results: During the observation period, 36 patients undergoing TLE for pocket infection (72.2%), endocarditis (25.0%) or other causes received a temporary pacemaker over the ISA. Mean age was 77.0 ± 10.7 years and 13.9% were female. Complete TLE could be achieved in 95.6% of leads. There were no major periprocedural complications. Intra-hospital mortality was 11.1% and major complications occurred in 30.6%. During long-term follow-up (23 ± 13 months), 8.3% had a relapse of local infection and 2.8% needed rehospitalization for re-intervention.

Conclusion: Temporary pacing using a standard permanent active fixation lead using the ISA was safe, with a low incidence of reinfections.

13 RISIKOFAKTOREN/ STOFFWECHSEL/LIPIDE

13.1

The new myokine myonectin is significantly associated with Type 2 diabetes in elderly patients

A. Leiherer¹, A. Muendlein², K. Geiger², C. H. Saely¹, B. Larcher³, A. Mader³, M. Maechler², L. Sprenger², B. Mutschlechner², M. Benda², P. Fraunberger⁴, H. Drexel²

¹Private University of the Principality of Liechtenstein, Triesen, Liechtenstein

²Vorarlberg Institute for Vascular Investigation & Treatment (VIVIT), Feldkirch, Austria

³Department of Medicine I, Academic Teaching Hospital Feldkirch, Feldkirch, Austria

⁴Medical Central Laboratories Feldkirch, Feldkirch, Austria

Introduction: The novel myokine myonectin is predominantly expressed in skeletal muscle and is involved in the regulation of metabolic homeostasis. A putative association between myonectin and type 2 diabetes mellitus (T2 DM) has been discussed controversially in current literature. The association between myonectin and T2 DM at different ages is still obscure and thus is addressed in the present study.

Methods: We measured myonectin in 410 vascular risk patients with a mean age of 66 years. Myonectin did not correlate with age ($r = -0.19$; $p = 0.697$).

Results: From our patients 219 (53%) were >65 years, with a mean age of 74 years and $191 \leq 65$ years, with a mean age of 57 years. The prevalence of T2 DM was 40.6% vs. 42.4% in the older as compared to the younger age group. Myonectin concentrations were significantly decreased in elderly patients with T2 DM compared to non-diabetic subjects (1.8 vs. 4.2 ng/ml; $p = 0.002$), whereas no significant difference was observed in younger patients (2.6 vs. 2.3 ng/ml; $p = 0.183$). Concordantly, regression analysis revealed an unadjusted odds ratio (OR) of 0.24 [0.07–0.81] ($p = 0.021$) for the association between myonectin and T2 DM in elderly patients but not in younger patients (OR = 1.08 [0.80–1.45]; $p = 0.609$). The association between myonectin and T2D; remained significant after adjusting for sex, body mass index, LDL cholesterol, HDL cholesterol, current smoking, as well as statin intake in elderly but remained non-significant in younger patients (OR = 0.23 [0.07–0.81]; $p = 0.021$ vs. OR = 1.05 [0.76–1.46]; $p = 0.769$).

Conclusion: We conclude that plasma myonectin levels are significantly associated with T2 DM, particularly in elderly vascular risk patients.

13.2

Long-term physical activity modulates adipsin and ANGPTL4 serum levels, a potential link to the lipid metabolism

M. Lenz¹, R. Schönbauer¹, S. Stojkovic¹, M. Lichtenauer², V. Paar², C. Gatterer¹, C. Schukro¹, M. Emich³, M. Fritzer-Szekeres⁴, J. Strametz-Juraneck⁵, M. Sponder¹

¹Innere Medizin II, Abteilung für Kardiologie, Meduni Wien, Wien, Austria

²Paracelsus Medical University of Salzburg, Department of Cardiology, Salzburg, Austria

³Austrian Federal Ministry of Defence, Austrian Armed Forces, Vienna, Austria

⁴Labor Medizin, Meduni Wien, Vienna, Austria

⁵Rehabilitation Centre Bad Tatzmannsdorf, Bad Tatzmannsdorf, Austria

Introduction: Within the presented prospective study, we aimed to illuminate the effect of long-term physical exercise on serum levels of adipsin and angiotensin-like 4 (ANGPTL4). Although past studies already outlined the effects of acute exercise, our trial design aimed to depict the development under long-term physical activity conditions.

Methods: 98 participants were included in the study and were asked to perform eight months of moderate physical activity for at least 150 minutes/week and/or vigorous-intensity exercise for at least 75 minutes/week. According to initial performance and performance gain throughout the study period, four groups were formed and subsequently compared. Blood sampling for the determination of routine laboratory parameters was done at baseline, after 2, 6, and 8 months. Additionally, adipsin and ANGPTL4 serum levels were concurrently quantified using commercially available ELISA kits.

Results: The study cohort consisted of 98 participants (61.2 % male) with an average age of 49.3 ± 6.7 years. Adipsin and ANGPTL4 were found to be strongly influenced by long-term physical exercise. Participants displaying a performance gain of >2.9 % throughout the study showed significantly increased serum levels of both biomarkers.

Conclusion: Serum levels of adipsin and ANGPTL4 were closely tied to the individual performance gain of the participating probands. An association of adipsin levels, initial performance, and serum triglycerides was found at baseline. Interestingly, this interrelationship was not detectable after eight months of physical training. This finding might indicate adipsin's involvement in linking triglyceride-balance to individual performance and energy demands in a homeostatic state.

13.3

Correlation of cholesterol efflux capacity with femoral and carotid plaque volume

M. Noflatscher¹, M. Hunjadi², M. Schreinlechner¹, P. Sommer¹, P. Deutingner³, D. Lener¹, F. Mair¹, M. Theurl¹, K. Rudolf¹, A. Bauer¹, A. Ritsch², P. Marschang⁴

¹Medizinische Universität Innsbruck, Kardiologie und Angiologie, Innsbruck, Austria

²Medizinische Universität Innsbruck, Gentherapie, Innsbruck, Austria

³Medizinische Universität Innsbruck, Innsbruck, Austria

⁴Zentralkrankenhaus Bozen, Innere Medizin, Bozen, Italy

Introduction: Introduction: Atherosclerosis is a systemic multifocal disease that can cause the narrowing and occlusion of arteries resulting in cardiovascular disease (CVD). Hypercholesterolemia plays a pivotal role in the pathogenesis of atherosclerotic plaques by the accumulation of cholesterol in the arterial wall. Cholesterol efflux mediated by HDL is capable of transporting cholesterol from the periphery back to the liver in a process called reverse cholesterol transport. Cholesterol efflux capacity (CEC) is inversely correlated with cardiovascular risk and has been proposed as a surrogate marker for reverse cholesterol transport. In this study, we set out to study a possible association between CEC and peripheral plaque volume.

Methods: Methods: Since lipid lowering therapy interferes with CEC, we studied a subset of 177 patients (median age 64; 48.6 % women) without lipid-lowering medication that had been included in a study of 443 patients with at least one cardiovascular risk factor or established CVD. CETP-mediated cholesterol ester transfer was measured by quantifying the transfer of cholesterol ester from radiolabelled exogenous HDL to apoB-containing lipoproteins. CEC was determined using cAMP treated 3H-cholesterol-labeled J774 cells. Plaque volume in the carotid and the femoral artery was measured using a 3D ultrasound system equipped with a semi-automatic software.

Results: Results We found a strong inverse correlation between CEC and high total plaque volume ($p=0.027$) in patients without lipid-lowering therapy. On the other hand, there was no correlation between LDL cholesterol, lipoprotein(a) and CETP-mediated cholesterol ester transfer.

Conclusion: Conclusion CEC correlates inversely with peripheral atherosclerosis in patients not taking lipid-lowering therapy, further strengthening its role as a cardiovascular biomarker.

13.4

Type 2 diabetes and congestive heart failure are mutually independent predictors of the presence of albuminuria

M. Maechler¹, A. Vonbank², B. Larcher², A. Mader², L. Sprenger¹, B. Mutschlechner¹, M. Benda¹, A. Leihner³, A. Muendlein¹, H. Drexel¹, C. H. Saely³

¹Vorarlberg Institute for Vascular Investigation & Treatment (VIVIT), Feldkirch, Austria

²Department of Medicine I, Academic Teaching Hospital Feldkirch, Feldkirch, Austria

³Private University of the Principality of Liechtenstein, Triesen, Liechtenstein

Introduction: Albuminuria is a well-known characteristic of diabetic nephropathy and it is also present in a large portion of patients with congestive heart failure (CHF). However, the single and joint effects of type 2 diabetes mellitus (T2 DM) and CHF on albuminuria are unknown. This issue therefore was addressed in the present study.

Methods: We investigated 180 patients with CHF, of whom 83 had T2 DM (CHF+/T2 DM+) and 97 did not have diabetes (CHF+/T2 DM-) and 223 controls without CHF, of whom 39 had T2 DM (CHF-/T2 DM+) and 184 did not have diabetes (CHF-/T2 DM-).

Results: The prevalence of albuminuria was lowest in CHF-/T2 DM- subjects (8.7%). When compared to this group it was significantly higher in CHF-/T2 DM+ (23.1%, $p=0.010$), CHF+/T2 DM- (38.1%, $p<0.001$) and CHF+/T2 DM+ patients (62.7%, $p<0.001$). It was highest in CHF+/T2 DM+ patients, in whom it was higher than in CHF-/T2 DM+ ($p<0.001$) and in CHF+/T2 DM- ($p=0.001$) patients; a trend towards a higher prevalence of albuminuria in CHF-/T2 DM+ patients vs. CHF+/T2 DM- patients did not reach statistical significance ($p=0.093$). In logistic regression analysis, CHF and T2 DM were mutually independent predictors of albuminuria, when adjusted for age, sex, body mass index, LDL cholesterol, history of smoking and hypertension, as well as for the use of statins and ACE inhibitors/angiotensin II receptor blockers (OR 2.57 [95% CI 1.47–4.51]; $p=0.001$ and OR 4.15 [2.18–7.88]; $p<0.001$, respectively).

Conclusion: We conclude that T2 DM and CHF are mutually independent predictors of albuminuria.

13.5

Type 2 diabetes and risk of major cardiovascular events in peripheral artery disease versus coronary artery disease patients

C. H. Saely¹, A. Vonbank², B. Larcher², A. Mader², M. Maechler³, L. Sprenger³, B. Mutschlechner³, M. Benda³, A. Leihner¹, A. Muendlein³, H. Drexel³

¹Private University of the Principality of Liechtenstein, Triesen, Liechtenstein

²Department of Medicine I, Academic Teaching Hospital Feldkirch, Feldkirch, Austria

³Vorarlberg Institute for Vascular Investigation & Treatment (VIVIT), Feldkirch, Austria

Introduction: The prevalence of type 2 diabetes (T2 DM) is higher in peripheral artery disease (PAD) than in coronary

artery disease (CAD) patients, and PAD overall confers higher cardiovascular risk than CAD. How the incidence of major cardiovascular events compares between PAD and CAD patients when analyses are stratified by the presence of type 2 diabetes (T2 DM) is unclear and is addressed in the present study.

Methods: We prospectively recorded major cardiovascular events and death over 10.0 ± 4.7 years in 923 patients with stable CAD, of whom 26.7% had T2 DM and in 292 patients with PAD, of whom 42.1% had T2 DM. Four groups were analyzed: CAD patients without diabetes (CAD/T2 DM-; $n=677$), CAD patients with T2 DM (CAD/T2 DM+; $n=246$), PAD patients without diabetes (PAD/T2 DM-; $n=169$) and PAD patients with T2 DM (PAD/T2 DM+; $n=123$).

Results: When compared to the incidence of MACE in CAD+/T2 DM- patients (25.1%), it was significantly higher in CAD+/T2 DM+ patients (35.4%; $p<0.001$), in PAD+/T2 DM- patients (30.2%; $p=0.022$) and in PAD+/T2 DM+ patients (47.2%; $p<0.001$). Patients with both PAD and T2 DM in turn were at a higher risk than CAD+/T2 DM+ or PAD+/T2 DM- patients ($p=0.001$ and $p<0.001$, respectively). The incidence of MACE did not differ significantly between PAD+/T2 DM- and CAD+/T2 DM+ patients ($p=0.413$). Compared to patients with CAD, Cox regression analyses after multivariate adjustment showed an adjusted hazard ratio of 1.46 [1.14–1.87], $p=0.002$ for the presence of PAD. Conversely, T2 DM increased the risk of MACE after multivariate adjustment in CAD and PAD patients (adjusted HR 1.58 [1.27–1.98], $p<0.001$).

Conclusion: In conclusion, our data show that T2 DM and the presence of PAD are mutually independent predictors of MACE. Patients with both PAD and T2 DM are at an exceedingly high risk of MACE.

13.6

Congestive heart failure and the metabolic syndrome are mutually independent predictors of non-alcoholic fatty liver disease

M. Maechler¹, A. Vonbank², B. Larcher², A. Mader², L. Sprenger¹, B. Mutschlechner¹, M. Benda¹, A. Leihner³, A. Muendlein¹, H. Drexel¹, C. H. Saely³

¹Vorarlberg Institute for Vascular Investigation & Treatment (VIVIT), Feldkirch, Austria

²Department of Medicine I, Academic Teaching Hospital Feldkirch, Feldkirch, Austria

³Private University of the Principality of Liechtenstein, Triesen, Liechtenstein

Introduction: Non-alcoholic fatty liver disease (NAFLD) is associated with both the metabolic syndrome (MetS) and congestive heart failure (CHF). The MetS is highly prevalent in CHF patients; however, the single and joint associations of the MetS and CHF with NAFLD have not been investigated yet. This issue therefore is addressed in the present study.

Methods: We investigated 202 patients with CHF and 670 controls who did not have signs or symptoms of CHF and in whom significant coronary artery disease was ruled out angiographically. The presence of NAFLD was determined using the validated fatty liver index (FLI).

Results: The prevalence of the MetS was 61.9% in CHF patients and 45.7% in controls ($p<0.001$). FLI values and prevalence rates of NAFLD (FLI ≥ 60) in non-CHF subjects without MetS were 40 ± 25 and 25.0%, respectively. They were significantly higher in non-CHF, but MetS patients (71 ± 22 , $p<0.001$ and 69.3%, $p<0.001$, respectively), in CHF patients without

MetS (54 ± 24 , $p < 0.001$ and 42.9% , $p = 0.002$, respectively) and in CHF patients with MetS (76 ± 20 , $p < 0.001$ and 82.4% , $p < 0.001$, respectively). In multivariate analysis of covariance, the MetS and CHF proved to be mutually independent predictors of FLI after adjustment for age, sex, BMI, LDL-C, history of smoking and hypertension ($F = 296.94$; $p < 0.001$ and $F = 21.68$; $p < 0.001$, respectively); concordantly, the MetS and CHF independently predicted the presence of NAFLD in logistic regression analyses, with adjusted odds ratios of 6.67 [4.83–9.21]; $p < 0.001$ and 2.52 [1.67–3.79]; $p < 0.001$, respectively.

Conclusion: We conclude that CHF and the MetS are mutually independent predictors of NAFLD.

13.7

The Ceramide- and Phosphatidylcholine-based coronary event risk test2 (CERT2) and cardiovascular mortality in men and women with Type 2 Diabetes

A. Leiberer¹, A. Muendlein², C. H. Saely¹, B. Larcher³, A. Mader³, M. Maechler², L. Sprenger², B. Mutschlechner², M. Benda², R. Laaksonen⁴, M. Laaperi⁴, A. Jylha⁴, P. Fraunberger⁵, H. Drexel²

¹Private University of the Principality of Liechtenstein, Triesen, Liechtenstein

²Vorarlberg Institute for Vascular Investigation & Treatment (VIVIT), Feldkirch, Austria

³Department of Medicine I, Academic Teaching Hospital Feldkirch, Feldkirch, Austria

⁴Zora Biosciences, Espoo, Finland

⁵Medical Central Laboratories Feldkirch, Feldkirch, Austria

Introduction: The recently introduced Coronary Event Risk Test version 2 (CERT2) is a validated cardiovascular risk predictor score that uses circulating ceramide and phosphatidylcholine concentrations.

Methods: We here aimed at investigating the power of CERT2 to predict cardiovascular mortality in 280 male and 121 female patients with type 2 diabetes (T2 DM).

Results: Prospectively, we recorded 55 cardiovascular deaths in men and 19 in women during a mean follow-up time of 7.6 ± 3.6 and 8.1 ± 3.4 years respectively. Overall, cardiovascular survival decreased with increasing CERT2 risk categories (Fig. 1). In Cox regression models, CERT2 significantly predicted the incidence of cardiovascular mortality in male patients with T2 DM (unadj. HR 1.82 [1.39–2.37] per standard deviation; $p < 0.001$), the unadj. HR in women was 1.36 [0.83–2.22]; $p = 0.228$). After adjustment for age, BMI, current smoking, LDL cholesterol, HDL cholesterol, hypertension, and statin use the

HR in men was 1.73 [1.31–2.29]; $p < 0.001$) and in 1.40 [0.83–2.36]; $p = 0.210$ women. Interaction terms CERT2 \times gender were non-significant both in univariate analysis ($p = 0.354$) and after multivariate adjustment ($p = 0.359$).

Conclusion: We conclude that sex does not significantly impact the association of CERT2 with cardiovascular mortality in patients with T2 DM.

13.8

Type 2 diabetes, chronic kidney disease and major cardiovascular events in patients with established coronary artery disease

L. Sprenger¹, A. Vonbank², B. Larcher², A. Mader², M. Maechler¹, B. Mutschlechner¹, M. Benda¹, A. Leiberer³, A. Muendlein¹, H. Drexel¹, C. H. Saely³

¹Vorarlberg Institute for Vascular Investigation & Treatment (VIVIT), Feldkirch, Austria

²Department of Medicine I, Academic Teaching Hospital Feldkirch, Feldkirch, Austria

³Private University of the Principality of Liechtenstein, Triesen, Liechtenstein

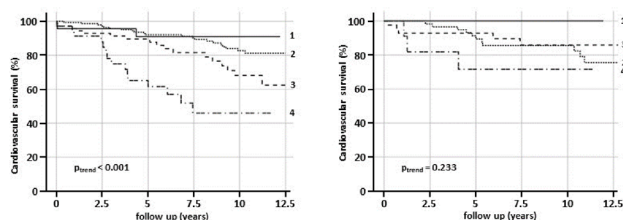
Introduction: Both type 2 diabetes (T2 DM) and chronic kidney disease (CKD) confer a high risk of cardiovascular disease (CVD), and these conditions frequently coincide. The aim of this study was to investigate the single and joint effects of T2 DM and CKD on major cardiovascular events (MACE) in a high-risk population of patients with established coronary artery disease (CAD).

Methods: We prospectively investigated 1460 patients with angiographically proven CAD over 10.4 ± 4.8 years, of whom 454 (30.8 %) had T2 DM and 251 (17.1 %) had CKD.

Results: MACE occurred more frequently in T2 DM patients than in non-diabetic subjects (40.4 % vs 28.7 %, $p < 0.001$) and in patients with CKD (eGFR < 60 ml/min/1.73 m²) than in those with an eGFR ≥ 60 ml/min/1.73 m² (51.6 % vs 28.3 %, $p < 0.001$). When both, T2 DM and CKD were considered, 863 subjects had neither T2 DM nor CKD, 346 had T2 DM but not CKD, 148 did not have diabetes but had CKD, and 103 had both T2 DM and CKD. When compared with the incidence of MACE among patients with neither T2 DM nor CKD (25.3 %), MACE occurred more frequently in patients with T2 DM who did not have CKD (35.8 %; $p < 0.001$) as well as in non-diabetic patients with CKD (47.6 %; $p < 0.001$) and occurred most frequently in patients with both, T2 DM and CKD (57.4 %; $p < 0.001$), in whom the incidence of MACE was higher than in those with T2 DM but not CKD ($p < 0.001$) or those without T2 DM but with CKD ($p = 0.025$); the incidence of MACE was higher in non-diabetic CKD patients than in T2 DM patients who did not have CKD ($p = 0.041$). In Cox regression analysis, T2 DM (HR = 1.46 [1.20–1.78]; $p < 0.001$) and CKD (HR = 1.81 [1.45–2.27]; $p < 0.001$) were mutually independent predictors of MACE after multivariate adjustment.

Conclusion: We conclude that T2 DM and CKD are mutually independent risk factors for MACE in patients with established CAD. CAD patients with both CKD and T2 DM are an extremely high risk for MACE.

Cardiovascular survival of T2DM patients according to CERT2



The Kaplan Meier plot indicates the cardiovascular survival according to the CERT2 risk categories ranging from low risk (1) to very high risk (4) for men (left) and women (right).

Fig. 113.7

14 VITIEN

14.1

Prevalence of cardiac amyloidosis in patients undergoing transcatheter edge-to-edge mitral valve repair

C. Donà¹, C. Nitsche¹, M. Koschutnik¹, S. Koschatko¹, V. Dannenberg¹, A. Kammerlander¹, G. Goliash¹, P. Bartko¹, M. Schneider¹, T. Traub-Weidinger², M. Hacker², C. Hengstenberg¹, J. Mascherbauer¹

¹Medizinische Universität Wien – Innere Medizin II, Klinik für Kardiologie, Wien, Austria

²Medizinische Universität Wien – Universitätsklinik für Radiologie und Nuklearmedizin, Wien, Austria

Introduction: Cardiac amyloidosis (CA) is associated with severe aortic stenosis, however, its prevalence in patients with severe mitral regurgitation in elderly patients is unknown.

Methods: Patients scheduled for transcatheter edge-to-edge mitral valve repair (TMVR) were prospectively screened for CA using 99 m technetium-3,3-diphosphono-1,2-propanodicarboxylic acid (DPD) bone scintigraphy and subsequent serum as well as urine free light-chain quantification in case of a positive DPD scan, defined as visual cardiac uptake based on the Perugini grading scale.

Results: Out of 100 patients undergoing TMVR, 28 patients (28.0 %) had a positive DPD-scan (DPD+). 14 patients (14.0 %) showed Perugini grade I enhancement, 9 patients (9.0 %) grade II enhancement, and in 5 patients (5.0 %), grade III enhancement was present. 28 patients suffered from TTR and two from AL-amyloidosis (one patient had a combination of TTR and AL-amyloidosis). When compared to patients with a negative scan (DPD-), DPD+ patients presented with similar baseline characteristics such as age (DPD- vs DPD+ 76y/o vs 77y/o, $p=0.44$), gender (female; 62.7 % vs 50.0 %, $p=0.25$), coronary artery disease (59.7 % vs 42.9 %, $p=0.13$), previous valve surgery (25.4 % vs 14.3 %, $p=0.24$) and atrial fibrillation (68.7 % vs 78.6 %, $p=0.33$). Also, NYHA functional class and EuroScore II were similar (NYHA \geq III; 85.1 % vs 82.1 %, $p=0.72$, and EuroScore II 9.9 ± 9.8 % vs 7.0 ± 4.8 %, $p=0.21$, respectively). On echocardiography, DPD+ patients presented with more pronounced left and right ventricular hypertrophy (interventricular septum: 15 mm vs 13 mm, $p < 0.01$) but similar left ventricular ejection fraction (44.9 % vs 42.3 %, $p=0.34$). At 3-months after TMVR, DPD+ patients showed significant improvement in BNP serum levels when compared to DPD- patients (DPD+ vs DPD-: $+315 \pm 2569$ pg/ml vs -2404 ± 8696 pg/ml, $p=0.03$), while NYHA functional class remained unchanged (NYHA improvement \geq I class: 57.6 % vs 50.0 %, $p=0.52$).

Conclusion: In this single centre experience, CA was highly prevalent among elderly patients with severe mitral regurgitation scheduled for TMVR. TMVR in CA patients resulted in significant improvement of NT-pro BNP levels. Future studies need to clarify the prognostic relevance of CA in this specific patient population.

14.2

Percutaneous transcatheter edge-to-edge repair of severe tricuspid regurgitation with off-label use of the mitraclip-system after failed surgical tricuspid repair—a case report

K. Danninger¹, M. Rammer¹, M. Suppan¹, R. Binder¹

¹Klinikum Wels-Grieskirchen, Wels, Austria

Background: Percutaneous transcatheter edge-to-edge repair of severe tricuspid regurgitation (TR) with off-label use of the MitraClip-system has shown promising results. We here-with report a case with early-recurrent severe functional TR after surgical tricuspid valve repair and aortocoronary bypass graft surgery.

Case summary: We present a 65-year-old man who underwent aortocoronary bypass graft surgery and surgical tricuspid valve repair with a cosgrove band (36 mm) annuloplasty because of coronary artery disease with ischaemic cardiomyopathy (left ventricular ejection fraction 35 %) and severe secondary TR due to annular dilatation. After the operation the patient was haemodynamically unstable and continually dependent on vasopressors. Echocardiographic evaluation revealed recurrent severe functional TR. Due to the inability to wean the patient from inotropic support over four weeks and the high risk of repeat open heart surgery the heart team decision was to go for a minimally invasive interventional approach using the MitraClip-system to treat the severe TR.

Results: The procedure was performed in the cathlab under general anaesthesia with transoesophageal echocardiography and fluoroscopic guidance. The cosgrove band complicated the echocardiographic guidance as well as the placement of the clip. Finally, 1 XTR-Clip was placed between the septal and the anterior leaflet.

Conclusion: Tricuspid regurgitation improved from massive to mild with a mean pressure gradient of 2 mm Hg. Three days after the procedure the patient could be transferred from the intensive care unit to the general ward and was released from hospital 24 days later in good physical condition. A follow-up echocardiography 4 months later still showed only mild TR.

14.3

Aortic stenosis reexpanded—a novel approach to determine aortic valve area with phase contrast cardiovascular magnetic resonance imaging

F. Troger¹, I. Lechner², M. Reindl², C. Tiller², M. Holzknicht², M. Pamminer¹, S. Reinstadler², A. Bauer², B. Metzler², A. Mayr¹, G. Klug²

¹Universitätsklinik für Radiologie, Innsbruck, Austria

²Universitätsklinik für Innere Medizin III, Kardiologie und Angiologie, Innsbruck, Austria

Introduction: Transthoracic echocardiography (TTE) has become the diagnostic standard for assessing AS, mainly because of its advantages in comparison to the gold standard of cardiac catheterization. However, its inaccuracies in determining SV and AVA call for a more precise and dependable method. PC-CMR is an aspiring tool to push these boundaries. Therefore, the aim of our study was to validate a novel approach based on phase contrast cardiovascular magnetic resonance imaging

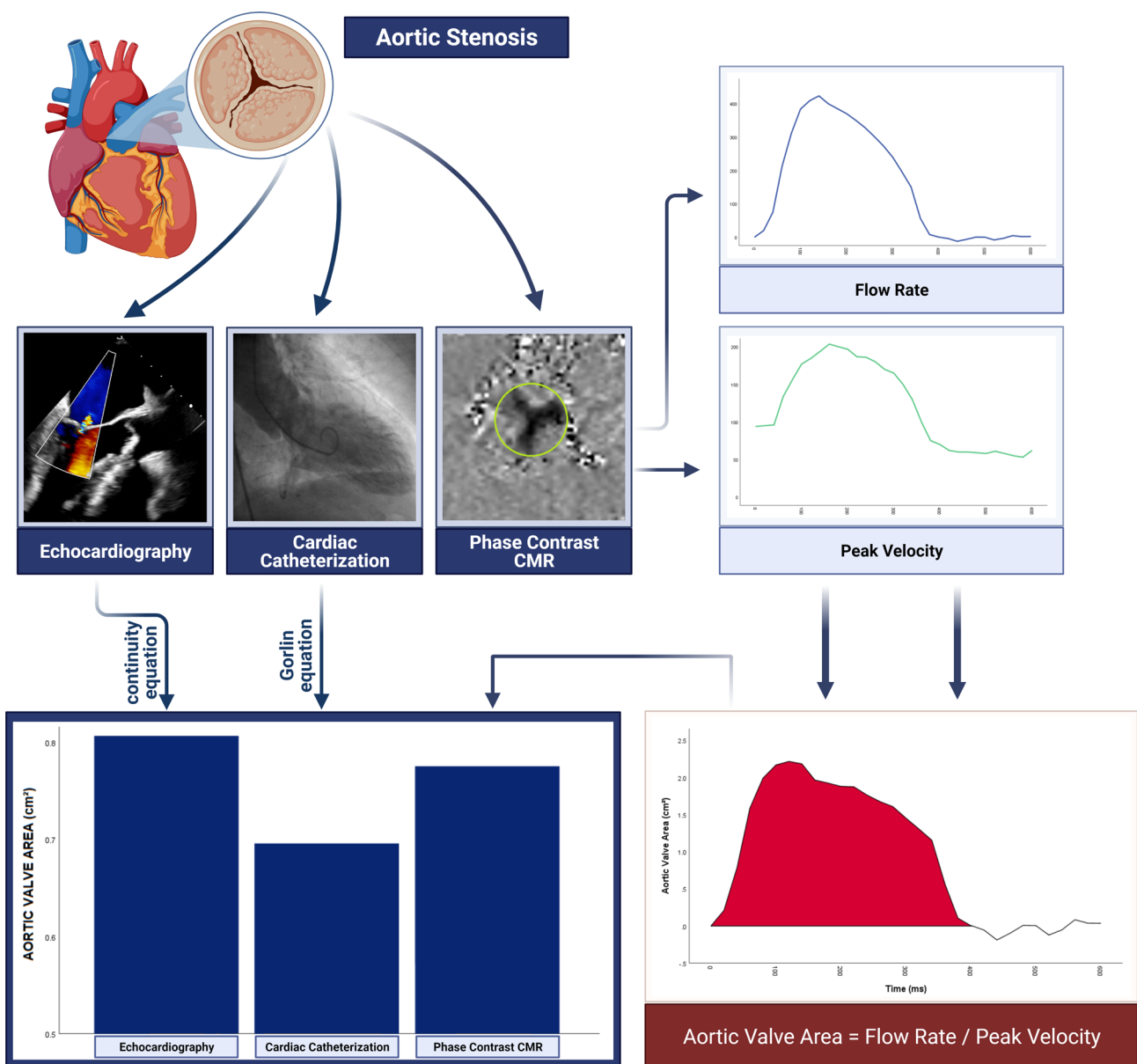


Fig. 1114.3 Many ways lead to Rome—several approaches to determine the aortic valve area, with phase-contrast CMR yielding solid values comparable to invasive measurement

(PC-CMR) against invasive and echocardiographic determination of stroke volume (SV) and aortic valve area (AVA) in aortic stenosis (AS).

Methods: PC-CMR was performed in 50 patients with moderate or severe AS (age 72 years, interquartile range (IQR): [66–78], 48 % of patients with low-flow states). All of them were referred to invasive evaluation of AS by cardiac catheterization. Additionally, transthoracic echocardiography (TTE) was performed. Aortic valve area (AVA) was determined by PC-CMR (AVA-CMR) via plotting momentary flow across the valve against momentary flow velocity. AVA-CMR at different time points over the entire cardiac cycle was compared to invasively determined AVA, calculated according to the Gorlin-formula. Stroke volumes (SV) were determined by the Fick-principle, pressure gradients according to the modified Bernoulli-equation.

Results: SV by PC-CMR correlated strongly with cine-CMR without significant bias ($r: 0.730, p < 0.001$); SV by PC-CMR: 85 ± 31 ml; SV by cine-CMR: 85 ± 19 ml, $p = 0.829$). Peak gradients

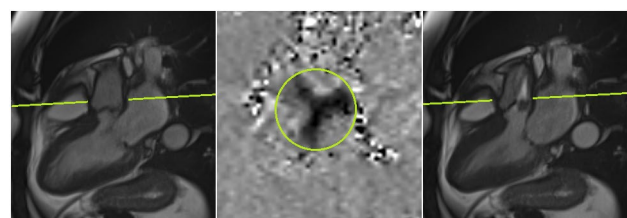


Fig. 2114.3 Cine 3-Chamber CMR (left end-diastolic, right end-systolic) and phase contrast-CMR (end-systolic, middle) in the displayed layer of the aortic valve of a patient with severe aortic stenosis

determined by PC CMR showed inverse correlation with AVA by PC-CMR ($r: 0.371; p = 0.008$). Mean AVA during the whole systolic phase correlated moderately ($r: 0.544, p < 0.001$) to invasive AVA with a small bias (AVA by CMR: 0.78 ± 0.25 cm² versus

invasive AVA: $0.70 \pm 0.23 \text{ cm}^2$, bias: 0.08 cm^2 , $p=0.017$). Inter-methodical correlation and bias of AVA as measured by TTE and invasively (AVA by TTE: $0.81 \pm 0.23 \text{ cm}^2$, $r: 0.580$, $p < 0.001$, bias 0.11 cm^2 , $p < 0.001$) showed similar values.

Conclusion: PC-CMR provides a reliable option to yield solid SV values in patients with moderate to severe aortic stenosis. Continuous determination of flow volumes and velocities is able to determine AVA in an easy-to-use manner with good correlation and virtually no bias to invasively determined AVA. Our novel approach highlights the diagnostic potential of PC-CMR for non-invasive AS grading, especially when echocardiographic findings are inconclusive.

Conclusion: TS classical LF/LG AS can be reliably predicted by a resting Vmax $>3.5 \text{ m/s}$ or a resting MPG $>35 \text{ mm Hg}$. Further imaging for subclassification is not needed in this situation.

Publisher's Note Springer Nature remains neutral with regard to jurisdictional claims in published maps and institutional affiliations.

14.4

Resting peak jet velocity $>3.5 \text{ m/s}$ in classical low-flow, low-gradient aortic stenosis indicates true-severity

J. Kellermair¹, S. Saeed², J. Kammler¹,
H. Blessberger¹, D. Kiblböck¹, C. Steinwender¹

¹Klinik für Kardiologie und Internistische Intensivmedizin, Kepler Universitätsklinikum Linz, Linz, Austria

²Department of Heart Disease, Haukeland University Hospital, Bergen, Norway, Bergen, Norway

Introduction: Classical low-flow, low-gradient (LF/LG) aortic stenosis (AS) is subclassified into a true-severe (TS) and a pseudo-severe (PS) subform using low-dose dobutamine stress echocardiography (DSE). A resting peak jet velocity (Vmax) $>3.5 \text{ m/s}$ or a mean transvalvular gradient (MPG) $>35 \text{ mm Hg}$ suggests the presence of TS classical LF/LG AS, but there is no data to support this. The aim of this study was therefore to investigate whether a resting Vmax $>3.5 \text{ m/s}$ or MPG $>35 \text{ mm Hg}$ reliably predicted diagnosis of TS classical LF/LG AS.

Methods: One hundred (100) consecutive patients with classical LF/LG AS were prospectively recruited. All patients underwent DSE for subcategorization. The impact of Vmax and MPG for the presence of the TS subform were analyzed.

Results: TS classical LF/LG AS was diagnosed in 72 patients. Resting Vmax and resting MPG predicted true-severity with an ROC-AUC of 0.737 (95%CI: 0.635–0.838; $p < 0.001$) and 0.725 (95%CI: 0.615–0.834; $p < 0.001$), respectively (Fig. 1). The optimal positive predictive values (PPV) for the diagnosis of TS classical LF/LG AS were obtained with a resting Vmax $>3.5 \text{ m/s}$ or resting MPG $>35 \text{ mm Hg}$. In a multivariate logistic regression analysis, Vmax $>3.5 \text{ m/s}$ was independently associated with a 5.33-fold odds-ratio of TS classical LF/LG AS (OR 5.33; 95%CI: 1.34–21.18, $p=0.018$)

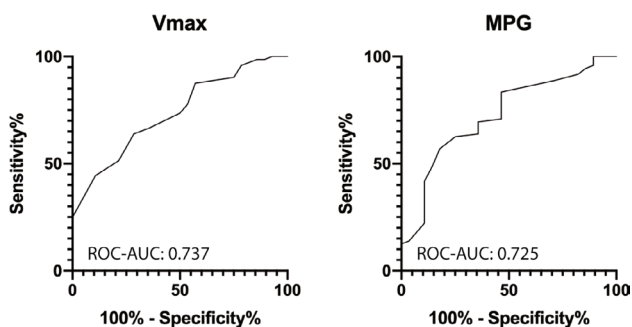


Fig. 1 | 14.4